Pacific Gas and Electric Company

David H. Oatley
Vice President and
General Manager

Diablo Canyon Power Plant
P.O. Box 56
Avila Beach, CA 93424

805.545.4350
Fax: 805.545.4234

October 3, 2003

PG&E Letter DIL-03-012

U.S. Nuclear Regulatory Commission
ATTN: Document Control Desk
Washington, DC 20555-0001

Docket No. 72-26
Diablo Canyon Independent Spent Fuel Storage Installation
Submittal of License Application Amendment 2 (TAC No. L23399)

Dear Commissioners and Staff:

This letter submits Amendment 2 to the Diablo Canyon Independent Spent Fuel Storage Installation (ISFSI) License Application. The ISFSI license application was submitted to the Nuclear Regulatory Commission (NRC) by Pacific Gas and Electric Company (PG&E) on December 21, 2001, in PG&E Letter DIL-01-002. The application included a Safety Analysis Report (SAR), Environmental Report (ER), and other required documents in accordance with 10 CFR 72. Amendment 1 to the application was previously submitted to the NRC on October 15, 2002, in PG&E Letter DIL-02-010.

Amendment 2 updates the ISFSI SAR part of the application to incorporate responses to NRC requests for additional information (RAIs), responses to informal NRC questions and comments related to previously submitted RAI responses and related topics, and to make explicit reference to applicable calculation packages submitted to the NRC. Amendment 2 incorporates information into the SAR from the following PG&E letters previously submitted to the NRC:

- DIL-01-004, 12/21/01, Non-Proprietary Calculation Packages
- DIL-02-005, 05/16/02, Geoscience Calculation Packages
- DIL-02-007, 06/04/02, Holtec Proprietary Reports
- DIL-02-009, 10/15/02, Response to NRC RAIs
- DIL-02-011, 10/15/02, Holtec Proprietary Reports
- DIL-03-002, 02/14/03, Response to NRC Comments on RAI Responses
- DIL-03-003, 03/27/03, Revised Response to RAI 5-1
- DIL-03-004, 03/27/03, Response to Additional Slope Stability Questions
- DIL-03-005, 03/27/03, Response to Comments on Blasts and Explosions
- DIL-03-006, 03/27/03, Holtec Proprietary Report
- DIL-03-007, 05/06/03, Response to Additional Slope Stability Questions

NMSS01

- DIL-03-008, 06/13/03, Response to Additional Blast and Explosion Questions
- DIL-03-010, 07/28/03, Response to Additional Blast and Explosion Questions
- DIL-03-011, 10/3/03, Response to Transporter Lateral Restraints RAI

Amendment 2 to the ISFSI SAR is enclosed.

If you have any questions regarding this amendment, please contact Mr. Terence Grebel at (805) 545-4160.

Sincerely,

David H. Oatley
Vice President and General Manager - Diablo Canyon

Enclosure

cc:	Diablo Distribution
	Brian Gutherman
cc/enc:	Diane Curran, Esq.
	James R. Hall
	David A Repka, Esq.
	Robert K. Temple, Esq.
	Robert R. Wellington, Esq.
	Jacquelyn C. Wheeler

DCL-03-012

UNITED STATES OF AMERICA
NUCLEAR REGULATORY COMMISSION

In the Matter of PACIFIC GAS AND ELECTRIC COMPANY Diablo Canyon Power Plant Units 1 and 2	Docket No. 72-26

AFFIDAVIT

David H. Oatley, of lawful age, first being duly sworn upon oath says that he is Vice President and General Manager – Diablo Canyon of Pacific Gas and Electric Company, that he is familiar with the content thereof; that he has executed Amendment 2 to the Diablo Canyon Independent Spent Fuel Storage Installation license application on behalf of said company with full power and authority to do so; and that the facts stated therein are true and correct to the best of his knowledge, information, and belief.

David H. Oatley
Vice President and General Manager - Diablo Canyon

Subscribed and sworn to before me this 3rd day of October 2003.

Notary Public
State of California
County of San Luis Obispo

CHUCK MACKEY
Commission # 1397647
Notary Public - California
San Luis Obispo County
My Comm. Expires Feb 1, 2007

DIABLO CANYON ISFSI
SAFETY ANALYSIS REPORT
FILING INSTRUCTIONS

Filing Instructions (Discard when filing has been completed)

Remove Current Sheets	Insert Amendment 2 Sheets
VOLUME 1	
List of Current Pages (6 pages)	List of Current Pages (6 pages)
SAR Contents i through iv	SAR Contents i through iii
Chapter 2	
Contents i through viii	Contents i through viii
2.2-1 through 2.2-13	2.2-1 through 2.2-15
2.3-1 through 2.3-3	2.3-1 through 2.3-3
2.4-1 through 2.4-3	2.4-1 through 2.4-4
2.6-1 through 2.6-61	2.6-1 through 2.6-67
	Table 2.3-1
Table 2.6-1	Table 2.6-1
Table 2.6-7	Table 2.6-7
Table 2.6-8 Sheets 1 of 2 through 2 of 2	Table 2.6-8 Sheets 1 of 2 through 2 of 2
Chapter 3	
Contents i through iii	Contents i through iii
3.3-1 through 3.3-17	3.3-1 through 3.3-17
Table 3.4-1 Sheets 1 of 2 through 2 of 2	Table 3.4-1 Sheets 1 of 2 through 2 of 2
VOLUME 2	
Chapter 4	
Contents I through v	Contents I through v
4.2-1 through 4.2-28	4.2-1 through 4.2-31
4.3-1 through 4.3-9	4.3-1 through 4.3-9
4.4-1 through 4.4-16	4.4-1 through 4.4-19
4.7-1 through 4.7-5	4.7-1 through 4.7-6
Figure 4.2-2	Figure 4.2-2

DIABLO CANYON ISFSI
SAFETY ANALYSIS REPORT
FILING INSTRUCTIONS

Filing Instructions (Discard when filing has been completed)

Remove Current Sheets	Insert Amendment 2 Sheets
Chapter 5	
Contents i through iii	Contents i through iii
5.1-1 through 5.1-12	5.1-1 through 5.1-13
Figure 5.1-1 Sheets 1 of 3 through 3 of 3 Figure 5.1-2 Sheets 1 of 2 through 2 of 2	Figure 5.1-1 Sheets 1 of 3 through 3 of 3 Figure 5.1-2 Sheets 1 of 2 through 2 of 2
Chapter 7	
Contents i through v	Contents i through v
7.4-1 through 7.4-3 7.5-1 through 7.5-4	7.4-1 through 7.4-3 7.5-1 through 7.5-4
Table 7.4-1 Sheets 1 of 3 through 3 of 3 Table 7.4-2 Sheets 1 of 2 through 2 of 2 Table 7.5-3 Table 7.5-4	Table 7.4-1 Sheets 1 of 3 through 3 of 3 Table 7.4-2 Sheets 1 of 2 through 2 of 2 Table 7.5-3 Table 7.5-4
Chapter 8	
Contents i through iv	Contents i through iii
8.1-1 through 8.1-12 8.2-1 through 8.2-61	8.1-1 through 8.1-12 8.2-1 through 8.2-66
Table 8.2-11	Table 8.2-11
Chapter 10	
Contents i through iii	Contents i through iii
10.2-1 through 10.2-16	10.2-1 through 10.2-17

DIABLO CANYON ISFSI
SAFETY ANALYSIS REPORT

LIST OF CURRENT PAGES

Page No.	Amendment	Page No.	Amendment	Page No.	Amendment
CONTENTS		2.1-1		2.6-15	2
		2.1-2		2.6-16	2
i	2	2.1-3		2.6-17	2
ii	2	2.1-4		2.6-18	2
iii	2	2.1-5		2.6-19	2
		2.1-6		2.6-20	2
GLOSSARY		2.2-1	2	2.6-21	2
		2.2-2	2	2.6-22	2
1	1	2.2-3	2	2.6-23	2
2	1	2.2-4	2	2.6-24	2
3	1	2.2-5	2	2.6-25	2
4	1	2.2-6	2	2.6-26	2
5	1	2.2-7	2	2.6-27	2
6	1	2.2-8	2	2.6-28	2
7	1	2.2-9	2	2.6-29	2
8	1	2.2-10	2	2.6-30	2
		2.2-11	2	2.6-31	2
CHAPTER 1		2.2-12	2	2.6-32	2
		2.2-13	2	2.6-33	2
I	1	2.2-14	2	2.6-34	2
Ii	1	2.2-15	2	2.6-35	2
1.1-1		2.3-1	2	2.6-36	2
1.1-2		2.3-2	2	2.6-37	2
1.1-3		2.3-3	2	2.6-38	2
1.1-4		2.4-1	2	2.6-39	2
1.1-5		2.4-2	2	2.6-40	2
1.2-1	1	2.4-3	2	2.6-41	2
1.2-2	1	2.4-4	2	2.6-42	2
1.3-1		2.5-1		2.6-43	2
1.3-2		2.5-2		2.6-44	2
1.4-1		2.5-3		2.6-45	2
1.5-1		2.6-1	2	2.6-46	2
Table 1.1-1	1	2.6-2	2	2.6-47	2
Table 1.1-2		2.6-3	2	2.6-48	2
		2.6-4	2	2.6-49	2
CHAPTER 2		2.6-5	2	2.6-50	2
		2.6-6	2	2.6-51	2
i	2	2.6-7	2	2.6-52	2
ii	2	2.6-8	2	2.6-53	2
iii	2	2.6-9	2	2.6-54	2
iv	2	2.6-10	2	2.6-55	2
v	2	2.6-11	2	2.6-56	2
vi	2	2.6-12	2	2.6-57	2
vii	2	2.6-13	2	2.6-58	2
viii	2	2.6-14	2	2.6-59	2

LIST OF CURRENT PAGES

LIST OF CURRENT PAGES

LIST OF CURRENT PAGES

Page No.	Amendment
Figure 4.3-1	
Figure 4.3-2	
Figure 4.3-3	
Figure 4.3-4	
Figure 4.3-5	
Figure 4.3-6	
Figure 4.4-1	
Figure 4.4-2	
Figure 4.4-3, Sheet 1	
Figure 4.4-3, Sheet 2	
Figure 4.4-3, Sheet 3	
Figure 4.4-3, Sheet 4	
Figure 4.4-4	
CHAPTER 5	
i	2
ii	2
iii	2
5.1-1	2
5.1-2	2
5.1-3	2
5.1-4	2
5.1-5	2
5.1-6	2
5.1-7	2
5.1-8	2
5.1-9	2
5.1-10	2
5.1-11	2
5.1-12	2
5.1-13	2
5.2-1	
5.3-1	
5.4-1	
Table 5.1-1	
Figure 5.1-1, Sheet 1	2
Figure 5.1-1, Sheet 2	2
Figure 5.1-1, Sheet 3	2
Figure 5.1-2, Sheet 1	2
Figure 5.1-2, Sheet 2	2
CHAPTER 6	
i	
6.1-1	
6.2-1	
6.3-1	
CHAPTER 7	
i	2
ii	2
iii	2
iv	2
v	2
7.1-1	
7.1-2	
7.1-3	
7.1-4	
7.1-5	
7.2-1	
7.2-2	
7.2-3	
7.2-4	
7.2-5	
7.2-6	
7.2-7	
7.2-8	
7.3-1	
7.3-2	
7.3-3	
7.3-4	
7.3-5	
7.3-6	
7.4-1	2
7.4-2	2
7.4-3	2
7.5-1	2
7.5-2	2
7.5-3	2
7.5-4	2
7.6-1	
7.7-1	
Table 7.2-1	
Table 7.2-2	
Table 7.2-3	
Table 7.2-4	
Table 7.2-5	
Table 7.2-6	
Table 7.2-7	
Table 7.2-8, Sheet 1	
Table 7.2-8, Sheet 2	
Table 7.3-1	
Table 7.3-2	
Table 7.3-3	
Table 7.3-4	
Table 7.4-1, Sheet 1	2
Table 7.4-1, Sheet 2	2
Table 7.4-1, Sheet 3	2
Table 7.4-2, Sheet 1	2
Table 7.4-2, Sheet 2	2
Table 7.4-3	
Table 7.4-4	
Table 7.5-1	
Table 7.5-2	
Table 7.5-3	2
Table 7.5-4	2
Figure 7.3-1	
Figure 7.3-2	
Figure 7.3-3	
Figure 7.3-4	
CHAPTER 8	
i	2
ii	2
iii	2
8.1-1	2
8.1-2	2
8.1-3	2
8.1-4	2
8.1-5	2
8.1-6	2
8.1-7	2
8.1-8	2
8.1-9	2
8.1-10	2
8.1-11	2
8.1-12	2
8.2-1	2
8.2-2	2
8.2-3	2
8.2-4	2
8.2-5	2

LIST OF CURRENT PAGES

LIST OF CURRENT PAGES

DIABLO CANYON ISFSI
SAFETY ANALYSIS REPORT

CONTENTS

VOLUME 1

DIABLO CANYON ISFSI
SAFETY ANALYSIS REPORT

CONTENTS

VOLUME 2

DIABLO CANYON ISFSI
SAFETY ANALYSIS REPORT

CONTENTS

VOLUME 2 (continued)

DIABLO CANYON ISFSI
SAFETY ANALYSIS REPORT

CHAPTER 2

SITE CHARACTERISTICS

CONTENTS

CHAPTER 2

SITE CHARACTERISTICS

CONTENTS (Continued)

DIABLO CANYON ISFSI
SAFETY ANALYSIS REPORT

CHAPTER 2

SITE CHARACTERISTICS

TABLES

CHAPTER 2

SITE CHARACTERISTICS

FIGURES

SITE CHARACTERISTICS

FIGURES (Continued)

CHAPTER 2

SITE CHARACTERISTICS

FIGURES (Continued)

CHAPTER 2

SITE CHARACTERISTICS

FIGURES (Continued)

CHAPTER 2

SITE CHARACTERISTICS

FIGURES (Continued)

2.2 NEARBY INDUSTRIAL, TRANSPORTATION, AND MILITARY FACILITIES

2.2.1 OFFSITE POTENTIAL HAZARDS

2.2.1.1 Description of Location and Routes

Industry in the vicinity of the Diablo Canyon ISFSI site is mainly light and of a local nature, serving the needs of agriculture in the area. Food processing and refining of crude oil are the major industries in the area, although the numbers employed are not large. Less than 8 percent of the work force in San Luis Obispo County is engaged in manufacturing. The largest industrial complex is Vandenberg Air Force Base, located approximately 35 miles south-southeast of the DCPP site in Santa Barbara County.

Port San Luis Harbor and the Point San Luis Lighthouse property are located approximately 6 miles south-southeast of the DCPP site. The Point San Luis Lighthouse is located on a 30-acre parcel of land. Until 1990, the US Coast Guard owned the lighthouse property. In 1990 the Port San Luis Harbor District, owners and operators of the Port San Luis Harbor, were granted ownership of the lighthouse and the 30 acres, except for approximately 3 acres of land, in 3 parcels, which the Coast Guard retained as owners in order to operate and maintain the modern light station and navigating equipment located on those 3 acres.

Located approximately 6 miles east-southeast of the DCPP site is the Port San Luis tanker-loading pier. The pier is located on property that is owned by the Port San Luis Harbor District and leased by UNOCAL, which built and owns the pier. However, this pier is no longer active as tanker traffic into Port San Luis has been discontinued.

US Highway 101 is the main arterial road serving the coastal region in this portion of California. It passes approximately 9 miles east of the site, separated from it by the Irish Hills. US Highway 1 passes approximately 10 miles to the north and carries moderate traffic between San Luis Obispo and the coast. The nearest public access from a US highway is by county roads in Clark Valley, 5 miles north, and See Canyon, 5 miles east. Access to the site is by Avila Beach Drive, a county road, to the entrance of the PG&E private road system.

The Southern Pacific Transportation Company provides rail service to the county by a route that essentially parallels US Highway 101. It passes approximately 9 miles east of the site, separated from it by the Irish Hills. There is no spur track into the DCPP site.

Coastal shipping lanes are approximately 20 miles offshore. Prior to 1998, there were local tankers coming into and out of Estero Bay, which is north of the DCPP site. There is no further tanker traffic in either Port San Luis or Estero Bay. The local tanker terminal at Estero Bay closed in 1994, and Avila Pier ceased operation in 1998. Petroleum products and crude oil are no longer stored at Avila Beach since the storage tanks there were removed in 1999. However, some petroleum products and crude oil continue to be stored at Estero Bay, approximately 10 miles from the DCPP site.

The San Luis Obispo County Regional Airport is located 12 miles east of the DCPP site. The airport served, as a 4 year average between 1998 and 2001, approximately 16,000 air transport (AT) (i.e., commercial or air taxi) landing and departure operations per year. Air transport was provided primarily by turbo-prop or smaller aircraft that seat no more than 41 people with a gross weight of no more than 30,000 pounds.

The airport also served, as a 4 year average between 1998 and 2001, approximately 7,560 total landings and departures of private aircraft per month. These consisted mostly of aircraft that seat no more than 8 people, with an average gross weight of less than 12,500 pounds. Although there are no specific air traffic restrictions over DCPP, most air traffic into and out of the San Luis Obispo County Regional Airport does not approach within 5 miles of the ISFSI site because of the mountainous terrain.

There is a federal flight corridor (V-27) approximately 5 miles east of the ISFSI that is used for aircraft flying between Santa Barbara and Big Sur areas, with an estimated 20 flights per day per year-2001 data. The majority of the aircraft using this route are above 10,000 ft. Sometimes this corridor is used also for traffic into San Luis Obispo County Regional Airport and, in this case, has traffic that passes as close as 1 mile of the ISFSI site at an elevation of 3,000 ft. However, this portion of the route is normally only used for aircraft to align for instrument landing. The more commonly used approach route for visual landings passes 8 miles from the Diablo Canyon ISFSI site on the far side of the San Luis Range.

There is also a military training route (VR-249), which runs parallel to the site and its center is approximately 2 miles off shore. This training route is not frequently used. (Estimated based on data from the period of September 2001 and September 2002 at approximately 50 flights per year). Its use requires a minimum of 5 miles visibility, and the flights are to maintain their altitude between sea level and 10,000 ft.

There is a municipal airport near Oceano, located 15 miles east-southeast of the DCPP site, which accommodates only small (12,500 pounds or less) private planes. The traffic at this airport is estimated to be no more than 2,200 flights per month. The Camp San Luis Obispo airfield is located 8 miles northeast of the DCPP site, but is now shown as helicopter use only.

The peak Vandenberg Air Force Base employment is approximately 4,400 people, including 3,200 military and 1,200 civilian personnel. At the Vandenberg Air Force Base, there are between 15 to 20 missiles fired per year and currently, missions are flown in a range varying from due west to a southeasterly direction, depending upon launch site and mission. The Vandenberg's Intercontinental ballistic missile tests launch from sites on north base, and typically fly due west. The Vandenberg Air Force Base's spacelift missions typically launch from sites on the southern part of the base, and fly in a southerly direction. The polar orbit launches are launched in a southerly direction. As a result, none of these launches would bring missiles in the vicinity of the ISFSI facility.

There is a potential for missions in the future to fly in a northwesterly direction, but Vandenberg Air Force Base will have safeguards in place to ensure there is no potential for the missile to impact on land outside of Vandenberg Air Force Base's boundary (same techniques used to protect the cities of Lompoc, Santa Barbara, etc., and requires the immediate destruction of any missile that deviates from its intended trajectory.). Deviation from a planned trajectory and destruction of a missile is considered a low probability event by the Air Force.

Vandenberg Air Force Base's most northerly missile launch site is approximately 25 miles south of the DCPP site. Vandenberg Air Force Base is also designated as an alternate landing site for the space shuttles, but has not been used for that purpose to date. The landing approach for a space shuttle would be normally west to east, and does not bring the shuttles within 30 miles of the ISFSI site. Because of the distance to Vandenberg Air Force Base, limited flights, trajectory of the missiles and space shuttle, and the safeguards in place to protect errant launches, there is no credible hazard from this facility.

The nearest US Army installation is the Hunter-Liggett Military Reservation located in Monterey County, approximately 45 miles north of the DCPP site. The California National Guard (CNG) maintains Camp Roberts, located on the border of Monterey County and San Luis Obispo County, southeast of the Hunter-Liggett Military Reservation and approximately 30 miles north of the DCPP site. The CNG also maintains Camp San Luis Obispo, located in San Luis Obispo County, approximately 10 miles northeast of the DCPP site. In addition, as noted earlier, a US Coast Guard Light station is located in Avila Beach on property commonly known as the Point San Luis Lighthouse property.

No significant amounts of any hazardous products are commercially manufactured, stored, or transported within 5 miles of the DCPP site. Within 6 to 10 miles of the site, up to 1998, 1 to 2 local tankers per month offloaded oil for storage at Avila Beach. However, such shipments no longer occur and oil is no longer transported through or stored at Avila Beach. Due to very limited industry within San Luis Obispo County and the distances involved, any hazardous products or materials commercially manufactured, stored, or transported in the areas between 5 and 10 miles from the site are not considered to be a significant hazard to the ISFSI.

2.2.1.2 Hazards from Facilities and Ground Transportation

The ISFSI is located in a remote, sparsely populated, undeveloped area. The ISFSI site is in a canyon, which is east and above DCPP Units 1 and 2, and is directly protected on two sides by hillsides. There are no industrial facilities (other than DCPP), public transportation routes, or military bases within 5 miles of the ISFSI. Therefore, activities related to such facilities do not occur near the ISFSI and, thus, do not pose any hazard to the ISFSI.

Local shipping tankers may come within 10 miles of the DCPP site, but will remain outside of a 5-mile range. Coastal shipping lanes are approximately 20 miles offshore. Therefore, shipping does not pose a hazard to the ISFSI.

No commercial explosive or combustible materials are stored within 5 miles of the site, and no natural gas or other pipelines pass within 5 miles of the site. Therefore, there is no potential hazard to the ISFSI from any explosions or fires involving such materials.

Since there are no rail lines or public transportation routes within 5 miles of the ISFSI location, no credible explosions involving truck or rail transportation events need to be considered, pursuant to Regulatory Guide 1.91 (Reference 1). Similarly, explosions involving shipping events offshore at the DCPP site are unlikely. Although the shortest distance from the ISFSI location to the ocean is approximately 1/2-mile, there is no shipping traffic within 5 miles of this location. Therefore, consistent with the guidance of Regulatory Guide 1.91, explosions involving shipping events are not considered credible accidents for the ISFSI.

2.2.1.3 Hazards from Air Crashes

Aircraft crashes were assessed in accordance with the guidance of NUREG-0800, Section 3.5.1.6, Aircraft Hazards (Reference 2). Although this guidance applies to power reactor sites, the analysis of aircraft crash probabilities on the site is not dependent on the nature of the site other than size of the facility involved and, thus, the guidance of NUREG-0800 can be applied to the Diablo Canyon ISFSI site.

As specified in NUREG-0800, the probability of aircraft crashes is considered to be negligibly low by inspection and does not require further analysis if the three criteria specified in Item II.1 of Section 3.5.1.6 are met. In particular, Criterion 1 of Section 3.5.1.6 specifies that the plant-to-airport distance, D, must be greater than 10 statute miles, and the projected annual number of operations must be less than $1{,}000D^2$. San Luis Obispo County Regional Airport is at a distance of 12 miles, with annual flight totals of approximately 92,330, which is less than $1{,}000(12)^2$ or 144,000. The airport at Oceano is 15 miles away, with flight totals of no more than approximately 26,400 per year, which is less than $1{,}000(15)^2$ or 225,000. Vandenberg Air Force Base is 35 miles away and flight totals there are not expected to be more than $1{,}000(35)^2$ or 1,225,000 per year (or more than 3,300 each day). Therefore, based on current data, Criterion 1 is met. However, the airways that are in the vicinity of the Diablo Canyon ISFSI have been analyzed below.

Criterion 2 specifies that the facility must be at least 5 statute miles from the edge of military training routes. There is a military training flight corridor (VR-249) that is within approximately 2 miles of the Diablo Canyon ISFSI site. This route is evaluated below.

Criterion 3 specifies that the facility must be at least 2 statute miles beyond the nearest edge of a federal airway, holding pattern, or approach pattern. There is a federal airway

(V-27) whose edge is within approximately 1 mile east of the ISFSI site. As a result, this route is evaluated below.

Evaluation of Airways

For situations where federal airways or aviation corridors pass through the vicinity of the ISFSI site, the probability per year of an aircraft crashing into the site (P_{fa}) is estimated in accordance with NUREG-0800. The probability depends on factors such as altitude, frequency, and width of the corridor and corresponding distribution of past accidents. Per NUREG-0800, the following expression is used to calculate the probability:

$$P_{fa} = C \times N \times A/w$$

Where:

C	=	Inflight crash rate per mile for aircraft using airway
w	=	Width of airway (plus twice the distance from the airway edge to the site when the site is outside the airway) in miles
N	=	Number of flights per year along airway
A	=	Effective area of the site in square miles

The following analysis was completed per DOE-STD 3014-96 (Reference 5) to determine effective crash area. In this analysis conservative factors have been used for maximum skid distance and maximum wingspan. Based on the available information on aircraft type, size, and the location of the site these factors are very conservative.

In DOE-STD-3014-96:

The effective crash area is: $A_{eff} = A_f + A_s$

where:

$$A_f = (WS + R)(H\cot\Phi) + (2)(L)(W)(WS)/R + (L)(W)$$

and

$$A_s = (WS + R)(S)$$

where:

A_f	=	effective fly-in area;
A_s	=	effective skid area;
WS	=	aircraft wingspan; (reference Table B-16 of DOE-STD 3014-96)
R	=	length of diagonal of the facility,
H	=	facility height;

cotΦ	=	mean on the cotangent of the aircraft impact angle; (reference Table B-17 of DOE-STD 3014-96)
L	=	length of facility;
W	=	width of facility;
S	=	aircraft skid distance; (reference Table B-18 of DOE-STD 3014-96)

For Commercial Aircraft:

A_f = (98 + 511)(20)(10.2) + (2)(500)(105)(98)/511 + (500)(105)
A_f = 196,872 $ft^2/(5{,}280\ ft/mile)^2$ = 0.0071 sq miles

and

A_s = (WS + R)(S) = (98 + 511)(700) = 426,300 $ft^2/(5{,}280\ ft/mile)^2$
= 0.0153 sq miles

For General Aviation Aircraft:

A_f = (73 + 511)(20)(10.2) + (2)(500)(105)(73)/511 + (500)(105)
A_f = 186,636$ft^2/(5{,}280\ ft/mile)^2$ = 0.0067 sq miles

and

A_s = (WS + R)(S) = (73 + 511)(700) = 408,800 $ft^2/(5{,}280\ ft/mile)^2$
= 0.0147 sq miles

For Military Aircraft:

A_f = (110 + 511)(20)(10.2) + (2)(500)(105)(110)/511 + (500)(105)
A_f = 201,787 $ft^2/(5{,}280\ ft/mile)^2$ = 0.0072 sq miles

and

A_s = (WS + R)(S) = (110 + 511)(700) = 0.0156 sq miles

For calculating A_s the skid distance is based on the layout of the facility which is surrounded on three sides by hills and is actually up against one of these hills, which limits the potential crash angle and limits the possible skid distance. The fourth side is protected by a drop off in terrain with a slope of greater than 1:1. The maximum distance on the unprotected side is estimated at less than 700 ft. Since the site is protected and limited from skidding aircraft on three sides, the use of the 700 ft is conservative.

Commercial = A_{eff} = A_f + A_s = 0.0071 + 0.0153 = 0.0224 sq miles

General Aviation = A_{eff} = A_f + A_s = 0.0067 + 0.0147 = 0.0214 sq miles

Military = $A_{eff} = A_f + A_s$ = 0.0072 + 0.0156 = 0.0228 sq miles

<u>For local traffic on V-27:</u>

V-27 use for local aircraft is usually limited to instrument landings for aircraft arriving from the south and instrument departures to the south from runway 11, or circle to land approaches on runway 29, and instrument departures to the south from runway 29 at San Luis Obispo County Regional Airport. As stated above, there are on average approximately 16,000 AT landings and takeoffs per year. It is estimated, using the San Luis Obispo County Regional Airport scheduled airline flight information located at the web address: http://www.sloairport.com/flightinfo.html, that 65 percent of the AT traffic is coming from or departing to the south. Based on airport data over a four-year period from 1998 to 2001 there was an average of 1,781 AT landings per year at San Luis Obispo County Regional Airport under instrument conditions. This would result in (1,781 x 0.65) or 1,157 landings per year, which is doubled to 2,314 operations to account for takeoffs. For the private aircraft usage, there are on average approximately 7,560 total landings and takeoffs per month at the San Luis Obispo County Regional Airport of which it is estimated that 65 percent are from or to the south. Based on airport data over a four-year period from 1998 to 2001 there was an average of 1,430 general aviation landings per year at San Luis Obispo County Regional Airport under instrument conditions. As a result, N for general aviation (1,430 x 0.65) or 930 landings, which is doubled to 1,860 operations to account for takeoffs.

Published holding patterns exist for arrivals at CREPE and CADAB intersections and for missed approaches at Morro Bay VOR. The CREPE Intersection is 11 miles and the CADAB Intersection 21 miles from the ISFSI site. Both holding patterns place the aircraft further from the ISFSI site and therefore do not need to be considered. The ISFSI site distance to the Morro Bay VOR is approximately 6 miles and the holding pattern places the aircraft closer to the ISFSI. Since the Morro Bay VOR holding pattern is used for missed approaches, it is conservatively estimated that 5 percent of all instrument landing approaches are missed and each aircraft remains in the holding pattern for 10 passes. For commercial traffic N is increased by 579 flights (2,314/2 x 0.05 x 10) and general aviation by 465 flights (1,860/2 x 0.05 x10).

Per NUREG-0800, C for commercial aircraft is provided as 4×10^{-10}. Per the Aircraft Crash Risk Analysis Methodology Standards (ACRAM), a C value of 1.55×10^{-7} was used in this analysis. Per federal guidelines, the width of the airway is 8 miles and the center is approximately 5 miles from the site. As a result, (w) is conservatively taken to equal 10 miles.

For commercial flights:

$$P1a_{fa} = CxNxA/w = (4 \times 10^{-10}) \times (2{,}314 + 579) \times (0.0224)/(10) = 2.59 \times 10^{-9}$$

For general aviation flights:

$$P1bfa = CxNxA/w = (1.55 \times 10\text{-}7) \times (1{,}860 + 465) \times (0.0214)/10 = 7.7 \times 10\text{-}7$$

Total local aircraft crash potential:

$$P1fa = P1afa + P1bfa = 2.59 \times 10\text{-}9 + 7.7 \times 10\text{-}7 = 7.72 \times 10\text{-}7$$

For commercial traffic flying on V-27 and not landing locally:

V-27 is a federal flight route from the Santa Barbara area northwest to the Big Sur area. Most of the aircraft on this route are normally flying at altitudes above 10,000 ft, with some smaller aircraft at elevations as low as 3,500 ft. Per the FAA Standards Office, the number of aircraft on this route is conservatively estimated at 20 per day or 7,300 per year. Using the same data as above and adjusting for the number of flights:

$$P2_{fa} = CxNxA/w = (4 \times 10^{-10}) \times (7{,}300) \times (0.0224)/(10) = 6.53 \times 10^{-9}$$

For military aircraft flying on VR-249:

VR-249 is a military training route, which requires 5 miles visibility and the ceilings above 3,000 ft. The aircraft may be traveling between sea level and 10,000 ft. The route is used very infrequently and is estimated to have approximately 50 flights a year. In the area of the Diablo Canyon ISFSI this route is provided for normal flight modes and is not expected to include any high-stress maneuvers. The majority of the aircraft flying this route over the past 12 months were F-18s. In addition, there have been a limited number of C-130, F-16 and EA6B aircraft and some helicopters using this route. For this calculation, N is conservatively taken to be 75 flights. The center of the route is approximately 2 miles off shore; therefore, (w) is conservatively set at 1 mile in this calculation. There was no data provided in the NUREG for military aircraft that would support this route and as a result the in flight crash probability for F-16s accepted in the Private Fuel Storage SER of 2.736×10^{-8} was used.

$$P3_{fa} = CxNxA/w = (2.736 \times 10^{-8}) \times (75) \times (0.0228)/(1) = 4.68 \times 10^{-8}$$

Military ordnance on aircraft on VR-249

Based on information provided by the Naval Air Station at Lemoore, which flies a majority of the flight on VR-249, aerial bombs are not carried. .However, because of recent events, other ordnance such as air-to-air missiles and cannon/machine guns might be carried on a very small number of the military aircraft on this route. Accidental firings of air-to-air missiles or aircraft guns have not been reported. In addition, air-to-air ordnance does not have a large explosive charge and would not be expected to cause major damage to non-aircraft targets.

VR-249 is a visual route, which requires a minimum of 5 miles of visibility and minimum ceilings of 3,000 ft. Aircraft using this route normally remain offshore and do not fly directly over the Diablo Canyon Power Plant or the Diablo Canyon ISFSI. Based on the type of ordnance the miniscule probability of an accidental discharge, and the visual requirements of the route the potential for any possible interaction between the ordnance and the ISFSI is not credible.

Summary of aircraft hazards

As stated above, and with the exception of the traffic related to VR-249, Morro Bay VOR and from V-27, the landing patterns and distance to the local airports would not significantly increase the probability of a crash at the ISFSI site. In addition, there are no designated airspaces, which are within the limits of Criterion 2 of NUREG-0800. As result, the total aircraft hazard probability at the Diablo Canyon ISFSI site is equal to the sum of the individual probabilities calculated above.

$$\text{Total} = P1_{fa} + P2_{fa} + P3_{fa} = (7.72 \times 10^{-7}) + (6.53 \times 10^{-9}) + (4.68 \times 10^{-8}) = 8.26 \times 10^{-7}$$

Based on the above calculation, the total aircraft hazard probability is determined to be approximately 8.26×10^{-7}, which is less than the threshold of 1×10^{-6} specified in the Private Fuel Storage SER for acceptable frequency of aircraft impact into a facility from all types of aircraft.

PG&E is aware the NRC is considering revising security regulations, which may affect aircraft hazard requirements relating to aircraft hazards. Following adoption of any new security regulations by the NRC, PG&E will comply with any such revised requirements as appropriate.

2.2.1.3.1 Estimates of Future Potential Hazards from Air Crashes

The projected growth of civilian flights can be based on Federal Aviation Administration (FAA) long-range forecast (FAA, 1999). This includes commercial aircraft operations for air carriers and commuter/air taxi takeoff and landings at all US towered and non-towered airports. In the FAA forecasts, that the commercial aircraft operations are projected to increase from 28.6 million in 1998 to 47.6 million in 2025. That results in a projected increase of 66 percent by 2025.

In addition, the annual number of general aviation operations at all towered and non-towered airports in the US is projected by the FAA to increase from 87.4 million in 1998 to 99.2 million in 2025. That results in a projected increase of 14 percent by 2025. Based on the above potential increases in traffic, the crash probability for local traffic on VR-27 would increase to 8.82×10^{-7} and for commercial traffic not landing locally to 1.08×10^{-8} by the year 2025.

The FAA also predicts that the military traffic will not increase appreciably, if at all in the foreseeable future. As a result the probability of a crash on VR 249 will remain at 5.6×10^{-8}.

Considering all of the FAA projections, the cumulative aircraft crash probabilities increases to 9.4×10^{-7} in 2025, which is still less than the threshold of 1×10^{-6} specified in the Safety Evaluation Report concerning the Provide Fuel Storage Facility, Docket No. 72-22, as an acceptable frequency for impact into the facility from all types of aircraft.

2.2.2 ONSITE POTENTIAL HAZARDS

2.2.2.1 Structures and Facilities

At the DCPP site, including the ISFSI storage site, there are no cooling towers or stacks with a potential for collapse. Therefore, such hazards need not be considered for any potential effects on the ISFSI.

There are 500-kV transmission lines that run in close proximity of the ISFSI storage site and on the hill above it (Figure 2.2-1). A 500-kV transmission line drop is postulated as a result of a transmission tower collapse or transmission line hardware failure near the ISFSI storage site and the cask transfer facility (CTF), as discussed on Section 8.2.8. The worst-case fault condition for a cask is that which places a cask in the conduction path for the largest current. This condition is the line drop of a single conductor of one phase with resulting single line-to-ground fault current and voltage-induced arc at the point of contact.

It is concluded that the postulated transmission line break will not cause the affected cask components to exceed either normal or accident condition temperature limits and that localized material damage at the point of arc on the shell of the overpack and transfer cask water jacket is bounded by accident conditions discussed in Sections 8.2.2 (tornado missile) and 8.2.11 (loss of shielding, HI-TRAC transfer cask water jacket). As a result of the considerations, it is apparent that the postulated transmission line break does not adversely affect the thermal performance of either system.

In addition to the 500-kV lines, the towers that support these lines were evaluated for any potential effect (Figure 2.2-1). They have been evaluated, and although the towers could fail as a result of a severe wind event, there would be no separation of the towers from their foundations, and the towers on the hillside would not have credible contact with the ISFSI storage site. However, the towers, which are located near the ISFSI storage site could, in these events, collapse and strike either the MPC while at the CTF or the loaded overpacks stored on the pads. As a result, as discussed in Section 8.2.16, this impact potential has been evaluated, and it does not adversely affect the MPC or the loaded overpacks.

2.2.2.2 Hazards from Fires

The ISFSI or the fuel storage systems have no credible exposure to fires caused by offsite transportation accidents, pipelines, or manufacturing facilities because of the distance to these transportation routes and the lack of facilities in the proximity of the site. However, there are onsite sources that were evaluated.

Fires are classified as human-induced or natural phenomena design events in accordance with ANSI/ANS 57.9, Design Events III and IV (Reference 3). To identify sources and to establish a conservative design basis for onsite exposure, a walkdown was performed of the CTF, ISFSI storage site, and the complete transportation route from the FHB/AB to the CTF and ISFSI storage site. Based on that walkdown, the following fire events are postulated:

(1) Onsite transporter fuel tank fire

(2) Other onsite vehicle fuel tank fires

(3) Combustion of other local stationary fuel tanks

(4) Combustion of other local combustible materials

(5) Fire in the surrounding vegetation

(6) Fire from mineral oil from the Unit 2 transformers

The potential for fire is addressed for both the HI-STORM 100 overpack and the HI-TRAC transfer cask. Locations where the potential for fire is addressed include the ISFSI storage pad; the area immediately surrounding the ISFSI storage pad, including the CTF; and along the transport route between DCPP and the ISFSI storage pad. These design-bases fires and their evaluations are detailed in Section 8.2.5. This section also discusses various administrative controls to ensure that any fire cannot exceed a design basis for the transfer and storage cask. These administrative controls are further defined in Section 8.2.5 and the evaluations done in support of that section.

For the evaluation of the onsite transporter and other onsite vehicle fuel tank fires (Events 1 and 2), it is postulated that the fuel tank is ruptured, spilling all the contained fuel, and the fuel is ignited. The fuel tank capacity of the onsite transporter is limited to a maximum of 50 gallons of fuel. The maximum fuel tank capacity for other onsite vehicles in proximity to the transport route and the ISFSI storage pads is assumed to be 20 gallons. As discussed in Section 8.2.5, the results of the Holtec analyses for transporter fuel tank rupture fire indicate that neither the storage cask nor the transfer cask undergoes any structural degradation and that only a small amount of shielding material (concrete and water) is damaged or lost. This analysis bounds the 20-gallon onsite vehicle fuel tank fire (Event 2).

The location of any transient sources of fuel in larger volumes, such as tanker trucks, will be administratively controlled to provide a sufficient distance from the CTF , and transport route during transport operations to ensure the total energy received is less than the design-basis fire event. As discussed in Section 8.2.5 an analysis was performed for a ruptured 2000-gallon gasoline tanker truck and determined that it does not result in exceeding the design basis of the storage casks.

All onsite stationary fuel tanks (Event 3) are at least 100 ft from the nearest storage cask, the transport route, and the CTF (Figure 2.2-1). Therefore, there is at least a 100-ft clearance between combustible fuel tanks and the nearest cask in transport, at the CTF, or on the ISFSI storage pads. These existing stationary tanks have been evaluated, but due to their distances to the transport route or the storage pads, the total energy received by the storage cask or the transporter is insignificant compared to the design basis fire event. These tanks will be periodically filled by standard tanker trucks with a capacity of three to four thousand gallons. As discussed in Section 8.2.5, the location of any tanker truck will be administratively controlled to ensure the total energy potentially received at the ISFSI is less than the design basis event. In addition, during transport operations, all filling will be suspended and these gasoline tanker trucks, will not be allowed within the owner-controlled area. This will be administratively controlled in accordance with the Diablo Canyon ISFSI Technical Specification Cask Transportation Evaluation Program.

For the ISFSI site, the restricted area not covered by the storage pads will be covered with crushed rock approximately 12 inches deep. The outer fence will be separated from the inner fence by a distance of approximately 20 ft. The isolation zone (i.e., the region between the fences) will also be covered with crushed rock approximately 12 inches deep. A maintenance program will control any significant growth of vegetation through the crushed rock. Therefore, the surface of the restricted area will be noncombustible.

No combustible materials will be stored within the security fence around the ISFSI storage pads at any time. In addition, prior to any cask operation involving fuel transport, a walkdown of the general area and transportation route will be performed to assure all local combustible materials (Event 4), including all transient combustibles, are controlled in accordance with administrative procedures.

The native vegetation (Event 5) surrounding the ISFSI storage pad is primarily grass, with no significant brush and no trees. Maintenance programs will prevent uncontrolled growth of the surrounding vegetation. As discussed in Section 8.2.5, a conservative fire model was established for evaluation of grass fires, which has demonstrated that grass fires are bounded by the 50-gallon transporter fuel tank fire evaluation.

The potential fire from mineral oil in the Unit 2 transformers (Event 6) has been evaluated in Section 8.2.5 and found to be bounded by the design basis fire.

In summary, as discussed in Section 8.2.5, the potential effects of any of these postulated fires have been found to be insignificant or acceptable. The physical layout of the Diablo Canyon ISFSI and the administrative controls on fuel sources ensure that the general design criteria related to fire protection specified in 10 CFR 72.122(c) are met (Reference 4).

2.2.2.3 Onsite Explosion Hazards

The storage site has no credible exposure to explosion caused by transportation accidents, pipelines, or manufacturing facilities because of the distance to these transportation routes and the lack of facilities in the proximity of the site. However, there are potential onsite hazards that must be evaluated.

Explosions are classified as human-induced or natural phenomena design events in accordance with ANSI/ANS 57.9 Design Events III and IV. To determine the potential explosive hazards, which could affect the ISFSI or the fuel transportation system, a walkdown of the ISFSI storage area and the transportation route from the FHB/AB was completed. The following explosion sources and event categories have been identified and evaluated in Section 8.2.6:

(1) Detonation of a cask transporter or an onsite vehicle fuel tank

(2) Detonation of propane bottles transported past the ISFSI storage pad

(3) Detonation of compressed gas bottles transported past the ISFSI storage pad

(4) Detonation of large stationary fuel tanks in the vicinity of the transport route

(5) Explosive decompression of a compressed gas cylinder

(6) Detonation of the bulk hydrogen storage facility

(7) Detonation of acetylene bottles stored on the east side of the cold machine shop

Figure 2.2-1 shows the location of the stationary potential sources (sources 4, 6 and 7). Events 1, 2, 3, and 5 are assumed to occur in the vicinity of the ISFSI storage pads, CTF, or transport route and potentially affect both the loaded overpack and the transfer cask. Events 4 through 7 occur in the vicinity of the transport route and affect the transfer cask. This section also discusses various administrative controls to ensure that any potential explosion hazards will meet the Regulatory Guide 1.91 criteria or methodologies. These administrative controls are further defined in Section 8.2.6 and the evaluations done in support of that section.

In all of the above evaluations, the effect on the loaded overpacks or transport cask are either minimal or not credible, and there will be no loss of function. For Events 1 through 3, as discussed in Section 8.2.6, the risk of exceeding the Regulatory Guide 1.91 overpressure criterion of 1 psi is not significant. In addition the transportation practices and the physical distance to the storage pads, CTF, or transporter are controlled by administrative procedures. For Event 4, the distance of the existing fuel tanks from the transportation route precludes any effect on the transportation of the spent fuel to the storage pads or CTF. Event 5 concerns decompression of gas cylinders and the possible missile damage to the transfer cask and overpack. The evaluation performed in Section 8.2.6 shows that this is not a credible event and that there would be no significant damage or loss of function by this event. Event 6 involves the transportation of the transfer cask past a potential hydrogen explosion hazard (Figure 2.2-1). Section 8.2.6 discusses the evaluation that was performed for this event. The evaluation shows that the probability of a detonation at the moment the transporter is in the vicinity is so small that it is not credible per the guidelines of Regulatory Guide 1.91. Event 7 was evaluated in Section 8.2.6 where it is shown that the detonation of the acetylene bottles stored on the east side of the cold machine shop was not a credible event based on configuration, restraints, and lack of an ignition source.

Also under Event 1, it not only refers to an average 20-gallon vehicle fuel capacity, but also a 2,000-gallon gasoline tanker truck that transports fuel near the ISFSI facility. This truck will only be in this area momentarily while passing by the ISFSI facility and will be under administrative controls for its speed and continued movement through the area on its way to and from the vehicle maintenance shop that is located approximately 2,000 ft northeast of the ISFSI pad. As discussed in SAR 8.2.6, a probabilistic risk assessment was performed and it was determined, based on the use of administrative controls and the restriction for movement and stopping within the separation distance calculated based on the 1 psi Regulatory Guide 1.91 criterion, that the risk is insignificant.

The Cask Transportation Evaluation Program will be developed, implemented, and maintained to ensure that no additional hazards are introduced either at the storage pads, CTF, or on the transportation route during onsite transport of the loaded overpacks or transfer cask. That program will include limitation on hazards and will require a transportation route walkdown prior to any movement of the transporter with nuclear fuel between the FHB/AB and the CTF, and between the CTF and the storage pads. The walkdown will require the evaluation or removal of any identified hazards prior to the movement of the transporter. The program will also control all movement of vehicles or activities during onsite transport that could have an adverse effect on the loaded overpacks or transfer cask.

2.2.2.4 Chemical Hazards

A walkdown of all chemical hazards was performed in the ISFSI storage pad and CTF areas, and along the transportation route. Chemical hazards were identified that could have an effect on the ISFSI or the transportation system. To ensure minimum potential for chemical hazards, the administrative program provided to control fire and explosive hazards will also include identification, control, and evaluation of hazardous chemicals.

2.2.3 SUMMARY

In summary, there are no credible accident scenarios involving any offsite industrial, transportation, or military facilities in the area around the DCPP site that will have any significant adverse impact on the ISFSI. In addition, there are no potential onsite fires, explosions, or chemical hazards that would have a significant impact on the ISFSI.

2.2.4 REFERENCES

1. Regulatory Guide 1.91, Evaluations of Explosions Postulated to Occur on Transportation Routes near Nuclear Power Plants, US Nuclear Regulatory Commission, February 1978.

2. Standard Review Plan for the Review of Safety Analysis Reports for Nuclear Power Plants, USNRC, NUREG-0800, July 1981.

3. ANSI/ANS 57.9, 1992, Design Criteria for an Independent Spent Fuel Storage Installation (Dry Storage Type), American National Standards Institute.

4. 10 CFR 72, Licensing Requirements for the Independent Storage of Spent Nuclear Fuel and High-Level Radioactive Waste.

5. DOE-STD-3014-96 Accident Analysis for Aircraft Crash Into Hazardous Facilities, US Department of Energy, October 1996.

2.3 METEOROLOGY

The meteorology of the Diablo Canyon area is described in Section 2.3 of the DCPP FSAR Update. Information in the FSAR Update includes discussion of the regional climatology, local meteorology, topographical information, onsite meteorological measurement program, and diffusion estimates for the Diablo Canyon owner-controlled area, which includes the ISFSI site. Relevant tables and figures supporting the discussion are included in the FSAR Update.

Meteorological conditions for the ISFSI site are expected to be the same as for DCPP since the ISFSI site is located approximately 0.22 miles and slightly uphill from the DCPP facilities. No significant changes in climate or meteorological characteristics can occur within such a short distance and, thus, existing meteorological measurements for DCPP are expected to be equally applicable to the ISFSI. Diffusion estimates at the ISFSI site are provided in Section 2.3.4.

The FSAR Update is maintained up to date by PG&E through periodic revisions made in accordance with 10 CFR 50.71(e). Hence, the information contained in the FSAR Update is current, and no further revision is necessary for applicability to the ISFSI. Therefore, in accordance with the guidance of Regulatory Guide 3.62, material from Section 2.3 of the FSAR Update is incorporated herein by reference in support of the ISFSI license application. The following paragraphs provide a brief summary of various discussions from Section 2.3 of the FSAR Update.

2.3.1 REGIONAL CLIMATOLOGY

The climate of the area is typical of the central California coastal region and is characterized by small diurnal and seasonal temperature variations and scanty summer precipitation. The prevailing wind direction is from the northwest, and the annual average wind speed is about 10 mph. In the dry season, which extends from May through September, the Pacific high-pressure area is located off the California coast, and the Pacific storm track is located far to the north. Moderate to strong sea breezes are common during the afternoon hours of this season while, at night, weak offshore drainage winds (land breezes) are prevalent. There is a high frequency of fog and low stratus clouds during the dry season, associated with a strong low-level temperature inversion.

The mountains that extend in a general northwest-to-southeast direction along the coastline affect the general circulation patterns. This range of mountains is indented by numerous canyons and valleys, each of which has its own land-sea breeze regime. As the air flows along this barrier, it is dispersed inland by the valleys and canyons that indent the coastal range. Once the air enters these valleys and canyons, it is controlled by the local terrain features.

The annual mean number of days with severe weather conditions, such as tornadoes and ice storms at west coast sites, is zero. Thunderstorms and hail are also rare phenomena, the average occurrence being less than 3 days per year. The maximum-recorded precipitation in the San Luis Obispo region is 5.98 inches in 24 hours at San Luis Obispo. The 24-hour maximum occurred on March 4, 1978.

The maximum-recorded annual precipitation at San Luis Obispo was 54.53 inches during 1969. The average annual precipitation at San Luis Obispo is 21.53 inches. There are no fastest mile wind speed records in the general area of Diablo Canyon, surface peak gusts at 46 mph have been reported at Santa Maria, California, and peak gusts of 84 mph have been recorded at the 250 ft level at the Diablo Canyon site.

The monthly average temperatures for San Luis Obispo from 1948 to 2000 are provided in Table 2.3-1.

2.3.2 LOCAL METEOROLOGY

The average annual temperature at the ISFSI site is approximately 55°F (based on measurements made at the DCPP primary meteorological tower). Generally, the warmest mean monthly temperature occurs in October, and the coldest mean monthly temperature occurs in December. The highest hourly temperature, as recorded at one of the recording stations, is 97°F in October 1987, and Diablo Canyon experienced below-freezing temperatures in December 1990 for several hours. Essentially no snow or ice occurs at the ISFSI site.

Solar radiation data considered representative of the Diablo Canyon ISFSI site is collected by the California Irrigation Management Information System (CIMIS), Department of Water Resources, at the California Polytechnic State University in San Luis Obispo, California. The CIMIS collection site is about 12 miles northeast of the Diablo Canyon ISFSI site. For a period of record between May 1, 1986 and December 31, 1999, the maximum measured incident solar radiation (insolation) values at the CIMIS site were 766 g-cal/cm^2 per day for a 24-hour period and 754 g-cal/cm^2 per day for a 12-hour period, both on June 1, 1989. The daily (24-hour) average for the period of record was 430 g-cal/cm^2 per day. For the Diablo Canyon ISFSI site, the insolation values would likely be lower than the CIMIS values because of more frequent fog in the ISFSI area.

The average annual precipitation at the DCPP site is approximately 16 inches. The highest monthly total recorded between 1967 and 1981 was 11.26 inches. The greatest amount of precipitation received in a 24-hour period was 3.28 inches. These maxima were recorded in January 1969 and March 1978, respectively. The maximum hourly amount recorded in the Diablo Canyon area during the same period is 2.35 inches.

The highest recorded peak wind gust at the primary meteorological tower is 84 mph, and the maximum-recorded hourly mean wind speed is 54 mph. Persistence analysis of wind directions in the Diablo Canyon area shows that, despite the prevalence of the marine inversion and the northwesterly wind flow gradient along the California coast, the long-term accumulation of emissions in any particular geographical area downwind is virtually impossible. Pollutants injected into the marine inversion layer of the coastal wind regime are transported and dispersed by a complex array of land-sea breeze regimes that exist all along the coast wherever canyons or valleys indent the coastal range.

Topographical influences on both short-term and long-term diffusion estimates are pronounced in that the ridge lines east of the ISFSI location extend at least to the average height of the marine inversion base. The implications of this barrier are:

(1) Any material released that is diverted along the coastline will be diluted and dispersed by the natural valleys and canyons, which indent the coastline.

(2) Any material released that is transported over the ridgeline will be distributed through a deep layer because of the enhanced vertical mixing due to topographic features.

2.3.3 ONSITE METEOROLOGICAL MEASUREMENT PROGRAM

The current onsite meteorological monitoring system supporting DCPP operation will serve as the onsite meteorological measurement program for the ISFSI. The system consists of two independent subsystems that measure meteorological conditions and process the information into useable data. The measurement subsystems consist of a primary meteorological tower and a backup meteorological tower. The program has been designed and continually updated to conform with Regulatory Guide 1.23.

A supplemental meteorological measurement system is also located in the vicinity of DCPP. The supplemental system consists of two Doppler acoustic sounders and six tower sites. Data from the supplemental system are used for emergency response purposes to access the location and movement of any radioactive plume.

2.3.4 DIFFUSION ESTIMATES

For ISFSI dose calculations required by 10 CFR 72.104, (normal operations and anticipated occurrences), site boundary χ/Q values range from 9.2×10^{-8} to 3.4×10^{-6} sec/m^3 and nearest residence χ/Q values range from 2.0×10^{-8} to 4.2×10^{-7} sec/m^3. These values are taken from Table 11.6-13 of the DCPP FSAR Update and have been determined to be applicable to the ISFSI site. They will be used, as appropriate, for dose calculations related to normal operations and anticipated occurrences.

Compliance with 10 CFR 72.106 requires calculation of design basis accident doses at the controlled area boundary (site boundary for the Diablo Canyon ISFSI), which is about 400 meters from the ISFSI at its closest point. Based on information from the DCPP FSAR Update, Section 2.3.4 and Table 2.3-41, a χ/Q of 4.5×10^{-4} sec/m^3 has been determined to be a conservative estimate applicable to the ISFSI site and will be used for accident dose calculations.

2.4 SURFACE HYDROLOGY

Hydrologic information pertaining to the Diablo Canyon area in general has been documented in the DCPP FSAR Update (Reference 1). Much of this information pertains also to the ISFSI location since the hydrologic characteristics in the Diablo Canyon area do not vary significantly in the general vicinity of the ISFSI and power plant facilities. Specific features relevant to hydrologic engineering at the ISFSI location are described in this section, with reference to supporting information in the FSAR Update where appropriate.

2.4.1 HYDROLOGIC DESCRIPTION

The topography and an outline of the drainage basin in the region surrounding the ISFSI site are shown in Figure 2.4-1. This map is reproduced from the US Geological Survey (USGS) Port San Luis and Pismo Beach 7.5-minute topographic quadrangles. The basin drains to Diablo Creek, which discharges into the Pacific Ocean. Figure 2.4-2 shows the Diablo Creek drainage basin to a larger scale. The basin encompasses approximately 5 square miles and is bounded by ridges reaching a maximum elevation of 1,819 ft above mean sea level (MSL) at Saddle Peak, located approximately 2 miles to the east of the ISFSI.

The hydrologic characteristics of the ISFSI site are influenced by the Pacific Ocean on the west and by local storm runoff collected from the basin drained by Diablo Creek. The maximum and minimum flows in Diablo Creek are highly variable. Average flows tend to be nearer the minimum flow value of 0.44 cfs. Maximum flows reflect short-term conditions associated with storm events. Usually within 1 or 2 days following a storm, flows return to normal. Flows during the wet season (October-April) vary daily and monthly. Dry season flows are sustained by groundwater seepage and are more consistent from day to day, tapering off over time. There is no other creek or river within the site area or the drainage basin.

Water is supplied to DCPP from three sources: Diablo Creek, two site wells, and an ocean water desalinization plant that has been used since 1985. The Diablo Creek collection point is located upstream and to the east of the 500-kV switchyard.

2.4.2 FLOODS

The DCPP FSAR Update addresses flood considerations pertinent to the power plant facilities at Diablo Canyon. The following discussion identifies flood considerations from the FSAR Update that are pertinent to the ISFSI location. Topography and ISFSI site structures limit flood design considerations to local floods from Diablo Creek. The canyon confining Diablo Creek will remain intact and is more than sufficient to channel any conceivable flood without any hazard to the ISFSI. Channel blockage from any landslides downstream of the ISFSI location and to an extent sufficient to flood the ISFSI area is not possible because of the topographic location and elevation of the ISFSI.

There are no dams or natural features in Diablo Creek that would hinder or retain runoff for a significant period of time. At the ISFSI, runoff can be efficiently drained by the adjacent natural and constructed drainage features.

If the culverts and drainage out of the ISFSI area become plugged during periods of high precipitation, water may locally and temporarily pond. Drainage in the vicinity of the ISFSI is shown in Figure 2.4-3. No significant ponding should occur since, due to the open terrain and location, any additional runoff into the ISFSI area will drain away from the facility toward Diablo Creek or the ocean. No adverse impact is expected on ISFSI operation or spent fuel confinement.

Two water reservoirs constructed in rock and located in the vicinity of the ISFSI maintain redundant water supplies in support of operation of Units 1 and 2. If the reservoirs were to overflow due to an unlikely accumulation of runoff from high precipitation, the local topography would cause water to drain toward the creek and ocean. No adverse impact on the ISFSI would be expected from overflow of the reservoirs.

2.4.3 PROBABLE MAXIMUM FLOOD (PMF) ON STREAMS AND RIVERS

Diablo Creek is the only significant channel for the drainage basin within which the ISFSI is located. This drainage basin includes approximately 5.2 square miles. The potential PMF upstream of the location of the power plant facilities was found to have a peak discharge of approximately 6,900 cfs, with a total volume of approximately 4,300 acre-ft for a 24-hour storm.

As documented in the DCPP FSAR Update, the drainage capacity of Diablo Creek through this area is more than sufficient to efficiently channel the PMF volume directly into the Pacific Ocean with no retention time. This volume of water discharged from the Diablo Creek basin will not cause any local flooding around the power plant or overtop the switchyards, even if the 10-ft diameter culvert passing under the switchyards were to temporarily plug. If the culvert were plugged, any water impounded east of the 500-kV switchyard would be discharged along Diablo Creek Road (elevation of approximately 250 ft MSL opposite the ISFSI) and through the stilling basin located between the switchyards. The floodwaters would pass through the diversion scheme with adequate freeboard near each switchyard, on the opposite side of the canyon, and below the elevation of the ISFSI (310 ft MSL). The water released would not cause any flooding of the ISFSI.

2.4.4 POTENTIAL DAM FAILURES (SEISMICALLY INDUCED)

There are no dams in the watershed area. Outside the watershed area, any seismic-induced failure of dams would not affect the ISFSI.

2.4.5 PROBABLE MAXIMUM SURGE AND SEICHE FLOODING

Due to the elevation of the ISFSI, there is no credible scenario that would create any flooding from a maximum surge or seiche.

2.4.6 PROBABLE MAXIMUM TSUNAMI FLOODING

Due to the elevation of the ISFSI, a maximum tsunami would not cause any flooding to the ISFSI.

The maximum combined wave runup from a distantly generated tsunami is 30 ft (Reference 1, Section 2.4.6.1.3), and the maximum combined wave runup for near shore tsunamis is 34.6 ft relative to a mean lower low water (MLLW) reference datum (Reference 1, Section 2.4.6.1.4). This is significantly lower than the elevation of the Diablo Canyon ISFSI site at 310 ft above mean sea level (MSL) (312.6 ft above MLLW) or the transporter route at 80 ft above MSL.

Additional data and analysis related to the maximum possible tsunami are provided in Reference 2 (PG&E Response to NRC Question 2-14).

2.4.7 ICE FLOODING

Flooding due to ice melt events is not credible because of the mild climate and infrequency of freezing temperatures in the region.

2.4.8 FLOOD PROTECTION REQUIREMENTS

No cooling water canals, reservoirs, rivers or streams are used in operation of the ISFSI. There are no channel diversions in the region that can alter any water flow patterns so as to affect the ISFSI. Hence, low flow conditions need not be considered.

Based on these considerations, there are no credible hydrological scenarios that can adversely affect the ISFSI. Thus, specialized hydrological engineering considerations and flood protection requirements for the ISFSI facilities are not necessary. Only typical grading and drainage provisions for storm runoff are needed.

2.4.9 ENVIRONMENTAL ACCEPTANCE OF EFFLUENTS

SAR Section 3.3.1.7.2 indicates that there are no radioactive wastes created by the HI-STORM 100 System while in storage at the storage pads, transport to or from the CTF, or at the CTF.

Environmental Report Sections 2.5, 4.1, and 4.2 address the environmental effects of potential effluents from the ISFSI. It is concluded that surface runoff from the ISFSI has no radioactive contamination and will not adversely affect the surrounding ecosystem.

Diablo Creek is the only source of surface water other than ocean water used at DCPP for support of power plant operation. No water is used to support ISFSI operation. Potable water used to support ISFSI administration is provided by existing systems at DCPP. Such support of ISFSI administrative activities will be provided according to plant procedures. No other significant surface or groundwater sources exist or are used in this area. There is no public use of any surface waters or groundwater from the Diablo Canyon site. Therefore, no detailed analysis of acceptance of effluents by surface waters or groundwater due to ISFSI operation is relevant.

2.4.10 REFERENCES

1. PG&E, Units 1 and 2 Diablo Canyon Power Plant, Final Safety Analysis Report Update, Revision 14, November 2001.

2. PG&E Letter DIL-02-009 to the NRC, Response to NRC Request for Additional Information for the Diablo Canyon ISFSI Application, October 15, 2002.

2.6 GEOLOGY AND SEISMOLOGY

The Diablo Canyon Independent Spent Fuel Storage Installation (ISFSI) will be located directly inland from the power plant on a graded bedrock hillslope adjacent to the DCPP raw water reservoir (Figure 2.6-1). It was desirable to select a site having bedrock properties and earthquake response characteristics comparable to those of the bedrock beneath the Diablo Canyon power block, such that existing DCPP design-basis ground motions could be used in the design of the ISFSI.

In this section, the geologic and seismologic conditions in the region are described and evaluated. Detailed information is provided regarding the earthquake vibratory ground motions, foundation characteristics, and slope stability at the ISFSI and CTF sites. Information regarding foundation characteristics and slope stability also is provided for the transport route between the power block and the CTF. The information is in compliance with the criteria in Appendix A of 10 CFR 100, and 10 CFR 72.102, and meets the format and content recommendations of Regulatory Guide 3.62. Several commercial technical computer software programs were used to assist in the analyses performed for Section 2.6.

An external, independent Seismic Hazards Review Board advised on the studies carried out for this section of the licensing submittal. A letter summarizing the conclusions of the consulting board is provided in Reference 1, as are the names and affiliations of the project team responsible for preparation of this section.

Definitions

For the purposes of Section 2.6, the following definitions and boundaries were used to describe the ISFSI study area and plant site region, as illustrated on Figure 2.6-1 (definitions of other terms used in this report are in the glossary at the front of the report):

- plant site region: the area of the Irish Hills and vicinity within a 10-mile radius of the Diablo Canyon ISFSI

- plant site area: the area within the DCPP boundary

- ISFSI study area: the area extending along the nose of the ridge behind the power plant and encompassing the ISFSI site and CTF site

Conclusions

Geologic, seismologic, and geotechnical investigations for the ISFSI yielded the following conclusions:

- The ISFSI will be founded on bedrock that is part of the same continuous, thick sequence of sandstone and dolomite beds upon which the DCPP power block is sited. The shear wave velocity characteristics of the rock at the ISFSI and CTF sites are within the same range as those at the power block. Additionally, the ISFSI and CTF sites are approximately the same distance from the Hosgri fault zone, the controlling earthquake source for the DCPP. Thus, the foundation conditions and ground-motion response characteristics are the same as those at the DCPP (discussed in Section 2.6.1.10).

- Because the ground-motion response characteristics at the ISFSI are the same as those at the DCPP, the DCPP earthquake ground motions are appropriate for use in the licensing of the ISFSI, in accordance with 10 CFR 72.102(f) (discussed in Section 2.6.2).

- Because ISFSI pad sliding, slope stability, and the stability of the transporter are affected by longer-period ground motions than those characterized by the DCPP ground motions, response spectra having a longer-period component were developed. The longer-period component conservatively incorporates the near-fault effects of fault rupture directivity and fling. These spectra, referred to as the ISFSI long-period ground motions (ILP), and associated time histories, were used to analyze elements that may be affected by longer-period ground motions (discussed in Section 2.6.2.5).

- Several minor bedrock faults were observed at the ISFSI and CTF sites. These minor faults are not capable; hence, there is no potential for surface faulting at the ISFSI or CTF sites (discussed in Section 2.6.3).

- The sandstone and dolomite bedrock, including zones of friable rock, that underlies the ISFSI and CTF sites area is stable, and has sufficient capacity to support the loads imposed by the ISFSI pads and casks and the CTF without settlement or differential movement (discussed in Section 2.6.4).

- There are no active landslides or other evidence of existing ground instability at the ISFSI and CTF sites, or on the hillslope above the ISFSI site (discussed in Section 2.6.1.12).

- The stability of the hillslope and the slopes associated with the pads, CTF, and transport route under static and seismic conditions was analyzed using conservative assumptions regarding slope geometry, material properties, seismic inputs, and analytical procedures (discussed in Section 2.6.5). The analyses show that the slopes have ample factors of safety under static conditions. The cutslope above the ISFSI site may experience local wedge movements or small displacements if exposed to the design-basis earthquakes. Mitigation measures to address these movements are described in Sections 4.2.1.1.9.1 and 4.2.1.1.9.2.

- The transport route follows existing paved roads, except for a portion of the route that will be constructed to avoid a landslide at Patton Cove along the coast. The route will have foundation conditions satisfactory for the transporter (discussed in Section 4.3.3). Small debris flows could potentially close portions of the road during or immediately following severe weather (discussed in Section 2.6.5.4). Because the transport route will not be used during severe weather, the flows will not be a hazard to the transporter.

2.6.1 GEOLOGIC, SEISMOLOGIC AND GEOTECHNICAL INVESTIGATIONS

Extensive geologic, seismologic and geotechnical investigations were performed to characterize the ISFSI and CTF sites. These investigations included compilation and review of pre-existing information developed for construction of the power plant, the raw water reservoir, and the 230-kV and 500-kV switchyards, as well as extensive detailed investigations performed in the ISFSI study area. These investigations are described in References 2 and 3. The investigations focused on collecting information to address four primary objectives:

- to evaluate foundation properties beneath the ISFSI pads, the CTF facility, and the transport route

- to evaluate the stability of the proposed cutslopes and existing hillslope above the ISFSI pads and along the transport route

- to identify and characterize bedrock faults at the site

- to compare bedrock conditions at the ISFSI site with bedrock conditions beneath the DCPP power block for the purpose of characterizing earthquake ground motions

Investigations in the plant site area included interpretation of aerial photography, review of existing data and literature, and field reconnaissance. In particular, borehole and trench data collected in the 1960s and 1970s for the power plant were compiled, reviewed, and used to evaluate stratigraphic conditions beneath the power block and between the power block and the ISFSI site.

Investigations in the ISFSI study area and along the transport route were conducted to develop detailed information on the lithology, structure, geometry, and physical properties of bedrock beneath the ISFSI and CTF sites, and beneath the transport route. Investigations of the ISFSI and CTF site geology included 17 borings at 14 locations, 22 trenches and test pits, a seismic refraction survey, down-hole geophysics and televiewer surveys, petrographic analysis of rock samples, laboratory analysis of soil and rock properties, and detailed surface mapping (Reference 3). These data were used to develop a detailed geologic map of the plant site area, the ISFSI study area and transport route, and 12 geologic cross sections to illustrate the subsurface distribution of bedrock lithology and structure (Reference 37).

2.6.1.1 Existing Geologic, Seismologic, and Geotechnical Information

Existing geologic, seismologic, and geotechnical information includes that collected for licensing the operating DCPP, construction of the raw water reservoir, and construction of the 230-kV and 500-kV switchyards. Regional and site-specific geologic, seismologic and geotechnical investigations at the DCPP site are documented in Sections 2.5.1 and 2.5.2 of the DCPP Final Safety Analysis Report (FSAR) Update, submitted in support of continued operation of Units 1 and 2 (Reference 4). In response to License Condition Item 2.C.(7) of the Unit 1 Operating License DPR-80, issued in 1980, PG&E was required to reevaluate the seismic design bases for the DCPP. This reevaluation became known as the Long Term Seismic Program (LTSP). The program was conducted between 1985 and 1991. In June 1991, the Nuclear Regulatory Commission (NRC) issued Supplement Number 34 to the Diablo Canyon Safety Evaluation Report (Reference 5), in which the NRC concluded that PG&E had satisfied License Condition Item 2.C.(7). The LTSP evaluations are docketed in the LTSP Final Report (Reference 6) and the Addendum to the Final Report (Reference 7). The information presented herein summarizes and refers to the DCPP FSAR Update and LTSP reports.

Existing regional and site-specific geologic, seismologic and geotechnical information for the ISFSI is discussed in the following docketed references:

Regional physiography:	DCPP FSAR Update, Section 2.5.1.1.1
Geologic setting:	DCPP FSAR Update, Section 2.5.1.1.2.1 LTSP Final Report, Chapter 2
Tectonic features:	DCPP FSAR Update, Sections 2.5.1.1.2.2 and 2.5.1.1.2.3 LTSP Final Report, Chapter 2
Geologic history:	DCPP FSAR Update, Section 2.5.1.1.3 LTSP Final Report, Chapter 2
Regional geologic structure and stratigraphy:	DCPP FSAR Update, Sections 2.5.1.1.4 and 2.5.1.1.5 LTSP Final Report, Chapter 2
Geologic structure and stratigraphy of the plant site area:	DCPP FSAR Update, Section 2.5.1.2 LTSP Final Report, Chapter 2
Slope stability of the plant site area:	Slope Stability Report

Earthquake history and association of earthquakes with geologic structures:	DCPP FSAR Update, Sections 2.5.2.5 and 2.5.2.6 LTSP Final Report, Chapter 2
Maximum earthquakes affecting the plant site area:	DCPP FSAR Update, Section 2.5.2.9 LTSP Final Report, Chapter 3
Earthquake ground accelerations and response spectra:	DCPP FSAR Update, 2.5.2.10 and 3.71 LTSP Final Report, Chapter 4

The ISFSI is sited on a bedrock slope that was previously used as a source of fill materials for construction of the 500-kV and 230-kV switchyards. The first geologic and geotechnical studies in the area were performed by Harding Miller Lawson & Associates (HML) (Reference 9). The study was conducted prior to the borrow excavation to obtain information regarding the excavatability and suitability of the site materials for switchyard fills. Their investigations included borings, test pits, and refraction surveys. The depth of their explorations, however, was limited to the depth of the planned (and as-built) borrow excavation, and did not extend below the present post-excavation site elevations. All the material investigated by HML was removed during the borrow excavation and used for construction of the switchyard fills.

In addition, an assessment of slope stability near the DCPP was performed following the heavy winter storms of 1996-1997 (Reference 8). This report includes a map of landslides in the plant site area, and a slope stability analysis of the natural hillslope and cutslope between the power plant and the ISFSI.

2.6.1.2 Detailed ISFSI Study Area Investigations

Additional detailed geologic, seismic, and geotechnical studies were performed in the ISFSI study area. References 2 and 3 further describe the method, technical approach, and results of the detailed studies. The following field, office, and laboratory investigations were performed:

Activity	Documented in
Interpretation of 1968 aerial photography, by PG&E Geosciences Department (Geosciences) and William Lettis & Associates, Inc. (WLA)	Reference 37
Evaluation of previous geologic investigations in the power plant area, including borings by HML and others, by Geosciences and WLA	Reference 37
Detailed geologic mapping of structures and lithology, by Geosciences and WLA	Reference 37

Activity	Documented in
Analysis of rock mass strength, by Geosciences and WLA	Reference 37
Evaluation of rock fractures, by Geosciences and WLA	Reference 37
Analysis of potential rock slope stability, by Geosciences, WLA, and Geomatrix Consultants	References 38 thru 42
Geologic mapping of the power plant site and ISFSI study area, by WLA	Reference 43, Data Report A
Drilling and logging of 17 exploratory diamond-core borings at 14 locations at and near the ISFSI and CTF sites, by WLA	Reference 44, Data Report B
Implementation of two surface seismic refraction lines to measure compressional wave and shear wave velocities of shallow bedrock across the ISFSI site, by GeoVision	Reference 45, Data Report C
Suspension logging of compression and shear wave velocities from boreholes 98BA-1, -3 and -4, by GeoVision	Reference 45, Data Report C
Excavation and logging of 22 exploratory trenches at 14 locations to expose bedrock structures and lithology at the ISFSI site, by WLA	Reference 46, Data Report D
Natural gamma and caliper logging of borings 00BA-1 and -2, and optical televiewer imaging of all borings drilled in 2000 and 2001, by NORCAL Geophysical Consultants	Reference 47, Data Report E
Compilation of discontinuity data, by WLA	Reference 48, Data Report F
Soil testing of clay beds, by Cooper Testing Laboratories	Reference 49, Data Report G
Characterization of rock mass strength, by WLA	Reference 50, Data Report H
Rock strength testing of representative core samples, by GeoTest Unlimited	Reference 51, Data Report I
Petrographic analyses and x-ray diffraction testing of rock samples, by Spectrum Petrographics, Inc.	Reference 52, Data Report J
X-ray diffraction testing and petrographic analysis of clay beds, by Schwein/Christensen Laboratories, Inc.	Reference 53, Data Report K

2.6.1.3 General Description of the ISFSI Study Area

The location and topography of the ISFSI and CTF sites and the transport route are shown in Figures 2.6-1, 2.6-2, and 2.6-3. Detailed investigations of the seismotectonic setting performed for the LTSP (Reference 6, Chapter 2) show that the plant site area lies along the active tectonic boundary between the Pacific and North American plates in coastal Central California. It is located within the San Andreas fault system, about 48 miles west of the main San Andreas fault, and about 3 miles east of the offshore Hosgri fault zone. Current tectonic activity in the region is dominated by active strike-slip faulting along the Hosgri fault zone, and reverse faulting within the Los Osos/Santa Maria domain. The plant site area is on a structural subblock of the San Luis Range (the Irish Hills subblock, Figure 2.6-4), bordered on the northeast and southwest by the Los Osos and southwestern boundary zone reverse faults, respectively, and on the west by the Hosgri fault zone (Reference 6, Chapter 2, Figure 2-50). Since the end of the early Quaternary, the Irish Hills subblock has been slowly elevated along these bounding faults. Detailed mapping and paleoseismic investigations performed for the LTSP (Reference 6) and the DCPP FSAR Update, Section 2.5.1 show that no capable faults are present within the plant site area.

Within the Irish Hills structural subblock, the principal geologic structure is the northwest-trending Pismo syncline (termed the San Luis-Pismo syncline in the DCPP FSAR Update, Section 2.5.1.1.5.2). This 20-mile-long regional structure deforms rocks of the Miocene Monterey and Obispo formations, and the Pliocene Pismo Formation. Fold deformation occurred primarily during the Pliocene, and ceased sometime in the late Pliocene or early Quaternary. Detailed mapping of Quaternary marine terraces across the axis and flanks of the syncline during the LTSP (Reference 6, Plates 10 and 12) documents the absence of fold deformation and associated faulting within the Irish Hills structural subblock for at least the past 500,000 to 1,000,000 years (Reference 6, page 2-34).

The plant site area is situated on the eroded southwestern limb of the Pismo syncline (Figure 2.6-4), within Miocene bedrock of the Obispo Formation (Figure 2.6-5). This regional structure has subsidiary folds that are hundreds to 10,000 ft long and hundreds of feet wide (DCPP FSAR Update, Section 2.5.1.1.5.2, p. 2.5-19, -20). One of these structures, a small northwest-trending syncline, is located directly northeast of the power block (DCPP FSAR Update, Section 2.5.1.2.4.2, p. 2.5-32, -33, Figure 2.5-8). This is the same small syncline that extends across the western part of the ISFSI site (Figures 2.6-5, 2.6-6, and 2.6-7).

Along the coast, the Obispo and Monterey formations have been eroded and incised by former high stands of sea level, leaving a preserved sequence of marine terraces and terrace remnants (Figures 2.6-2 and 2.6-7). The foundation for the power block was excavated into rock below the lower two marine terraces, which are approximately 80,000 and 120,000 years old, respectively (Reference 6, Chapter 2). The power block is founded on competent sandstone and siltstone of the Obispo Formation, the same stratigraphic unit that underlies the ISFSI site.

The ISFSI will be on a prominent ridge directly south of the raw water reservoir and east of the DCPP (Figures 2.6-7 and 2.6-8). The ridge area was used formerly as a borrow source to derive fill material for construction of the 230-kV and 500-kV switchyards. The borrow excavation, completed in 1971, removed up to 100 ft of material from the ISFSI site area and extended deep into bedrock (Figures –2.6-2, 2.6-3, and 2.6-9 through 2.6-12). As a result, the ISFSI and CTF facilities will be founded on bedrock, and the foundation stability and seismic response will be controlled by the bedrock properties. The borrow area cutslope is 900 by 600 ft in plan view, and 300 ft high. The slope of the cut face varies between 2.5:1 and 4:1 (22 to 14 degrees). The former borrow activity at the site stripped surficial soil and weathered rock from the hillside above the ISFSI site, leaving a bedrock slope covered with a veneer of rock rubble. The proposed cutslopes south of the ISFSI pads will be cut entirely in bedrock.

The ISFSI site will be accessed via the transport route, which will follow existing paved roads, except where the road is routed inland from Patton Cove. The transport route starts at the power block, and ends at the ISFSI (Figures 2.6-1, 2.6-3, and 2.6-7).

2.6.1.4 Stratigraphy

2.6.1.4.1 Plant Site Area Stratigraphy

The plant site area is underlain by bedrock of the early and middle Miocene Obispo Formation, and middle Miocene diabase intrusions (References 10 and 6, Chapter 2). Geologic studies for the original DCPP FSAR Update classified bedrock at the power plant site as strata from the middle and late Miocene Monterey Formation. Subsequent studies published by the U.S. Geological Survey (Reference 10), and conducted during the LTSP (Reference 6, Chapter 2) and this ISFSI study reclassified most of the bedrock in the plant site area as part of the Obispo Formation.

Hall and others (Reference 10) divided the Obispo Formation into two members: a fine-grained, massively bedded, resistant zeolitized tuff (mapped as Tor), and a thick sequence of interbedded marine sandstone, siltstone, and dolomite (mapped as Tof) (Figures 2.6-6 and 2.6-7). During the current geologic investigations, the marine sedimentary deposits were further divided into three units, a, b, and c, based on distinct changes in lithology. Unit Tof_a occurs in the eastern part of the plant site area (entirely east of the ISFSI study area) and consists primarily of thick to massively bedded diatomaceous siltstone and tuffaceous sandstone. Unit Tof_b occurs in the central and west-central part of the plant site area, including the entire ISFSI study area and beneath the power block, and consists primarily of medium to thickly bedded dolomite, dolomitic siltstone, dolomitic sandstone, and sandstone. Unit Tof_c occurs in the western part of the plant site area and consists of thin to medium bedded, extensively sheared shale, claystone and siltstone.

Diabase and gabbro sills and dikes intrude the Obispo Formation in the plant site area. These intrusive rocks originally were mapped as a member of the Obispo Formation (Tod) by Hall (Reference 11), but later were reclassified as a separate volcanic formation (Tvr) by Hall and others (Reference 10), because the rocks intrude several different formations, and are not confined to the Obispo Formation. The nomenclature of Hall and others (Reference 10) has been adopted for this study, and these rocks are mapped as Tertiary volcanic rock (Tvr) in the plant site area. These intrusive rocks are well exposed in the north wall of Diablo Canyon, across from the ISFSI site (Reference 11). The diabase typically is a dark, highly weathered, low-hardness rock. It is altered and weak, has a fine crystalline structure, and weathers spheroidally. Petrographic analysis of hand samples shows the diabase is an altered cataclastic gabbro and diorite. The large diabase sill that intruded between dolomite and sandstone beds in the raw water reservoir area was entirely removed during borrow area excavation (Figures 2.6-10 and 2.6-11). There are no exposures of diabase remaining on the borrow area cutslope and no diabase was encountered in any of the boreholes or trenches excavated at the ISFSI study area. Deeper parts of the original intrusion are still exposed in the roadcut along Tribar Road east of and below the raw water reservoir (Figure 2.6-6).

Quaternary deposits generally cover bedrock within the plant site area (Figure 2.6-7). These unconsolidated sediments are discussed in Section 2.6.1.5.

2.6.1.4.2 ISFSI Study Area Stratigraphy

The ISFSI is sited on folded and faulted marine strata of unit Tof_b of the Obispo Formation (Figures 2.6-7 and 2.6-8). Unit Tof_b in the ISFSI study area has undergone a complex history of deposition, alteration, and deformation. Understanding the complexity of the geology and the various geologic processes giving rise to the current geologic conditions at the site is important for interpreting the stratigraphy and structural geology at the site. Based on analysis of surface and subsurface data, supplemented by petrographic analyses of rock lithology, mineralogy, and depositional history, the following events produced the current lithology and stratigraphic character of bedrock at the site (Figures 2.6-13 and 2.6-14). A detailed description of each of these processes is presented in Reference 37.

(1) Original marine deposition, including vertical and lateral facies changes within the dolomite and sandstone sequence

(2) Burial and lithification, followed by diagenesis and dolomitization

(3) Localized addition of petroliferous fluids

(4) Diabase intrusion, hydrothermal alteration, and associated deformation

(5) Tectonic deformation (folding and faulting)

(6) Surface erosion and weathering (both chemical and mechanical)

(7) Borrow excavation and stress unloading

Across the ISFSI site, unit Tof_b is significantly influenced by a lateral and vertical facies change from dolomite to sandstone. In the ISFSI site area, therefore, unit Tof_b has been further divided into a dolomite unit (Tof_{b-1}) and a sandstone unit (Tof_{b-2}). Figure 2.6-15 provides a generalized stratigraphic column illustrating the distribution of rock types within these two subunits. Unit Tof_{b-1} consists primarily of dolomite, dolomitic siltstone, fine-grained dolomitic sandstone, and limestone. Unit Tof_{b-2} consists primarily of fine- to medium-grained dolomitic sandstone and sandstone. Thin clay beds also are present in both units. The dolomite appears to be a diagenetic product of alteration from a limestone and/or calcareous siltstone and very fine sandstone parent rock. Primary deposition of limestone ($CaCO_3$) or calcareous siltstone occurred in a shallow to moderately deep marine environment. Following burial and lithification, the replacement of calcium by magnesium (dolomitization) during diagenesis of the limestone or siltstone formed dolomite ($CaMg(CO_3)_2$).

The contact between the dolomite and sandstone (units Tof_{b-1} and Tof_{b-2}) marks a facies change from a deep marine dolomite sequence to a sandstone turbidite sequence. The contact varies from sharp to gradational, and bedding from one unit locally interfingers with bedding of the other unit. For purposes of mapping, the contact was arbitrarily defined as the first occurrence (proceeding down-section) of medium- to coarse-grained dolomitic sandstone below the dolomite. Surface and subsurface geologic data were used to construct 12 cross sections across the site and transport route (Reference 37). The interfingering nature of the dolomite/sandstone contact beneath the ISFSI study area is illustrated on cross sections A-A', B-B''', D-D', F-F', I-I', and L-L' (Figures 2.6-10, 2.6-11, 2.6-16, 2.6-17, 2.6-18, and 2.6-19, respectively). Some of the thin, interfingering beds provide direct evidence for the lateral continuity and geometry (attitude) of bedding within the hillslope (for example, between boring 01-F and 00BA-1 on section I-I').

Analysis of the cross sections shows that the facies contact between the dolomite and sandstone (units Tofb-1 and Tofb-2) generally extends from northwest to southeast across the ISFSI study area, with sandstone of unit Tofb-2 primarily in the north and northeast part of the area, and dolomite of unit Tofb-1 primarily in the south and southwest part of the area. The three-dimensional distribution of the facies contact is well illustrated by comparing cross sections B-B''' and I-I' (Figures 2.6-11–and 2.6-18). This distribution of the two units reflects a cyclic transgressive/regressive/transgressive marine sequence during the Miocene.

The division of unit Tof_b into two subunits also allows for a detailed interpretation of the geologic structure (folds and faults) in the ISFSI study area. This understanding provides the basis for evaluating the distribution of rock types in the area, and for selecting appropriate rock properties for foundation design and slope stability analyses at the ISFSI, as discussed in Sections 2.6.1.7, 2.6.1.8, 2.6.4.2, and 2.6.5.

2.6.1.4.2.1 Dolomite (Unit Tof_{b-1})

The slope above the ISFSI, including most of the borrow area excavation slope, is underlain by dolomite (Figure 2.6-8). The dolomite is exposed as scattered outcrops across the excavated slope, along the unpaved tower access road (Reference 43, Data Report A), in the upper part of most borings in the ISFSI study area (Reference 44, Data Report B), and in most exploratory trenches (Reference 46, Data Report D). The dolomite consists predominately of tan to yellowish-brown, competent, well-bedded dolomite, with subordinate dolomitic siltstone to fine-grained dolomitic sandstone, and limestone (Figure 2.6-20). Petrographic analyses of hand and core samples from, and adjacent to, the ISFSI study area show that the rock consists primarily of clayey dolomite, altered clayey carbonate and altered calcareous claystone, with lesser amounts of clayey fossiliferous, bioclastic and brecciated limestone, fossiliferous dolomite, and friable sandstone and siltstone (Reference 52, Data Report J, Tables J-1 and J-2). As described in the petrographic analysis, the carbonate component of these rocks is primarily dolomite; thus the general term dolomite and dolomitic sandstone is used to describe the rock.

The dolomite crops out on the excavated borrow area slope as flat to slightly undulating rock surfaces. The rock is moderately hard to hard, and typically medium strong to brittle, with locally well defined bedding that ranges between several inches to 10 ft thick in surface exposures and boreholes. Bedding planes are laterally continuous for several tens of feet, as observed in outcrops, and may extend for hundreds of feet based on the interpreted marine depositional environment. The bedding planes are generally tight and bonded. Unbonded bedding parting surfaces are rare and generally limited to less than several tens of feet, based on outcrop exposures.

2.6.1.4.2.2 Sandstone (Unit Tof_{b-2})

Sandstone of unit Tof_{b-2} generally underlies the ISFSI study area below about elevation 330 ft (Figure 2.6-8). Typically, the rocks in this subunit are well-cemented, hard sandstone and dolomitic sandstone, and lesser dolomite beds.

The well-cemented sandstone encountered in the borings and trenches is tan to gray, moderately to thickly bedded, and competent (Figure 2.6-21). The rock is well sorted, fine- to coarse-grained, and is typically well cemented with dolomite. Petrographic analyses show that the sandstone is altered, and that its composition varies from arkosic to arenitic, with individual grains consisting of quartz, feldspar, dolomite, and volcanic rock fragments (Reference 52, Data Report J). The rock is of low to medium hardness, is moderately to well cemented, and is medium strong. The matrix of some samples contains a significant percentage of carbonate and calcareous silt to clay matrix (probably from alteration). Petrographic analyses show that the carbonate is primarily dolomite. Thus, these rocks are referred to as sandstone and dolomitic sandstone. Bedding in places is well defined, and bedding plane contacts are tight and well bonded. Similar to the dolomite beds, unbonded bedding surfaces within the sandstone are rare and generally limited to less than several tens of feet, based on limited outcrop exposure.

2.6.1.4.2.3 Friable Bedrock

Distinct zones of friable bedrock are present within the generally more cemented sandstone and dolomite (Figures 2.6-8, 2.6-15, and 2.6-22). In some cases, the friable bedrock appears to reflect the original deposit, with no subsequent dolomitization. In other cases, the friable bedrock appears to be related to subsequent chemical weathering or hydrothermal alteration. The friable beds within units Tof_{b-1} and Tof_{b-2} have been designated with the subscript (a). Unit Tof_{b-1a} consists primarily of altered or weathered dolomite or dolomitic siltstone that has a block-in-matrix friable consistency, or simply a silt and clay matrix with friable consistency. The friable rock is of low hardness and is very weak to weak. Unit Tof_{b-2a} consists primarily of friable sandstone, is of low hardness, and is very weak to weak. In many cases, the friable sandstone is the original sandstone that has been chemically weathered or altered to a clayey sand (plagioclase and lithics altered to clay). In other cases, the friable sandstone simply lacks dolomite cementation and retains its original friable nature.

The vertical thickness of the friable rock encountered in borings ranges from less than 1 ft to 32 ft. The friable zones extend laterally for tens of feet in trench exposures, and up to about 200 ft were assumed to correlate between borings (Reference 37). As illustrated on cross section I-I' (Figure 2.6-18), the zones of friable rock are more common, and possibly more laterally continuous, in the sandstone than in the dolomite.

2.6.1.4.2.4 Clay Beds

Clay beds are present within both the sandstone and dolomite units. Clay beds were observed in several trenches (Figures 2.6-23 and 2.6-24) and in many of the borings (Figures 2.6-25 and 2.6-26). Because clay beds are potential layers of weakness in the hillslope above the ISFSI site, they were investigated in detail, (Reference 37). The clay beds generally are bedding-parallel, and commonly range in thickness from thin partings (less than 1/16 inch thick) to beds 2 to 4 inches thick; the maximum thickness encountered was about 8.5 inches. The clay beds are yellow-brown, orange-brown, and dark brown, sandy and silty, and stiff to hard. Petrographic analyses show that the clay contains marine microfossils and small rock inclusions; the rock inclusions are angular pieces of dolomite that are matrix-supported, and have no preferred orientation or shear fabric (Reference 53, Data Report K). In the trenches, the clay beds locally have slickensides and polished surfaces. The clay beds typically are overconsolidated (due to original burial), as supported by laboratory test data (Reference 49 , Data Report G), and, where thick, have a blocky structure.

The clay beds encountered in the borings were recorded on the boring logs (Reference 44, Data Report B). In addition, in most of the borings, the clay beds also were documented in situ by a borehole televiewer. The televiewer logs show that the clay beds generally are in tight contact with the bounding rock, and are bedding-parallel (Reference 47, Data Report E). The clay beds range from massive having no preferred shear fabric, to laminated having clear shear fabric. The shear fabric is interpreted to be the result of tectonic shearing during folding and flexural slip of the bedding surfaces. The shear fabric does not reflect gravitational sliding, because features indicative of sliding, such as disarticulation of the rock mass, tensional fissures, and geomorphic expression of a landslide on pre-construction aerial photographs, are not present.

Clay Beds in Dolomite

Clay beds are more common, thicker, and more laterally continuous in the dolomite (unit Tof_{b-1}). Examination of the continuity of clay beds within and between adjacent trenches, roadcuts, and borings provided data on the lateral continuity (persistence) of the clay beds (Reference 37). Individual clay beds exposed in the trenches and roadcuts appear to be persistent over distances of between tens of feet to more than 160 ft, extending beyond the length of the exposures. The exposed clay beds are wavy and have significant variations in thickness along the bed. Thinner clay beds (less than about 1/4 inch thick) typically contain areas where asperities on the surfaces of the bounding adjacent hard rock project through or into the thin clay. The bedding surfaces are all irregular and undulating, with the height (amplitude) of the undulation greater than the thickness of the clay beds, such that the clay beds likely will have rock-to-rock contact locally during potential sliding, producing an overall increase in the average shear strength of the clay bed surface. A correlation of clay beds within the slope above the ISFSI site is shown on cross section I-I' (Figure 2.6-18). These correlations indicate that at least some clay beds extend over several hundred feet into the hillslope. However, some beds clearly do not correlate: for example, the clay beds exposed in trenches T-14 and T-15 are not found in nearby boring 01-I.

Clay Beds in Sandstone

Clay beds are less common, generally thinner, and less laterally continuous in the sandstone (unit Tof_{b-2}). Clay beds observed in the sandstone generally are less than 1/4 inch thick. These thinner clay beds are difficult to correlate laterally between borings and, at least locally, are less than 50 to 100 ft in lateral extent. For example, as shown on cross sections B-B' and I-I' (Figures 2.6-11 and 2.6-18), clay beds were not encountered in boring 01-B, but were encountered in borings 01-A and 01-H, 50 to 100 ft away.

Clay Moisture Content

The clay beds encountered in the borings and trench excavations in both the dolomite and sandstone were moist. Clay beds uncovered in the trenches dried out after exposure during the dry season, and became hard and desiccated. When wetted during the rainy season, the clay in the trenches became soft and sticky (Reference 46, Data Report D, Trench T-11). Possible local perched water tables, as observed in boring 01-F and evident elsewhere in the plant site area (Section 2.5, Subsurface

Hydrology), also may soften the upper portions of the clay beds during the rainy season in the ISFSI study area.

Clay Composition

X-ray diffraction analyses (Reference 53, Data Report K) show that the clay-size fraction of the clay beds consists of three primary minerals: kaolinite (a clay), ganophyllite (a zeolite), and sepiolite (a clay). The silt-size fraction of the sample consists primarily of rock and mineral fragments of quartz, dolomite/ankerite, and calcite. Petrographic examination of the clay (Reference 53, Data Report K) shows a clay matrix having matrix-supported angular rock fragments and no shear fabric. Included rock fragments have evidence of secondary dolomitization of original calcite (limestone), and localized post-depositional contact alteration. Some samples contain microfossils (benthic foraminifera). The ganophyllite minerals appear to be expansive, as evidenced by swelling of one sample (X-1 from trench T-14A) after thin-section mounting. Sample X-2 also had a significant percentage of ganophyllite, and a high plasticity index (PI) of 63 (References 49 and 53, Data Reports G & K).

The presence of microfossils confirms the clay is depositional in origin, and was not formed by alteration or weathering of a lithified host rock. The clay is interpreted to reflect pelagic deposition in a marine environment.

2.6.1.4.2.5 Diabase (Tvr)

Diabase is exposed in the roadcut along Tribar Road and probably underlies the eastern portion of the raw water reservoir area. The diabase is part of the Miocene diabase intrusive complex in Diablo Canyon near the switchyards (Reference 10). A large diabase body was removed during grading for the raw water reservoir pad and the borrow cut area. This body of diabase likely was continuous with the diabase exposed along Tribar Road. Currently, no diabase is exposed on the borrow cut slope, and diabase was not encountered in any of the borings or trenches in the ISFSI study area. The diabase exposed along Tribar Road has been altered to a friable rock, and is soft to dense and easily picked apart; it is judged to be similar in engineering properties to the friable sandstone and friable dolomite found in the ISFSI study area. Though diabase was not encountered elsewhere in the ISFSI study area during field investigations, it is possible that other small dikes or sills of diabase may be encountered during excavation for the ISFSI pads or cutslope.

2.6.1.5 Geomorphology and Quaternary Geology

The geomorphology and Quaternary geology of the plant site area is dominated by a flight of coastal marine terraces, deep fluvial incision along Diablo Creek, and deposition of alluvial and colluvial fans at the base of hillslopes. Quaternary deposits cover bedrock across most of the power plant property, except in the ISFSI study area, where extensive borrow excavation in the 1970s removed the Quaternary deposits. These deposits accumulated in distinctive geomorphic landforms that include coastal marine terrace platforms, debris and colluvial fans at the base of hills and swales, landslides on hillslopes and sea cliffs, and alluvium along the floor of Diablo Canyon. The distribution of Quaternary deposits and landforms are shown on Figures 2.6-7 and 2.6-8.

2.6.1.5.1 Marine Terraces

Several marine terraces form broad coastal platforms within the western part of the power plant property (Figure 2.6-7). The power plant and associated support facilities and buildings are constructed on these terraces (Figure 2.6-2). Discontinuous remnants of older and higher terraces also are present locally across the ISFSI study area. Each of these marine terraces consists of a relatively flat, wave-cut bedrock platform, a thin layer of marine sand and cobble sediments, and surficial deposits of colluvium, alluvium, and eolian sediments. The "staircase" of bedrock platforms resulted from a combination of regional uplift, sea level fluctuations, and wave erosion.

The locations and elevations of marine terraces along the coast from Avila Beach to Montaña de Oro and Morro Bay, including the area of the power plant, were initially characterized during studies for PG&E's Long Term Seismic Program (Reference 6).. Several terraces were mapped in more detail for the ISFSI studies, and the location of the inner edge (or shoreline angle) of the terraces was estimated (Figure 2.6-7). Well-developed, wave-cut bedrock platforms and their associated terraces exist in the plant site area at elevations of about 30 to 35 ft (Q_1 terrace), 100 to 105 ft (Q_2 terrace), and 140 to 150 ft (Q_3 terrace), and form relatively level bedrock surfaces under the surficial Quaternary deposits along the coast. The platforms slope gently seaward at angles from 2 degrees to 3 degrees, and are bordered landward by steep (50 degrees to 60 degrees, Reference 6) former sea cliffs that are now largely covered by thick surficial deposits. A sequence of Pleistocene to Holocene colluvial fans covers the landward portion of the coastal terraces. These deposits consist of crudely bedded clay, clayey gravel, and sandy clay, and have distinct paleosol and carbonate horizons. The lower, Pleistocene fan deposits are very stiff and partly consolidated; they have highly weathered clasts, carbonate horizons, and an oxidized appearance. The upper, Holocene deposits are unconsolidated and have a higher organic contact; they do not have argillic or carbonate horizons.

Near the ISFSI site, discontinuous remnants of a higher marine terrace are present. The terrace has an approximate shoreline angle elevation of 290 ft (Q_5 terrace) (Figure 2.6-7). The terrace deposits consist of a basal layer of marine sand and gravel overlain by colluvial sandy clay and clayey gravel. This terrace may be coeval with an estuarine deposit of black clay having interfingering white shell hash that crops out beneath the edge of the 500-kV switchyard fill (Figure 2.6-7). The clay appears to have been deposited in an estuarine environment by an ancient marine embayment into Diablo Canyon. Most of the Q_5 terrace, however, has been eroded by incision along Diablo Creek, or is buried by younger stream terrace and landslide deposits, or switchyard and road fills.

The thickness of the terrace deposits (depth to bedrock) varies greatly, from less than 10 ft to greater than 80 ft. Extensive grading for the DCPP and related facilities and parking areas has substantially modified the morphology and thickness of terrace deposits in some locations. The current thickness of terrace deposits, therefore, is locally dependent on site-specific grading activities.

2.6.1.5.2 Inland Quaternary Deposits

Diablo Creek has carved a deep channel into bedrock, causing oversteepening of the slopes along the canyon walls. Some thin, narrow, channel deposits, and one locally preserved stream terrace veneered by colluvial deposits, are present in the canyon. The rate and extent of erosion, however, generally has been dominant over sedimentation in the canyon, and alluvial deposits are relatively thin and of limited extent. Substantial reaches along the lower part of the creek were artificially filled, channeled, and altered during development of the power plant and related facilities, particularly around the 230-kV and 500-kV switchyards, which are constructed on large fill pads across the bottom of the canyon.

Slopes in the Irish Hills are extensively modified by mass wasting processes, including landslides, debris flows, creep, gully and stream erosion, and sheet wash. Extensive grading to form level platforms for the power plant and related facilities along the back edge of the coastal terraces has greatly modified the lower portions of most slopes in the plant site area. Large, deep-seated landslide complexes are present on the slopes of Diablo Canyon south of the 230-kV and 500-kV switchyards (Figure 2.6-7). These features consist of large (exceeding 100 acres), deep-seated, coalescing, bedrock landslides. The dip of bedrock strata in the vicinity of these large slides is downslope, suggesting the failure planes for these slides probably occurred within the bedrock along clay beds and bedding contacts. Some slides may have occurred at the contact between bedrock and overlying weathered bedrock and colluvium, or along contacts between Obispo Formation bedrock and relatively weaker diabase.

The large landslide complexes have been considerably modified by erosion, and fluvial terraces and possible remnants of the Q_5 marine terrace appear to have been cut into the toes of some of the slides. These conditions suggest they are old features that likely formed prior to the Pleistocene-Holocene transition, during a wetter climate. These large slide complexes, therefore, appear to have a stable configuration under the present climatic conditions, which have persisted during the Holocene (past 10,000 years or so).

Debris-flow scars and deposits are found along some of the steeper slopes (Figure 2.6-7). The debris flows originate where colluvium collects in topographic swales or gullies on the upper and middle slopes. Debris flows usually are triggered by periods of severe weather that allow development of perched groundwater within hillside colluvial deposits. Following initial failure, the saturated mass flows rapidly down drainage channels, commonly scouring the bottom of the channel and increasing in volume as it travels downslope. The flow stops and leaves a deposit of poorly sorted debris at a point where the slope angle decreases. Debris fans formed by accumulation of successive debris flows are present at the mouths of the larger canyons and gullies in the area (Figure 2.6-7).

2.6.1.6 Structure

2.6.1.6.1 Regional Structure

Bedrock structure in the plant site region is dominated by the northwest-trending Pismo syncline (Figure 2.6-4), which forms the core of the Irish Hills (References 10 and 11). The regional bedrock structure and tectonic setting are described in the DCPP FSAR Update, Section 2.5.1.1 (Reference 4), and LTSP Final Report, Chapter 2 (Reference 6), and are summarized in Section 2.6.2 of this report. The following sections describe the structural setting of the ISFSI study area, including the distribution of bedrock folds, faults, and joints in the area.

2.6.1.6.2 ISFSI Study Area Structure

Bedrock in the ISFSI study area has been deformed by tectonic processes and possibly by the intrusion of diabase. The detailed stratigraphic framework described above provides the basis for analyzing the geologic structure in the site area.

Geologic structures in the ISFSI study area include folds, faults, and joints and fractures. The distribution and geometry of these structures is important for evaluating rock mass conditions and slope stability because (1) folds in the bedrock produce the inclination of bedding that is important for evaluating the potential for out-of-slope, bedding-plane slope failures; and (2) faults and, to a lesser extent, joints in the bedrock produce laterally continuous rock discontinuities along which potential rock failures may detach in the proposed cutslopes.

The distribution and geometry of folds and faults in the bedrock were evaluated through detailed surface geologic mapping, trenches, and borings (References 2 and 3). Data from these studies were integrated to produce geologic maps (Figures 2.6-6, 2.6-7, and 2.6-8) and geologic cross sections (for example, Figures 2.6-10, 2.6-11, and 2.6-16 through 2.6-19). The cross sections were prepared at various orientations to evaluate the three-dimensional distribution of structures. Bedding attitudes were obtained from surface mapping (including roadcut and trench exposures) and from boreholes (based on visual inspection of rock core integrated with oriented televiewer data). These bedding attitudes were used to constrain the distribution of bedrock lithologies and geometry of bedding shown on the cross sections.

2.6.1.6.2.1 Folds

Similar to the power plant, the ISFSI is located on the southwestern limb of the regional Pismo syncline (Figure 2.6-4). As shown on the geologic maps (Figures 2.6-6, 2.6-7, and 2.6-8) and cross sections (Figures 2.6-10, 2.6-11, and 2.6-16 through 2.6-19), bedrock in the ISFSI study area is deformed into a small, northwest-trending syncline and anticline along the western limb of the larger regional Pismo syncline. On the ridge southeast of the ISFSI study area, nearly continuous outcrops of resistant beds expose the small anticline and an en echelon syncline (Figures 2.6-6, 2.6-7, and 2.6-17). These folds are relatively tight and sharp-crested, have steep limbs, and plunge to the northwest.

Within the ISFSI study area, the northwest-plunging anticline appears to be the northwestward continuation of the anticline that is exposed in the ridge top at the Skyview Road overlook area (Figure 2.6-1). The anticline varies from a tight chevron fold southeast of the ISFSI study area, to a very broad-crested open fold across the central part of the area. The northwestward shallowing of dips along the anticlinal trend appears to reflect a flattening of fold limbs up-section. In the ISFSI study area, the broad crest of the fold is disrupted by a series of fold-parallel, minor faults (Figure 2.6-11). The minor faults displace the fold axis, as well as produce local drag folding, which tends to disrupt and complicate the fold geometry. The axis of this broad-crested anticline is approximately located on the geologic map (Figure 2.6-8).

The en echelon syncline at the ridge crest along Skyview Road projects to the northwest along the southwestern margin of the ISFSI study area. From the southeast to the northwest, the syncline changes into a northwest-trending monocline, and then back into a syncline (Figures 2.6-6 and 2.6-7). In the ISFSI study area, the syncline opens into a broad, gently northwest plunging (generally less than 15 degrees) fold with gently sloping limbs (generally less than 20 degrees). Bedding generally dips downslope to the northwest in the upper part of the slope above the ISFSI site, and perpendicular to the slope to the southwest and west in the lower part of the slope. Small undulations in the bedding reflect the transition from a tight syncline to a relatively flat monocline, or "shoulder," and then back to a broad, northwest-plunging syncline. These localized interruptions to the northwestern plunge of the fold may be caused by the diabase intrusion and localized doming associated with the intrusion (compare diagrams C and D on Figure 2.6-13).

As discussed above and shown on cross sections B-B''', D-D', and F-F' (Figures 2.6-11, 2.6-16, and 2.6-17), the western limb of the small syncline varies from steeply dipping (approximately 70 degrees northwest) across the southern part of the plant site area, to gently dipping (approximately 30 degrees northwest) beneath the power block. This change in the dip of the syncline across the plant site area mirrors the change in dip described above across the ISFSI study area. Based on the geometry of the syncline, bedrock beneath the power block consists of sandstone (unit Tof_{b-2}), underlain by dolomite (unit Tof_{b-1}) (Figure 2.6-11). The power block is located on the same stratigraphic sequence exposed in the ISFSI study area; however, the sequence is approximately 400 ft lower in the stratigraphic section. As shown on cross section B-B''' (Figure 2.6-11), boreholes drilled during foundation exploration for the power block encountered calcareous siltstone having abundant foraminifera. This description of the rock is very similar to the dolomite of unit Tof_{b-1}; thus, the lower contact between units Tof_{b-1} and Tof_{b-2} is interpreted to be beneath the power block area.

Folding occurred during growth of the northwest-trending, regional Pismo syncline in the Pliocene to early Quaternary (Reference 6). The smaller folds at and near the ISFSI study area are parasitic secondary folds along the southwestern limb of the larger Pismo syncline. Because of their structural association with the Pismo syncline, the folding in the area is interpreted to have occurred during the Pliocene to early Quaternary (Figure 2.6-8). Some localized fold deformation also may have accompanied the earlier Miocene diabase intrusions.

2.6.1.6.2.2 Faults

Numerous minor, bedrock faults occur within the ISFSI study area (Figures 2.6-27 and 2.6-28). Based on displaced lithologic and bedding contacts, most of the faults have vertical separations of a few inches to a few feet. At least five faults show vertical separation of several tens of feet. Slickensides and mullions on the fault surfaces generally show strike-slip to oblique strike-slip displacement.

The faults trend generally northwest, subparallel to the local fold axes (Figure 2.6-29). They dip steeply to near-vertical, generally 70 to 90 degrees, both northeast and southwest. They consist of interconnecting and anastomosing strands, in zones up to 5 ft wide. The faults have documented lengths of tens of feet to a few hundred feet, and are spaced from several tens of feet to hundreds of feet apart across the ISFSI study area, based on trench exposures and surface geologic mapping.

The fault surfaces within bedrock vary from tightly bonded or cemented rock/rock surfaces, to relatively soft slickensided clay/rock and clay film contacts. Individual faults are narrow, ranging in width from less than an inch to about 2 ft. Fault zones contain broken and slickensided rock, intermixed clay and rock, and locally soft, sheared, clayey gouge. The thickness of fault gouge and breccia is variable along the faults.

Cross section B-B''' (Figure 2.6-11) illustrates the subsurface stratigraphy and structure beneath the ISFSI pads. As shown on the map (Figure 2.6-8) and cross section, five minor faults clearly juxtapose dolomite (Tof_{b-1}) against sandstone (Tof_{b-2}), and truncate individual friable beds. Vertical separation across individual faults ranges from about 10 ft to greater than 50 ft, based on displacements of friable beds and the contact between units Tof_{b-1} and Tof_{b-2}. Total vertical separation across the entire fault zone exceeds 50 ft; cumulative displacement is down on the northeast. As described previously, the contact between dolomite and sandstone (units Tof_{b-1} and Tof_{b-2}) beneath the pads is based on the first occurrence of medium to coarse-grained sandstone, and there is no evidence of significant facies interfingering between the two units beneath the pads that would obscure the amount of displacement. Therefore, the interpretation of vertical separation of bedrock along the faults is given a relatively high degree of confidence.

Subhorizontal slickensides indicate that the minor faults in the ISFSI study area have predominantly strike-slip displacement (Figure 2.6-30). Using a typical range of a 10-degree to 20-degree rake on the slickensides and the vertical separation, total fault displacement is estimated to be several tens to several hundreds of feet. The faults trend subparallel to the axis of the Pismo syncline, and trend approximately 35 to 55 degrees more westward than the offshore Hosgri fault zone (Figure 2.6-29).

The faults in the ISFSI study area may be continuous with several other minor faults having similar characteristics exposed along strike in dolomite in the Diablo Creek roadcut about 800 ft to the north (Figures 2.6-6, 2.6-7, and 2.6-30). Given this correlation and the presence of several hundred feet of strike-slip displacement, the faults may be at least several thousand feet long. Interpretation of pre-borrow excavation aerial photography shows that the faults are not geomorphically expressed in the ISFSI study area (Figure 2.6-31) and there is no evidence of displaced Quaternary deposits along the fault traces.

In the analysis of slope stability (Section 2.6.5), the faults are assumed to form high-angle parting surfaces along the lateral margins of potential rock slides, rock wedges, and topple blocks. Fault-bounded structural blocks are shown on Figure 2.6-8, and on cross section B-B''' (Figure 2.6-11). The age and noncapability of the faults are discussed in Section 2.6.3.

2.6.1.6.2.3 Bedrock Discontinuities

Extensive data on bedrock discontinuities were collected from the borings and trenches within the ISFSI study area to assess their orientation, intensity, and spatial variability (Reference 48, Data Report F). The discontinuity data were used in the failure analysis of the ISFSI cutslopes (Section 2.6.5). Bedrock discontinuities include joints, faults, bedding, and fractures of unknown origin. These discontinuities, in particular joints, are pervasive throughout bedrock in the ISFSI study area (Figure 2.6-20). Steeply dipping faults and joint sets are the dominant discontinuities, giving the rock mass a subvertical fabric. Random and poorly developed low-angle joints also occur subparallel to bedding. The fault discontinuities are described in Section 2.6.1.6.2.2. Joint discontinuities are described below.

Joint contacts vary from tight to partially tight to slightly open; joint surfaces are slightly smooth to rough, and have thin iron oxide or manganese coatings (Reference 50, Data Report H). Joint lengths in trenches and outcrops typically range from a few feet to about 20 ft, and typical joint spacings range from about 6 inches to 4 ft, with an observed maximum spacing of about 14 ft (Reference 48, Data Report F, Table F-6). The intersections of various joints, faults, and bedding divide the bedrock into blocks generally 2 ft to 3 ft in dimension, up to a maximum of about 14 ft. Rock blocks formed by intersecting joints larger than those described above generally are keyed into the rock mass by intact rock bridges or asperity interlocking. The largest expected "free" block in the rock mass is, therefore, estimated to be on the order of about 14 ft in maximum dimension.

Both the well-cemented sandstone and the dolomite contain numerous joints. The jointing typically is confined to individual beds or groups of beds, giving the bedrock a blocky appearance in outcrop. Joints are less well developed and less common in the friable sandstone and friable dolomite. Linear zones of discoloration in the friable rock may represent former joints and small faults, but these zones are partially recemented, and not as frequent or obvious as joints in the harder rock.

The character of joints also differs between the upper, dilated zone of bedrock (generally within the upper 4 ft in the ISFSI study area, but conservatively estimated to extend to a maximum of 20 ft deep, particularly toward the edges of the old borrow cut where the amount of rock removed in 1971 is minimal) and the underlying zone of "tight" bedrock. Joints are generally tight to open in the upper zone. In the lower zone, the joints and other structures are tight and, in places, bonded and healed. This is well demonstrated in the borehole optical televiewer logs (Reference 47, Data Report E), which show the joints are typically tight and/or partly bonded throughout the borings. In both zones, the joints are locally clay-filled, and commonly contain thin fillings of clay, calcite, dolomite, and locally, gypsum. Joints and fractures in the borings are very closely to widely spaced (less than 1/16-inch to 3-ft spacing), with local crushed areas between joints.

In general, the joints group into two broad sets: a west- to west-northwest-striking set, and a north-northwest-striking set. In some trenches, fractures from both sets are present, whereas some show a scatter in orientation within a general northwest-southeast orientation. The variation in orientation and density of the joints with both strata and location across the ISFSI study area shows that the joints are limited in continuity.

The general northwest-southeast-trending character of the joints in the ISFSI study area is consistent with both the overall northwest-trending regional structural grain. Local variations in discontinuity orientations and intensity are attributed to rheological differences between dolomite and sandstone and their friable zones, as well as to proximity to the minor faults that cut across the area.

2.6.1.7 Stratigraphy and Structure of the ISFSI Pads Foundation

Figure 2.6-32 illustrates the expected bedrock conditions that will be encountered in the foundation excavation for the ISFSI pads at the assumed pad subgrade elevation of 302 ft (Reference 37). The pads will be founded primarily on dolomitic sandstone of unit Tof_{b-2} and dolomite of unit Tof_{b-1}. Dolomitic sandstone generally underlies most of the site; dolomite underlies the eastern end of the site. The proposed cutslopes above the site are generally underlain by dolomitic sandstone in the western and central parts of the cut, and by dolomite in the upper and eastern parts of the cut.

Locally, friable sandstone (Tof_{b-2a}) and friable dolomite (Tof_{b-1a}) underlie the foundation of the ISFSI pads and the proposed cutslopes (Figure 2.6-32). Because the zones are highly variable in thickness and continuity, their actual distribution likely will vary from that shown on Figure 2.6-32. In particular, a large body of friable dolomite underlies the southeastern portion of the proposed cutslope. Other smaller occurrences of friable sandstone and dolomite probably will be encountered in the excavation. These friable rocks locally have dense, soil-like properties; thus, specific analyses were performed to assess the foundation properties and slope stability of these friable rock zones (Reference 51, Data Report I). Small zones of friable diabase may be found in the excavation, as discussed in Section 2.6.1.4.2.5. This rock has properties similar to the friable sandstone.

In two places beneath the foundation of the ISFSI pads, clay beds within dolomite and sandstone are expected to daylight or occur within 5 ft of the base of the foundation (Figure 2.6-32). Additional clay beds may be exposed in the foundation of the pads. Although available geologic data do not document the presence of clay beds that will daylight in the ISFSI cutslope, some may be encountered when the cuts are made.

In addition, a zone of minor noncapable faults trends northwest across the central and eastern part of the ISFSI pads (Figures 2.6-8 and 2.6-11) (Section 2.6.3). The faults have vertical separations of 10 ft to 30 ft, and locally juxtapose different bedrock units.

2.6.1.8 Stratigraphy and Structure of the CTF Foundation

The CTF site lies about 100 ft directly northwest of the northwest corner of the ISFSI site (Figure 2.6-8). The CTF site is on the same west limb of the small anticline that underlies the ISFSI site (Figure 2.6-8, Section 2.6.1.6.2.1). Borings 00BA-3 and 01-CTF-A show the CTF will be founded on sandstone (unit Tof_{b-2}) and friable sandstone (unit Tof_{b-2a}), similar to the rock at the ISFSI site (Figures 2.6-8 and 2.6-32). The CTF site is located along the northwestern projection of the small bedrock faults at the ISFSI site, and similar faults and joints are expected to be encountered in the excavation for the CTF. Although no clay beds were encountered in borings 00BA-3 and 01-CTF-A, clay beds may underlie the site at deeper elevations (Reference 37). The dip of the bedrock at the CTF site appears to be near-horizontal. In the cutslope west of the CTF site, bedrock dips moderately to the northeast, into the slope (Figure 2.6-7).

2.6.1.9 Stratigraphy and Structure of the Transport Route

The transport route begins at the power block and ends at the ISFSI. The route will follow existing paved Plant View, Shore Cliff, and Reservoir roads (Figure 2.6-1), except where routed north of the intersection of Shore Cliff and Reservoir roads to avoid an existing landslide at Patton Cove. The lower two-thirds of the route traverses thick surficial deposits, including marine terrace, debris-flow, and colluvial deposits of varying thicknesses (Reference 37). These surficial deposits overlie two units of the Obispo Formation bedrock: unit Tof_b sandstone and dolomite, and unit Tof_c thinly to thickly bedded claystone, siltstone, and shale. The upper third of the route is on engineered fill, directly above dolomite and sandstone bedrock (units Tof_{b-1} and Tof_{b-2}) of the

Obispo Formation (Figure 2.6-7). Locally, the road is on a cut-and-fill bench cut into the bedrock.

In the geologic description below, approximate stations have been assigned to assist in defining distances between locations, starting from the power block and ending at the ISFSI (Figure 2.6-7). Although not surveyed, this informal stationing is standard engineering format to represent the distance, in feet, from the beginning of the route outside the power block to the station location (for example, 21+00 is 2,100 ft from the beginning). The specific conditions along the route are discussed below.

<u>Station 00+00 (south side of power block) to 20+00 (near Reservoir Road)</u>: The transport route generally follows Plant View Road and Shore Cliff Road. The route starts at the power block and crosses flat, graded topography on the lower coastal marine terrace (Q_2) (Figure 2.6-3). Behind the power block, the route is founded on sandstone (Tof_b) of the Obispo Formation. From there to near Reservoir Road, the transport route is founded on surficial deposits 10 to 40 ft thick, and engineered fill in excavations made during construction of the power plant. The surficial deposits consist primarily of debris-flow and colluvial deposits that overlie the marine bedrock terrace platform (Figures 2.6-7 and 2.6-16). These deposits range in age from middle Pleistocene to Holocene, and consist of overconsolidated to normally consolidated clayey sand and gravelly clay. The deposits contain some carbonate cementation and paleosols, and typically are stiff to very stiff (medium dense to dense). Bedrock below the marine terrace platform consists of east-dipping sandstone (Tof_b) from station 00+00 to about 07+00, and steeply dipping claystone and shale (Tof_c) from about 07+00 to 20+00. Because of the thickness of the overburden, bedrock structure will have no effect on the foundation stability of the road.

Station 20+00 to 34+00 (near Shore Cliff Road to Hillside Road): From station 20+00 to 26+00, the transport route will be on a new road north of the intersection of Shore Cliff Road and Reservoir Road to avoid an existing landslide at Patton Cove (Section 2.6.1.12.1.1; Figures 2.6-6, 2.6-7, and 2.6-19). A 5- to 50-ft-thick prism of engineered fill will be placed to achieve elevation from the lower part of the marine terrace to the upper part of the marine terrace as the road U-turns uphill. The engineered fill will overlie overconsolidated to normally consolidated Pleistocene debris-flow and colluvial deposits 20 to 80 ft thick that cover the marine bedrock platform (Q2), which in turn overlie steeply dipping claystone and shale of unit Tofc below the marine platform.

Along Reservoir Road, the route follows the higher part of this terrace, generally over the marine platforms Q_2 and Q_3. The surficial deposits consist of debris-flow and colluvial deposits up to 80 ft thick along the base of the ridge behind parking lot 8 (Figure 2.6-19). Bedrock below the marine terrace is claystone and shale (Tof_c) from station 26+00 to 29+50, and sandstone (Tof_b) from station 29+50 to 34+00.

Station 34+00 (Reservoir Road at Hillside Road) to 49+00 (along Reservoir Road): The route follows Reservoir Road to the raw water reservoir area. The road traverses the west flank of the ridge on an engineered cut-and-fill bench constructed over unit Tof_b dolomite and sandstone, and thin colluvium and debris-flow fan deposits. Bedding, as exposed in the roadcut, dips 30 to 50 degrees into the hillslope, away from the road. Engineered fill on sandstone and dolomite underlies the inboard edge of the road, and a wedge of engineered fill over colluvium generally underlies the outboard edge of the road (Figures 2.6-7, 2.6-11, and 2.6-19).

Bedrock joints exposed in this part of the route are similar to those at the ISFSI site. Joints are generally of low lateral persistence, confined to individual beds, and are tight to open. Joint-bounded blocks are typically well keyed into the slope, with the exception of a 1- to 3-foot-thick outer dilated zone. No large unstable blocks or adverse structures prone to large-scale sliding were observed.

Station 49+00 (along Reservoir Road) to 53+50 (ISFSI pads): The route leaves the existing Reservoir Road and crosses the power plant overview parking area. The route will be placed on new engineered fill up to 5 ft thick that will overlie thin engineered fill (up to 4 ft thick) that was placed over sandstone and friable sandstone (Tof_{b-2} and Tof_{b-2a}), the same rock types that underlie the ISFSI pads and CTF site.

Bedrock structures beneath this part of the route are inferred to be joints and small faults, similar to those exposed at the ISFSI site (Figure 2.6-8). The faults would trend generally northwest, and dip steeply northeast and southeast, to vertical. The primary joint sets are near-vertical (Section 2.6.1.6.2.3). This part of the road is on flat topography, and bedrock structure will have no effect on the foundation stability of the road.

An expanded description of this section of the transport route is provided in Reference 76 (PG&E Response to NRC Request 5).

2.6.1.10 Comparison of Power Block and ISFSI Bedrock

Bedrock beneath the ISFSI was compared to bedrock beneath the power block based on stratigraphic position, lithology, and shear wave velocity. Based on these three independent lines of evidence, the bedrock beneath the ISFSI and the power block is interpreted to be part of the same stratigraphic sequence, and to have similar bedrock properties and lithology.

Stratigraphic Position

Cross section B-B''' illustrates the stratigraphic correlation of bedrock between the ISFSI site and the power block site (Figure 2.6-11). As shown on the cross section, the power block and ISFSI are located on the same continuous, stratigraphic sequence of sandstone and dolomite of unit Tof_b of the Obispo Formation. As mentioned previously, the sequence at the power block is approximately 400 ft lower in the stratigraphic section.

The bedrock of the same continuous, stratigraphic sequence as that beneath the power block is exposed directly along strike in roadcuts along Reservoir Road (Figure 2.6-2). The bedrock exposed in the roadcut consists of dolomite, dolomitic siltstone, and dolomitic sandstone of unit Tof_{b-1}.

Lithology

As described in the DCPP FSAR Update, Section 2.5.1.2.5.6, p. 2.5-42, Figures 2.5-9 and 2.5-10) bedrock beneath the power block consists predominantly of sandstone, with subordinate thin- to thick-bedded slightly calcareous siltstone (for examples, see boring descriptions on Figures 2.6-11 and 2.6-19). The rocks are described as thin-bedded to platy and massive, hard to moderately soft and "slightly punky," but firm. These lithologic descriptions are similar to those for the rocks at the ISFSI site, and the rocks are interpreted to be the same lithologies.

The "calcareous siltstone" described in the DCPP FSAR Update is probably dolomite or dolomitic siltstone comparable to unit Tof_{b-1}. For example, based on the geologic descriptions of the rocks, the "siltstone" and "sandstone" encountered in 1977 in power block boring DDH-D is interpreted to be the dolomite and dolomitic sandstone of unit Tof_{b-1} observed at the ISFSI site.

Boring logs from the hillslope between the power block and the ISFSI site, included in the DCPP FSAR Update (Figures 2.5-22 to 2.5-27; Appendix 2.5C, plates A-1 to A-19), describe bedrock as tan and gray silty sandstone and tuffaceous sandstone (Figures 2.6-11 and 2.6-19). These rocks are moderately hard and moderately strong. The rock strata underlying this slope dip into the hillside and correlate with the sandstone and dolomite strata exposed on the west flank of the ridge (and west limb of the syncline) that are exposed in roadcuts along Reservoir Road south of the ISFSI site (Figures 2.6-6, 2.6-7, and 2.6-20) and in the deeper part of the borings at the ISFSI site.

Shear Wave Velocity

Shear wave velocity data from the power block site and the ISFSI site are summarized on Figures 2.6-33 and 2.6-34. Velocity data in Figure 2.6-35 are from borehole surveys at the ISFSI site (Reference 45, Data Report C), and comparative velocities at the power block site are from the DCPP FSAR Update. As evident from the figures, shear-wave velocities from surface refraction and borehole geophysical surveys at the ISFSI site are within the same range as those obtained at the power block site. The velocity profiles at both sites are consistent with a classification of "rock" for purposes of characterizing ground-motions (Reference 12).

2.6.1.11 Groundwater

Refer to Section 2.5, Subsurface Hydrology.

2.6.1.12 Landslides

2.6.1.12.1 Landslide Potential in the Plant Site Area

Slopes in the Irish Hills are subjected to mass-wasting processes, including landslides, debris flows, creep, gully and stream erosion, and sheet wash (Reference 9). Extensive grading in the plant site area to create level platforms for structures along Diablo Canyon and the coastal terraces has modified the lower portions of most of the slopes near the plant site.

Debris-flow scars and deposits occur on, and at the base of, slopes in the plant site area. The debris flows initiate where colluvium collects in topographic swales or gullies, and are usually triggered by periods of severe weather. Debris-flow fans, caused by the accumulation of successive debris flows, form at the mouths of the larger canyons and gullies in the area. Several typical gullies that have colluvium-filled swales, debris-flow chutes, and debris-flow fans at the bottom of the chutes are found on the slope above parking lots 7 and 8, south of the power plant (Figures 2.6-5 and 2.6-7).

During landslide investigations in 1997, PG&E identified a large, (exceeding 100 acres) ancient landslide complex on the slopes of Diablo Canyon, directly east of the 230- and 550-kV switchyards (Reference 9, Figure 2.6-7). The dip of the bedrock in the vicinity of these large slides is downslope, contributing to slope instability (Reference 9, Figure 21). This structure suggests the failure planes for these slides are probably within the bedrock along bedding contacts, clay beds, and possibly along the intrusive contacts between Obispo Formation bedrock and the altered diabase.

The large landslide complex is subdued, and has been considerably modified by erosion. Thin stream-terrace deposits and remnants of the Q_5 430,000-year-old marine terrace at elevation 290 ±5 ft appear to have been cut into the toes of some of the slides. These relations indicate the landslides are old, and likely formed in a wetter climate during the middle to late Pleistocene. The landslides appear to be stable under the present climatic conditions. There is no geomorphic evidence of activity in the Holocene (past 10,000 years or so). Additionally, the 500-kV switchyard embankment fill in the canyon provides a partial buttress to the toe of the old landslide deposit, and serves to help stabilize the landslide. The switchyard shows evidence of no post-construction slope movement. The complex lies entirely east of the ISFSI, and does not encroach, undermine, or otherwise affect the ISFSI.

Patton Cove Landslide

The Patton Cove landslide (Figure 2.6-36) is a deep-seated rotational slump located at a small cove adjacent to Shore Cliff Road along the coast, about one-half mile east of the power plant (Figures 2.6-6, 2.6-7, and 2.6-17) (Reference 9, p. 78-83). Shore Cliff Road was constructed on engineered fill benched into marine-terrace and debris-flow fan deposits directly east of the slide. Cracks within Shore Cliff Road suggest that the landslide may be encroaching headward beneath the road. The landslide is approximately 125 ft long, 400 ft wide, and 50 ft deep. The slide occupies nearly the full height of the bluff face, which is inclined about 1.3:1 (H:V).

Slide movement was first documented in 1970 by Harding Lawson Associates (HLA) (Reference 13). In 1970, the head scarp of the slide was approximately 15 ft south of the toe of the fill that supports Shore Cliff Road. In the 31 years since slide movement was first documented, the slide mass has been episodically reactivated by heavy rains and continued wave erosion at the toe of the slide along the base of the sea cliff.

Renewed activity of the landslide in the winter of 1996/1997 coincided with development of numerous en echelon cracks in the asphalt roadway and walkway along Shore Cliff Road. In the winter of 1999/2000, a water line separated beneath the paved roadway in the vicinity of the cracks. Comparison of pre- and post-construction topographic maps shows that the locations of these cracks coincide approximately with the contact between the road fill wedge and the underlying colluvium, suggesting that deformation in this area may be caused by fill settlement or creep. However, the arcuate pattern of the cracks and proximity to the Patton Cove landslide suggest that incipient landsliding is encroaching into the roadway. The cracks also are located in the general area of a crescent-shaped marine terrace riser mapped prior to road construction (Reference 4, Figure 2.5-8). The mapped terrace riser is more likely a subdued landslide headscarp.

To avoid the potential hazard of the landslide and unstable fill, the transport route will be constructed north of the existing road (Patton Cove Bypass, Figure 2.1-2), where the Patton Cove slide will pose no hazard (Section 2.6.1.12.3). The closest approach of the transport route will be about 100 ft north of the cracks at the intersection of Shore Cliff and Reservoir roads.

Significant movement of the upper Patton Cove landslide, if it occurs, will not impact the proposed transport route of the Patton Cove Bypass because its headward migration is limited by the depth of the slide, which is controlled by the elevation of the higher wavecut platform. The geometry of the landslide is such that it is unlikely to extend much farther landward because it would require either (a) an extremely low slide plane angle in the alluvial fan deposits or (b) a deeper slide plane that cuts through the bedrock materials. These scenarios are both considered to be very unlikely. The current head of the upper slide is located 110 ft from the edge of the proposed transport route. Continued movement of the lower slide, however, will probably continue to destabilize the upper slide and cause additional movements and increased cracking in Shore Cliff Road.

As discussed in SAR Section 2.2.2.3, a Cask Transportation Program will be developed and implemented to require a walkdown of the transportation route prior to any transport operations. This walkdown will ensure that no hazards are present from the Patton Cove landslide as evidenced by severe cracking of the roadway surface.

Additional information on the potential impact of the Patton Cove landslide on the transport route is provided in Reference 75 (PG&E Response to NRC Question 2-17).

An inclinometer was installed on the road shoulder closest to the slide in November 2000 to monitor the depth and rate of future movements. The inclinometer has recorded small movements near the contact between the base of the fill and the underlying colluvium and debris-flow deposits.

2.6.1.12.2 Landslide Potential at the ISFSI and CTF Sites

Detailed investigation of landslides in the plant site area (Reference 9) shows there are no existing deep-seated landslides or shallow slope failures at the ISFSI and CTF sites. Field mapping and interpretation of 1968 aerial photography (Figure 2.6-31) during the ISFSI site investigations confirmed the absence of deep-seated bedrock slides or shallow slope failures at the site.

Excavation of the existing slope at the ISFSI site was completed in 1971. No stability problems were encountered during excavation using bulldozers and scrapers, and the slope has been stable, with minimal surface erosion, since 1971. Prior to excavation of the slope, Harding Miller Lawson (HML) (Reference 9) described a shallow landslide in weathered bedrock (Figure 2.6-10) along a "shale seam" in their exploratory trench A (Reference 9, Plate D-3). This feature was less than 15 ft deep, and was removed entirely, along with underlying intact bedrock, to a depth of about 75 ft during excavation of the slope. Zones of "fractured, decomposed, and locally brecciated sandstone, siltstone, and shale" and "breccia and clay zones" described in HML trench A are interpreted to be friable dolomite zones and steep faults.

The Harding Miller Lawson landslide is apparent on 1968 black-and-white aerial photography, and is expressed by a subtle, arcuate headscarp, hummocky landscape, and locally thicker vegetation, probably reflecting high soil moisture within the slide debris (Figure 2.6-31). The slide was located along a slight swale in colluvial soils and possibly weathered bedrock that mantled the slope prior to excavation. The slide mass appears to have moved northeast along the axis of the swale, and not directly downslope. Because bedding is interpreted to dip to the northwest in this area, the landslide probably was not a bedrock-controlled failure. There is no evidence of deep-seated bedrock landslides on the 1968 aerial photographs; the ISFSI study area appears as a stable, resistant bedrock ridge in the photos.

Because surficial soils were removed from the ISFSI site area during past grading, there is no potential for surficial slides to adversely affect the site. There is no evidence of bedrock landslides below the ISFSI site or along the southern margin of Diablo Canyon near the raw water reservoir. Reservoir facilities (including the water treatment plant) and paved areas between the ISFSI and CTF sites and Diablo Canyon show no evidence of sliding or distress. Because the 290-foot Q_5 marine terrace is preserved locally across the ISFSI study area, it is apparent that no deep-seated bedrock slides have occurred since formation of the 430,000-year-old terrace, and the ridge is interpreted to be stable. Some shallow debris-flow failures and slumps were identified in surficial soil on the outermost 3 ft to 4 ft of weathered rock in the steep (45 to 65 degrees) slope below the raw water reservoir (Figure 2.6-7). These failures are shallow, and do not pose a stability hazard to the ISFSI or CTF sites, which are set more than 180 ft back from the top of the slope.

2.6.1.12.3 Landslide Potential Along the Transport Route

The transport route is located 100 ft north of the headscarp of the active Patton Cove landslide (Figure 2.6-7). Based on detailed mapping, borings, and an inclinometer, the landslide headscarp is defined by a series of cracks at the intersection of Shore Cliff and Reservoir Roads. A cross section through the landslide is shown in Figure 2.6-17. The geometry and depth of the slide plane indicate further headward encroachment of the landslide toward the transport route is not likely.

Where the transport route follows Reservoir Road at the base of the bedrock hillslope north from near Hillside Road, there are no bedrock landslides. Sandstone beds in the hillslope above the road dip obliquely into the slope at about 30 to 50 degrees (Figures 2.6-7, 2.6-11, and 2.6-19). These beds extend continuously across much of the hillside, providing direct evidence of the absence of bedrock slope failures (Figure 2.6-5). Small faults and joints in the rock mass do not appear to adversely affect potential slope stability, and the existing roadcut and natural slopes have no evidence of any slope failures.

Kinematic analyses of the bedding and fractures along the road were performed where the road borders the bedrock slope (Section 2.6.5.4.1). Two portions of the route were analyzed: a northern part from approximately station 43+00 to 49+00 (Figure 2.6-37), and a northwesterly stretch from approximately station 35+00 to 42+00 (Figure 2.6-38). The rock mass is stable against significant wedge or rock block failures; however, the analysis indicates that rock topple failure from the cutslope into the road is possible. Field evaluations indicate such failures would be localized and limited to small blocks. The existing drainage ditches on the inboard edge of the road would catch these small topple blocks.

Several colluvial or debris-flow swales are present above the transport route along Reservoir Road (Figures 2.6-5 and 2.6-7). These swales have been the source of past debris flows that primarily have built the large fans on the marine terraces over the past tens of thousands of years. Additional debris flows could develop within these swales during severe weather events, similar to those described elsewhere in the Irish Hills following the 1997 storms (Reference 8). Holocene debris-flow fan deposits extend to just below the road alignment, indicating that future debris flows could cross the road. However, large graded benches for an abandoned leach field system are present above a portion of the Reservoir Road, and concrete ditches and culverts are present in swale axes. These existing facilities will catch and divert much of the debris from future debris flows above the road. However, two debris-flow chutes are present above the road northwest of Hillside Road; this part of Reservoir Road is not protected from these potential debris flows. Based on the thickness of the colluvium in the swales (5 to 10 ft), and the slope profile, the maximum depth of debris on the road following severe weather is estimated to be less than 3 ft, which easily could be removed after the event.

2.6.1.13 Seismicity

A detailed analysis of the earthquake activity in south-central coastal California was presented in Reference 6. The report included the historical earthquake record in the region since 1800, instrumental locations from 1900 through May 1988, and selected focal mechanisms from 1952 to 1988. From October 1987 through May 1988, the earthquake catalog incorporated data recorded by the PG&E Central Coast Seismic Network (CCSN). This station network has operated continuously since then to monitor earthquake activity in the region.

The seismicity in the region is illustrated in two frames on Figure 2.6-39: (a) historical earthquakes of magnitude 5 and greater since 1830, and (b) instrumentally recorded seismicity of all magnitudes from 1973 through September 1987. Epicentral patterns of the microearthquakes (Figure 2.6-39) show that most of activity within the region occurs to the north, beneath the Santa Lucia Range and north of San Simeon, and in the southern onshore and offshore region south of Point Sal. Earthquakes in the southern offshore region extend westward to the Santa Lucia Bank area. Within about 15 miles of the ISFSI, small, scattered earthquakes occur between the Los Osos fault and faults of the Southwest Boundary fault zone (including the Irish Hills subblock (Section 2.6.1.3), in the nearshore region within Estero Bay, and along the Hosgri fault zone. Focal mechanisms along the Hosgri fault zone show right-slip displacement along nearly vertical fault planes (Reference 6, Figures 2-30 and 2-36).

McLaren and Savage (Reference 14) updated the earthquake record and present well-determined hypocenters and focal mechanisms for earthquakes recorded from October 1987 through January 1997 by the CCSN and by the U.S. Geological Survey, from north of San Simeon to the southern region near Point Arguello (Figure 2.6-40). No significant earthquakes occurred during this time period, and no significant change in the frequency of earthquake activity was observed. The largest event recorded was the local (Richter) magnitude 5.1 (duration magnitude 4.7) Ragged Point earthquake on 17 September 1991 northwest of San Simeon (Figure 2.6-40 inset). The focal mechanism of this event is oblique thrust, typical of nearby recorded earthquakes. Earthquake data since January 1997 also do not show any significant change in the frequency or epicentral patterns of seismic activity in the region.

The seismicity data presented in Reference 14 is consistent with the LTSP observations and conclusions (Reference 6). Specifically:

- Epicentral patterns of earthquakes have not changed. As shown in Figure 2.6-40, microearthquakes continue to occur to the north, along a northwest trend to San Simeon, east of the Hosgri fault zone, and in the southern offshore region.

- Selected seismicity cross sections A-A' through D-D' along the Hosgri fault zone (Figure 2.6-41) show that onshore and nearshore hypocenters extend to about 12-kilometers depth, consistent with the seismogenic depth range reported for the region (Reference 6). Seismicity cross section B-B', across the Hosgri fault zone, shows the Hosgri fault zone is vertical to steeply dipping. The earthquakes projected onto cross sections C-C' and D-D' are evenly distributed in depth.

- Focal mechanisms along the Hosgri fault zone (Figure 2.6-42) are primarily strike slip, consistent with the LTSP conclusion that the Hosgri is a northwest-trending, vertical, strike-slip fault (Reference 6). Mechanisms from events within the Los Osos/Santa Maria domain show oblique slip and reverse fault motion, consistent with the geology.

- The location of the 1991 Ragged Point earthquake in the San Simeon region, as well as its size and focal mechanism, are consistent with previous earthquakes in the region.

2.6.2 VIBRATORY GROUND MOTIONS

2.6.2.1 Approach

10 CFR 72.102(f) states the following "The...DE for use in the design of structures must be determined as follows:

(1) For sites that have been evaluated under the criteria of Appendix A of 10 CFR 100, the DE must be equivalent to the safe shutdown earthquake (SSE) for a nuclear power plant."

Thus, DCPP ground motions are considered to be the seismic licensing basis, in accordance with 10 CFR 72.102(f), for the evaluation ISFSI design ground motions. Seismic analyses for the ISFSI used ground motions that meet or exceed the DCPP ground motions.

Vibratory ground motions were considered in the design and analyses (Section 8.2.1) of (1) the ISFSI pads, (2) the CTF, including the reinforced concrete support structure and structural steel, (3) the ISFSI casks and cask anchorage, (4) ISFSI pad sliding and cutslope stability, (5) transport route slope stability, and (6) transporter stability.

The approach used for developing the ground motion characteristics to be used for design and analysis of the ISFSI SSCs consisted of the following.

- Use the DCPP ground motions (Section 2.6.2.2) as the basis for developing the ISFSI design ground motions, in accordance with 10 CFR 72.102(f).

- Compare the earthquake source and distance and ISFSI site conditions with those at the DCPP to confirm the applicability of the DCPP ground motions to the ISFSI site.

- Because ISFSI pad sliding and cutslope stability, transport route slope stability, and transporter stability may be affected by longer-period ground motions than those characterized by the DCPP ground motions, develop appropriate response spectra for the analysis of these elements, conservatively taking into account the additional influence of near-fault effects, such as fault rupture directivity and fling, that have been recorded in recent large earthquakes.

- Develop, as necessary, spectra-compatible time histories for use in analyses and design.

2.6.2.2 DCPP Licensing-Basis Ground Motions

The basis for the DCPP design ground motions is discussed in the DCPP FSAR Update, Sections 2.5.2.9, 2.5.2.10, and 3.7.1. There are three design ground motions for the DCPP: the design earthquake (DE), DCPP FSAR Update, Figures 2.5-20 and 2.5-21; the double design earthquake (DDE), DCPP FSAR Update, Section 3.7.1.1; Reference 4; and the Hosgri earthquake (HE), DCPP FSAR Update, Figures 2.5-29 through 2.5-32, which was incorporated into the DCPP seismic design basis as part of the seismic reevaluation of applicable existing structures by PG&E, and is now required as part of the licensing basis at the plant.

As discussed in the DCPP FSAR Update, the seismic qualification basis for the plant is the original design earthquakes (DE and DDE), plus the HE evaluation, along with their respective analytical methods, acceptance criteria, and initial conditions. Future additions and modifications to the plant are to be designed and constructed in accordance with these seismic design bases. In addition, as discussed in the DCPP FSAR Update, certain future plant additions and modifications are to be checked against the insights and knowledge gained from the Long Term Seismic Program (LTSP) to verify that the plant's "high-confidence-of-low-probability-of-failure" (HCLPF) values remain acceptable (Reference 4). As part of the Long Term Seismic Program, response spectra were developed for verification of the adequacy of seismic margins of certain plant structures, systems, and components (Reference 6). The DE, DDE, HE, and LTSP spectra are defined for periods up to 1.0 second, 1.0 second, 0.8 second, and 2.0 seconds, respectively.

2.6.2.3 Comparison of Power Block and ISFSI Sites

The Diablo Canyon ISFSI site is located in the plant site area of the licensed DCPP; therefore, the applicability of the DCPP ground motions to the ISFSI site was evaluated by comparing the ground-motion response characteristics of the ISFSI site with those of the plant site, and by comparing the distance from the controlling seismic source to the plant with the distance from the controlling source to the ISFSI.

As described in Section 2.6.1.4.2 and shown in Figures 2.6-6 and 2.6-11, the power block and the ISFSI are sited on bedrock that is part of the same, continuous, thick sequence of sandstone and dolomite beds of unit b of the Obispo Formation. In the classification of site conditions used for purposes of ground-motion estimation, both of these sites are in the "rock" classification (Reference 12).

Shear-wave velocity profiles from both sites are compared in Figure 2.6-35. As these comparisons indicate, shear-wave velocities from surface refraction and borehole geophysical surveys at the ISFSI site are within the same range as those obtained at the power block site. The velocity profiles at both sites are consistent with the "rock" classification for purposes of ground-motion estimation (Reference 12).

The earthquake potential of the significant seismic sources in the region was characterized during development of the DCPP FSAR Update and the Long Term Seismic Program (Reference 6). The Hosgri fault zone, at a distance of 4.5 kilometers, was assessed to be the controlling seismic source for the DCPP (Reference 4, Sections 2.5.2.9 and 2.5.2.10; Reference 6, Chapters 3 and 4). The ISFSI is approximately 800 ft to 1,200 ft east of the power block, and is thus only slightly farther from the Hosgri fault zone (Figure 2.6-4).

Therefore, because both sites are classified as rock, and because within the rock classification they have similar ranges of shear-wave velocities, and the distance to the controlling seismic source is essentially the same, the DCPP ground motions are judged to be applicable to ISFSI design.

2.6.2.4 Spectra for ISFSI Pads, Casks and Cask Anchorage, and CTF

The DE, DDE, HE, and LTSP spectra (Figures 2.6-43 and 2.6-44; the DE is one-half the DDE and is not shown) are applicable to the analysis of the pads, casks and cask anchorage, and CTF (Reference 55) (Section 8.2.1.2).

For cask anchorage design, the design spectra were defined by the HE spectrum for periods up to 0.8 second, and the LTSP spectrum for periods up to 2.0 seconds. New three-component, spectrum-compatible time histories were developed for the HE and LTSP by modifying recorded ground motions using the spectral matching procedure described by Silva and Lee (Reference 15). The recorded time histories used in the spectral matching were selected based on their similarity to the DDE, HE and LTSP earthquakes. The NRC Standard Review Plan spectral matching criteria (Section 3.7.1, NUREG-0800) were followed for 4-percent, 5-percent, and 7-damping; however, the NUREG requirement for a minimum value for the power spectral density (PSD) based on an NRC Regulatory Guide 1.60 spectral shape is not applicable to the spectral shapes of the HE or LTSP. The objective of the minimum PSD requirement was met by requiring the spectrum of each time history to be less than 30 percent above and 10 percent below the target spectrum. This ensures that no Fourier amplitudes are deficient in energy for the frequency range of interest.

2.6.2.5 ISFSI Long-Period Earthquake (ILP) Spectra and Time Histories For Pad Sliding, Slope Stability, and Transporter Stability Analyses

Because ISFSI pad sliding and cutslope stability, transport route slope stability, and transporter stability may be affected by longer-period ground motions than those characterized by the DCPP ground motions, PG&E has developed longer-period spectra and associated time histories for the analysis of pad sliding, slope stability, and transporter stability (References 54, 56, 57, and 58). These are referred to as the ISFSI long period (ILP) ground motions (Figures 2.6-45 and 2.6-46). The ILP spectra represent 84th percentile horizontal and vertical spectra, at damping values of 2 percent, 4 percent, 5 percent, and 7 percent, that extend out to a period of 10 seconds.

New information has become available from analytical studies of near-fault strong-motion recordings of large earthquakes in the past decade to evaluate the influence of near-fault effects, such as fault rupture directivity and tectonic deformation (fling), especially on ground motions in the longer-period range. PG&E has incorporated the influence of rupture directivity and fling in the ILP spectra and time histories (References 54, 56, 57, and 58) used for the analyses of pad sliding, slope stability, and transporter stability.

Development of the ILP horizontal spectra (Figure 2.6-46) incorporated the following assumptions and considerations:

- Although the LTSP (Reference 6) considered alternative styles of faulting for the Hosgri fault zone, the weight of the evidence favored strike-slip, and subsequent earthquake data and geologic and geophysical data interpretations (References 14 and 16) indicate the style of faulting is strike slip. Therefore, ground-motion characteristics appropriate for strike-slip earthquakes were used.

- The effect of directivity was analyzed for the case in which rupture begins at the southern end of the Hosgri fault zone, progresses 70 kilometers to the northwest where it passes at a closest distance of 4.5 kilometers from the plant site, and continues an additional 40 kilometers to the northwest end of the Hosgri fault zone. This assumption is conservative, because this rupture scenario has the greatest directivity effects at the site.

- The ILP horizontal spectrum at 5-percent damping at periods less than 2.0 seconds envelopes the DDE, HE, and LTSP spectra.

- The spectrum based on the Abrahamson and Silva (Reference 17) attenuation relation is consistent with the envelope of the DDE, HE, and LTSP spectra at 2 seconds, and has the same slope-with-period as the Sadigh (Reference 18) and Idriss (References 19, 20, and 21) attenuation relations, so it was used to extrapolate the envelope spectrum to 10 seconds. This spectrum is the 84th percentile horizontal spectrum.

- The 5-percent-damped horizontal spectra were increased to assure they envelope the Hosgri spectra at 4-percent and 7-percent damping ratios. Scaling factors for computing spectra at damping values other than 5 percent are from Abrahamson and Silva (Reference 17).

- Abrahamson's (Reference 22) and Somerville and others' (Reference 23) models were used to scale the average horizontal spectrum, to compute the fault-normal and fault-parallel ground-motion components, incorporating directivity effects.

- The fault-normal component was increased in the period range of 0.5 second to 3.0 seconds to account for possible directivity effects for earthquakes having magnitudes less than 7.2 at periods near 1 second.

- Because fling can occur on the fault-parallel component for strike-slip faults, a model was developed (Reference 57) to compute the 84th percentile ground motion due to tectonic fling deformation at the ISFSI accompanying fault displacement on the Hosgri fault zone in a magnitude 7.2 earthquake. The fling arrival time was selected, and the fling and the transient fault-parallel ground motion were combined so as to produce constructive interference of the fling and the S-waves, resulting in a conservative fault-parallel ground motion.

Development of the ILP vertical spectra (Figure 2.6-46) incorporated the following assumptions and considerations:

- The ILP vertical spectrum at 5-percent damping at periods less than 2 seconds is defined by the envelope of the DDE, HE, and LTSP (Reference 4) spectra.

- Current empirical attenuation relations (References 17, 18, and 24) were used to estimate the vertical-to-average-horizontal ratio for periods greater than 2 seconds; the value of two-thirds is conservative. The envelope vertical spectrum at 5-percent damping at periods less than 2 seconds was extended to a period of 10 seconds using two-thirds the average horizontal spectrum.

- The 5-percent-damped vertical spectra were increased to assure they envelop the Hosgri spectra at 4 percent and 7 percent damping ratios. Scaling factors for computing spectra at damping values other than 5 percent are from Abrahamson and Silva (Reference 17).

Five sets of spectrum-compatible acceleration time histories were developed to match the ILP ground motions spectra (References 56 and 58). The recordings in the table below were selected because they are from strike-slip earthquakes of magnitude 6.7 or greater, recorded at distances less than 15 kilometers from the fault, and contain a range of characteristics of near-fault ground motions.

Earthquake	Magnitude	Recording	Distance (km)	Site Type
1992 Landers	7.3	Lucerne	1.1	Rock
1999 Kocaeli	7.4	Yarimca	8.3	Soil
1989 Loma Prieta	6.9	DCPP	6.1	Rock
1940 Imperial Valley	7.0	El Centro #9	6.3	Soil
1989 Loma Prieta	6.9	Saratoga	13.0	Soil

The NRC Standard Review Plan spectral matching criteria (Section 7.1, NUREG-0800) recommends 75 frequencies for spectral matching. Augmented frequency sampling at 104 frequencies was used to account for the broader frequency range being considered for the ISFSI analyses. The interpolation of the response spectral values was done using linear interpolation of log spectral acceleration and log period. The NRC requirement permits not more than 5 of the 75 frequencies to fall below the target spectrum, and no point to fall below 0.9 times the target spectrum. This requirement was adhered to with the 104 frequencies.

The time histories were matched to the target spectra at 5-percent damping. The mean response spectrum of the five sets must envelop the target to meet the criteria of SRP 3.7.1. This criterion was applied to the damping values of 2 percent, 4 percent, 5 percent, and 7 percent.

The fault-parallel time histories were modified to include the effects of fling.

2.6.2.6 Transport Route and Transporter Design-Basis Ground Motions

As discussed in Section 2.6.1.9 and shown in Figures 2.6-6 and 2.6-7, the transport route is underlain by Obispo Formation bedrock consisting of unit b dolomite and sandstone (the same bedrock as at the power block and ISFSI sites), and unit c claystone and shale. Varying thicknesses of dense soil deposits overlie the bedrock.

Because the transport route is about the same distance from the Hosgri fault zone as the DCPP and the ISFSI sites, the ILP spectra are appropriate for use along the transport route where the route is constructed on bedrock and where the transport route crosses surficial deposits over bedrock (approximately two-thirds of the route)

(Section 2.6.1.9). An evaluation of the impact of a seismic event occurring during cask transport is discussed in Section 8.2.1.2.1.

2.6.3 SURFACE FAULTING

Potentially active faults at Diablo Canyon and in the surrounding region were identified and characterized in the DCPP FSAR Update, Section 2.5.3, the LTSP Final Report, Chapter 2, and the LTSP Addendum (Reference 7, Chapter 2). Together, these documents provide a comprehensive evaluation of the seismotectonic setting and location of capable faults in the plant site region, and document the absence of capable faults beneath the power block and in the plant site area. These studies used detailed mapping of Quaternary marine terraces and paleoseismic trenching to document the absence of middle to late Pleistocene faulting in the plant site area, including the ISFSI study area (Reference 6, p. 2-38, Plates 10 and 12). Hence, there are no capable faults at the ISFSI site.

Several minor bedrock faults were encountered in trenches at the ISFSI site during site characterization studies (described in Section 2.6.1.6.2.2). These faults are similar to minor faults that are commonly observed throughout the Miocene Obispo and Monterey formations in the Irish Hills (DCPP FSAR Update, Section 2.5.1; References 9 and 11). Similar minor bedrock faults encountered beneath the power block strike generally northwest to west, dip 45 degrees to 85 degrees, and have displacements of up to several tens of feet (Reference 4, Section 2.5.1.2.5.6, Figure 2.5-14).

The faults at the ISFSI site (Figure 2.6-8) are near-vertical (dip generally 70 to 90 degrees) and trend northwest, subparallel to the regional structural trend of the Pismo syncline (Figure 2.6-29). As described in Section 2.6.1.6.2.2, individual faults have vertical separation of a few tens of feet or less; cumulative vertical separation across the fault zone is greater than 50 ft, down on the northeast (Figure 2.6-11). Subhorizontal slickensides on the fault plane indicate a significant component of oblique strike slip, so total displacement is hundreds of feet. Detailed site investigations, including mapping and trench excavations, show that the individual faults generally extend across the ISFSI site and at least across the lower slope above the ISFSI.

The faults do not align with any significant bedrock fault in the plant site area (Figures 2.6-4 and 2.6-6), nor do the faults have major stratigraphic displacement. The origin of the faults may be related to one or more of three possible causes, all prior to 1 million years ago.

The faults most likely formed during a period of regional transtensional deformation during the Miocene, when normal and strike-slip faulting occurred in the region. This most directly explains the observed normal-oblique slip on the fault zone. A transition to transpressional deformation occurred during the late Miocene to Pliocene, and is well expressed in the offshore Santa Maria Basin and along the Hosgri fault zone (Reference 6). The minor bedrock faults at the ISFSI site were subsequently rotated during the growth of the Pismo Syncline, although the faults occur near the flat-lying crest of a small parasitic anticline and, thus, have not been rotated significantly. Given this origin, the faults formed during the Miocene, contemporaneous with the transtensional formation of Miocene basins along the south-central coast of California, prior to 5 million years ago.

Alternatively, the minor faults may be secondary faults related to growth of the regional Pismo syncline (Figure 2.6-4), as concluded for the small bedrock faults at the power block (Reference 4, p. 2.5-49, -50). As shown on Figure 2.6-29, the faults trend subparallel to the axis of the Pismo syncline, and are located near the crest of a small anticline on the southwestern limb of the syncline. The apparent oblique displacements observed on the faults may be related to bending-moment normal faults and right shear along the axial plane of the small anticline that formed in the Pliocene to early Quaternary. The zone of minor faulting may have used the area of diabase intrusion as an area of crustal weakness to accommodate tensional stresses along the axial plane of the anticline. As described in Reference 4, pages 2.5-14, -33, -34, and in the LTSP reports (Reference 6, p. 2-34 to -38; and Reference 7, p. 2-10), growth of the Pismo syncline and related folds ceased prior to 500,000 years to 1,000,000 years ago. Thus, the observed minor faults also ceased activity prior to 500,000 years to 1,000,000 years ago.

A third alternative explanation for origin of the minor bedrock faults is that they are related to intrusion of the diabase into the Obispo Formation. Diabase is present locally in the ISFSI study area. Forceful intrusion, or magmatic stoping of the diabase may have produced faulting in response to stresses induced by the magma intrusion in the adjacent host rock. Hydrothermal alteration is extensive in the diabase. The friable sandstone and dolomite in the ISFSI study area are spatially associated with the zone of faulting (Figures 2.6-8 and 2.6-11), indicating the faults may have acted as a conduit for hydrothermal solutions. Assuming the hydrothermal fluids were associated with the diabase intrusion, the minor faults predate, or are contemporaneous with, intrusion of the diabase. Diabase intrusion into the Obispo Formation occurred in the middle Miocene (References 10 and 11), indicating the faulting would have occurred prior to or contemporaneous with the diabase intrusion in the middle Miocene, more than 10 million years ago. The faulting may have originated by transtensional regional deformation, as described above, then subsequently was modified by diabase intrusion.

In addition to their probable origin related to transtensional deformation in the Miocene (or to growth of the Pismo syncline in the Pliocene to early Quaternary, or to intrusion of the diabase in the middle Miocene), several additional lines of evidence indicate the minor faults are not capable and do not present a surface faulting hazard at the site:

- As described in the Reference 6, pages 2-37 to -39, Plates 10 and 12), the Quaternary marine terrace sequence in the plant site vicinity is not deformed, providing direct stratigraphic and geomorphic evidence demonstrating the absence of capable faulting. The minor faults observed at the ISFSI site project northwest across, but do not visibly displace, any of the lower marine terrace platforms, within a limit of resolution of ±5 ft, indicating the absence of deformation in the past 120,000 years. Assuming the displacement does not die out at the coast, this resolution is enough to recognize the greater-than-50-ft of vertical separation on the faults at the ISFSI site.

- As described in Reference 4, p. 2.5-35 to -50, Figures 2.5-13 to 2.5-16, similar northwest-trending minor faults were mapped in bedrock in the power block area. Detailed trenching investigations of these faults and mapping of the power block excavation provided direct observation that they do not displace and, hence, are older than the late Pleistocene (120,000 years old) marine terrace deposits. By analogy, the minor faults at the ISFSI site also would be older than late Pleistocene.

- Interpretation of aerial photographs taken before the 1971 excavation of the ISFSI site area (former borrow area) and construction of the raw water reservoir (Figure 2.6-31), shows there are no geomorphic features in the ISFSI study area (tonal lineaments, drainage anomalies, scarps) indicative of displacement of the minor faults prior to grading. The landscape in the ISFSI study area is interpreted to have formed in the middle to late Quaternary, about 430,000 years ago, based on the preserved remnants of marine terraces in the surrounding site area.

Based on these lines of evidence, the minor faults observed in bedrock at the ISFSI site are not capable; hence, there is no potential for surface faulting at the ISFSI site.

2.6.4 STABILITY OF SUBSURFACE MATERIALS

2.6.4.1 Scope

An extensive program of field investigations, in situ testing, and laboratory testing was conducted to define the static and dynamic characteristics of the soil and rock materials. The scope of the program is summarized in Table 2.6-1. A detailed discussion of the test procedures and results is presented in References 44, 45, and 48 through 51, Data Reports B, C, F, G, H, and I, and Reference 9. The results are summarized below.

2.6.4.2 Subsurface Characteristics

The geology at the subgrade of the foundation of the ISFSI pads (elevation about 302 ft, 8 ft below the pad grade) is shown in Figure 2.6-32. The subsurface beneath the ISFSI pads consists of dolomite (Tof_{b-1}), sandstone (Tof_{b-2}), friable dolomite (Tof_{b-1a}), and friable sandstone (Tof_{b-2a}) (Section 2.6.1.7). The bedrock contains minor faults and joints (Section 2.6.1.6.2). The groundwater table is near elevation 100 ft, about 200 ft below the foundation elevation. Clay beds of limited extent occur at a few locations under the ISFSI pads, below the surface of the cutslope, and in the existing slope above the pads (Section 2.6.1.7).

The geology at the CTF foundation grade is shown in Figure 2.6-32. At this grade (elevation about 286 ft), the bedrock consists of sandstone and friable sandstone (Section 2.6.1.8). At the site, the sandstone may have a few minor faults and joints, similar to those described in Section 2.6.1.6.2. Because the rocks are the same, the static and dynamic engineering properties of the rock at the foundation of the CTF were selected to be the same as those at the ISFSI pads.

The transport route traverses thick surficial deposits along nearly two-thirds of its route, including a new 500-foot-long section of thick, engineered fill near Patton Cove. It is constructed on engineered fill placed on dolomite and sandstone for the rest of its length (Section 2.6.1.9).

The detailed geologic characteristics of these rock units are described in Section 2.6.1.4.2.

2.6.4.3 Parameters for Engineering Analysis

2.6.4.3.1 ISFSI and CTF Sites

The static and dynamic engineering properties for use in foundation analyses of the rock at the ISFSI and CTF sites are as follows:

Density: A density of 140 pounds per cubic ft (pcf) was chosen as appropriate for foundation analyses (Reference 51, Data Report I).

Strength: A friction angle for the rock mass of 50 degrees was chosen as appropriate for foundation analyses. This friction angle is consistent with that used in the slope stability analyses (Section 2.6.5.1.2.3).

Poisson's ratio: A representative value of Poisson's ratio of 0.22 for dolomite and sandstone was selected as appropriate for analyses. A representative value of 0.23 was selected for friable rock. These values were derived from seismic velocity measurements in the bedrock below the footprint of the pads (Reference 59), and laboratory-based measurements (Reference 60) on samples of bedrock from beneath the pads (Reference 37 and Reference 51, Data Report I).

Young's modulus: Representative values of Young's modulus of between 1.34 times 10^6 psi (mean) and 2.0 times 10^6 psi (84^{th} percentile upper bound) for dolomite and sandstone were selected as appropriate for analyses. A representative value of 0.2 times 10^6 psi was selected for friable rock. These values were derived from seismic velocity measurements in the bedrock below the footprint of the pads (Reference 59), and laboratory-based measurements (Reference 60) on samples of bedrock from beneath the pads (Reference 37 and Reference 51, Data Report I).

2.6.4.3.2 Slopes

Static and dynamic engineering properties of soils and rock at the ISFSI site for use in slope stability analyses are as follows:

Rock Strength: A friction angle of 50 degrees for the rock mass was selected for stability analyses of the hillslope above the ISFSI pads. A range of friction angles between 16 degrees and 46 degrees for rock discontinuities was selected for stability analyses of the cutslopes behind the ISFSI pads. Further discussion of rock strength parameters is provided in Sections 2.6.5.1.2.3 and 2.6.5.2.2.3.

Clay Bed Strength and Unit Weight: The following parameters were defined for clay:

- unit weight, 115 pcf (Reference 49, Data Report G)
- shear strength, drained, $c' = 0$ psf; $ø' = 22$ degrees
- shear strength, undrained, lower of $c = 800$ psf and $ø=15$ degrees or $ø = 29$ degrees.

Further discussion of clay strength parameters is provided in Section 2.6.5.1.2.3.

Shear wave velocities: Representative values of shear wave velocities were selected for stability analyses (Section 2.6.5.1.3.2). These values were based on suspension geophysical surveys in boreholes beneath the footprint of the pads, as well as on data summarized in the Addendum to the LTSP Final Report (Reference 7, Chapter 5, Response to Question 19).

Dynamic shear modulus and damping values: Relationships of the dynamic shear modulus and damping values with increasing shear strain were selected for stability analyses (Section 2.6.5.1.3.2), based, in part, on literature review and dynamic tests of DCPP rock core samples performed in 1977 and 1988 (Reference 41).

Additional considerations for the selection of rock and clay properties for specific static and dynamic stability analyses, and the calculation of seismically induced displacements are presented in Section 2.6.5.1.3.

2.6.4.3.3 Transport Route

As described earlier, the transport route generally follows existing Plant View, Shore Cliff, and Reservoir roads (Figure 2.6-7). The specifications for the construction of these roads required all fills to be compacted to 90-percent relative density, and the upper 2.5 ft to be compacted to 95-percent relative density. Fills on slopes were benched and keyed a minimum of 6 ft into the hillside. Based on these requirements, the road base and subgrade material are expected to be at least as capable for transporter loads and earthquake ground motions as the underlying rock and soil.

The new section of the transport route near Patton Cove will be constructed on engineered fill, as will a section of the route near the CTF (Figure 2.6-7). These fills and the overlying road subgrade also will be constructed to the same specifications as the existing roads. Both new roadway sections will support the imposed loads.

Where the transport route follows Plant View, Shore Cliff and Reservoir roads to Hillside Road, the alignment is founded on marine terrace deposits overlain by dense colluvial deposits. The remaining portions of the route, on Reservoir Road (beyond station 34+00), are founded on cuts made in the dolomite and sandstone. The static and dynamic engineering properties of the rock and soil deposits underlying the transport route are summarized in Reference 9, Tables 1 and 2.

2.6.4.4 Static Stability

The ISFSI pads will be founded on dolomite, sandstone, friable dolomite, and friable sandstone (Figure 2.6-32). The CTF will be founded on sandstone and friable sandstone (Figure 2.6-32). This bedrock will support the proposed facilities without deformation or instability (References 61 and 71). The borrow excavation removed between 75 ft and 100 ft of rock from the ISFSI and CTF sites. As a result, the existing rock is overconsolidated, and facility loads are likely to be much less than the former overburden loading on the rock (calculated to be about 10,000 to 14,000 psf). The overconsolidated state of the rock mass in the foundation precludes any settlement, including differential settlement between rock types, under the planned loading conditions.

As discussed in the DCPP FSAR Update, Section 2.5.4, there are no mines or oil wells in the plant site area. The two makeup-water wells draw water from fractured bedrock that is fed groundwater from the shallow alluvium along Diablo Creek (Section 2.5). No subsidence has been observed, nor is any expected, near these wells, which are approximately 2,500 ft east of the ISFSI.

Similarly, there is no evidence of solution features or cavities within the dolomite and sandstone strata, or in the friable dolomite and friable sandstone, beneath the ISFSI, or in the plant site area. Hence, there is no potential for karst-related subsidence or settlement at the ISFSI or CTF sites.

There is no potential for differential settlement across the different rock units (sandstone, dolomite, friable sandstone, friable dolomite) at the ISFSI, because the rock is well consolidated, joints and fractures are tight, and the friable rocks have almost no joints. Although no piping voids in the friable rocks are expected beneath the ISFSI pads, very small voids (a few inches across) are possible, as found in the friable dolomite in one of the trenches (Reference 46, Data Report D, trench T-20A). The foundation will be below the dilated zone for the borrow area cutslope (observed to be at about 4 ft in the trenches), and the rock mass is expected to be tight, with no open fractures. The rock mass is also overconsolidated, having had 100 ft of rock overburden removed from the location of the borrow area in the vicinity of the ISFSI for construction of the raw water reservoir and the 230-kV and 500-kV switchyards (Figure 2.6-10).

There is no potential for displacement on the faults at the sites, because the faults are not capable (Section 2.6.3). No differential displacement or settlement is expected during potential ground shaking.

2.6.4.5 DYNAMIC STABILITY

The ISFSI is located entirely within bedrock. There are no loose, saturated deposits of sandy soil beneath the pads or CTF site, and the groundwater table is near elevation 100 ft, about 200 ft below the foundation level. Therefore, there is no potential for liquefaction at either site.

The CTF foundation will be embedded into rock at least 20 ft below grade, as shown on Figure 2.6-32. This precludes the development of unstable foundation blocks under static or dynamic loading conditions.

Because the transport route subgrade will be on engineered fill on rock and well-consolidated surficial deposits, no liquefaction or other stability problems are expected.

An analysis was performed to verify pad stability during an earthquake (Reference 72). This analysis included the inertial effects of the pad and pre-existing structures. Additional information is provided in Reference 75 (PG&E Response to NRC Question 2-16) and Reference 76 (PG&E Response to NRC Request 2).

2.6.4.6 POTENTIAL FOR CONSTRUCTION PROBLEMS

No significant construction-related problems are anticipated for preparation of the ISFSI and CTF foundations subgrade. The permanent groundwater table is about 200 ft below the planned foundation elevations (Section 2.5), and groundwater is not expected to rise to within the zone of foundation influence. The rock mass is generally tight, and does not have significant voids or soft zones that would require grouting or dental work, with the possible exception of small piping voids related to the friable dolomite. The fractures are tight or filled, and are tightly confined by the surrounding competent rock. The prepared foundation pads will be level, and will be a considerable distance from descending slopes, thus precluding development of unstable blocks or foundation loads into slopes.

2.6.5 SLOPE STABILITY

The ISFSI is located on the lower portion of a hillslope that has been modified by excavation for borrow materials during the construction of the DCPP. Construction of the ISFSI pads, the CTF, and portions of the transport route will include cutslopes and fills. The purpose of this section is to examine the stability of the hillslope and the cuts and fills. For each slope, the static and seismic stability were analyzed, and the potential seismically induced displacements were estimated.

The analyses, which are summarized in Table 2.6-2, show that the hillslope and the cutslopes above the ISFSI are generally stable under modeled seismic inputs, slope geometries, and material properties. The seismically induced displacements of the rock mass above the ISFSI, estimated using very conservative assumptions, are small. Under the modeled seismic loads, small rock wedges appear to be susceptible to movement in the cutslopes around the pads. These potential hazards will be mitigated by setbacks in slope design, rock anchors, and debris fences, as discussed in Section 4.2.1.1.9.1. The slopes along the transport route and below the CTF are stable.

For each slope analysis, the objectives and scope of the stability analysis are defined, and the analysis methods are described. The slope geometry and selection of material properties are then given. Finally, the results of the analyses for the hillslope above the ISFSI, the ISFSI cutslopes, the slope below the CTF, and slopes along the transport route are presented.

2.6.5.1 Stability of the Hillslope above the ISFSI

A critical section of the hillslope above the ISFSI was analyzed to examine the static and dynamic stability of the jointed rock mass along postulated slide surfaces. Analyses also were conducted to estimate potential seismically induced displacements due to the vibratory ground motions derived in Section 2.6.2. In addition, an analysis was conducted to evaluate the conservatism of the analysis parameters and examine the geologic data to estimate past displacements due to earthquakes. In Reference 76 (PG&E Response to NRC Request 3), PG&E has performed additional evaluations to address: (a) the potential for a generalized slip-circle type failure of the cutslopes and hill slope above the ISFSI and (b) the effect of the cutslope (i.e., the proposed excavation for construction of the ISFSI) on the stability of the hill slope above the ISFSI. The results of the evaluations found that the clay bed failure of the slopes governed the design and the effect of the cutslope on slope stability was minimal.

2.6.5.1.1 Geometry and Structure of Rock Mass Slide Models

Cross section I-I' (Figure 2.6-18) parallels the most likely direction of potential slope failure, and illustrates the geometry of bedding in the ISFSI study area for analysis of slope stability. The cross section shows apparent dips, and the facies variation and interfingering of beds between the dolomite and sandstone (units Tof_{b-1} and Tof_{b-2}) beneath the slope. The clay beds, where orientation and extent are critical to this evaluation of slope stability, have been correlated based on stratigraphic position, projection of known bedding attitudes, and superposition of sandstone and dolomite beds (clay beds have not been allowed to cross cut dolomite or sandstone beds, but have been allowed to cross facies changes). These clay beds, as drawn, are a conservative interpretation of their lateral continuity for the analysis of the stability of the slope.

Individual clay beds that are, in places, thick (more than about 0.5-inch thick) in the dolomite, may continue up to several hundred feet. Thinner clay beds are less laterally continuous. On cross section I-I' (Figure 2.6-18), clay beds are not shown to extend continuously through the slope, but are terminated at set distances from exposures in boreholes, trenches, or outcrops, reflecting the estimates of possible lateral continuity. Because of the generally limited lateral continuity of the clay beds, potential large surfaces (greater than several hundred feet in maximum dimension) likely would require sliding on several clay beds, and stepping between beds on joints and in places through rock in a "staircase" profile. Stepping between basal clay failure surfaces would probably be localized where the individual clay beds are stratigraphically close and are thin and pinch out. Other likely locations for stair-stepping failure or structural boundaries for possible rockslide margins are at changes in structural orientation (transitions from monocline to syncline), and along the lateral margins of the slide. These limit the size of potential rock masses. Faults at the site are subparallel to the potential down-slope motion, and impart a strong near-vertical fabric in the rock mass. It is likely that lateral margins for potential larger rockslides would develop, at least partially, along these faults.

Based on the above considerations, three rock mass slide models, comprising ten potential slide surfaces, were defined for cross section I-I' of the hillslope:

Model 1. A shallow slide mass model (Figure 2.6-47) involving sliding rock masses along shallow clay beds encountered in trench T-14A and boring 01-I. It toes out at the upper part of the tower access road.

Model 2. A medium-depth slide mass model (Figure 2.6-48) involving sliding rock masses along clay beds encountered at depths of between about 25 ft and 175 ft in borings 01-F, 00BA-1, and 01-I, and trench T-11D. It toes out on the slope between the ISFSI and below the tower access road.

Model 3. A deep slide mass model (Figure 2.6-49) involving sliding along deep clay beds encountered in borings 01-H, 01-F, 00BA-1, and 01-I at depths of between about 50 ft and 200 ft. It toes out behind or below the proposed ISFSI cutslope and pads.

Model 1 has been segmented into two possible geometries, labeled 1a and 1b on Figure 2.6-47. These two modeled slide blocks daylight at a clay bed encountered in trench T-14A (model 1a), or along the projected dip of a clay bed encountered in boring 01-I. The failure headscarp/tension break-up zone extends upward from the inferred maximum upslope extent of the clay bed in trench T-14A (model 1a), or from the inferred likely uphill extent of a clay bed encountered in boring 01-I.

Model 2 has been segmented into three subblocks: 2a, 2b, and 2c (Figure 2.6-48). The three blocks daylight along a clay bed encountered in trench T-11D (2a and 2b), or along the dip projection of a clay bed encountered in boring 00BA-1 (2b). Model 2a breaks up near trench T-14A at the location of a major structural discontinuity for potential slide blocks; the transition between the monocline and syncline where the bedding geometry (strike and dip) changes. Models 2b and 2c break up from the basal failure planes in a "stair-stepping" manner between clay beds, and have a common headscarp that daylights about 50 ft above the brow of the 1971 borrow cut excavation. The geometry of the headscarp break-up zone is inferred to be controlled by the uphill limit of clay beds encountered in the borings, and dominant steep joint fabric in the rock mass.

Model 3 has been segmented into three subblocks: 3a, 3b, and 3c. The three blocks daylight in the ISFSI pads cutslope, or at the base of the cutslope (Figure 2.6-49). All three modeled blocks have basal slide surfaces along clay beds encountered in borings 01-F, or 00BA-1 and 01-I. Models 3a and 3b break up with headscarp/tension zones at the location of the structural change in bedding geometry described for model 2a (3a and 3b), or about 75 ft above the top of the borrow cut (3c) at an inferred maximum uphill extent of clay beds encountered in boring 01-I. Model 3 has been further segmented into 3c-1, which daylights beyond the ISFSI pads, and 3c-2, which daylights at the base of the first cutslope bench.

For all models, the toe daylight geometry reflects the propensity for failure planes to break out along bedding planes and along the projection of clay beds. In contrast, the geometry of the headscarp/tension failure was inferred to be controlled by the dominant steep (greater than 70 degrees) joint/fault fabric in the rock mass.

2.6.5.1.2 Static Stability Analysis

2.6.5.1.2.1 Method

The static stability analysis of the hillslope was conducted using the computer program UTEXAS3 (Reference 26). Spencer's method, a method of slices that satisfies force and moment equilibria, was used in the analysis.

2.6.5.1.2.2 Assumptions

The following assumptions were made:

- The clay beds are saturated. This assumption is reasonable, because during the rainy season, rainfall would infiltrate the slope through the fractured rock and perch temporarily on the clay beds, and would saturate at least the upper part of the clay.

- There is little water in the slope. This assumption is reasonable, because the groundwater table is about 200 ft below the ISFSI site, and the rock is fractured and well-drained. There are no springs from perched water tables near the ISFSI slope.

- The lateral margins of the potential slide masses have no strength. This is conservative, because the margins of a potential failure wedge would, in part, follow discontinuous joints, small faults, and, in part, break through rock. Friction between rock surfaces and by asperity overriding, or shearing along the lateral slide margins would provide some resistance to sliding.

- The upper 20 ft of the rock mass forming the head of a potential sliding mass has been modeled as a tension crack, that is, the zone has been given no strength. This assumption is conservative, because the dilated zone is only about 4 ft deep (Reference 37).

- The head of the slide below the tension crack would break irregularly along joints and clay beds and through some rock. The strength assigned to this rock mass is discussed below.

- The orientation, continuity, and extent of the clay beds is assumed to be as shown on cross section I-I'. This is reasonable, because the extent of the clay beds and their dip is based on extensive geologic data from the ISFSI study area.

- The strength of the clay (discussed below) is assumed to apply along the entire length of a clay bed, as shown on cross section I-I'. This is conservative, because the clay beds are commonly thin and irregularly bedded, providing rock contact through the beds, thereby increasing the strength.

2.6.5.1.2.3 Material Properties

Drained and undrained clay-bed strength parameters were developed from the results of strength and index testing performed on clay-bed samples collected from borings and trenches excavated at the site. Strength tests consisted of consolidated-undrained triaxial compression tests (CU) with pore pressure measurements, drained and undrained monotonic direct-shear tests, and undrained cyclic direct-shear tests (Reference 49, Data Report G). Atterberg limits tests were conducted on the clay-bed samples to measure their liquid limits (LL) and plasticity indices (PI). Drained strength parameters were developed from the results of the CU triaxial and drained monotonic direct-shear tests, and from published empirical correlations with Atterberg limits. Drained strength was taken as the post-peak strength (defined as strength at the maximum displacement) from the drained direct-shear tests, and the lower of either the stress at 5 percent axial strain or the post-peak strength for the CU tests. Undrained strength parameters were developed from the results of the CU triaxial, undrained monotonic and cyclic direct-shear, and Atterberg limits tests. As with the drained strength parameters, the undrained strength was taken as post-peak strength from the monotonic direct-shear tests, and the lower of either the stress at 5 percent axial strain or the post-peak strength for the CU tests.

Undrained strength parameters c = 800 psf and ø = 15 degrees were determined from analysis of the undrained strength data (Figure 2.6-50). Similarly, c' = 0 psf, and ø' = 22 degrees were selected based on analysis of the drained strength data (Figure 2.6-51). Because the overburden pressure under the original ground surface is higher than the consolidation pressure used in most of the laboratory strength tests, overconsolidation effects are likely present in the laboratory test results. This effect was conservatively removed at low confining pressures by estimating corresponding undrained shear strengths for a maximum overconsolidation ratio (OCR) of 3.0 and determining an equivalent friction angle, as shown in Figure 2.6-50, of 29 degrees (with no cohesion). Accordingly, undrained strength parameters were selected as the lower of ø = 29 degrees and ø = 15 degrees (Figure 2.6-50). Strength envelopes for the clay beds are described in Reference 73.

An expanded description of the development of clay bed strength is provided in Reference 76 (PG&E Response to NRC Request 3).

Two different empirical methods were used to develop in situ rock mass strength envelopes for the dolomite and sandstone (units Tof_{b-1} and Tof_{b-2}): Barton and Choubey (Reference 27), and Hoek and Brown (Reference 28).

The Barton-Choubey method estimates the in situ shear strength of naturally occurring rock discontinuities (joints, bedding planes, faults) in relatively hard rock on the basis of field and laboratory measurements of discontinuity properties. Mean and standard deviation determinations of unconfined compression strengths for hard rock at the DCPP ISFSI are provided in Reference 63. The base friction angle along rock discontinuities based on laboratory tests (Reference 62) was used as input for the Barton-Choubey method. Shear strength envelopes for discontinuity surfaces within the shallow rock mass at the ISFSI site were used in the stability analyses of surficial rock mass sliding, wedge, and topple slope failures in the proposed cutslope above the ISFSI, and frictional sliding along shallow rock discontinuities below the foundation of the ISFSI pads. The range of strength envelopes for dolomite (Tof_{b-1}) and sandstone (Tof_{b-2}) discontinuities calculated using the Barton-Choubey method (Reference 64) are plotted in Figure 2.6-52, using the derived stress-strain data.

The Hoek-Brown method is an empirically based approach that develops nonlinear shear-strength envelopes for a rock mass, and accounts for the strength influence of discontinuities (joints, bedding planes, faults), mineralogy and cementation, rock origin (for example, sedimentary or igneous), and weathering. The resulting rock-mass shear-strength envelopes were used for evaluation of the ISFSI pads and CTF foundation properties, and for stability analyses of potential bedrock failures within jointed confined rock at the ISFSI site. The Hoek-Brown method is for rock masses having similar surface characteristics, in which there is a sufficient density of intersecting discontinuities such that isotropic behavior involving failure along multiple discontinuities can be assumed. The method is not for use when failure is anticipated to occur largely through intact rock blocks, or along discrete, weak, continuous failure planes (such as weak bedding interfaces). The structure (or failure) geometry must be relatively large with respect to individual block size. The rock mass conditions and relative size differences between rock blocks, potential deep-seated masses, and the ISFSI and CTF foundations for which the Hoek-Brown criterion is being applied are appropriate and meet these rock-mass requirements. Strength envelopes for dolomite and sandstone calculated using the Hoek-Brown method (Reference 65) are plotted in Figures 2.6-53 and 2.6-54, using the derived stress-strain data.

A strength envelope having a friction angle, ø, of 50 degrees and cohesion, c, of zero was selected for the portion of the rock mass consisting of dolomite (unit Tof_{b-1}) and sandstone (Tof_{b-2}) below the dilated zone (Figures 2.6-53 and 2.6-54) (Reference 65). This envelope is lower than (but approximately parallel to) the envelopes for either dolomite or sandstone derived from the empirical Hoek-Brown method, and is more nearly equal to the post-peak strength envelope for the friable sandstone derived from laboratory tests of nonjointed rock blocks. The interpreted post-peak strength envelope for the friable rocks has a friction angle, ø, of 51.2 degrees and cohesion, c, of zero (Figure 2.6-55) (Reference 49). Accordingly, a ø of 50 degrees was also selected for the friable rocks.

Reference 76 (PG&E Response to NRC Request 1) provided additional justification for the rock mass strength material properties developed using the Hoek-Brown methodology.

2.6.5.1.2.4 Results

The static factors of safety computed using UTEXAS3 (Reference 26) for the ten slide surfaces analyzed are shown in Table 2.6-3 (Reference 68). The table shows that, in all cases, the computed factor of safety varies between 1.62 and 2.86. It is, therefore, concluded that the hillslope is stable.

2.6.5.1.3 Seismically Induced Displacements

2.6.5.1.3.1 Method

The selected slide surfaces were analyzed to estimate the potential for earthquake-induced displacements by using the concept of yield acceleration proposed by Newmark (Reference 29) and modified by Makdisi and Seed (Reference 30). The procedure used to estimate permanent displacements involved the following steps:

- A yield acceleration, k_y, at which a potential sliding surface would develop a factor of safety of unity, was estimated using limit-equilibrium, pseudostatic slope-stability methods. The yield acceleration depends on the slope geometry, the phreatic surface conditions, the undrained shear strength of the slope material, and the location of the potential sliding surface.

- Computations were made using UTEXAS3 (Reference 26) to identify sliding masses having the lowest yield accelerations. A two-stage approach was used that consisted of first calculating the normal stresses on the failure plane under pre-earthquake (static) loading conditions using drained strength properties. For each slice, the normal effective stress on the failure plane was then used to calculate the undrained strength on the failure plane. In the second stage of the analysis, horizontal seismic coefficients were applied to the potential sliding mass, and the stability analysis was repeated using the undrained strengths calculated at the end of the first stage. The yield acceleration was calculated by incrementally increasing the horizontal seismic coefficient until the factor of safety equaled unity.

  The material properties used for the UTEXAS3 analysis (unit weights and shear strength) were the same as those for the static stability calculations. Drained rock strengths were used for both stages of the yield acceleration analysis. Drained clay strengths were used for the first stage and a bilinear undrained strength envelope was used for the clay beds in the second stage of the analysis.

- The seismic coefficient time history (and the maximum seismic coefficient, kmax) induced within a potential sliding mass was estimated using two-dimensional, dynamic finite-element methods. The seismic coefficient is the ratio of the force induced by an earthquake in a sliding block to the total mass of that block. Alternatively, the seismic coefficient time history can be obtained directly by averaging acceleration values from several finite-element nodes within the sliding block at each time interval, as long as variations in the accelerations between nodes are not substantial. Development of seismic coefficient time histories is further discussed in Reference 76 (PG&E Responses to NRC Requests 4 and 7).

- Earthquake-induced seismic coefficient time histories (and their peak values, kmax) for the potential sliding surfaces were computed using the two-dimensional, dynamic finite-element analysis program QUAD4MU (Reference 31). This is a time-step analysis that incorporates a Rayleigh damping approach, and allows the use of different damping ratios in different elements. The program uses equivalent linear strain-dependent modulus and damping properties, and an iterative procedure to estimate the nonlinear strain-dependent soil and rock properties.

- The QUAD4MU program (Reference 31) was used to analyze three slide surfaces (1b, 2c, and 3c) for which the calculated yield acceleration values were the lowest (Table 2.6-3). Because the base of the finite element mesh is at a depth of 300 ft, and because QUAD4MU only allows the input motion to be applied at the base, the base motion was first computed by deconvolving the surface ground motion using a one-dimensional wave propagation analysis (SHAKE, Reference 32) to obtain motions at the level of the base of the two-dimensional finite-element model.

- For a specified potential sliding mass, the seismic coefficient time history of that mass was compared with the yield acceleration, ky. When the seismic coefficient exceeds the yield acceleration, downslope movement will occur along the direction of the assumed failure plane. The movement will decelerate and will stop after the level of the induced acceleration drops below the yield acceleration, and the relative velocity of the sliding mass drops to zero. The accumulated permanent displacement was calculated by double-integrating the increments of the seismic coefficient time history that exceed the yield acceleration.

Reference 75 (PG&E Response to NRC Question 2-18) provided the results of a two-dimensional FLAC analysis that was performed to demonstrate the reasonableness of the displacements calculated using the described Newmark-type approach.

2.6.5.1.3.2 Material Properties

The material properties needed for the QUAD4MU analyses are the unit weight, the shear modulus at low shear strain, G_{max}, and the relationships describing the modulus reduction and damping ratio increase with increasing shear strain (Reference 40, , Figures 7 and 8). The rock mass was modeled as having a unit weight and shear wave velocity that vary with depth, based on field measurements of shear wave velocity and laboratory values for unit weight. The shear wave velocity profile used is shown in Reference 40, Figure 6.

2.6.5.1.3.3 Seismic Input

The seismic input consisted of the five sets of time histories developed to match the ILP ground-motion spectra (Section 2.6.2.5). Both fault-parallel and fault-normal components were defined for each of the five motions postulated to occur on the Hosgri fault zone at a distance of 4.5 kilometers from the site. Because the strike of the Hosgri fault zone is 36 degrees from the orientation of cross section I-I', the input motions were rotated to the direction of cross section I-I'. For a specified angle of rotation, there will be 10 rotated earthquake motions along I-I', because the fault-normal component will be either positive (to the east) or negative (to the west) and each needs to be considered separately.

2.6.5.1.3.4 Analysis

Acceleration time-histories were calculated for 26 locations within the three selected slide surfaces (1b, 2c, and 3c) (Reference 41, Figure 2). Average acceleration time histories were computed for each rock mass. Sensitivity studies using a cross section having a slightly different orientation indicated that the calculated peak accelerations are not significantly influenced by orientation or the total height of the hillslope.

Because the slope at the ISFSI site is a rock slope and its seismic response is anticipated to be generally similar to the input rock motions, the earthquake-induced deformation was first estimated using a Newmark-type analysis for a sliding block on a rigid plane (Reference 29). An estimated yield acceleration of 0.20 g (Table 2.6-4) was used to calculate the deformation of the sliding block. The displacement was computed for the negative direction (representing down-slope movement) only. The down-slope permanent displacement of the sliding block was integrated by using rock motions in the positive direction (representing up-slope direction) only. These preliminary displacement estimates were used to help in selecting the ground-motion time histories that provided the largest permanent displacement.

Table 2.6-4 shows the calculated down-slope permanent displacements (for the five sets of rotated rock motions) following the Newmark sliding block approach. The results (for a rotation angle ø = 36 degrees) indicate that, on average, ground-motion sets 1, 3, and 5 provided the largest displacements (2.4 ft to 2.9 ft). A sensitivity analysis was performed to evaluate the effect of the uncertainty in the direction of cross section I-I' (Figure 2.6-18) relative to the fault strike (Figure 2.6-29). For this analysis, ø was varied by ±10 degrees. As shown in Table 2.6-4, for a ø of 46 degrees, ground-motion set 1 (with a negative fault-normal component) and set 5 (with a positive fault-normal component) produced the largest displacements (3.3 ft and 2.8 ft, respectively). This is because the fault-normal components are stronger than the fault-parallel components in most cases, and for a ø of 46 degrees, the I-I' direction is closer to the fault-normal direction. Set 3, when combined with the negative fault-normal component, produced 2.8 ft of displacement; however, when combined with the positive fault-normal component, produced a much smaller displacement than that of set 5. Based on the rigid sliding block analyses, two rotated ground motions: set 1 motions (rotated 46 degrees with a negative fault-normal component) and set 5 motions (rotated 46 degrees with a positive fault-normal component) were used in the two-dimensional finite-element analyses (Reference 40).

The potential sliding masses and the node points of the computed acceleration time histories were used to develop average-acceleration time histories for each sliding mass. The seismic coefficient time histories were then double integrated to obtain earthquake-induced displacements for any specified yield acceleration. As mentioned before, the integration was made for the ground-motion amplitudes exceeding the yield acceleration in the positive direction only, and the resulting displacement was computed for potential sliding in the down-slope direction. The relationships between calculated displacement and yield acceleration, k_y, for the three potential sliding masses considered are presented in Reference 41, Figures 5 and 6, for input motion sets 1 and 5, respectively. The normalized relationships between calculated displacement and yield acceleration ration, k_y/k_{max}, for the three potential sliding masses considered are presented on Figures 7 and 8 of Reference 41, for input motions sets 1 and 5, respectively.

2.6.5.1.3.5 Results

The earthquake-induced down-slope displacements for the potential slip surfaces analyzed are summarized on Table 2.6-5. Computed permanent displacements using ground-motion set 1 as input range from about 3.1 ft, for sliding mass 1b, on the upper slope, to about 1.4 ft, for sliding mass 3c, on the lower slope. Computed displacements using ground-motion set 5 as input were lower, and ranged from 2.4 ft, for sliding mass 1b, to about 0.6 foot, for sliding mass 3c.

Sliding mass 1b (located in the upper portion of the slope) daylights at a horizontal distance of about 400 ft from the toe of the cutslope behind the pads. As mentioned above, the computed displacements for this sliding mass ranged between 2.4 ft and 3.1 ft. Sliding mass 2c (located in the middle of the slope) daylights about 100 ft from the toe of the cutslope. The computed displacements for this sliding mass ranged between 2.5 ft and 3 ft. The computed displacements for sliding mass 3c (located in the lower portion of the slope) ranged between 0.6 ft and 1.4 ft. Two additional potential sliding masses were analyzed in addition to 3c: sliding mass 3c-1, which daylights 70 ft beyond the north edge of the ISFSI pads, and sliding mass 3c-2, which daylights at the first bench on the cutslope behind the pads (Figure 2.6-56). The computed displacements for sliding mass 3c-1 ranged between 0.4 ft and 1.2 ft. For sliding mass 3c-2, the computed displacements ranged between 0.8 ft and 2.0 ft, depending on the input motion used in the analysis. Given the planned mitigation measures for the ISFSI (Section 4.2.1.1.9), none of the potential displacements indicated by any of the rock mass models would impact the ISFSI pads.

2.6.5.1.3.6 Estimating Displacements Based on Geologic Data

Potential slide mass displacement can be estimated by evaluating past performance of the hillslope above the ISFSI site. As described below, the topographic ridge upon which the ISFSI site is located has been stable for the past 500,000 years or more (Reference 37; Reference 6, p. 2-38). A geologic analysis of slope stability, therefore, provides insights into the minimum shear strength and lateral continuity of the clay beds used in the analysis and, hence, a check on the conservatism of the assumptions used to analyze the stability of the hillslope above the ISFSI site.

Geomorphic and geologic data from mapping and trenching in the ISFSI study area show no evidence of past movements of large rock masses on the slope above the ISFSI (Reference 37). Analysis of pre-construction aerial photographs shows no features indicative of such landslides: no arcuate scarps, no vegetational lineaments indicative of filled fissures, and no textural differences in the rock exposures or slopes indicative of a broken rock mass at the ISFSI study area. Similarly, the many trenches excavated into the slope, the tower access road cuts, the extensive outcrops exposed by the 1971 borrow cut, and the many borings exposed no tension cracks or fissure fills on the hillslope (References 43, 44 and 46, Data Reports A, B, and D). Open cracks or soil-filled fissures greater than 1 foot to 2 ft in width would be easily recognized across the slope, given the extensive rock exposure provided by the borrow cut. Therefore, it is reasonable to conclude that any cumulative displacement in the slope greater than 3 ft would have produced features that would be evident in rock slope. The absence of this evidence places a maximum threshold of 3 ft on the amount of cumulative slope displacement that could have occurred in the geologic past.

The hillslope at the ISFSI site is older than at least 500,000 years, because remnants of the Q_5 (430,000 years old) marine terrace are cut into the slope west of the ISFSI site (Reference 37; Reference 6, p. 2-18). Preservation of the terrace documents that the slope has had minimal erosion (a few tens of feet) since that time. Moreover, gradual reduction of the ridge by erosion at the ISFSI site would not destroy deep tension cracks or deep disruption of the rock mass; these features would be preserved as filled fractures and fissures, even as the slope is lowered.

The topographic ridge upon which the ISFSI site is located is presumed to have experienced strong ground shaking from numerous earthquakes on the Hosgri fault zone during the past several hundred thousand years. Studies for the LTSP (Reference 6) estimated a recurrence interval of 11,350 years for a magnitude 7.2 earthquake on the Hosgri fault zone. Assuming that deep cracks from rock mass movements during the past 400,000 years would have been preserved, approximately 35 to 40 large earthquakes have occurred during the past 400,000 years without causing significant (greater than 3 ft) cumulative slope displacement.

2.6.5.1.3.7 Assessment of Conservatism in Displacement Estimates

Because a major portion of the rock mass slide surfaces analyzed is along clay beds, an approximate analysis of the slope at its pre-borrow excavation configuration was conducted to assess the degree of conservatism associated with the assumptions used in the analysis, in particular, the lateral continuity and shear strength of the clay beds. The calculation consisted of extending the potential slide surfaces 1a and 1b (located in the upper part of the slope) to the pre-excavated ground surface, and varying the undrained strength of the clay bed until a yield acceleration corresponding to a displacement of 4 inches was calculated. Ground-motion sets 1 and 5, multiplied by 1.6 and rotated through the same angle as in the previous analysis (ϕ = 46 degrees) were used. Several combinations of the undrained strength parameters c and ϕ were considered in the analysis. The results indicate that the calculated undrained clay bed shear strength is significantly greater than the undrained shear-strength parameters developed from laboratory test data. It is reasonable to conclude, therefore, that the clay bed strength properties used in the analyses are conservative (that is, the clay beds are thin, with rock-to-rock contact through some of the length of the bed that increases the strength), and that the clay beds are more limited in lateral extent than was assumed in analysis.

2.6.5.2 Stability of Cutslopes

Construction of the ISFSI will involve preparing cutslopes along the southwestern, southeastern, and northeastern margins of the site (Figure 2.6-32). The stability of these cutslopes was evaluated using kinematic, pseudostatic, and dynamic analyses.

2.6.5.2.1 Kinematic Analysis

Three potential failure modes were identified for analysis of the cutslopes along the margins of the ISFSI site (Reference 38):

- planar sliding on a single discontinuity
- wedge sliding on the intersection of two discontinuities
- toppling of blocks

2.6.5.2.1.1 Method

Kinematic analyses, based on the collected fracture data, were performed for each of the three ISFSI site cutslopes: east cutslope (northeast), back cutslope (southeast), and west cutslope (southwest), proposed to be excavated at an inclination of 70 degrees. Discontinuity data from the trenches and outcrops in the area of each cutslope (Reference 48, Data Report F) were applied in the analysis (Figures 2.6-57, 2.6-58, and 2.6-59). Data from outcrops along Reservoir Road were applied in the analyses of the slope above the road (Figures 2.6-37 and 2.6-38).

Using the Markland procedure (Reference 32), discontinuities were analyzed for three modes of rock block failure. All kinematic analyses used a friction angle (ø) of 28 degrees to represent sliding resistance along dilated joints or discontinuities in the rock mass. This friction angle value represents a conservative estimate for rock friction, and was selected on the basis of laboratory direct-shear test data on borehole core joints, and estimation of in situ shear strength using the Barton-Choubey method (Figure 2.6-52). Discontinuities generally are 2 ft to 4 ft long, and locally up to 14 ft long (Reference 48, Data Report F).

2.6.5.2.1.2 East Cutslope

Kinematic analyses of the east cutslope are shown on Figure 2.6-57. The analysis shows low potential for toppling failure, as only a few random discontinuities plot within this failure envelope. There is a moderate to high potential for planar sliding failure, as numerous discontinuities from discontinuity set 2, as well as some random discontinuities, plot within the planar sliding failure envelope. Potential also exists for wedge sliding along the intersection lines between discontinuity sets 1 and 2, and between sets 2 and 4; though these intersections plot very close to the failure envelope, these lines represent the average orientation of the set and there is a scatter of orientations around this mean. Thus, there is a moderate to high potential for planar sliding, and a moderate to high potential for wedge sliding failures in the east cutslope.

2.6.5.2.1.3 Back Cutslope

Kinematic analyses of the back cutslope are shown on Figure 2.6-58. The analysis shows low potential for toppling failure, as only a few random discontinuities plot within this failure envelope. Planar sliding failure represents a low to moderate potential, as a few discontinuities from sets 1 and 2, as well as a number of random discontinuities, plot within the planar sliding failure envelope. Potential exists for wedge sliding along the intersection line of discontinuity sets 2 and 3, whereas another intersection (1 and 3) plots outside but relatively close to the failure envelope and should be considered a potential hazard, given that these lines represent the average orientation of the set and that there is a scatter of orientations around this mean. Thus, there is a high potential for wedge failure and minor planar sliding failure in the back cutslope.

Reducing the rock friction angle value to a value appropriate to represent the strength of the bedding-parallel clay beds results in a larger failure envelope, and introduces the possibility of planar sliding failures along the clay beds in the back cutslope and in the hill above the ISFSI site. Static and dynamic modeling of potential sliding along clay beds is presented in Sections 2.6.5.1.2 and 2.6.5.1.3.

A portion of the back cutslope will be in friable dolomite. This material does not behave as a jointed rock mass but, rather, behaves as a stiff soil. The potential exists for slumps within this material.

2.6.5.2.1.4 West Cutslope

Analyses of the west cutslope are shown on Figure 2.6-59. The west cutslope shows a high potential for topple failure. The majority of discontinuity set 2, as well as some fractures from set 1, plot within the zone of potential failure for toppling. However, analyses of planar and wedge sliding failures show low and very low potential, respectively, for these modes of failure in the west cutslope, as very few discontinuities (and none belonging to any of the defined sets) fall within the failure envelope for planar sliding, and none of the discontinuity intersections fall within the failure envelope for wedge sliding failure. Thus, the failure mode for the west cutslope is topple failure. A portion of the southwest side of the ISFSI slope will be in a fill prism; therefore, the topple failure mode would not be applicable there.

2.6.5.2.1.5 Results

None of the three potential failure modes described above pose a threat to the ISFSI, because potential displacements will be mitigated using conventional methods and appropriate setback distances from the toe of cutslopes, as discussed in Section 4.2.1.1.9.

2.6.5.2.2 Pseudostatic Analyses of Potential Wedge Slides

A pseudostatic seismic analysis of the wedges identified in the kinematic analysis was conducted to assess cutslope stability under seismic loads.

2.6.5.2.2.1 Geometry and Dimensions of Wedge Blocks

The size of potential wedge block failures in the ISFSI cutslope (Figure 2.6-32) will be controlled, in part, by the spacing, continuity, and shear strength of discontinuities in the rock mass. Both the dolomite (unit Tof_{b-1}) and sandstone (unit Tof_{b-2}) bedrock at the site are jointed and faulted. Joints and faults in friable dolomite and friable sandstone are less well developed and do not control the mechanical behavior of this rock; rather, strength of the friable rock is controlled primarily by the cementation properties of the rock.

The orientation of the joint sets varies somewhat across the site; however, field measurements of the discontinuities (Reference 48, Data Report F) document two primary, steeply dipping, joint sets: a west- to northwest-striking set, and a north-northwest- to north-striking set. The joints are continuous for about 1 foot to about 14 ft, and commonly die out or terminate at subhorizontal bedding contacts. Field observations from surface exposures and trenches show that the joints commonly are slightly open or dilated in the upper 4 ft, probably due to the stress unloading from the 1971 borrow excavation and surface weathering. Dilation of the joints reduces the shear strength of the discontinuity. To be conservative, the zone of near-surface dilation was assumed to extend to a depth of 20 ft on the ISFSI cutslope.

Joints in the dolomite typically are spaced about 1 ft to 3 ft apart, and divide the rock mass into blocks having an average dimension of 1 foot to 3 ft; typical maximum dimensions are about 14 ft (Reference 48, Data Report F, Table F-6). Twenty ft was conservatively assumed to be the maximum block size in the wedge block stability analysis. This dimension would allow for multiple-block wedges to form in the cutslope.

2.6.5.2.2.2 Method

Kinematic analyses (Section 2.6.5.2.1) show that the proposed east and back cutslopes along the southeast margin of the ISFSI pads have potential for wedge slides. The back cutslope would be the highest, and also has the least stable geometry with respect to rock mass discontinuities. Pseudostatic wedge analyses of these cutslopes were performed to evaluate the potential for shallow wedge slides along joints emerging on the cut faces through the zone of stress-relieved rock (Reference 39). Analyses were performed using SWEDGE (Reference 34) a computer program for the analysis of translational slip of surface wedges in rock slopes defined by two intersecting discontinuity (joint, fault, shear, or fracture) planes, a slope face, and an optional tension crack. The program performs analyses using two techniques: probabilistic analyses (probability of failure), and deterministic analyses (factor of safety). For probabilistic analyses, variation or uncertainty in discontinuity orientation and strength values can be accounted for, resulting in safety factor distribution and prediction of failure probability. For deterministic analyses, a factor of safety is calculated for a specified wedge geometry and a set of strength parameters.

Results from the kinematic analysis show that the most critical wedges are formed by intersections between steeply dipping, northwest-trending faults and joints that intersect at a high oblique angle. These fault/joint intersections plunge steeply to the northwest, and some could daylight on the proposed back cut. These wedge geometries were specifically modeled in the SWEDGE analyses. Planar sliding along low-angle clay beds is addressed in Section 2.6.5.1.3.

Probabilistic analyses were performed to evaluate the overall susceptibility of the slope to wedge failure, and to evaluate the sensitivity of failure to variations in material strength, geometry, and water conditions. Twenty-six separate model runs were performed using the probabilistic approach. Each probabilistic model run included 1,000 Monte Carlo iterations of input parameter variations to generate a probability distribution. After completing the probabilistic analyses, deterministic analyses were performed for the most critical modeled conditions in terms of probability of failure, and size and weight of wedge. Sixteen separate deterministic models were run that included variations in slope height and inclination, wedge geometry (with and without tension cracks), and degree of water saturation.

2.6.5.2.2.3 Rock Wedge Strength Parameters

Strength values derived from the Barton-Choubey method (Reference 27) (Figure 2.6-52) were used for the analyses of potential shallow rock wedge failures of rock blocks along existing discontinuities within the stress-relieved outermost rock zone directly behind the cutslope face. Cohesion was neglected. The friction angles selected and used in the probabilistic analyses ranged from 16 degrees (clay-coated faults) to 46 degrees (clay-free joints), and from about 26 degrees to 31 degrees, respectively, for the deterministic analyses.

2.6.5.2.2.4 Assumptions

The following assumptions and parameters were used for the pseudostatic analysis:

- Three 70-degree cutslope geometrics were analyzed for the back cutslope: a 20.5-ft-high cutslope, a 31.8-ft-high cutslope, and 52.3-ft-high cutslope. The 20.5-ft-high cutslope models potential failures from base of cut to the intermediate bench(Figure 2.6-60). The 31.8-ft-high cutslope models potential failures from the intermediate bench to top of cut. The 52.3-ft-high cutslope models potential failures from base of cut to top of cut, at an "average" inclination of about 47 degrees.

- Each slope was evaluated with and without tension cracks, for example, in the case of the back cutslope, tension cracks were located at distances of

1.6 ft and 23 ft back from the crest of the slope. These distances are reasonable for a slope model, because the fractures at the ISFSI site have spacings of up to several feet, and the cutslope bench is 25 ft wide. One set of tension cracks (at 23 ft) specifically models the potential for tension cracks to develop along a backfilled trench for a drainage pipe at the back of the intermediate bench.

- Analyses were performed for each cutslope configuration using (1) a horizontal (out-of-slope) pseudostatic seismic coefficient of 0.5 g, and (2) dry and partially saturated rock mass (water levels at one-half the height of the slope). The value of 0.5 g (Reference 68) was derived using the procedure described by Ashford and Sitar (Reference 35), and is approximately two-thirds of the peak horizontal acceleration of 0.83 g from the LTSP spectra shown in Figure 2.6-43. This level of reduction has been shown to be appropriate for pseudostatic analyses of slopes (Reference 35).

2.6.5.2.2.5 Results

The results of the pseudostatic probabilistic SWEDGE analysis for the back cutslope and the east cutslope are presented in Tables 2.6-6 and 2.6-7, respectively. Results of the deterministic analyses for these cutslopes are presented in Table 2.6-8. The probabilistic analyses show that rock wedges in the modeled cutslopes (Figure 2.6-60) have a low probability of failure in a dry condition. The probability of failure increases significantly with partial saturation of the slope and the addition of seismic force. The largest predicted wedge, with a factor of safety less than 1.0, weighs 4,475 kips and has an estimated face area of 2,649 square ft (Table 2.6-6).

Deterministic analyses were performed to calculate support forces required to restrain the wedges and achieve a factor of safety of 1.3 under seismic loading conditions (Table 2.6-8). The calculated total support force to stabilize the largest predicted wedge to a factor of safety of 1.3 is 1,881 kips. For an assumed anchor spacing of 5 ft by 5 ft, this force translates to 32 kips per anchor (Table 2.6-8). The design of slope reinforcement to prevent wedges from displacing is described in Section 4.2.1.1.9 (Reference 69).

2.6.5.3 Slope Stability at CTF Site

In a previous submittal examining the stability of the slope behind DCPP Unit 1 (Reference 9, p. 30-36), it was shown that displacements along the interface between colluvial and terrace deposits within the underlying bedrock would be limited. The results of this analysis also indicate that the farthest extent of these estimated displacements is at the uppermost edge of the colluvium/bedrock interface, which is more than 100 ft west of the CTF (Figure 2.6-7), and similar to the relationship shown in cross sections B-B''' and L-L' (Figures 2.6-11 and 2.6-19). Therefore, slope-related displacements at the CTF site are estimated to be nil.

2.6.5.4 Slope Stability Along the Transport Route

2.6.5.4.1 Static Stability

As discussed in Section 2.6.1.12.3, the Patton Cove landslide is more than 100 ft from the transport route, and it is not likely to encroach headward to where it would affect the route.

Small debris flows (up to 3 ft deep on the road) could impact the roadway as they issue from the swales on the steep slopes above the road (Section 2.6.1.12.3). These debris flows occur infrequently during or shortly following severe rainstorms (Reference 7), and are relatively easy to clear from the road.

Kinematic analyses of the stability of the slope above the transport route are shown on Figures 2.6-37 and 2.6-38. (Reference 38, Figures 7 and 8). The north-trending slope (station 43+00 to 46+00) shows moderate potential for toppling failure, as a large portion of set 1 plots within this failure envelope. There is low potential of planar sliding failure, and very low potential for wedge sliding failure. Due to the very low inclination of the northwest-trending slope (station 35+00 to 43+00), this slope shows low potential for all three failure modes. Thus, the only potentially significant failure mode is for small topple failures along the transport route cutslopes.

Reference 76 provided an additional static stability assessment for portions of the transport route on rock. Where the transport route is founded on rock begins at approximately Stations 34+50 and continues uphill to the CTF at station 53+50. Along the southern part of this section (station 34+50 to 46+10), the rock beddings dip into the slope and thus makes it kinematically unlikely for slope movements to daylight at the slope face. Along the northern section (station 46+10 to 53+50), the rock beddings show a gentle out-of-slope dip and thus it is kinematically feasible to have out-of-slope movement along possible clay beds that parallel the bedding.

Reference 76 (PG&E Response to NRC Request 5) concluded the following:

The northern section of the transport route on rock, between stations 46+10 and 53+50, has bedding that dips gently out of the slope. Potential rock mass slide models on clay bed or rock discontinuities are kinematically feasible. Potential slide mass models were developed based on conservative interpretations of geological information from surfacing mapping, trenching, and exploratory boring as shown on Section M-M'. Static slope stability analysis for the two rock slide models indicates that the minimum static factor of safety is 2.07, which is higher than the 1.5 that is typically required for static slope stability. This demonstrates the slope has ample safety factors against static slope failure.

The southern section of this alignment, between stations 34+50 and 46+10, has rock bedding that dips into the hillslope making slope failure on bedding not possible.

Kinematic analysis of joints along the transport route also shows that failure of the bedrock below the transport route is not possible.

Based on the above evaluation and documentation provided in References 74 and 76 (Attachment 5-1), it is concluded that the portions of transport route on rock have adequate static factor of safety against rock mass sliding on clay beds.

2.6.5.4.2 Dynamic Stability and Displacements

Stability analyses using the ILP ground motions (Section 2.6.2.5) were performed on the hillslope behind Unit 2 using cross section L-L' (Figure 2.6-19). Borings drilled during investigations for the power block along the slope provided data for modeling the slope. Reference 76 (PG&E Response to NRC Request 6) provided additional information on material properties used for the transport route stability evaluations and PG&E submitted Revision 3 of Reference 74 that provides technical bases for the material properties. The results of these analyses indicate the bedrock slope and the transport route that crosses it are expected to undergo only minor displacements of about 1.0 ft or less during the possible occurrence of the ILP ground motions (References 50, 51, and 52).

An additional location, shown on cross section D-D' (Figure 2.6-16), along the transport route also was modeled, and the responses to the ILP ground-motions were assessed in a similar manner. Results from this analysis show that this location also is expected to undergo only minor displacements of about l.0 ft or less.

PG&E has revised the dynamic slope stability calculations (References 74, 42, and 71) for the transport route incorporating the inertial mass of the transporter, a new section of the transport route with two slide mass models, and revised seismic coefficient time histories for the three slide masses in sections of the transport route underlain by surficial deposits. The transport route slopes' estimated displacement magnitude of 1.5 ft is smaller than that computed for the ISFSI pad's slope (Reference 41) and is not indicative of an unstable slope. Thus, the transport route slope remains stable during and after a design basis earthquake. Further details of the revised stability analyses for the transport route are provided in Reference 76 (PG&E Response to NRC Request 7).

2.6.6 <u>REFERENCES</u>

1. PG&E Letter DIL-01-006 to the NRC, Submittal of Seismic Hazards Review Board Final Report, December 21, 2001.

2. PG&E Letter DIL-01-004 to the NRC, Submittal of Non-Proprietary Calculation Packages, December 21, 2001.

3. PG&E Letter DIL-01-005 to the NRC, Submittal of Geologic Data Reports, December 21, 2001.

4. PG&E, Units 1 and 2 Diablo Canyon Power Plant, Final Safety Analysis Report Update, Revision 14, November 2001.

5. USNRC, Supplement Number 34 to NUREG-0675, Safety Evaluation Report for Diablo Canyon Power Plant, Units 1 and 2, June 1991.

6. PG&E, Final Report of the Diablo Canyon Long Term Seismic Program, 1988.

7. PG&E, Addendum to the 1988 Final Report of the Diablo Canyon Long Term Seismic Program, 1991.

8. PG&E, Assessment of Slope Stability Near the Diablo Canyon Power Plant (Response to NRC Request of January 31, 1997), 1997.

9. Harding Miller Lawson Associates, Soil Investigation, Intake and Discharge Lines, Borrow Area, and Switchyards for Unit 1, Diablo Canyon Site, San Luis Obispo County, California, 1968.

10. C. A. Hall, Jr., W. G. Ernst, S. W. Prior, and J. W. Siese, Geologic Map of the San Luis Obispo-San Simeon Region, U.S. Geological Survey Miscellaneous Investigation I-1097, 1979.

11. C. A. Hall, Jr., Geologic Map of the Morro Bay South and Port San Luis Quadrangles, San Luis Obispo County, California, U.S. Geologic Survey Miscellaneous Field Studies Map MF-511, scale 1:24,000, 1973.

12. N. A. Abrahamson, and K. Shedlock, Overview [of Special Issue of SRL on Attenuation Relations], Seismological Research Letters, v. 68, no. 1, p. 9-23, 1997.

13. Harding Lawson Associates, Landslide Investigation, Diablo Canyon Site, San Luis Obispo County, California, 1970.

14. M. K. McLaren, and W. U. Savage (in press), "Seismicity of South-central coastal California", October 1987 through January 1997, accepted for publication in Bull. Seis. Soc. America, 2001.

15. W. J. Silva, and K. Lee, WES RASCAL: Code for Synthesizing Earthquake Ground Motions, State-of-the-Art for Assessing Earthquake Hazards in the United States, Report 24, U. S. Army Waterways Experiment Station, Misc. Paper S-73-1, 1987.

16. K.L. Hanson, W.R. Lettis, J.R. Wesling, K.I. Kelson, and L. Mezger, Quaternary Marine Terraces, South-Central Coastal California: Implications for Crustal Deformation and Coastal Evolution: in Quaternary Coasts of the United States: Marine and Lacustrine System, SEPM Special Publication No. 48, p 323-332, 1992.

17. N. A. Abrahamson, and W. J. Silva, Empirical Response Spectral Attenuation Relations for Shallow Crustal Earthquakes, Seis. Res. Let. Vol 68, p 94-127, 1997.

18. K. Sadigh, C.Y. Chang, J.A. Eagan, F. Makdisi, R.R. Youngs, Attenuation Relationships for Shallow Crustal Earthquakes Based on California Strong Motion Data, Seis. Res. Let., vol. 68, p 180-189, 1997.

19. I. M. Idriss, Selection of Earthquake Ground Motions at Rock Sites, report prepared for the Structural Division, Building and Fire Research Laboratory, National Institute of Standards and Technology, Department of Civil Engineering, University of California, Davis, 1991, included in Idriss (1992).

20. M. Idriss, Updated Standard Error Terms, Memo to Phalkun Tan, April 17, 1994.

21. M. Idriss, An Overview of Earthquake Ground Motions Pertinent to Seismic Zonation, Proc. Fifth International Conference on Seismic Zonation, vol. III, p 2111-2126, 1995.

22. N. A. Abrahamson, Effects of Directivity on Probabilistic Seismic Hazard Analyses, Earthquake Engineering Research Institute, Proceedings, Sixth International Conference on Seismic Zonation, Palm Springs, California, 2000.

23. P. G. Somerville, N. F. Smith, R. W. Graves, and N. A. Abrahamson, Modification of Empirical Strong Motion Attenuation Relations to Include the Amplitude and Duration Effects of Rupture Directivity, Seismological Research Letters, v. 68, p. 199-222, 1997.

24. K. W. Campbell, Empirical Near-Source Attenuation Relationships for Horizontal and Vertical Components of Peak Ground Acceleration, Peak Velocity and Pesudo Absolute Acceleration Response Spectra, Seis. Res. Let. Vol 68, p 154-179, 1997.

25. Deleted in Amendment 2.

26. S. G. Wright, UTEXAS3, A Computer Program for Slope Stability Calculations, Shinoak Software, Austin, Texas, 1991.

27. N. R. Barton, and V. Choubey, The Shear Strength of Rock Joints in Theory and Practice, Rock Mechanics, v. 10, no. 1-2, p. 1-54, 1977.

28. E. Hoek, Rock Engineering Course Notes, Hoek's Corner, University of Toronto, www.rocscience.com last updated May 2003.

29. N. M. Newmark, Effects of Earthquakes on Dams and Embankments, Geotechnique, v. 15, no. 2, p. 139-160, 1965.

30. F. I. Makdisi, and H. B. Seed, Simplified Procedure for Estimating Dam and Embankment Earthquake-Induced Deformations, Journal of the Geotechnical Engineering Division, American Society of Civil Engineers, v. 104, no. GT7, p. 849-867, 1978.

31. M. Hudson, I. M. Idriss, and Beikae, (QUAD4MU) User's Manual for a Computer Program to Evaluate the Seismic Response of Soil Structures Using Finite-Element Procedures and Incorporating a Compliant Base, Center for Geotechnical Modeling, University of California, Davis, 1994.

32. P. B. Schnabel, J. Lysmer, and H. B. Seed, SHAKE: A Computer Program for Earthquake Response Analysis of Horizontally Layered Sites, Report EERC 72-12, Earthquake Engineering Research Center, University of California, Berkeley, 1972.

33. Deleted in Amendment 2.

34. Rocscience, Inc., SWEDGE, Probabilistic Analyses of the Geometry and Stability of Surface Wedges, version 3.06, 1999.

35. S. A. Ashford, and N. Sitar, Seismic Response of Steep Natural Slopes, Report No. UCD/EERC-94/05, College of Engineering, University of California, Berkeley, 1994.

36. Deleted in Amendment 2.

37. PG&E Calculation No. 52.27.100.731 (GEO.DCPP.01.21), "Analysis of Bedrock Stratigraphy and Geologic Structure at the DCPP ISFSI Site."

38. PG&E Calculation No. 52.27.100.732 (GEO.DCPP.01.22), "Kinematic Stability Analysis for Cutslopes at DCPP ISFSI Site."

39. PG&E Calculation No. 52.27.100.733 (GEO.DCPP.01.23), "Pseudostatic Wedge Analysis of DCPP ISFSI Cutslopes (SWEGE Analysis)."

40. PG&E Calculation No. 52.27.100.735 (GEO.DCPP.01.25), "Determination of Seismic Coefficient Time Histories for Potential Sliding Masses Along Cut Slope Behind ISFSI Pad."

41. PG&E Calculation No. 52.27.100.736 (GEO.DCPP.01.26), "Determination of Earthquake-Induced Displacements of Potential Sliding Masses on ISFSI Slope."

42. PG&E Calculation No. 52.27.100.739 (GEO.DCPP.01.29), "Determination of Coefficient Time Histories for Potential Sliding Masses on DCPP ISFSI Transport Route."

43. Diablo Canyon ISFSI Data Report A, "Geologic Mapping in the Plant Site and ISFSI Site Areas," Revision 1, December 17, 2001.

44. Diablo Canyon ISFSI Data Report B, "Borings in ISFSI Site Area," Revision 1, December 17, 2001.

45. Diablo Canyon ISFSI Data Report C, "1998 Geophysical Investigations at the ISFSI Site Area (Agbabian Associates and GeoVision)," Revision 1, December 17, 2001.

46. Diablo Canyon ISFSI Data Report D, "Trenches in the ISFSI Site Area," Revision 1, December 17, 2001.

47. Diablo Canyon ISFSI Data Report E, "Borehole Geophysical Data (NORCAL Geophysical Consultants, Inc.)," Revision 0, November 5, 2001.

48. Diablo Canyon ISFSI Data Report F, "Field Discontinuity Measurements," Revision 1, December 17, 2001.

49. Diablo Canyon ISFSI Data Report G, "Soil Laboratory Test Data (Cooper Testing Laboratory), Revision 1, December 17, 2001.

50. Diablo Canyon ISFSI Data Report H, "Rock Strength Data and GSI Sheets," Revision 0, November 5, 2001.

51. Diablo Canyon ISFSI Data Report I, "Rock Laboratory Test Data (GeoTest Unlimited)," Revision 1, December 2001.

52. Diablo Canyon ISFSI Data Report J, "Petrographic Analysis and X-Ray Diffraction of Rock Samples (Spectrum Petrographics, Inc.)," Revision 0, November 5, 2001.

53. Diablo Canyon ISFSI Data Report K, "Petrogrpahic and X-Ray Diffraction Analyses of Clay Beds (Schwein/Christensen Laboratories, Inc.)," Revision 0, November 5, 2001.

54. Calculation GEO.DCPP.01.11, Development of ISFSI Spectra."

55. PG&E Calculation 52.27.100.747, "Development of Freefield Ground Motion Storage Cask Spectra and Time Histories for the Used Fuel Storage Project."

56. PG&E Calculation 52.27.100.724, "Development of Time Histories with Fling."

57. Calculation GEO.DCPP.01.12, "Development of Fling Model for Diablo Canyon ISFSI."

58. PG&E Calculation 52.27.100.723, "Development of Spectrum Compatible Time Histories."

59. PG&E Calculation 52.27.100.711 (GEO.DCPP.01.01), "Development of Young's Modulus and Poisson's Ratios for DCPP ISFSI Based on Field Data."

60. PG&E Calculation 52.27.100.725 (GEO.DCPP.01.15), "Development of Young's Modulus and Poisson's Ratio Values for DCPP ISFSI Based on Laboratory Data."

61. PG&E Calculation 52.27.100.713 (GEO.DCPP.01.03), "Development of Allowable Bearing Capacity for DCPP ISFSI Pad and CTF Stability Analyses."

62. Calculation GEO.DCPP.01.18, "Determination of Basic Friction Angle Along Rock Discontinuities at DCPP ISFSI Based on Laboratory Tests."

63. Calculation GEO.DCPP.01.17, "Determination of Mean and Standard Deviation of Unconfined Compression Strengths for Hard Rock at DCPP ISFSI Based on Laboratory Tests."

64. Calculation GEO.DPCP.01.20, "Development of Strength Envelopes for Shallow Discontinuities at DCPP ISFSI Using Barton Equations."

65. Calculation GEO.DCPP.01.19, "Development of Strength Envelopes for Jointed Rock Mass at DCPP ISFSI Using Hoek-Brown Equations."

66. Calculation GEO.DCPP.01.16, "Development of Strength Envelopes for Non-jointed Rock at DCPP ISFSI Based on Laboratory Data."

67. PG&E Calculation 52.27.100.734 (GEO.DCPP.01.24), "Stability and Yield Acceleration Analysis of Cross-Section I-I."

68. Calculation GEO.DCPP.01.05, "Determination of Pseudostatic Acceleration Coefficient for Use in DCPP ISFSI Cutslope Stability Analyses."

69. PG&E Calculation 52.27.100.718 (GEO.DCPP.01.08), "Determination of Rock Anchor Design Parameters for DCPP ISFSI Cutslope."

70. PG&E Calculation 52.27.100.716 (GEO.DCPP.01.06), Development of Lateral Bearing Capacity for DCPP CTF Stability Analysis."

71. PG&E Calculation 52.27.100.740 (GEO.DCPP.01.30), "Determination of Earthquake Induced Displacements of Potential Sliding Masses Along DCPP ISFSI Transport Route."

72. Calculation GEO.DCPP.03.01, "Determination of Earthquake-Induced Displacements of Potential Sliding Mass."

73. PG&E Calculation 52.27.100.741 (GEO.DCPP.01.31), "Development of Strength Envelopes for Clay Beds at DCPP ISFSI."

74. PG&E Calculation 52.27.100.738 (GEO.DCPP.01.28), "Stability and Yield Acceleration Analysis of Potential Sliding Masses Along DCPP ISFSI Transport Route."

75. PG&E Letter DIL-02-009 to the NRC, Response to the NRC Request for Additional Information for the Diablo Canyon ISFSI Application, October 15, 2002.

76. PG&E Letter DIL-03-004 to the NRC, Supplemental Slope Stability Responses to Additional NRC Questions for the Diablo Canyon ISFSI Application, March 27, 2003.

TABLE 2.3-1

MONTHLY AVERAGE TEMPERATURES
FOR SAN LUIS OBISPO
(1948 to 2000) [a]

Month	Temp (°F)	Month	Temp (°F)
Jan	52.2	Jul	65.2
Feb	54.1	Aug	66.0
Mar	54.6	Sep	65.8
Apr	56.9	Oct	63.3
May	58.9	Nov	58.2
Jun	62.4	Dec	53.3

[a] Information from Western Regional Climate Center

TABLE 2.6-1

SOIL AND ROCK TEST PROGRAM

Type of Properties	Soil		Rock	
	Tests Conducted	Reference	Tests Conducted	Reference
Basic properties	Classification, identification, unit weight, saturation	References 44 and 49, Data Report B and Data Report G	Classification, identification, JRC, (mi)	References 44 and 50, Data Report B and Data Report H
Strength, deformation (static)	Drained, undrained triaxial strength, direct shear	Reference 49 Data Report G	Drained and undrained triaxial strength, unconfined compression, direct shear, Poisson's ratio, Young's modulus	Reference 51 Data Report I
Strength, deformation (dynamic)	Triaxial, drained, undrained strain vs. damping, strain vs. shear modulus	Reference 49 Data Report G		
Field and in situ properties			Field discontinuity, shear wave and compression wave velocity, Poisson's ratio, Young's modulus	References 48 and 45 Data Report F and Data Report C

TABLE 2.6-7

PSEUDOSTATIC PROBABILISTIC SWEDGE ANALYSES OF ISFSI EAST CUTSLOPE

Run	Cut Height[1] (ft)	Discontinuity[2] A	Discontinuity[2] B	Mean Friction Angle[3] (ø)	Tension Crack Distances[4] (ft)	Seismic Force[5] (g)	Water Unit Weight[6] (kips/ft^3)*	Probability of Failure	Factor of Safety	Wedge Weight (kips)*	Wedge Face Area (ft^2)
East cut P1	23.3	76/08 (4)	67/239 (2)	35.0 (A) 36.0 (B)	None	None	None	0.20	1.08	33.96	446.0
East cut P2	23.3	76/08 (4)	67/239 (2)	35.0 (A) 36.0 (B)	1.64	None	None	0.12	1.08	33.96	446.0
East cut P3	23.3	76/08 (4)	67/239 (2)	35.0 (A) 36.0 (B)	None	None	0.031	0.31	1.02	33.96	446.0
East cut P4	23.3	76/08 (4)	67/239 (2)	35.0 (A) 36.0 (B)	None	0.50	None	1.0	0.65	33.96	446.0
East cut P5	23.3	76/08 (4)	67/239 (2)	35.0 (A) 36.0 (B)	None	0.50	0.031	1.0	0.54	33.96	446.0
East cut P6	23.3	88/98 (1)	67/239 (2)	36.0 (A) 36.0 (B)	None	None	None	0.97	0.31	23.81	469.8
East cut P7	23.3	88/98 (1)	67/239 (2)	36.0 (A) 36.0 (B)	None	0.50	0.031	0.99	0	23.81	469.8

*1 kip = 1000 pounds

[1] Cut height geometry from PG&E/Enercon drawing, PGE-009-SK-001, 9/12/01.

[2] Mean dip and dip direction of intersecting joints (set number indicated in parentheses) that were identified by kinematic analyses in Reference 38, as forming potential wedges. Geometry of discontinuity is defined by the dip/dip convention. (Reference 39, Table 23-1). Numbers in brackets refer to Joint Set identification (Table 23-1).

[3] Mean rock discontinuity friction angle determined by Barton-Choubey method.

[4] Tension crack distance is the distance between the top of the wedge block crest and tension crack location, measured along strike of discontinuity A.

[5] Seismic force recommended for pseudostatic wedge analyses.

[6] Water pressure of 0.031 kips/ft^3 approximates a condition in which water collects halfway up wedge-bounding discontinuities.

TABLE 2.6-8

PSEUDOSTATIC DETERMINISTIC SWEDGE ANALYSES OF ISFSI BACK CUTSLOPE AND EAST CUTSLOPE

Run	Cut[1] Height (ft)	Discontinuity[2] A	Discontinuity[2] B	Mean[3] Friction Angle	Tension[4] Crack Distance (ft)	Seismic[5] Force (g)	Water[6] Unit Weight (kips*/ft^3)	Bolt[7] Force (kips*)	Factor of Safety	Wedge Weight (kips*)	Wedge |Face Area (ft^2)	Penetration[8] Anchor Length (ft)	Per Anchor[9] Force (kips*)
Back cut D1RR	31.8	69/220 (2)	88/12 (3)	26.5 (A/B)	None	0.5	0.031	None	0	40.1	101.8		
Back cut D2R	31.8	69/220 (2)	88/12 (3)	26.5 (A/B)	None	0.5	0.031	41.8	1.39	40.1	101.8	6.6	18.6
Back cut D3R	31.8	88/12 (3)	24/232 (4)	26.5 (A) 30.5 (B)	23.0	0.5	0.031	None	0.62	1783.8	1059.9		
Back cut D4R	31.8	88/12 (3)	24/232 (4)	26.5 (A) 30.5 (B)	23.0	0.5	0.031	796.4	1.30	1783.8	1059.9	13.1	33.9
Back cut D5R	52.3	88/12 (3)	24/232 (4)	26.5 (A) 30.5 (B)	23.0	0.5	0.031	None	0.63	4474.6	2649.1		
Back cut D6R	52.3	88/12 (3)	24/232 (4)	26.5 (A) 30.5 (B)	23.0	0.5	0.031	1881.0	1.30	4474.6	2649.1	23.0	32.1
Back cut D7R	20.5	69/220 (2)	88/12 (3)	26.5 (A/B)	4.92	0.5	0.031	-	0.27	10.12	41.94		
Back cut D8R	20.5	69/220 (2)	88/12 (3)	26.5 (A/B)	4.92	0.5	0.031	8.8	1.67	10.12	41.94	3.9	9.4
Back cut D9R	20.5	88/12 (3)	24/232 (4)	26.5 (A) 30.5 (B)	20.0	0.5	0.031	-	0.76	596.2	440.1		
Back cut D10R	20.5	88/12 (3)	24/232 (4)	26.5 (A) 30.5 (B)	20.0	0.5	0.031	189.2	1.31	596.2	440.1	16.4	19.4
East cut D1R	23.3	76/08 (4)	67/239 (2)	35.0 (A) 36.0 (B)	None	None	None	None	1.08	33.96	446.0		
East cut D2R	23.3	76/08 (4)	67/239 (2)	35.0 (A) 36.0 (B)	None	0.5	0.031	None	0.54	33.97	446.0		
East cut D3R	23.3	76/08 (4)	67/239 (2)	35.0 (A) 36.0 (B)	None	0.5	0.031	81.6	1.34	33.98	446.0	3.3	9.0
East cut D4R	23.3	88/98 (1)	67/239 (2)	36.0 (A/B)	None	None	None	None	0.31	23.81	469.8		
East cut D5R	23.3	88/98 (1)	67/239 (2)	36.0 (A/B)	None	0.5	0.031	None	0	23.81	469.8		
East cut D6R	23.3	88/98 (1)	67/239 (2)	36.0 (A/B)	None	0.5	0.032	83.8	1.43	23.81	469.8	3.3	8.4

*1 kip = 1000 pounds

1 Cut height estimated from PG&E Drawing Fig 4.2-6, Rev. A.

2 Mean dip and dip direction of intersecting joints (set number indicated in parentheses) that were identified by kinematic analyses in Reference 38 as forming potential wedge. Geometry of discontinuity is defined by the dip/dip direction convention. Refer to Table 23-1. Numbers in brackets refer to Joint Set identification in Table 23-1, Reference 38.

3 Mean rock discontinuity friction angle determined by Barton Equation as developed in Reference 64.

4 Tension crack distance is the distance between the top of the wedge block crest and tension crack location measured along strike of discontinuity A. Wedges modeled in runs D3-D6 were unrealistically long and narrow when tension cracks were not included. Final runs therefore include tension cracks at 23 feet behind the slope face.

TABLE 2.6-8

[5] Seismic force recommended for pseudostatic wedge analyses as defined in Reference 68.

[6] Water pressure of 0.031 kips/ft^3 represents approximately a condition with water collecting halfway up wedge-bounding discontinuities.

[7] Total force required to stabilize block to the listed factor of safety.

[8] Length of anchor in meters required to penetrate modeled wedge sliding plane, assuming an anchor inclination of 15° below horizontal, and plunge direction perpendicular to slope face. Additional length is required to provide anchor anchorage and capacity in sound rock behind the failure wedge.

[9] Per anchor force calculated by dividing wedge face area by 50% to account for wedge margins that are not suitable for providing anchor restraint, and then dividing this value by the required anchor force, and assuming one anchor per 22.6 ft^2, which represents an anchor pattern spacing of 5.0 feet.

CHAPTER 3

PRINCIPAL DESIGN CRITERIA

CONTENTS

CHAPTER 3

PRINCIPAL DESIGN CRITERIA

TABLES

DIABLO CANYON ISFSI
SAFETY ANALYSIS REPORT

CHAPTER 3

PRINCIPAL DESIGN CRITERIA

FIGURES

3.3 DESIGN CRITERIA FOR SAFETY PROTECTION SYSTEMS

The Diablo Canyon ISFSI is designed for safe storage of spent nuclear fuel and associated nonfuel hardware. The ISFSI storage facility in general, and the HI-STORM 100 System storage casks in particular, are designed to protect the MPC contents and prevent release of radioactive material under normal, off-normal, and accident conditions in accordance with applicable regulatory requirements contained in 10 CFR 72 (Reference 1). Section 3.2 provides the design criteria for environmental conditions and natural phenomena for ISFSI SSCs. This section provides the other design criteria for the ISFSI SSCs.

3.3.1 HI-STORM 100 SYSTEM

3.3.1.1 General

The primary safety functions of each of the major components comprising the Diablo Canyon ISFSI are summarized below, with appropriate references to the HI-STORM 100 System FSAR (Reference 2) or other sections of this SAR for additional information. Table 3.4-6 provides a list of ASME Code alternatives for the HI-STORM 100 System.

3.3.1.1.1 Multi-Purpose Canister

The MPC is comprised of a cylindrical, strength-welded shell, fuel basket, lid, vent and drain port cover plates, and a welded closure ring. The MPC provides criticality control, decay heat removal, shielding, and acts as the primary confinement boundary for the storage system. The MPC may contain, at prescribed fuel basket locations, a damaged fuel container (DFC) that provides confinement, structural support, and retrievability for damaged fuel assemblies or fuel debris. A detailed description, design drawings, and a summary of the design criteria for the MPCs are provided in Sections 1.2.1.1, 1.5, and 2.0.1, respectively, of the HI-STORM 100 System FSAR, as amended by LAR 1014-1 (Reference 3).

3.3.1.1.2 HI-STORM 100SA Overpack

The HI-STORM 100SA overpack is a rugged, heavy-walled, cylindrical, steel structure. The structure is comprised of inner and outer concentric, carbon-steel shells, a baseplate, and a bolted top lid (comprised of steel plates and a concrete shield) with integral outlet vents. The annulus between the inner and outer shells is filled with concrete. A shortened, seismically-anchored version of the overpack, denoted as the HI-STORM 100SA, is used at the Diablo Canyon ISFSI.

The overpack provides support and protection for the MPC during normal, off-normal, and accident conditions including natural phenomena such as tornadoes and earthquakes; provides radiation shielding; and facilitates rejection of decay heat from the MPC to the environs to ensure fuel cladding temperatures remain below acceptable limits. Detailed descriptions, design drawings, and a summary of the design criteria for the overpack are provided in Sections 1.2.1.2.1, 1.5, and 2.0.2, respectively, of the HI-STORM 100 System FSAR, as amended by LAR 1014-1.

3.3.1.1.3 HI-TRAC 125 Transfer Cask

The HI-TRAC 125 transfer cask is a rugged, heavy-walled, cylindrical steel vessel weighing a maximum of 125 tons during use. The cask guides, retains, protects, and supports the MPC during load handling and transfer operations, including submersion in the SFP where the MPC is loaded. During load handling operations to and from the SFP with a loaded MPC, the transfer cask retains the unwelded MPC lid using a top lid retention device. The transfer cask also limits MPC vertical dynamic loading to within acceptable design-basis limits in the event of a postulated load drop inside the FHB/AB by using a removable bottom-mounted impact limiter. The transfer cask also features a single bottom lid that is removed at the CTF to facilitate the transfer of the MPC to or from the overpack. While submerged, the transfer cask prevents most of the exterior surfaces of the MPC from becoming contaminated by preventing contact with the SFP water.

Upon removal from the SFP, the transfer cask provides shielding to maintain personnel exposure ALARA, and facilitates heat transfer from the MPC to the environs. A more detailed description, and a summary of the design criteria for the transfer cask are provided in Sections 1.2.1.2.2, and 2.0.3, respectively, of the HI-STORM 100 System FSAR; and in Sections 5.1 and 10.2 of this SAR. A modified version of the HI-TRAC 125 transfer cask, known as HI-TRAC 125D, will be used to support Diablo Canyon ISFSI operations. See Section 4.2.3.2.4 for more detailed discussion of HI-TRAC 125D.

3.3.1.2 Protection by Multiple Confinement Barriers and Systems

3.3.1.2.1 Confinement Barriers and Systems

The HI-STORM 100 System provides several confinement barriers for the radioactive contents. Intact fuel assemblies have cladding that provides the first boundary within the MPC preventing release of the fission products. (The MPC confinement and radiological evaluations do not take credit for the cladding.) A DFC prevents the dispersal of gross particulates within the MPC for any fuel assemblies classified as damaged fuel or fuel debris. The MPC is a strength-welded enclosure that provides the confinement boundary for all normal, off-normal and accident conditions, including natural phenomena. The MPC confinement boundary is defined by the MPC baseplate, shell, lid, port cover plates, and the welds joining these components, as shown in Figure 3.3-1. The closure ring provides a redundant boundary. Refer to the drawings in Section 1.5 of the HI-STORM 100 System FSAR for details of the MPC confinement boundary design.

3.3.1.2.2 Cask Cooling

The HI-STORM 100 System provides decay heat removal both during processing and final storage of the MPC. As described previously, the transfer cask conducts heat from the MPC until the MPC is transferred to the overpack where convective cooling is established as depicted in Figure 3.3-2. The thermal design of the HI-STORM 100 System is discussed in detail in Chapter 4 of the HI-STORM 100 System FSAR, as amended by LAR 1014-1, and in Section 4.2.3.3.3 of this SAR.

3.3.1.3 Protection by Equipment and Instrumentation Selection

3.3.1.3.1 Equipment

The cask transporter and CTF provide protection functions to the MPC and are discussed in Sections 3.3.3 and 3.3.4, respectively.

3.3.1.3.2 Instrumentation

No instrumentation is required for storage of spent nuclear fuel and associated nonfuel hardware at the Diablo Canyon ISFSI. Due to the welded closure of the MPC, the passively-cooled storage cask design, and the Diablo Canyon ISFSI TS requirement for periodic checks of the casks, the loaded overpacks do not require continuous surveillance and monitoring or operator actions to ensure the safety functions are performed during normal, off-normal or postulated accident conditions.

3.3.1.4 Nuclear Criticality Safety

The HI-STORM 100 System is designed to ensure the stored fuel remains subcritical with k_{eff} less than 0.95 under all normal, off-normal, and accident conditions. A detailed discussion of the criticality analyses for the HI-STORM 100 System is provided in Chapter 6 of the HI-STORM 100 System FSAR, as amended by Holtec LAR 1014-1. Section 4.2.3.3.5 of this SAR includes a summary discussion of the HI-STORM 100 System criticality design.

3.3.1.4.1 Control Methods for Prevention of Criticality

The design features and control methods used to prevent criticality for all MPC configurations are the following:

(1) Incorporation of permanent neutron absorbing material (Boral) attached to the MPC fuel basket walls with a minimum required loading of the ^{10}B isotope.

(2) Favorable geometry provided by the MPC fuel basket.

(3) Loading of certain fuel assemblies is performed in water with a soluble boron content as specified in the Diablo Canyon ISFSI TS.

There are a number of conservative assumptions used in the HI-STORM 100 System criticality analyses, including not taking credit for fuel burnup, fuel-related burnable neutron absorbers, and only crediting 75 percent of ^{10}B isotope loading in the Boral neutron absorbers. A complete list of the conservative assumptions in the HI-STORM 100 System criticality analyses is provided in Section 6.1 of the HI-STORM 100 System FSAR, as amended by LAR 1014-1.

3.3.1.4.2 Error Contingency Criteria

Provisions for error contingency are built into the criticality analyses discussed in Chapter 6 of the HI-STORM 100 System FSAR, as amended by LAR 1014-1. Because biases and uncertainties are explicitly evaluated in the analyses, it is not necessary to introduce additional contingency for error.

3.3.1.4.3 Verification Analyses

The criticality analyses for the HI-STORM 100 System were performed using computer codes validated for use in this application under the Holtec International Quality Assurance Program. A discussion of the analysis and the applicable computer codes is provided in Section 6.1 of the HI-STORM 100 System FSAR, as amended by LAR 1014-1. Criticality benchmark experiments are discussed in Section 6.5 of the HI-STORM 100 System FSAR, as amended by LAR 1014-1.

3.3.1.5 Radiological Protection

Radiation exposure due to the release of material from the storage system is precluded by the confinement boundary design, as discussed in Section 3.3.1.2. The confinement boundary is designed to maintain its integrity during all normal, off-normal, and accident conditions including natural phenomena. Radiation exposure due to direct and sky shine radiation is minimized to the extent practicable through the use of the "time, distance, and shielding" philosophy. This philosophy is implemented at the Diablo Canyon ISFSI through access control, minimization of required maintenance, and the design of the HI-STORM 100 System.

3.3.1.5.1 Access Control

The Diablo Canyon ISFSI storage pads are surrounded by two fences. The inner is a protected area fence in compliance with the requirements of 10 CFR 73.55. The outer is a restricted area fence in compliance with 10 CFR 20. Only authorized personnel with a need to be in these areas will be permitted entrance. These areas do not require the continuous presence of operators or maintenance personnel. During normal storage operations, the HI-STORM 100 System requires only infrequent, short-duration personnel activity to perform necessary checks on the material condition of the casks and to ensure the overpack air ducts are free of blockage. Higher occupancy times with a greater number of personnel will occur during placement of loaded overpacks at the storage pads and during construction of any additional storage pads. These activities will be governed by the DCPP radiation protection program to ensure occupational radiation exposures are maintained ALARA. Chapter 7 and Section 9.6 provide additional details regarding the implementation of access control at the Diablo Canyon ISFSI.

3.3.1.5.2 Shielding

The HI-STORM 100 System is designed to minimize radiation doses to DCPP personnel and the public through the use of a combination of concrete, lead, and steel shielding. The HI-STORM 100 System is designed to meet the annual dose limit of 25 mrem specified in 10 CFR 72.104 for annual dose at the DCPP owner-controlled-area boundary. The steel shell of the overpack includes concentric inner and outer shells. The annulus between the shells is filled with unreinforced concrete. The requirements for the unreinforced concrete used for shielding are stated in Appendix 1.D to the HI-STORM 100 System FSAR. The steel overpack lid is designed with steel-encased concrete shields to minimize the dose contribution due to sky shine.

The transfer cask is also fabricated from concentric steel shells. The annulus between the shells is filled with lead to provide significant gamma shielding while maintaining the diameter of the transfer cask small enough for loading into the SFP. The transfer cask also includes a water jacket surrounding the main body of the cask. The water jacket is filled with water after the loaded MPC and transfer cask are removed from the SFP to allow as much structural shielding as possible to be designed into the transfer cask without exceeding the 125-ton design weight. Water is not required in the water jacket to provide adequate shielding while there is water inside the MPC cavity. The water in the water jacket provides necessary shielding for neutrons after the water is drained from the inside of the MPC. The MPC lid, the transfer cask top lid, and the bottom shield are designed to provide necessary shielding during onsite transport of the transfer cask in the horizontal position.

The objective of shielding is to ensure that radiation dose rates at the following locations are below acceptable levels for those locations:

- Immediate vicinity of the storage cask
- Restricted area boundary
- Controlled area (site) boundary

Dose rates in the immediate vicinity of the loaded overpack are an important factor in consideration of occupational exposure. A design objective for the maximum average radial surface dose rate has been established as 60 mrem/hr. Areas adjacent to the inlet and exit vents that pass through the radial shield are limited to 60 mrem/hr. The average dose rate at the top of the overpack is limited to less than 60 mrem/hr.

A detailed discussion of the HI-STORM 100 System generic shielding evaluation, including modeling, source-term assumptions, and resultant dose rates is provided in Chapter 5 of the HI-STORM 100 System FSAR, as amended by LAR 1014-1 (Reference 3). The site-specific shielding analysis is discussed in Section 7.3. Estimated occupational exposures and offsite doses for fuel loading, cask handling activities, and storage at the Diablo Canyon ISFSI have been evaluated for DCPP fuel and are discussed also in Sections 7.4 and 7.5.

3.3.1.5.3 Radiological Alarm Systems

The HI-STORM 100 System, when used outside the FHB/AB, does not produce any solid, liquid, or gaseous effluents. Release of loose contamination is not a factor because the HI-STORM overpack is not submerged in the SFP or otherwise subject to contamination. The transfer cask and MPC are submerged in the SFP, but contamination of the MPC is limited to the top of the MPC lid by the annulus seal, which prevents SFP water from coming into contact with the sides and bottom of the MPC. Upon removal from the SFP, the transfer cask and top of the MPC will be decontaminated. Therefore, the inadvertent release of loose contamination from the transfer cask produces a negligible dose effect.

The dose rates for a given storage cask at the Diablo Canyon ISFSI will be stable and decreasing over time due to the decay of the fuel sources stored inside. There is no credible event that could cause an increase in dose rate from the casks.

Based on the foregoing, there is no need for either airborne or area radiological alarms at the Diablo Canyon ISFSI storage pads or CTF. Radiological alarms, if required for operations inside the FHB/AB, will be implemented under the DCPP radiological protection program.

3.3.1.6 Fire and Explosion Protection

There are no combustible or explosive materials associated with the HI-STORM 100 System, except for the fuel contained in the cask transporter fuel tank. Such materials will not be permanently stored within the Diablo Canyon ISFSI protected area. The cask transporter may be parked within the ISFSI, which has been evaluated. However, for conservatism, several hypothetical fire and explosion events were evaluated for the Diablo Canyon ISFSI. Design criteria for fires and explosions are discussed in Section 2.2 and summarized in Section 3.4.

The generic fire evaluations for both the loaded overpack and the loaded transfer cask are described in Section 11.2.4 of the HI-STORM 100 System FSAR. The fire evaluations assume a maximum of 50 gallons of combustible fuel. Therefore, any transport vehicle used to move the loaded overpack or transfer cask is limited by the

Diablo Canyon ISFSI TS to 50 gallons. A site-specific fire evaluation for the Diablo Canyon ISFSI site is provided in Section 8.2.5.

Small overpressures may result from accidents involving explosive materials that are stored or transported near the storage site. Explosion is an accident loading condition evaluated in Section 3.4.7.2 of the HI-STORM 100 System FSAR. A Diablo Canyon ISFSI explosion evaluation for transport to and from the CTF, at the CTF, and at the ISFSI storage pads is discussed in Section 8.2.6.

3.3.1.7 Materials Handling and Storage

3.3.1.7.1 Spent Fuel Handling and Storage

Spent fuel will be moved within the DCPP SFP and loaded into the HI-STORM 100 System in accordance with Diablo Canyon ISFSI TS, DCPP TS, and plant procedures. Only fuel assemblies meeting the burnup, cooling time, decay heat, and other limits of the Diablo Canyon ISFSI TS and SAR Section 10.2 will be loaded. Administrative controls will be used to ensure that no unauthorized fuel assemblies are loaded into the HI-STORM 100 System. The Diablo Canyon ISFSI TS and SAR Section 10.2 limits on fuel assemblies authorized for loading, in combination with the design features of the cask system described earlier in this section, ensure that:

- The keff for the stored fuel will remain less than 0.95.
- Adequate cooling will be provided to ensure peak fuel cladding temperature limits will not be exceeded.
- Radiation dose rates and accumulated doses to plant personnel and the public will be less than applicable limits.

The fuel selection process includes a review of reactor operating records for each fuel assembly and nonfuel hardware chosen for loading into the HI-STORM 100 System. Each fuel assembly will be classified as intact fuel, damaged fuel, or fuel debris, in accordance with the applicable definitions in the Diablo Canyon ISFSI TS and SAR Section 10.2. Fuel assemblies classified as damaged fuel or fuel debris are required to be placed in DFCs for storage in the HI-STORM 100 System.

Section 3.3.1.5 discusses contamination as it relates to the operation of the HI-STORM 100 System. The Diablo Canyon ISFSI TS and SAR Section 10.2 provide the necessary limits on MPC moisture removal, helium backfill, and helium leakage prior to declaring the MPC ready for storage. Chapter 8 of the HI-STORM 100 System FSAR, as amended by LAR 1014-1, provides generic operating procedures for all facets of fuel loading, MPC preparation, and cask handling. The general operating sequence specific to the Diablo Canyon ISFSI is discussed in Sections 5.1 and 10.2 of this SAR. Implementation procedures will be developed based on both generic and site-specific guidelines, as applicable.

The HI-STORM 100 System is designed to allow retrievability of the fuel, as necessary. If the situation warrants fuel retrieval, the MPC is removed from the overpack and returned to the FHB/AB in the transfer cask. The MPC cavity gas is cooled, in accordance with the requirements of the Diablo Canyon ISFSI TS and SAR Section 10.2 and the HI-STORM 100 System FSAR. The MPC is reflooded, the lid removed, and the fuel assemblies are returned to the SFP. Fuel removal activities take place entirely inside the FHB/AB, ensuring that any radiological conditions are controlled and maintained ALARA.

3.3.1.7.2 Radioactive Waste Treatment

There are no radioactive wastes created by the HI-STORM 100 System while in storage at the storage pads, transport to or from the CTF, or at the CTF. During fuel loading and cask preparation activities inside the plant facility, any radioactive wastes created (for example, from decontamination activities) will be treated and handled like any other radioactive waste under the DCPP radwaste management program.

3.3.2 ISFSI CONCRETE STORAGE PAD

The Diablo Canyon ISFSI includes a number of individual storage pads, which will be constructed periodically to meet fuel storage needs of DCPP. For simplicity, this discussion refers to a single storage pad. The design criteria are identical for all pads comprising the ISFSI.

3.3.2.1 General

The ISFSI concrete storage pad must be designed to support the weight of the loaded overpacks under all design basis static and dynamic conditions of storage. The pad must also be designed to support the studs that anchor the overpack to the pad and to maintain the integrity of the fastening mechanism embedded in the pad during a postulated design-basis event. The ISFSI pad has been evaluated for the physical uplift, pad sliding, and overturning moments caused by extreme environmental events (for example, tornado missiles, earthquakes, etc.). Therefore, the pad is engineered as a thick, heavily reinforced concrete structure. Concrete shrinkage and thermal stresses are evaluated in Reference 10. Steel reinforcement of the pad is described in Reference 11.

Because tipover of a cask installed in an anchored configuration is not a credible event, the pad does not need to be engineered to accommodate this non-mechanistic event. Since the lifting devices are designed, fabricated, inspected, maintained, operated, and tested in accordance with NUREG-0612 (Reference 4), a drop of the loaded overpack will not occur; therefore, a specific lifting height limit for the cask at the ISFSI is not required to be established. Based on these two criteria, there is no maximum limit on the hardness of the concrete pad and subgrade.

3.3.2.2 Natural Phenomena

The Diablo Canyon ISFSI concrete storage pad is engineered to perform its design function under all loadings induced by design basis natural phenomena. The design criteria for the natural phenomena applicable to the Diablo Canyon ISFSI site, including seismic loadings, tornado wind, and missile loadings, are discussed in Section 3.2.

3.3.2.3 Design Criteria

The ISFSI pad and its embedment steel design must comply with the ACI 349-97, NUREG-1536 (Reference 5) and with NRC draft Regulatory Guide DG-1098 as applicable. A new Proposed Appendix B to the ACI 349-97 (dated 10/01/00) was used. (It may be noted that the NRC took exception to the Appendix B [of the 97 Code] as stated in DG-1098.) Specifically, the design strength capacity of the embedded base plate, concrete bearing, and diagonal tension shear capacity are in accordance with the design provisions of ACI 349-97 and the embedded anchorage is to meet the ductile anchorage provisions of the Proposed Draft New Appendix B to ACI 349-97 (dated October 1, 2000). The materials of construction (for example, anchor stud material and additives in the pad concrete) have been chosen to be compatible with the environment at the Diablo Canyon ISFSI site. ISFSI pad design life is 40 years. The surface anchorage studs (i.e. SA-193 B7 Studs and the exposed embedment plates) will be properly coated for corrosion protection.

The use of an embedded steel structure underneath the cask and in the concrete storage pad is to be employed at the Diablo Canyon ISFSI. The purpose of the embedded structure is to permit the cask anchor studs to be preloaded, while the embedded steel structural connection to the concrete does not involve a preload. The embedded structure, while not part of the cask system, is designed in accordance with the AISC Manual of Steel Construction (Reference 6) and the ACI 349-97 requirements.

3.3.2.3.1 Load Combinations for the Concrete Storage Pad

Factored load combinations for ISFSI pad design are provided in the ACI-349-97 and supplemented by the factored load combinations from NUREG-1536 (Reference 5), Table 3.1 and NRC draft Regulatory Guide DG-1098, as applicable.

<u>Overturning and Sliding</u>

Since the casks at the Diablo Canyon ISFSI are anchored to the concrete pads, the load combinations from Table 3-1 of NUREG-1536 associated with gross sliding and overturning at the cask/pad interface are not applicable to the cask. The gross sliding of the loaded pad structure was evaluated using a dynamic non-linear seismic analysis to determine the extent of sliding. Pad overturning is not considered as a credible failure mechanism due to the size and geometry of the pad (that is, 68 ft wide by 105 ft long by 7.5 ft thick). The sliding analysis acceptance criteria is: The analysis is to show insignificant impact on the pad's ability to meet its functional requirements and the cask design qualifications as a result of potential pad sliding.

3.3.2.3.2 Load Combinations for the Cask Anchor Studs

The design of the cask anchor studs is governed by the ASME Code, Section III, Subsection NF and Appendix F (Reference 7). The applicable load combinations and allowable stress limits for the anchor studs attaching the cask to the intervening steel support structure are:

Normal Conditions:

Load Combination: D

Code Reference for Stress Limits: NF-3322.1 and NF-3324.6

Off-Normal Conditions:

Load Combination: D+F

Code Reference for Stress Limits: NF-3322.1 and NF-3324.6 with all stress limits increased by a factor of 1.33

Accident Conditions:

Load Combinations: D+E and D+W_t

Code Reference for Stress Limits: Appendix F, Sections F-1334 and F-1335

The axial stress in the cask anchors induced by pretensioning is kept below 75 percent of the material yield stress, such that during a seismic event the maximum stud axial stress remains below the limit prescribed for bolts in the ASME Code, Section III, Subsection NF, for Level D conditions.

3.3.2.3.3 Maximum Permissible Tornado Wind and Missile Load

During a tornado event, the HI-STORM 100 System may be subjected to a constant wind force and differential pressures. It may also be subjected to impacts by tornado-borne missiles. In contrast to a free-standing cask, the anchored cask system is capable of withstanding greater lateral pressures and impulsive loads from large missiles. The anchored HI-STORM 100SA cask design at the Diablo Canyon ISFSI has been analyzed assuming the lateral force from the site-specific design-basis, large-tornado-missile impact occurs at the worst-case height on the cask and the force created by the tornado wind action and differential pressure acts simultaneously at cask mid-height. The resulting overturning moment is bounded by the maximum seismic overturning moment applied to the cask anchorage embedment and the pad.

3.3.3 CASK TRANSPORTER

3.3.3.1 General

The cask transporter is a U-shaped tracked vehicle used for lifting, handling, and onsite transport of loaded overpacks and the transfer cask. The functional specification for the transporter is provided in Reference 12. The cask transporter does not have a suspension system (for example, springs). The transporter consists of the vehicle main frame, the lifting towers, an overhead beam system that connects the parallel lifting towers, a cask restraint system, the drive and control systems, and a series of cask lifting attachments. The casks are individually carried within the internal footprint of the transporter tracks (Sections 4.3 and 4.4 provide more detailed descriptions of cask transportation components and operating characteristics). The cask is supported by the lifting attachments that are connected to the overhead beam. The overhead beam is supported at the ends by a pair of lifting towers. The lifting towers transfer the cask weight directly to the vehicle frame and ultimately to the tracks and the transport route surface. The cask transporter has the added capability of being able to raise and lower an MPC between the transfer cask and the overpack when used in conjunction with the CTF. The transporter's CTF functions are contained in Section 2.3.3.1 of the HI-STORM 100 System FSAR, as amended by LAR 1014-1.

3.3.3.2 Design Criteria

The key design criteria for the cask transporter are summarized in Table 3.4-4. The bases for these criteria are discussed in the sections below.

3.3.3.2.1 Design Life

The cask transporter design life of 20 years has been established based on a reasonable length of time for a vehicle of its type with normal maintenance. The cask transporter may be replaced or recertified for continued use at the end of its design life.

3.3.3.2.2 Environmental Design Criteria

The cask transporter is an "all-weather" vehicle. It is designed to operate in both rain and snow over a temperature and humidity range that bounds the historical conditions at the Diablo Canyon site. Materials that would otherwise degrade in an coastal marine environment will be appropriately maintained.

A lightning strike on the cask transporter would not structurally affect the ability of the transporter to hold the load. Due to the massive amount of steel in the structure, the current would be transmitted to the ground without significantly damaging the transporter. However, the driver may be affected by a lightning strike. Therefore, the transporter design includes fail-safe features to automatically shutdown the vehicle into a safe, stopped, and braked condition if the operator is injured or incapacitated for any reason while handling a loaded cask.

Flooding is not a concern on the transport route as discussed in Section 3.2.2. Sources of fires and explosions have been identified and evaluated. Fixed sources of fire and explosion are sufficiently far from the transport route to not be of concern (Section 2.2). Mobile sources of fire and explosion, such as fuel tanker trucks, will be kept at a safe distance away from the transporter during cask movement through the use of administrative controls. The cask transporter is diesel-powered and is limited to a maximum fuel volume consistent with that used in the HI-STORM 100 System fire accident analysis. The hydraulic fluid used in the cask transporter is nonflammable.

3.3.3.2.3 Regulatory Design Criteria and Industry Standards

The transporter is designed, fabricated, inspected, maintained, operated, and tested in accordance with applicable guidelines of NUREG-0612, which allows the elimination of the need to establish a cask lift height limit.

3.3.3.2.4 Performance Design Criteria

As described in Section 4.4, the cask transporter must lift and transport either the loaded transfer cask or the loaded overpack, including the weight of all necessary ancillary lift devices such as rigs and slings. The loaded overpack, being the heavier of the two casks to be lifted, provides the limiting weight for the design of the transporter.

3.3.3.2.5 Stability Design Criteria

The cask transporter is custom designed for the Diablo Canyon site, including the transport route with its maximum grade of approximately 8.5 percent. It will remain stable and will not experience structural failure, tip over, or leave the transport route should a design-basis seismic event occur while the loaded transfer cask is being moved to the CTF, while transferring an MPC at the CTF, while moving a loaded overpack from the CTF to the storage pad, or while moving a loaded overpack on the storage pad. In addition, the cask transporter is designed to withstand design-basis tornado winds and tornado-generated missiles without an uncontrolled lowering of the load or leaving the transport route. All design criteria for natural phenomena used to design the cask transporter are specific to the Diablo Canyon site (Sections 3.2 and 3.4 provide further information).

3.3.3.2.6 Drop Protection Design Criteria

In accordance with NUREG-0612, prevention of a cask or MPC drop is provided by enhancing the reliability of the load supporting systems by design, using a combination of component redundancy and higher factors of safety than would normally be used for a commercial lift device. Load supporting components include the special lifting devices used to transfer the force of the payload to the cask transporter lift points (including attachment pins, as appropriate), the cask transporter lift points, the overhead beam, the lifting towers, and the vehicle frame. The design criteria for each of the components of the cask transporter are the following:

Slings and Special Lifting Devices

The transfer cask horizontal lift rig, HI-TRAC lift links, MPC downloader slings, overpack lifting brackets, and HI-STORM lift links are designed to applicable guidelines of NUREG-0612.

Cask Transporter Lift Points, Overhead Beam, Vehicle Body and Seismic Restraints

The cask transporter lift points, overhead beam, and load supporting members of the vehicle body (whose failure would result in an uncontrolled lowering of the load) are designed to applicable guidelines of NUREG-0612.

Lifting Towers

The lifting towers are designed with redundant drop protection features. The primary cask lifting device is the hydraulic system, which prevents uncontrolled cask lowering through the control of fluid pressure in the system. A mechanical backup load retaining device, independent of the hydraulic lifting cylinders, is provided in case of failure of the hydraulic system. This may consist of load blocks, pawl and detent, locking pins, or other suitably designed positive mechanical locking device.

3.3.3.2.7 Drive System Design Criteria

The cask transporter is capable of forward and reverse movement as well as turning and stopping. It includes an on-board engine capable of supplying enough power to perform its design functions. The cask transporter includes fail-safe service brakes (that is, brakes that automatically engage in any loss of power and/or independent emergency) and parking brakes. The brake system is capable of stopping a fully loaded cask transporter on the maximum design grade. The cask transporter is equipped with an automatic drive brake system that applies the brakes if there is a loss of hydraulic pressure or the drive controls are released. The cask transporter is not capable of coasting on a 10 percent downward grade with the brakes disengaged due to the resistance in the drive system.

3.3.3.2.8 Control System Design Criteria

The cask transporter is equipped with a control panel that is suitably positioned on the transporter frame to allow the operator easy access to the controls located on the control panel and, at the same time, allow an unobstructed view of the cask handling operations. The control panel provides for all-weather operation or will be enclosed in the cab. The control panel includes controls for all cask transporter operations including speed control, steering, braking, load raising and lowering, cask restraining, engine control and "dead-man" and external emergency stop switches.

The drive control system is capable of being operated by a single operator from an on-board console. The control panel contains all gauges and instruments necessary for the operator to monitor the condition and performance of both the power source and hydraulic systems. A cask lift-height indicator is provided to ensure the loaded casks are lifted only to those heights necessary to accomplish the operational objective in progress.

3.3.3.2.9 Cask Restraint Design Criteria

The cask transporter is equipped with a cask restraint to secure the cask during movement. The restraint is designed to prevent lateral and transverse swinging of the cask during cask transport. The restraint is designed to preclude damage to the cask exterior with padding or other shock dampening material used, as necessary.

3.3.4 CASK TRANSFER FACILITY

3.3.4.1 General

The ISFSI CTF is used in conjunction with the cask transporter to accommodate MPC transfers between the transfer cask and the overpack. The CTF is designed to position an overpack sufficiently below grade where the transfer cask can be mated to the overpack using the cask transporter. The CTF lifting platform acts as an elevator to raise and lower the overpack. In the full-up position, the overpack base is approximately 40 inches below grade. The surface of the CTF contains an approach pad that supports the loaded transporter and provides a laydown area for the transfer cask, cask transport frame, mating device, seismic restraint, and other load handling equipment.

3.3.4.2 Design Criteria

The rated load of the CTF lifting system is the bounding weight of a loaded overpack (360,000 lb). The design criteria for the specific subcomponents are discussed below. The CTF is designed to withstand a design-basis seismic event without an uncontrolled lowering of the lifted load. The design life of the CTF is 40 years. Design criteria for the CTF are summarized in Table 3.4-5 and presented in Reference 13.

3.3.4.2.1 Main Shell Design Criteria

A cylindrical steel shell forms the opening in the ground into which the overpack is lowered, provides the support for the lifting jacks, and provides a setdown location for the lifting platform when it is fully lowered. The main shell forms a cylindrical opening of approximately 150 inches in diameter and approximately 200 inches deep. Three extensions run the length of the cylinder and form the locations for the jacks. The shell is also equipped with a sump for collecting and disposing of incidental water from the CTF. The surrounding area is reinforced concrete. The resulting structure is a flat-surfaced pad with a steel-lined hole. The main shell is designed in accordance with applicable portions of ASME Section III, Subsection NF.

3.3.4.2.2 Lifting Jacks

Three lifting jacks provide the lifting force for the lifting platform. The jacks are located on the circumference of the main shell in the extensions. The jacks are supported at the top end and suspend the lifting platform by bearing on a traveling nut on each jack screw. All jacks operate in unison to keep the platform level through the entire travel range (approximately 160 inches). The jacks are interconnected with an electronic position monitoring and control system. The maximum lift speed of the jacks is 12 inches/minute and will not unwind on loss of the driver.

3.3.4.2.3 Drive and Control System

A drive and control system provides the power and control for the lifting jacks. Electrical power is supplied to each jack drive motor. The speed is reduced via one or more gearboxes. The relative position of each jack is monitoring by the drive and control system to stop all jacking if a mismatch is detected. Position switches limit the travel beyond established points. The control system is designed in accordance with applicable guidelines of NUREG-0612, Section 5.1.6 (2). The lifting jack design ensures the load will stop in position on a loss of electrical power to the drive and control system.

3.3.4.2.4 Lifting Platform

A lifting platform provides the support of the overpack and transmits the lifting jack force to the cask. Multiple beams or a single torsion box-type beam forms the lifting platform. The platform provides a level base on which the overpack rests. To interface with the lifting jacks, the platform has extensions that enter into each main shell extension. Uniform loading of the lifting platform is afforded by the location and controlled movement of the jacks. Radial stability of the lifting platform is provided by the main shell.

Wheeled or low-friction pad-type vertical guides or runners are provided to prevent damage to the main shell and lifting platform at the interface locations. The guides (or runners) are capable of restraining the lift platform under the maximum horizontal loading due to a design basis seismic event.

3.3.4.2.5 HI-STORM Mating Device

A mating device provides structural support and shielding at the interface between the top of the open overpack and the bottom of the transfer cask during MPC transfer operations. The mating device also facilitates the removal of the pool lid from the transfer cask prior to MPC transfer operations.

3.3.4.2.6 Top Shell Seismic Restraint

A removable top shell seismic restraint provides lateral structural support in the gap between the overpack and the CTF main shell (Reference 14).

3.3.4.2.7 Reinforced Concrete Support Structure

The reinforced concrete surrounding the shell is capable of supporting a loaded transporter and handling any seismic loads applied through the shell. The reinforced concrete base pad supports the CTF shell and a steel pedestal base that supports the lifting platform when it is in the full-down position. The approach pad is designed for the weight of the transporter with a loaded overpack. Independent tie-down blocks at the surface of the CTF will be provided to hold the transporter in place during the MPC transfer operation. The reinforced concrete structure is qualified to ACI-349-97 (Reference 8), NUREG-1536, and DG-1098, as applicable.

3.3.4.2.7.1 Design Load Combinations

Factored load combinations for the CTF concrete structure design are provided in the ACI 349-97 and supplemented by the factored load combinations from NUREG-1536 (Reference 5), Table 3.1, and NRC draft Regulatory Guide DG-1098 (Reference 9), as applicable.

3.3.5 REFERENCES

1. 10 CFR 72, Licensing Requirements for the Independent Storage of Spent Nuclear Fuel and High-Level Radioactive Waste.

2. Final Safety Analysis Report for the HI-STORM 100 System, Holtec International Report No. HI-2002444, Revision 0, July 2000.

3. License Amendment Request 1014-1, Holtec International, Revision 2, July 2001, including Supplements 1 through 4 dated August 17, 2001; October 2, 2001; October 12, 2001; and October 19, 2001; respectively.

4. Control of Heavy Loads at Nuclear Power Plants, USNRC, NUREG-0612, July 1980.

5. Standard Review Plan for Dry Cask Storage Systems, USNRC, NUREG-1536, January 1997.

6. Manual of Steel Construction, American Institute of Steel Construction, 9th Edition.

7. Boiler and Pressure Vessel Code, Section III, Division 1, Subsection NF, American Society of Mechanical Engineers, 1995 Edition including 1996 and 1997 Addenda.

8. ACI-349-97, Code Requirements for Nuclear Safety Related Concrete Structures, American Concrete Institute, (with Draft Appendix B [10/01/00]).

9. Draft Regulatory Guide DG-1098, Safety Related Concrete Structures for Nuclear Power Plants (Other than Reactor Vessel and Containment), USNRC, August 2000.

10. Calculation PGE-009-CALC-006, "ISFSI Cask Storage Pad Concrete Shrinkage and Thermal Stresses."

11. Calculation PGE-009-CALC-007, "ISFSI Cask Storage Pad Steel Reinforcement."

12. Holtec International Report No. HI-2002501, "Functional Specification for the Diablo Canyon Transporter."

13. Holtec International Report No. HI-2002570, "Design Criteria Document for the Diablo Canyon Cask Transfer Facility."

14. PG&E Calculation M-1058, "Cask Transfer Facility Seismic Restraint Configuration."

TABLE 3.4-1

DESIGN CRITERIA FOR ENVIRONMENTAL CONDITIONS AND NATURAL PHENOMENA APPLICABLE TO THE MAJOR ISFSI STRUCTURES, SYSTEMS, AND COMPONENTS

Design Criterion	Design Value	Reference Documents
Wind	80 mph with a gust factor of 1.1 Condition is bounded by tornado wind	Diablo Canyon ISFSI SAR Section 3.2.1
Tornado	200 mph maximum speed 157 mph rotational speed 43 mph translational speed 0.86 psi pressure drop 0.36 psi/sec pressure drop rate	Diablo Canyon ISFSI SAR Section 3.2.1, Table 3.2-1
Tornado Missiles	See Diablo Canyon ISFSI SAR Table 3.2-2	Diablo Canyon ISFSI SAR Section 3.2.1
Flood	Design-basis flooding event is not considered credible	Diablo Canyon ISFSI SAR Section Section 3.2.2
Seismic	See Diablo Canyon ISFSI SAR Section 3.2.3	Diablo Canyon ISFSI SAR Section 3.2.3
Snow & Ice	Design-basis snow and ice loadings are not considered credible	Diablo Canyon ISFSI SAR Section 3.2.4
Explosion	A fuel tank for the transporter, load handling equipment, or other vehicle 7-gallon propane bottles being transported via Reservoir Road Standard acetylene bottles transported to the vehicle maintenance shop via Reservoir Road A 250-gallon propane tank, a 2,000-gallon #2 diesel fuel oil tank, and a 3,000-gallon gasoline tank located in close proximity to each other and beside the main plant road and approximately 1,200 ft from the transport route to the ISFSI storage pad	Diablo Canyon ISFSI SAR Sections 2.2.2.3, 3.3.1.6, and 8.2.6

TABLE 3.4-1

Design Criterion	Design Value	Reference Documents
Explosion (continued)	The Unit 2 main bank transformers, which contain approximately 13,000 gallons each of mineral oil and are located 160 ft from the transport path Standard compressed gas bottles (air, nitrogen, argon, CO_2) located inside the RCA and near the El. 115' south gate Hydrogen gas facility adjacent to the transport route Acetylene bottles stored on the east side of the cold machine shop	
Fire	A fuel tank for the transporter, load handling equipment, or other vehicle Local stationary fuel tanks Local combustible materials Nearby grass/brush fire	Diablo Canyon ISFSI SAR Sections 2.2.2.2, 3.3.1.6, and 8.2.5
Ambient Temperatures	Annual Average = 55°F Minimum recorded was below freezing for a few hours. Maximum Recorded = 97°F Extreme Temperature Range = 24°F to 104°F	Diablo Canyon ISFSI SAR Sections 2.3.2, 3.2.7, 8.2.6, and 8.2.10
Insolation	766 g-cal /cm^2 maximum for a 24-hr period	Diablo Canyon ISFSI SAR Section 3.2.7

DIABLO CANYON ISFSI
SAFETY ANALYSIS REPORT

CHAPTER 4

ISFSI DESIGN

CONTENTS

DIABLO CANYON ISFSI
SAFETY ANALYSIS REPORT

CHAPTER 4

ISFSI DESIGN

CONTENTS (Continued)

DIABLO CANYON ISFSI
SAFETY ANALYSIS REPORT

CHAPTER 4

ISFSI DESIGN

TABLES

DIABLO CANYON ISFSI
SAFETY ANALYSIS REPORT

CHAPTER 4

ISFSI DESIGN

FIGURES

CHAPTER 4

ISFSI DESIGN

FIGURES (continued)

4.2 STORAGE SYSTEM

Final construction design and analysis of the Diablo Canyon ISFSI storage pad and the CTF will be completed during the detailed design phase of the project. No significant changes are anticipated from the information presented.

4.2.1 STRUCTURES

Major important-to-safety ISFSI structures and their site locations are described in the following sections:

- Section 4.2.1.1 Cask Storage Pads
- Section 4.2.1.2 CTF
- Section 4.2.2 Site Layout
- Section 4.2.3 Storage Casks

See Figure 2.1-2 for the location of the Diablo Canyon ISFSI site in relation to the power block. See Figure 4.1-1 for the Diablo Canyon ISFSI site layout and the immediate surroundings.

4.2.1.1 Cask Storage Pads

The Diablo Canyon ISFSI storage site is designed to include seven cask storage pads in a row. Each pad will accommodate up to 20 HI-STORM 100SA storage casks. Figure 4.1-1 shows the layout of the pads with the surrounding security fence, restricted area fence, and approximate dimensions. Seven storage pads provide sufficient storage space for DCPP spent fuel through plant decommissioning. The seismic design criteria for the cask storage pads are described in Section 3.2.3 and 3.3.2. Pad embedment design criteria are integrated with the storage cask pad design criteria, which is the primary focus of discussion in Section 3.3.2. A further discussion of the design criteria, analyses, and resulting design of the cask storage pads is provided here.

4.2.1.1.1 Function

The function of the cask storage pads is to provide a level, competent structural surface for placement of the loaded overpacks for all design-basis conditions of storage. The storage casks (overpacks) are to be anchored to the pad by 16, 2-inch diameter, SA 193 Gr. B7 studs.

4.2.1.1.2 Design Specifications

The cask storage pad design is based on a maximum, loaded-overpack weight of 360,000 lb each. This maximum weight bounds the maximum loaded weight of the overpacks proposed for use at the Diablo Canyon ISFSI. Each HI-STORM 100SA overpack proposed for use at the Diablo Canyon ISFSI can contain one of the following pressurized water reactor (PWR) fuel canisters: MPC-24, MPC-24E, MPC-24EF, or MPC-32, with maximum weights given in Table 4.2-1 of this SAR and shown in Table 3.2-1 of the HI-STORM 100 System FSAR (Reference 1), as amended by Holtec LAR 1014-1 (Reference 2). See Section 3.3.2 for more details on the storage pad design criteria.

4.2.1.1.3 Plans and Sections

The site plan, which shows the locations of the concrete storage pads in relation to the power plant facility, is shown in Figure 2.1-2. A cross section of a typical concrete storage pad plan is shown in schematic Figure 4.2-1.

4.2.1.1.4 Components

- **Embedment Steel Assembly**: This assembly consists of structural steel plates and rods. The function of this assembly is to properly distribute the loads imposed on the surface (by the storage casks) to the entire structure (Figure 4.2-2).

- **Reinforced Concrete**: The steel-reinforced concrete is designed for a mix with a compressive strength of 5,000 psi at 90 days. The reinforcing steel bars will have minimum 60,000-psi yield strength.

4.2.1.1.5 Design Bases and Safety Assurance

The cask storage pads are classified as important to safety in order to provide the appropriate level of quality assurance in the design and construction. This classification is consistent with the recommendation made in Section 2.0.4 of the HI-STORM 100 System FSAR, as amended by Holtec LAR 1014-1, for deployment of the anchored HI-STORM 100SA overpack at a high-seismic site. This ensures that the cask storage pads will perform their intended functions.

4.2.1.1.6 Storage Pad Design

The cask storage pads (total of seven) are structural units constructed of steel-reinforced concrete. Each concrete pad is approximately 68 ft wide by 105 ft long and 7.5 ft thick with longitudinal and transverse horizontal reinforcing bars near the top and bottom of the pads. The concrete compressive strength will be 5,000 psi at 90 days. The reinforcement bars will have minimum yield strength of 60,000 psi (Reference 17).

Each pad accommodates a center-to-center spacing of 17 ft for the overpacks. Each of the cask storage pads accommodates up to 20 loaded overpacks (4 rows of 5). The sides of each storage pad are designed with an additional apron to provide maneuvering room for the cask transporter before it is driven onto the pad. The pads are nearly flush with grade to allow direct access by the cask transporter. The casks will be installed on the pads in a prescribed loading sequence to assure pad stability for all design-basis accidents and to maintain design qualifications. The loading sequence will be proceduralized.

The cask storage pad is designed with an embedded steel structure having a steel plate ring (Figure 4.2-1) at the surface of the concrete that mates with the bottom of the cask. Each cask is compressed against the embedment plate using 16 studs. Each stud is preloaded to approximately 157,000 lbf. The preload is achieved by threading the SA193-B7 studs into a coupling steel block located on the underside of the embedment plate, buried in the concrete. The seismic tensile/bending loads imposed on the pad will then be resisted by the long A-36 steel rods connected to the bottom base plate (Figure 4.2-2). The base plates are designed to provide sufficient bearing area onto the concrete so as to be able to transfer loads by bearing. Shear loads from each cask will be carried through the embedment plate/coupling blocks into the concrete.

4.2.1.1.7 Storage Pad and Anchorage Analysis

The pad structural seismic analysis is performed by developing a finite-element model, using the ANSYS FEA Program (Reference 3) of a representative pad, which includes the casks and the supporting rock, to determine the potential for pad uplift and to calculate the stress fields in the concrete. The results of this static analysis are used in the design of the reinforcements to ensure that the bending moments are adequately carried by the pad, and that the stress limits of ACI 349-97 are satisfied. The specific pullout provisions of Appendix B are not applicable to anchorage and base plates of the proposed size. The anchorage is designed to meet the ductile-anchorage provisions of the October 1, 2000, Proposed Draft Appendix B to ACI 349-97 (Reference 4). The new Appendix B has since been officially issued as a part of ACI 349-01 (Reference 22). The methodology used assumes the loading imposed on the pad embedment structures is similar to an inverted column. Specifically, the design-strength capacity of the embedded base plate, concrete bearing, and diagonal tension-shear capacity computed in accordance with the design provisions of ACI 349-97 all exceed the required ductile design strength of the embedded anchor stud. Furthermore, the ultimate tensile strength of the reduced section at the thread root of the anchor bar is approximately 125 percent of the yield strength of the unreduced gross section of the anchor bar. Anchor bars are made of A36 steel, which has a well-defined yield plateau. Thus, if any overload occurs, the anchor bars will yield before any less ductile failure could occur. Lastly, the yield strength of the embedded anchor studs is more than 250 percent of the computed demand load on these bars to provide substantial margin against yielding. Reference 15 contains design and analysis information pertaining to the embedment support structure.

Supporting evidence that the concrete will not break out prior to failure of ductile metal members is provided in Reference 26. The tension tie-rods are not treated like anchors for the reasons stated above in the design philosophy. They are treated as inverted columns on base plates and are sized to have lower ultimate strength than the surrounding concrete strength in bearing and diagonal shear as provided by the provisions of the main body of the ACI 349 code. As such, the design ensures ductile behavior, which meets the intent of Appendix B to the ACI 349 code. Reference 15 provides various capacity calculations for different elements in the load path, thus providing the required evidence as stated above. Furthermore the design has substantial margin between the yield capacity of the weakest element (tension tie-rods) and the imposed tension pull-out demand load.

The load path for delivery of shear load into concrete is through the coupler at the top of the tension tie-rods. As such, the tension tie-rods are not relied on to deliver any shear load into concrete.

Lastly, the combination of the tension (pad flexure) and shear (pull-out) loading in the reinforcing steel and the minimum required steel area has been demonstrated and shown to have considerable margin.

The pad was evaluated for sliding. Section 8.2.1.2.3.2 describes the dynamic non-linear time history analysis that was performed to evaluate pad sliding. Overturning is not considered as a credible failure, considering the overall geometry of the structure.

4.2.1.1.7.1 Pad Static Analysis

A solid finite element model of the pad was developed (using the ANSYS FEA Program) to statically analyze the pad for loads imposed by the casks, as well as the pad-inertia loads, due to ZPA excitation from postulated bounding ground motions (Section 8.2.1.2.3.2). The static loading cases were performed for a range of ground/rock moduli of elasticity to account for variations in the rock properties. The earthquake loadings bound the other accidental loading conditions (for example, explosion and tower collapse) and natural phenomena accident conditions (for example, tornado and wind).

4.2.1.1.7.2 Cask Dynamic Analyses

The storage cask is analyzed by a nonlinear, time history analysis for bounding ground motions. The resulting anchorage loading at the concrete/embedment interface is used for the detailed analysis of the pad and the embedment steel (see Section 4.2.1.1.7.1 for a discussion of the pad static analysis). The cask dynamic analysis is explained further in Section 8.2.1.2.3.1.

4.2.1.1.8 Storage Pad Settlement

No pad settlement is anticipated as a result of the facility placement on the rock site (See Section 2.6.4.4 for more discussion).

4.2.1.1.9 Slope Stabilization Measures

The following sections discuss slope stabilization and rock fall mitigation measures being taken to ensure the storage casks are not adversely affected by debris flow and rock falls.

4.2.1.1.9.1 Cut Slope, Stabilization Design

As discussed in Sections 2.6.5.2.1 and 2.6.5.2.2, rock blocks exposed after cut-slope excavation have the potential to fall into the excavation under both static and seismic loading conditions. After excavation, cut-slope faces will be protected from weathering and minor raveling by a wire-mesh-reinforced shotcrete facing to stabilize the cut slope and prevent or minimize potential failures from occurring. To stabilize larger rock blocks, potentially prone to failure during seismic loading, rock anchors (Reference 18) will be installed in approximately 2- to 3-inch diameter holes on approximately 5-ft centers and drilled subhorizontally approximately 30 ft deep from the cut-slope faces (Figure 4.2-3). Square concrete pads with steel top plates will be formed and cast over the holes to distribute anchor loads to the rock surface. High-strength, corrosion-protected bar anchors will be inserted into the holes, grouted and stressed. Each bar will be installed and proof-tested as recommended by the Prestressed Tensioning Institute (PTI). Additional holes, one approximately every fifth anchor, will be drilled between anchor holes and lined with PVC drainpipe to ensure the slope remains free for draining. The actual pattern will be adjusted during construction, based on the conditions found.

4.2.1.1.9.2 Mitigation of Potential Displacements along Clay Beds

As discussed in Section 2.6.5.1.3, potential rock mass displacements along clay beds due to seismic ground motions are calculated to range from 1 to 3 ft on the clay beds located on the natural slope above the ISFSI site, and 1 ft to 2 ft on the clay beds inferred to daylight in the cut slope or pass just below the ISFSI site. The effects of these potential displacements will be mitigated, as described below.

Rocks dislodged by displacements along any of the several clay beds on the natural slope above the ISFSI site will be prevented from reaching the ISFSI site by a rockfall barrier constructed at the top of the ISFSI cut slope. This barrier will be designed to absorb and dissipate the kinetic energy of the rockfall and will be constructed of articulated steel posts, bundled wire ring steel nets, friction brake elements, anchoring and retaining ropes, and rock anchors.

Rocks offset by displacements along clay beds daylighting in the cut slope will be prevented from dislodging from the cut slope face by the wire-mesh-reinforced shotcrete facing and rock anchor system described in Section 4.2.1.1.9. The orientation of clay beds in the region of the cut slope is approximately parallel to the preferred rock anchor orientation, thereby minimizing the potential for damage to the anchors as a result of displacements along the clay beds. In the unlikely event that rock blocks are completely dislodged from the cut-slope face during a seismic event, the midslope bench width and offset distance from the slope base to the ISFSI pads are sufficient to accommodate the largest rock blocks as defined in
Section 2.6.5.2.2.

In the event displacements occur along clay beds inferred to pass beneath the site, it is expected that any displacements propagating upward will do so through the weaker rock surrounding the massive, heavily reinforced concrete pads, and not impose significant additional loads or displacements on the pads themselves.

The design basis criteria and analysis of potential slope instability mitigation features are further described and discussed in References 27 and 28.

4.2.1.2 CTF Support Structure

The CTF concrete support structure is a cylindrical, steel-lined structure, embedded in the rock, underground; made-up of steel-reinforced slabs and walls (Figure 4.2-4). This concrete structure houses the CTF steel shell structure consisting of a lift platform and associated mechanical equipment. The facility is designed with a sump for incidental water collection. An associated standpipe will accommodate a temporary, drop-in sump pump for water removal. When not in use, the facility will be enclosed with a cover for personnel safety and protection of the structure from the environment. The transporter tie down locations immediately adjacent to the CTF support structure is shown on Figure 4.2-4. The tie downs will be supported by rock anchor installations into the ground. Holtec Drawing 3770, showing the CTF shell structure, is provided in
Figure 4.4-3.

The CTF structure is fully and permanently embedded in the ground. The top of the structure is at grade and the bottom of the concrete base slab is approximately 20 ft below the surface of the adjacent competent rock (see Figure 4.2-4). Once the base slab is poured, the main shell steel structure is placed, plumbed and anchored to the base slab. Concrete is placed between the exterior surface of the main shell and the surrounding competent rock. Following concrete placement, the main shell remains embedded in the concrete.

The concrete portion of the facility is designed to transfer all loads to the rock in direct bearing of the concrete on the rock. The analysis demonstrates that all stresses in the concrete and the rock remain less than the allowable limits under all design conditions. Therefore, it is not necessary to anchor the concrete structure to the rock.

The design of the CTF is described in References 24 and 25. This calculation demonstrates that the concrete structure is capable of resisting all applied loads and adequately transferring these loads to the surrounding rock. This includes all applicable loads from the transporter, the CTF structure and the fully loaded cask. This calculation considers all operating loads in addition to other applicable loads including seismic. A removable seismic restraint provides lateral support in the gap between the overpack and the CTF main shell (Reference 21).

Holtec Calculation HI-2012626 (Reference 25), demonstrates the feasibility of the CTF conceptual design by modeling major components and developing the loads transmitted to the concrete support structure. The description of load paths is provided in Section 1.2 of the report. The demand and capacity of the main shell and various major components are provided in Attachment A, Section A.10. The summary of safety factors of the major components is provided in Attachment A, Section A.11. In addition to the information provided in HI-2012626, Drawing 3770 (SAR Figure 4.4-3) provides materials of construction and major dimensional information for the CTF. SAR Table 3.4-5 specifies that ASME Section III, Subsection NF, Appendix F, NUREG-0612, and ACI-349 (including draft Appendix B) are the governing codes for the design of the CTF. These codes provide requirements for design, materials, welding, inspection, brittle fracture testing, etc., which will be reflected in the final design and procurement documents. Fabrication, assembly, and test procedures will be developed in accordance with the design criteria and specifications, drawings, and applicable codes after final design is complete.

For added documentation, PG&E submitted the Holtec-proprietary design criteria document for the CTF (HI-2002570) to the NRC (Reference 23), which provides additional detail on codes and standards, as well as performance requirements. The aforementioned documents provide the complete set of information available regarding the design of the CTF, including the main shell, jack support platform, and lifting platform. The final design will be performed in accordance with these design criteria and codes and the detailed design documents will include all of the appropriate design details. After construction, the CTF will be functionally tested prior to use.

4.2.1.2.1 Function

The function of the CTF support structure is to provide a flat, concrete pad at the bottom of the facility to accommodate installation of the CTF steel shell and lift platform, and to provide a rigid, concrete pad on the surface for the cask transporter. The CTF lifting platform function is to raise and lower the overpack for MPC transfer operations.

4.2.1.2.2 Design Specifications

The structure will have provisions for a sump and sump pump to allow for removal of incidental rainwater. The CTF and its supporting structure will be qualified to withstand the design earthquake (DE), double-design earthquake (DDE), Hosgri earthquake (HE), and LTSP earthquakes without an uncontrolled lowering of the lifted load

(Section 3.3.4). The earthquake loading bounds the other accidental loading conditions (for example, tower collapse) and natural phenomena accident conditions (for example, tornado and wind). See Section 3.3.4 for a discussion of the CTF design criteria.

4.2.1.2.3 Static Analysis

The reinforced concrete was designed and evaluated for a transporter on top of the facility and the overpack in the CTF during the MPC transfer operation. The structure is designed for appropriate vertical and lateral loads imposed during the DE, DDE, HE and LTSP earthquakes. The concrete and the reinforcing steel have been designed in accordance with the requirements set forth in ACI 349-97 (Reference 4). A static, seismic analysis was performed on the CTF shell and lifting platform (Section 8.2.1).

4.2.1.2.4 CTF Structure Layout

The structure is located on the ISFSI site approximately 100 ft from the concrete storage pads (Figure 4.1-1).

4.2.2 SITE LAYOUT

A plan view of the ISFSI storage site layout is shown in Figure 4.1-1. This figure shows the functional features of the storage site, including the locations of the CTF, the security and restricted area fences, and the access road that leads up from the DCPP. A section view of the ISFSI storage site is shown in Figure 4.2-5. This figure provides separation distances from the pad to nearby features, including the cut-slope hillside to the south and east of the pad.

As shown in Figures 4.1-1 and 4.2-5, a removable fence is located between the security fence and the raw water reservoirs. This fence provides protection against false security alarms due to authorized personnel, who are working in the raw-water-reservoir area, inadvertently stepping into an alarmed zone. If work activities in the raw-water-reservoir area required the fence to be temporarily removed, it can be with the appropriate, accompanying security compensating measures.

4.2.3 STORAGE CASK DESCRIPTION

The HI-STORM 100 System is used to store spent fuel and associated nonfuel hardware in a dry configuration at the Diablo Canyon ISFSI storage site. At Diablo Canyon, a shortened and anchored version of the standard HI STORM 100 System overpack will be used. This system is referred to as the HI-STORM 100SA. The free-standing version of the HI-STORM 100 System has been certified by the NRC for general use at applicable onsite ISFSIs operated by a 10 CFR 50 license holder. An anchored version of the HI-STORM 100 System (HI-STORM 100A and SA) is proposed as part of Holtec LAR 1014-1. Holtec Drawing 3769, showing the HI-STORM 100SA overpack-to-ISFSI pad (anchor stud/sector lug) arrangement is provided in Figure 4.2-6.

4.2.3.1 Function

As discussed in Section 3.2, the HI-STORM 100 System is designed to store spent nuclear fuel and associated nonfuel hardware from DCPP under Diablo Canyon ISFSI site-specific normal, off-normal, and accident conditions of service, including the most severe design-basis natural phenomena in accordance with 10 CFR 72 (Reference 5). The HI-STORM 100 System design is summarized in Chapter 1 of this SAR and described in more detail in Chapters 1 and 2 of the HI-STORM 100 System FSAR, as amended by LAR 1014-1.

The HI-STORM 100 System is designed to permit testing, inspection, and maintenance of the systems. The acceptance test and maintenance programs of the HI-STORM 100 System are specified in Chapter 9 of the HI-STORM 100 System FSAR. Because of the passive nature of the HI-STORM 100 System, onsite inspection and maintenance requirements are minimal. Surveillance requirements associated with operational control and limits are described in Chapter 10. Inspection and testing of important-to-safety components are performed in accordance with the Holtec International or PG&E Quality Assurance Program, as applicable.

Each of the HI-STORM 100 System components is described in further detail in the following sections. Figures, or reference to figures, in the HI-STORM 100 System FSAR are provided to illustrate the components and their functions.

4.2.3.2 Description

In its final storage configuration, the HI-STORM 100 System consists of the following major components considered important to safety:

- Holtec multi-purpose canister
- Holtec damaged fuel container (DFC)
- HI-STORM 100SA overpack

Figure 4.2-7 (exploded isometric view) shows the components of the HI-STORM 100 System in its storage configuration with the HI-STORM 100SA overpack. The following sections provide a summary of the HI-STORM 100 System MPC, DFC, and overpack design bases and design relative to the storage requirements of the Diablo Canyon ISFSI. The Diablo Canyon onsite transporter is described in Section 4.3. Detailed operating guidance for MPC loading, onsite transport, and transfer of the MPC from the transfer cask to the HI-STORM overpack is provided in Sections 5.1 and 10.2 of this SAR. Design drawings for generic HI-STORM 100 System components, except the DFC, are contained in Section 1.5 of the HI-STORM 100 System FSAR, as amended by LAR 1014-1. A figure depicting the DFC is contained in Section 2.1 of the HI-STORM 100 System FSAR, as amended by Holtec LAR 1014-1.

The HI-TRAC 125 transfer cask is used to provide the necessary structural support, shielding, heat removal, and missile protection as well as the means to transfer the loaded MPC between the transfer cask and the HI-STORM 100SA overpack. The transfer cask is not used in the final storage configuration of the HI-STORM 100 System at the storage pads. Design drawings for a standard transfer cask are provided in Section 1.5 of the HI-STORM 100 System FSAR.

4.2.3.2.1 MPC

The MPC provides for confinement of radioactive materials, criticality control, and the means to dissipate decay heat from the stored fuel. It has the structural capability to withstand the loads created by all design basis accidents and natural phenomena. The MPC is a totally welded structure of cylindrical profile with flat ends. It consists of a honeycomb fuel basket, baseplate, MPC shell, MPC lid, vent and drain port cover plates, and closure ring. The MPCs, with different internal arrangements, can accommodate intact spent fuel, damaged fuel, fuel debris, and nonfuel core components, as discussed in Sections 3.1.1 and 10.2. The MPC lid provides top shielding and provisions for lifting the loaded MPC during transfer operations between the transfer cask and the overpack. The MPC fuel-basket assembly provides support for the fuel assemblies as well as the geometry and fixed neutron absorbers for criticality control. The MPC is constructed entirely from stainless steel, except for the neutron absorber (Boral, an aluminum alloy and boron carbide composite), and an aluminum washer in the vent and drain ports. A summary of the nominal physical characteristics of the MPC is provided in Table 4.2-1.

4.2.3.2.2 DFC

The DFC is used to contain fuel assemblies classified as damaged fuel or fuel debris in the as required by the Diablo Canyon ISFSI TS and SAR Section 10.2. Damaged fuel may be stored in both the MPC-24E and the MPC-24EF, however, storage of fuel debris is only allowed in the MPC-24EF. Storage of damaged fuel or fuel debris is not permitted in the MPC-24 or the MPC-32. The DFC is a long, square, stainless-steel container with screened openings at the top and bottom. Each DFC is inserted into a designated storage cell within the MPC. The function of each DFC is to retain the damaged fuel or fuel debris in its storage cell and provide the means for ready retrievability. The DFC permits gaseous and liquid media to escape into the interior of the MPC, but minimizes dispersal of gross particulates during all design basis conditions of storage, including accident conditions. The total quantity of fuel debris permitted in a single DFC is limited to the equivalent weight and special nuclear material quantity of one intact fuel assembly. Proposed HI-STORM 100 System FSAR Figure 2.1.2B in Holtec LAR 1014-1 shows the general arrangement of the MPC-24E/EF DFC.

The lifting device at the top of the DFC is designed to meet the requirements of ANSI N14.6 (Reference 6) in accordance with applicable guidelines of NUREG-0612 (Reference 7). As discussed in the Holtec LAR 1014-1, Appendix 3.AS, the DFC is designed to meet ASME Section III, Subsection NG (Reference 8) allowables for normal handling and ASME Section III, Appendix F allowables for loadings experienced during a postulated, cask-drop accident.

4.2.3.2.3 HI-STORM 100SA Overpack

The HI-STORM overpack is a rugged, heavy-walled, cylindrical, steel and concrete structure. The structure is made of inner and outer concentric carbon-steel shells, a baseplate, and a bolted lid (comprised of steel top plates and a concrete shield). The spacing of the carbon-steel inner and outer shells provides approximately 30 inches of annular space that is filled with unreinforced concrete for radiation shielding. The overpack is designed to permit natural circulation of air around and up the exterior shell of the MPC, via the chimney effect, to provide for the passive cooling of the spent fuel contained in the MPC. The cask has 4 air inlet ducts located at 90-degree spacing in the base of the cask and 4 air outlet ducts located in the top lid of the overpack. The cooling air enters the inlet ducts, absorbs heat from the MPC surface, and flows upward in the annulus between the MPC and exits at the outlet ducts.

A summary of the nominal physical characteristics of the overpack is provided in Table 4.2-2.

4.2.3.2.4 HI-TRAC 125 Transfer Cask

The transfer cask is used to facilitate transport of the loaded MPC from the FHB/AB to the CTF and transfer of the loaded MPC into the overpack for storage at the ISFSI storage pad. It provides the necessary structural, shielding, and heat removal design features to protect the spent fuel and personnel during fuel loading, MPC preparation, and MPC transfer operations. The transfer cask is a rugged, heavy-walled, cylindrical steel vessel comprised of inner and outer concentric shells, a bolted pool lid, a top lid, and an outer circumferential water jacket. The annulus between the inner and outer steel shells is filled with lead. As needed, the water jacket is filled with water for shielding after the loaded transfer cask is removed from the spent fuel pool (SFP) and placed in the cask washdown area, but before the MPC interior is drained of borated water. The lead and the water in the jacket provide gamma and neutron shielding for personnel working on or near the loaded MPC to ensure occupational exposures are as low as is reasonably achievable (ALARA) during operations. The transfer cask is designed for transient use, to contain the MPC, and to be submerged in the SFP to support fuel loading. It includes lifting trunnions to allow the loaded transfer cask and MPC to be placed into and removed from the SFP for decontamination and preparation of the MPC for storage. The maximum design weight of the transfer cask is 125 tons, including a fully loaded MPC-32 with water in the MPC cavity and no water in the water jacket. Additional physical characteristics of the transfer cask are provided in Table 4.2-3. Figure 4.2-8 (isometric view) shows the HI-TRAC transfer cask and Figure 4.2-7 shows an isometric view of the HI-STORM 100 SA System. A more detailed description, design drawings, and a summary of the design criteria for the transfer cask are provided in Sections 1.2.1.2.2, 1.5, and 2.0.3, respectively, of the HI-STORM 100 System FSAR.

An optional design of the HI TRAC 125 transfer cask is being used at the Diablo Canyon ISFSI. This optional design, known as the HI-TRAC 125D, was developed by Holtec International and will be implemented under the provision of 10 CFR 72.48 for generic use with the HI-STORM 100 System after Amendment 1 to the HI-STORM CoC is approved. Holtec proprietary Drawing 3438 (see Section 1.1) is being provided to the NRC under separate cover (see Reference 9). A non-proprietary drawing will be included in Revision 1 to the HI-STORM 100 System FSAR. The key differences between the generic HI-TRAC 125D and the generic HI-TRAC 125 design described above are as follows:

(1) The lower pocket trunnions have been removed as they are not needed to accommodate the Diablo Canyon ISFSI lifting and handling operations.

(2) Four attachment points with appropriate reinforcing steel have been added to the top of the transfer cask shell to allow for the use of temporary bumpers described below.

The generic HI-TRAC 125D design will be slightly modified for the site-specific use at the Diablo Canyon ISFSI. This modification adds attachment points at the top (Figure 4.2-9) and bottom (Figure 4.2-10) of the transfer cask for the attachment of temporary bumpers used while handling the transfer cask in the DCPP FHB/AB. These bumpers are not used outside the DCPP FHB/AB. See Chapter 5 for more detailed discussion of the bumpers and attachment points.

(3) The transfer lid has been replaced by a HI-STORM mating device (see Figure 4.2-11). This device eliminates replacing the pool lid with a transfer lid while in the FHB/AB, thus reducing personnel dose. This design allows for the removal of the pool lid to facilitate MPC transfer at the CTF. The shielding previously provided by the transfer lid when the transfer cask is in the horizontal orientation is provided by a removable bottom shield that is integral to the cask transport frame (see Figure 4.2-12).

(4) The bottom baseplate diameter has been increased and an additional bolt circle added with 16 holes to accommodate the HI-TRAC bottom shield, the HI-STORM mating device, and an optional impact limiter. Gussets have been added to the baseplate to provide additional strength.

(5) The water jacket design has been changed from channel-and-plate design to a rib-and-shell design to better facilitate fabrication and reduce the number of welded joints.

(6) The pool lid and drain line have been slightly modified to improve the quality of the bolted joint and improve the operability of the drain.

4.2.3.3 Design Bases and Safety Assurance

The governing codes used for the design and construction of the HI-STORM 100 System steel components are listed in HI-STORM 100 System FSAR, Table 2.2.6, and are summarized below. Clarifications on the applicability of ACI 349-85 (Reference 10) to the unreinforced concrete used in the HI-STORM 100 overpack are provided in Appendix 1.D to the HI-STORM 100 System FSAR, as amended by LAR 1014-1. Table 3.4-6 provides a list of ASME Code alternatives for the HI-STORM System.

- MPC

Pressure boundary	ASME Code Section III, Subsection NB
Fuel Basket	ASME Code Section III, Subsection NG

- DFC

Lifting Bolts	ANSI N14.6 per applicable guidelines of NUREG-0612, Section 5.1.6
Steel Structure	ASME Code Section III, Subsection NG

- Overpack

Steel	ASME Code Section III, Subsection NF
Unreinforced Concrete	ACI-349-85

- Transfer Cask

Steel Structure	ASME Code Section III, Subsection NF
Lifting Trunnion Blocks	ASME Code Section III, Subsection NF and ANSI N14.6 per applicable guidelines of NUREG-0612, Section 5.1.6
Lifting Trunnions	ANSI N14.6 per applicable guidelines of NUREG-0612, Section 5.1.6

The safety classification of the components comprising the HI-STORM 100 System were determined using NUREG/CR-6407 (Reference 11) as a guide. Section 4.5 provides the safety classification of the HI-STORM 100 System components and additional detail on safety classification of components used at the Diablo Canyon ISFSI.

4.2.3.3.1 System Layout

In its storage configuration, the HI-STORM 100 System consists of a fully-welded MPC placed inside of a vertical concrete overpack. Each MPC holds either 24 or 32 PWR spent fuel assemblies in an internal basket, depending on the particular MPC model. The specifics of the material approved for storage in the HI-STORM 100 System at the

Diablo Canyon ISFSI storage site are discussed in Sections 3.1.1 and 10.2 and the Diablo Canyon ISFSI TS.

The HI-STORM 100 System is illustrated in Figure 4.2-7. Cross-sections of the PWR MPC baskets and an outline of the DFC are shown in the figures contained in Sections 1.2 and 2.1, respectively, of the HI-STORM 100 System FSAR, as amended by LAR 1014-1.

The transfer cask is designed for repetitive, transient use to contain one MPC during fuel loading, MPC preparation for storage, and transfer of the sealed MPC to the CTF. The transfer cask provides necessary shielding, heat removal, and structural integrity during the short time it contains the loaded MPC. The transfer cask is shown in Figure 4.2-8.

4.2.3.3.2 Structural Design

The structural evaluation for the HI-STORM 100 System is contained in HI-STORM 100 System FSAR Chapter 3, as amended by LAR 1014-1, and in the accident analyses in Chapter 8 of this SAR. Structural evaluations and analyses of the HI-STORM 100 System components have been performed for all design basis normal, off-normal, and accident conditions and for design basis natural phenomena conditions in accordance with 10 CFR 72, Subpart L. The structural evaluations confirm that the structural integrity of the HI-STORM 100 System is maintained under all design-basis loads with a high level of assurance to support the conclusion that the confinement, criticality control, radiation shielding, and retrievability criteria are met.

The following discussion verifies that the Diablo Canyon ISFSI site-specific criteria are enveloped by the HI-STORM 100 System design.

4.2.3.3.2.1 Dead and Live Loads

Dead loads are addressed in the HI-STORM 100 System FSAR, Section 2.2.1.1. The dead load of the overpack includes the weight of the concrete and steel cask and the MPC loaded with spent fuel. As identified in HI-STORM 100 System FSAR Table 2.1.6, the dead load of the overpack with the loaded MPC is calculated assuming the heaviest PWR assembly (B&W 15-by-15 fuel assembly type, wt = 1,680 lb, including nonfuel hardware) that bounds the Diablo Canyon fuel dead load (1,621 lb). The stresses calculated for the dead loads of the MPC and the overpack are shown to be within applicable Code allowables and, therefore, meet the Diablo Canyon ISFSI design criteria in Section 3.2.5 for dead loads.

The overpack is designed for two live loads, both of which act on the top of the overpack: (a) snow loads, and (b) the mating-device and transfer cask weight (during transfer operations) containing a fully loaded MPC. The HI-STORM 100 System FSAR uses a conservative, worst-case ground snow load of 100 lb/ft^2 as shown in HI-STORM 100 System FSAR Table 2.2.8, which exceeds any anticipated Diablo Canyon ISFSI site snow load. The live load capacity of the overpack is shown in HI-STORM 100 System FSAR, Section 3.4.4.3.2.1, to exceed the live load imposed by the loaded transfer cask. Since the live loads used in the HI-STORM 100 System generic analysis meet or exceed those that would be expected at the Diablo Canyon ISFSI, the HI-STORM 100 System FSAR analysis bounds the Diablo Canyon ISFSI design criteria specified for live loads and dead loads in Section 3.2.

As described above, the transfer cask dead load includes the weight of the cask plus the heaviest loaded MPC. The stresses calculated for the dead loads of the MPC and the transfer cask are shown to be within applicable Code allowables and, therefore, meet the Diablo Canyon ISFSI design criteria in Section 3.2.5 for dead loads.

4.2.3.3.2.2 Internal and External Pressure

Internal and external pressure loads are addressed in the HI-STORM 100 System FSAR, Sections 3.4.4.3.1.2 and 3.4.4.3.1.7, respectively. The normal and off-normal condition design pressures for the MPC are 100 psig for internal pressure and 0 psig (ambient) for external pressure as shown in Table 2.2.1 of the HI-STORM 100 System FSAR, as amended by LAR 1014-1. For accident conditions, the design pressure for the MPC is 200 psig for internal pressure and 60 psig for external pressure. Table 4.2-4 provides the maximum calculated MPC pressures for two normal conditions; no fuel rods ruptured and 1 percent fuel rods ruptured. The resultant pressure for the 10 percent rods rupture off-normal condition is provided in Section 8.1.1 and is below the 100 psig design pressure. The calculations assumed design basis heat load and bounding maximum fuel rod off-gas and internal pressure for DCPP fuel, considering a site-specific bounding value for fuel rod internal pressure. The internal pressure calculations for the MPC-32 bound those for the MPC-24, MPC-24E, and MPC-24EF because there is less free volume and more fuel inside the MPC-32 cavity, which creates higher pressures for the scenarios analyzed.

The MPCs are backfilled with helium during fuel loading operations to a nominal pressure of 31.3 psig at a reference temperature of 70°F. The internal pressure rises in proportion to the rise in MPC cavity gas absolute temperature due to the decay heat emitted by the stored fuel and as temperatures equilibrate to those associated with the normal condition 80°F day/night annual average ambient temperatures evaluated in the thermal analysis. This normal condition ambient temperature is higher than, and is therefore bounding for, the average day/night ambient temperature at the Diablo Canyon ISFSI site (Reference 12, Section 1.2.1.3).

MPC internal pressures were also evaluated for postulated accident conditions, including 100 percent fuel rod cladding rupture, assuming all rod fill gas and a conservative fraction of fission product gases, are released from the failed rods into the MPC. The resultant pressure from the 100 percent fuel rod rupture is provided in Section 8.2.14 and is below the MPC accident design pressure of 200 psig.

The stresses resulting from the internal and external pressure loads were shown to be within Code allowables. The Diablo Canyon ISFSI TS and SAR Section 10.2 ensure that the characteristics of the DCPP fuel to be loaded in a HI-STORM 100 System are consistent with the bounding fuel limits for array/class 17x17A and 17x17B fuel assemblies in Appendix B to the HI-STORM 100 System CoC (Reference 13). The pressure evaluations have appropriately accounted for the gas volume produced by burnable poison rod assemblies and integral fuel burnable absorber (IFBA) rods.

4.2.3.3.2.3 Thermal Expansion

Thermal expansion-induced mechanical stresses due to nonuniform temperature distribution are identified in Section 3.4.4.2 of the HI-STORM 100 System FSAR, as amended by LAR 1014-1. There is adequate space (gap) between the MPC basket and shell, and between the MPC shell and overpack or transfer cask, to ensure there will be no interference during conditions of thermally induced expansion or contraction. Table 4.4.15 of the HI-STORM 100 System FSAR, as amended by LAR 1014-1, provides a summary of HI-STORM 100 System component temperature inputs for the structural evaluation, consisting of temperature differences in the basket periphery and MPC shell between the top and bottom portions of the HI-STORM PWR MPC (MPC-24, MPC-24E, MPC-24EF, and MPC-32). The temperature gradients were used to calculate resultant thermal stresses in the MPC that were included in the load combination analysis. The stresses resulting from the temperature gradients were shown to be within Code allowables. Section 3.4.4.2 of the HI-STORM 100 System FSAR provides a discussion of the analysis and results of the differential thermal expansion evaluation. The Diablo Canyon ISFSI TS and SAR Section 10.2 ensure that the characteristics of the DCPP fuel to be loaded in a HI-STORM 100 System meet the limits delineated in Section 3.1.1. These limits are consistent with the bounding fuel limits for array/class 17-by-17A and 17-by-17B fuel assemblies in Appendix B to the HI-STORM 100 System CoC. Therefore, the thermal expansion evaluation, discussed above, in the HI-STORM 100 System FSAR, as amended by LAR 1014-1, will bound the conditions at the Diablo Canyon ISFSI.

4.2.3.3.2.4 Handling Loads

Handling loads for normal and off-normal conditions are addressed in the HI-STORM 100 System FSAR, Sections 2.2.1.2, 2.2.3.1, and 3.1.2.1.1.2. The normal handling loads that were applied included vertical lifting and transfer of the overpack with a loaded MPC through all movements. The MPC and overpack were designed to withstand loads resulting from off-normal handling assumed to be the result of a vertical drop. In the case of Diablo Canyon, however, the vertical drop during onsite transport, outside the FHB/AB, is precluded with the use of a cask transporter that is designed, fabricated, inspected, maintained, and tested in accordance with NUREG-0612. Likewise, drops are precluded while the cask is lifted at the CTF since the CTF is designed, fabricated, inspected, operated, maintained, and tested in accordance with NUREG-0612. This approach is consistent with the provisions in the HI-STORM 100 System CoC described in Section 4.2.3.3.2.5 below. The preclusion of drop events was chosen as a design strategy to accommodate the anchored HI-STORM 100SA overpack, which requires a robust pad to ensure that the anchor studs and embedment structure remain fixed during postulated earthquake and tornado events.

The transfer cask is designed to withstand the loads experienced during routine handling, including lifting, upending, downending, and transfer to the CTF with a loaded MPC. Loads were increased by 15 percent in the analyses to account for dynamic effects from lifting operations (hoist load factor). The lifting trunnions, trunnion blocks, and load-bearing connection points (that is, pool lid bolted connections) were analyzed for normal handling loads, as described in Section 3.4.3.7 of the HI-STORM 100 System FSAR, as amended by LAR 1014-1.

4.2.3.3.2.5 Overpack/Transfer Cask Tipover and Drop

Outside the FHB/AB, tipover of a loaded overpack is a noncredible accident since the HI-STORM 100SA used at the Diablo Canyon ISFSI storage site is anchored to the ISFSI pad. When not on the ISFSI pad, the overpack will be either in the CTF or attached to the cask transporter (as described in Chapter 5). Both the CTF and the cask transporter are designed to preclude cask drops. The anchored HI-STORM 100SA overpack has been designed to withstand the worst-case, design-basis, seismic ground motion without failure of the anchor studs or the embedment. In addition, the anchored overpack has been analyzed for site-specific: (a) explosions, and (b) tornado wind concurrent with the impulse force of a large, design-basis, tornado-borne missile to verify that the anchorage design can resist the resultant overturning moment (Reference 19). The design criteria for the concrete storage pad and cask anchors are described in Section 3.3.2. The design and analysis of the concrete storage pad and anchorage embedment are discussed in Section 4.2.1.1.7. The analysis of the cask/pad interface under seismic loadings is described in Section 8.2.1.

The CTF and cask transporter are designed, fabricated, inspected, operated, maintained, and tested in accordance with NUREG-0612. Thus, there is no need to establish lift height limits or to postulate cask-drop events during transport to the pad, including activities at the CTF.

The cask lifting assembly on the transporter is a horizontal beam that is supported by towers at each end with hydraulic lifting towers. During movement of the transporter with the cask in a fixed elevation, a redundant load support system is used. This is further described in Section 4.3 and in Chapter 5.

4.2.3.3.2.6 Tornado Winds and Missiles

Design criteria for tornado wind and missile impact are discussed in Section 3.2.1 of this SAR. The HI-STORM 100 System is designed to withstand pressures, wind loads, and missiles generated by a tornado, as described in Section 2.2.3.5 of the HI-STORM 100 System FSAR. In Section 8.2.2, the analysis of the Diablo Canyon ISFSI site design-basis tornado, including pressures, wind loads, and missiles is discussed. The MPC confinement boundary remains intact under all design-basis, tornado-wind, and missile-load combinations.

Tornado-wind and missile loads are evaluated for the overpack and the transfer cask. In the case of the transfer cask, the loaded transfer cask is always maintained in a restrained condition by the handling equipment while it is in a vertical position. Tipover or instability due to tornado-wind or missile impact is therefore a noncredible accident for the transfer cask (HI-STORM 100 System FSAR, Sections 2.2.3.1 and 3.4.8). However, missile penetration effects on the transfer cask and overpack have been evaluated.

4.2.3.3.2.7 Flood

Flooding is addressed in Sections 3.2.2 and 8.2.3 of this SAR and in Sections 3.1.2.1.1.3 and 3.4.6 of the HI-STORM 100 System FSAR. The MPC is designed to withstand hydrostatic pressure (full submergence) up to a depth of 125 ft and horizontal loads due to water velocity up to 15 fps without tipping or sliding. The Diablo Canyon ISFSI and CTF are above probable maximum flood conditions; therefore, the HI-STORM 100 System FSAR evaluation bounds conditions at the Diablo Canyon ISFSI storage and CTF sites. Thus, the requirements of 10 CFR 72.122(b) are met with regard to floods.

4.2.3.3.2.8 Earthquake

Design criteria for earthquake loads at the Diablo Canyon ISFSI are discussed in Section 3.2.3. The results of the seismic analyses are discussed in Section 8.2.1. Analyses were performed using the DE, DDE, HE, and LTSP ground motions to verify that the Diablo Canyon ISFSI SSCs (including components of the HI-STORM 100 system) meet their design requirements of 10 CFR 72.122(b) with regard to earthquakes. Although not considered a licensing basis, PG&E has evaluated the effects of these recent data (ILP ground motions, Section 2.6.2.4.2) to ensure appropriate design margins are maintained.

4.2.3.3.2.9 Explosion Overpressure

Explosion overpressure loads are addressed in Sections 3.3.1.6 and 8.2.6.2.1 of this SAR and in Sections 3.4.7.2 and 11.2.11 of the HI-STORM 100 System FSAR. The HI-STORM 100 System MPC is analyzed and designed for accident external pressures up to 60 psig. The transfer cask overpressure design limit is 384 psig. The overpack is designed for steady-state and transient external pressures of 5 psig and 10 psig, respectively. As shown in Section 8.2.6, the Diablo Canyon ISFSI is not subject to credible explosions (that is, transient external pressures) that are in excess of 1 psig or are risk significant in accordance with Regulatory 1.91. Therefore, the HI-STORM 100 System bounds the expected overpressure due to explosions at the Diablo Canyon ISFSI, as required per 10 CFR 72.122(c).

4.2.3.3.2.10 Fire

Design criteria for fire loads are addressed in Section 3.3.1.6 and in the HI-STORM 100 System FSAR, Section 11.2.4. The HI-STORM 100 System was analyzed for a fire of 50 gallons of combustible fuel from the cask transporter encircling the cask, resulting in temperatures up to 1,475°F and lasting for a period of 3.6 minutes. The analysis also evaluated the post-fire temperatures of the system for the duration of 10 hours. The evaluation of this fire and its effect on both the loaded overpack and the loaded transfer cask is discussed in Section 11.2.4 of the HI-STORM 100 System FSAR. The results of the analysis show that the intense heat from the fire only partially penetrated the concrete-cask wall. This fire would cause less than 1 inch of concrete to exceed temperature limits, and would have a negligible effect on shielding or MPC and fuel temperatures.

For the Diablo Canyon ISFSI, the threat of fire was evaluated for a variety of potential sources in addition to the transporter fire, including a vehicle fuel tank, other local fuel tanks, other combustible materials, and a vegetation fire. The results of this evaluation are discussed in Section 8.2.5.

The HI-STORM 100 System design meets the Diablo Canyon ISFSI design criteria for accident-level thermal loads as required per 10 CFR 72.122(c).

4.2.3.3.2.11 Lightning

A lightning strike of the HI-STORM 100 System at the Diablo Canyon ISFSI is addressed in Sections 3.2.6 and 8.2.8. The lightning strike accident is also discussed in the HI-STORM 100 System FSAR, Sections 2.2.3.11 and 11.2.12. The analysis shows that the lightning will discharge through the steel shell of the overpack or the transfer cask to ground through a ground connector. The lightning current will discharge through the affected steel structure and will not affect the MPC, which provides the confinement boundary for the spent fuel.

Therefore, the HI-STORM 100 System design meets the Diablo Canyon ISFSI design criteria in Section 3.2.6 for lightning protection, as required in 10 CFR 72.122(b).

4.2.3.3.2.12 500-kV Line Drop

The Diablo Canyon ISFSI storage site is located underneath and adjacent to 500-kV transmission lines. The HI-STORM 100 System design criteria for a 500-kV transmission line dropping and striking the HI-STORM 100 overpack or transfer cask is similar to the lightning strike. Section 8.2.8 of this SAR discusses the analysis of this accident and demonstrates that the MPC remains protected. The HI-STORM 100 System, therefore, meets the requirements of 10 CFR 72.122(b) for the 500-kV line break.

4.2.3.3.3 Thermal Design

The environmental thermal design criteria for the Diablo Canyon ISFSI are discussed in Chapter 3.2.7. Thermal performance for the HI-STORM 100 System is addressed in Chapter 4 of the HI-STORM 100 System FSAR, as amended by LAR 1014-1. The HI-STORM 100 System is designed for long-term storage of spent fuel and safe thermal performance during onsite loading, unloading, and transfer operations. The HI-STORM 100 System is also designed to minimize internal stresses from thermal expansion caused by axial and radial temperature gradients. The thermal model and its benchmarking with full size cask test data is described in Reference 20.

The HI-STORM 100 System is designed to transfer decay heat from the spent fuel assemblies to the environment. The MPC design, which includes the all-welded honeycomb basket structure, provides for heat transfer by conduction, convection, and radiation away from the fuel assemblies, through the MPC basket structure and internal region, to the MPC shell. The internal MPC design incorporates top and bottom plenums, with interconnected downcomer paths, to accomplish convective heat transfer via the thermosiphon effect. The MPC is pressurized with helium, which assists in transferring heat from the fuel rods to the MPC shell by conduction and convection. Gaps exist between the basket and the MPC shell to permit unrestrained axial and radial thermal expansion of the basket without contacting the shell, thus minimizing internal stresses. The stainless steel basket conducts heat from the individual spaces for storing fuel assemblies out to the MPC shell.

The HI-STORM 100SA overpack design provides an annular space between the MPC shell and the inner steel liner of the overpack for airflow up the annulus. Relatively cool air enters the four inlet ducts at the bottom of the overpack, flows upward through the annulus removing heat from the MPC shell by convection, and exits the four outlet ducts at the top of the cask.

The thermal analysis, discussed in Chapter 4 of the HI-STORM 100 System FSAR, as amended by LAR 1014-1, was performed using the ANSYS and FLUENT (Reference 14) computer codes. The HI-STORM PWR MPCs (MPC-24, MPC-24E, MPC-24EF, and MPC-32) were evaluated to determine the temperature distribution under long-term, normal storage conditions, assuming the MPCs are loaded with design basis PWR fuel assemblies. Maximum-assembly, decay-heat-generation rates for fuel to be loaded into these two MPC models are specified in SAR Section 10.2. The decay-heat-generation limits vary by cooling time.

The thermal analysis assumed that the HI-STORM overpacks are in an array, subjected to an 80°F-annual-average ambient temperature, with full insolation. The annual-average temperature takes into account day-and-night and summer-and-winter temperatures throughout the year. The annual-average temperature is the principal design parameter in the HI-STORM 100 System design analysis, because it establishes the basis for demonstration of long-term spent nuclear fuel integrity. The long-term integrity of the spent fuel cladding is a function of the average-ambient temperature over the entire storage period, which is assumed to be at the maximum annual-average temperature in every year of storage for conservatism. The results of this analysis are presented in Tables 4.4.9, 4.4.26 and 4.4.27 of the HI-STORM 100 System FSAR, as amended by Holtec LAR 1014-1, for MPC-24, MPC-24E, MPC-24EF, and MPC-32, respectively. The results, summarized in HI-STORM 100 System FSAR Table 4.2-3, indicate that temperatures of all components are within normal condition temperature limits. These results bound the Diablo Canyon ISFSI site since the average-annual temperature at the site is only 55°F (Section 2.3.2).

Section 11.1.2 of the HI-STORM 100 System FSAR discusses the temperatures of the HI-STORM 100 System for a maximum off-normal, daily-average ambient temperature of 100°F, which is an increase of 20°F from the normal conditions of storage discussed above. The maximum off-normal temperatures were calculated by adding 20°F to the maximum normal temperatures from the highest component temperature for the MPC-24, MPC-24E, MPC-24EF, and MPC-32. All of the maximum off-normal temperatures are below the short-term peak fuel cladding temperature limits (HI-STORM 100 System FSAR Table 2.2.3). Therefore, all components are within allowable temperatures for the 100°F-ambient-temperature condition. Since the highest hourly temperature recorded at the Diablo Canyon Site is 97°F (Section 2.3.2), the HI-STORM 100 System FSAR evaluation bounds the Diablo Canyon ISFSI site.

The thermal analysis in the HI-STORM 100 System FSAR discussed above includes the following global assumptions: (a) the concrete pad is assumed to be an insulated surface (that is, no heat transfer to or from the pad is assumed to occur), (b) adjacent casks are assumed to be sufficiently separated from each other (that is, cask pitch is sufficiently large) so that their ventilation actions are autonomous, and (c) the cask is assumed to be subject to full solar insolation on its top surface as well as view-factor-adjusted solar insolation on its lateral surface, based on 12-hour insolation levels recommended in 10 CFR 71 (800g-cal/cm^2 averaged over a 24-hour period as allowed in NUREG-1567). The evaluation of insolation is further discussed in Section 4.4.1.1.8 of the HI-STORM 100 System FSAR, as amended by Holtec LAR 1014-1.

Ambient-temperature and incident solar radiation (insolation) values applicable to the ISFSI site are summarized in Section 2.3.2. The highest-recorded-hourly temperature at the Diablo Canyon site is 97°F and the lowest temperature was below freezing for a few hours. The annual-average temperature is approximately 55°F. The maximum insolation values for the ISFSI site are estimated to be 766 g-cal/cm^2 per day for a 24-hour period and 754 g-cal/cm^2 for a 12-hour period.

Second-order effects such as insolation heating of the concrete pad, heating of feed air traveling downward between casks and entering the inlet ducts of the reference cask, and radiative heat transfer from adjacent spent fuel casks were not explicitly modeled in the HI-STORM 100 System FSAR analysis.

Within a loaded transfer cask, heat generated in the MPC is transported from the contained fuel assemblies to the MPC shell. A small, diametrical air gap exists between the outer surface of the MPC and the inner surface of the transfer cask. Heat is transported across this gap by the parallel mechanisms of conduction, natural convection, and thermal radiation. Assuming that the MPC is centered and does not contact the transfer cask walls conservatively minimizes heat transport across this gap. Additionally, thermal expansion that would minimize the gap is conservatively neglected.

Heat is transported through the cylindrical wall of the transfer cask by conduction through successive layers of steel, lead, and steel. A water jacket, which provides neutron shielding for the transfer cask, surrounds the cylindrical steel wall. The water jacket is composed of a carbon steel shell attached to the outer shell of the transfer cask by radial fins. Conduction heat transfer occurs through both the water cavities and the fins. While the water jacket openings are sufficiently large for natural convection loops to form, this mechanism is conservatively neglected. Heat is passively rejected to ambient from the outer surface of the transfer cask by natural convection and thermal radiation.

In the vertical position, the bottom face of the transfer cask is in contact with a supporting surface. This face is conservatively modeled as an insulated surface. Because the transfer cask is not used for long-term storage in an array, radiative heat blocking does not need to be considered. The transfer cask top lid is modeled as a surface with convection, radiative heat exchange with air, and a constant, maximum-incident solar heat flux load. Insolation on cylindrical surfaces is conservatively based on 12-hour levels prescribed in 10 CFR 71 and averaged on a 24-hour basis. Concise descriptions of these models are described in Section 4.5 of the HI-STORM 100 System FSAR, as amended by LAR 1014-1.

The HI-STORM 100 System was analyzed for an extreme hot ambient temperature of 125°F averaged over a 72-hour time period. Section 8.2.10 of this SAR and Section 11.2.15 of the HI-STORM 100 System FSAR, as amended by LAR 1014-1, provide discussions of the analysis of this extreme temperature condition. The ambient temperature is applied coincident with full solar insolation. Resulting fuel cladding temperatures are well below their short-term temperature limit. The balance of the HI-STORM 100 System structure remains insignificantly affected. Since the extreme hot ambient temperature at the Diablo Canyon site is 104°F, the extreme hot ambient temperature evaluation in the HI-STORM 100 System FSAR bounds the conditions at Diablo Canyon.

The HI-STORM 100 System was also evaluated for a -40°F, extreme-low ambient temperature condition, as discussed in Section 4.4.3 of the HI-STORM 100 System FSAR. Zero decay heat generation from spent fuel, and no solar insolation were conservatively assumed. All materials of construction for the MPC and overpack will perform their design function under this extreme cold condition. Since the minimum temperature at the Diablo Canyon site is greater than 24°F (Table 3.4-1), the extreme low ambient temperature evaluation in the HI-STORM 100 System FSAR bounds the conditions at Diablo Canyon.

The thermal performance of the MPC to limit fuel cladding temperature inside the transfer cask during welding, draining, drying, and helium backfill operations, and during transportation of the loaded transfer cask to the CTF is bounded by the thermal evaluation performed with the MPC under a hypothetical, complete-vacuum condition. The vacuum condition is bounding for the other transient operational conditions mentioned above, because there is no fluid medium to transfer heat from the fuel to the MPC shell. In the other conditions, there is some amount of either helium or water in the MPC cavity to enhance heat transfer. All internal MPC heat transfer in the vacuum condition is through conduction and radiation.

Sections 4.5.1.1.4 and 4.5.2.2 of the HI-STORM 100 System FSAR, as amended by LAR 1014-1, discuss the thermal evaluation of the MPC under vacuum conditions and the resultant MPC and fuel cladding temperatures with design-basis heat load. Fuel cladding temperatures are shown in HI-STORM 100 System FSAR Table 4.5.9, and are all less than 1,000°F, which is less than the short-term temperature limit of 1,058°F. The design-basis heat load used for this evaluation bounds the heat load for all combinations of DCPP fuel to be loaded into the HI-STORM 100 System. The characteristics of the operations to be performed at Diablo Canyon are the same as those described in the HI-STORM 100 System FSAR. Therefore, the evaluations described in Section 4.5 of the HI-STORM 100 System FSAR, as amended by Holtec LAR 1014-1, bound operations at DCPP.

The above discussion demonstrates that the HI-STORM 100 System as deployed at the Diablo Canyon ISFSI meets the requirements of 10 CFR 72.122(h), 72.128(a)(4), and 72.236(f) and (g) for thermal design.

4.2.3.3.3.1 HI-STORM Overpack at the CTF

The site-specific design of the Diablo Canyon CTF involves transferring a loaded MPC into the overpack with the overpack located below grade in a vault. The thermal implications of the difference between a loaded overpack located in a vault and one located at grade level have been evaluated.

Under normal conditions, the loaded overpack will remain in the vault only for the time it takes to remove the transfer cask from atop the overpack, retrieve and install the overpack lid, and raise the overpack out of the vault with the CTF lift system. This is expected to take less than 4 hours and has an insignificant effect on heat removal and fuel cladding temperatures.

Under off-normal conditions, such as a power failure affecting the CTF lift system, the condition could last several hours, depending upon the time it takes to complete corrective actions to restore power, or to provide an alternate power source. The effect of a loss of electrical power on the ability of the overpack to transfer the heat from the MPC to the environs is discussed in Section 8.1.6. The time frame computed before short-term peak fuel cladding temperature limits are reached is a sufficient amount of time to initiate corrective actions described in Section 8.1.6.

Accident conditions, such as a failure of one lift jack screw, may result in the loaded overpack being in the down position for an extended period of time, depending upon the severity of the failure. This accident and the corrective actions are discussed in more detail in Section 8.2.17 and the Diablo Canyon ISFSI TS.

4.2.3.3.4 Shielding Design

Shielding design and performance for the HI-STORM 100 System is addressed in Section 3.3.1.5.2 and Chapter 7 of this SAR specifically for the Diablo Canyon ISFSI, and in Chapter 5 of HI-STORM 100 System FSAR for the HI-STORM 100 System generically. The HI-STORM 100 System is designed to maintain radiation exposure ALARA in accordance with 10 CFR 72.126(a). The concrete overpack is designed to limit the average external contact dose rates (gamma and neutron) to 60 mrem/hr on the sides, 60 mrem/hr on top, and 60 mrem/hr at the air inlets and outlets based on HI-STORM design basis fuel.

The overpack is a massive structure designed to provide gamma and neutron shielding of the spent fuel assemblies stored within the MPC. Most of the side shielding is provided by the overpack, although the MPC structure is credited in the shielding model. The overpack steel inner shell, the concrete-filled annulus, and the steel outer shell provide radiation shielding for the side of the overpack. The steel MPC lid and the overpack lid provide axial shielding at the top. The MPC lid is approximately 10 inches thick and is stainless steel. The overpack lid consists of a 4-inch thick steel top plate and steel-encased concrete. The lid shield configurations differ between the HI-STORM 100 and the HI-STORM 100S designs as shown on the respective drawings in Section 1.5 of the HI-STORM 100 System FSAR, as amended by LAR 1014-1. In both designs, particular emphasis is placed on providing overpack lid shielding above the annulus between the MPC and the overpack inner shell, which is a streaming path.

The configuration of the inlet and outlet ducts in relation to the MPC prevents a direct radiation-streaming path from the MPC to outside the cask. The duct dose rates are further reduced by the installation of duct photon attenuators to minimize scatter (Figure 4.2-7). The HI-STORM 100 System design allows for necessary personnel access during inspection and maintenance operations, while keeping dose rates ALARA. The HI-STORM 100 System FSAR, Section 5.1.1, as amended by LAR 1014-1, provides generic calculated dose rates around the sides and top of the HI-STORM 100S overpack. Predicted Diablo Canyon ISFSI dose rates and site-specific dose evaluations are presented in Chapter 7 for the HI-STORM 100 System, and meet the requirements of 10 CFR 72.104 and 72.106.

The transfer cask provides shielding to maintain occupational exposures ALARA in accordance with 10 CFR 20, while also maintaining the maximum load on the FHB crane hook to 125 tons or less. The plant specific dose rates for a transfer cask loaded with design basis fuel are used to perform the occupational exposure estimate for MPC loading, closure, and transfer operations, as described in Chapter 7 of this SAR. The actual dose rates from a loaded transfer cask during operations in support of loading fuel for the Diablo Canyon ISFSI will be lower because the actual MPCs to be loaded will not contain design-basis fuel in every fuel storage location. Occupational exposures during transfer cask operations will be monitored and maintained ALARA in accordance with the DCPP radiation protection program and the requirements of 10 CFR 20.

The above discussion demonstrates that the HI-STORM 100 System as used at the Diablo Canyon ISFSI meets the requirements of 10 CFR 72.104, 72.106, 72.128(a)(2), and 72.236(d) for shielding design.

4.2.3.3.5 Criticality Design

Criticality of the HI-STORM 100 System is addressed in Section 3.3.1.4 of this SAR and Chapter 6 of the HI-STORM 100 System FSAR, as amended by Holtec LAR 1014-1. The HI-STORM 100 System is designed to maintain the spent fuel subcritical in accordance with 10 CFR 72.124(a) and (b) with the MPC materials and geometry. The acceptance criterion for the prevention of criticality is that k_{eff} remain below 0.95 for all normal, off-normal, and accident conditions.

Criticality safety of the HI-STORM 100 System depends upon the following four principal design parameters:

- Administrative limits on the maximum fuel assembly enrichment and physical properties acceptable for storage in the MPC
- The inherent geometry of the fuel basket designs within the MPC, including the flux-traps in the MPC-24, MPC-24E, and MPC-24EF (water gaps for loading fuel into submerged MPCs)
- The incorporation of permanent, fixed, neutron-absorbing panels (Boral) in the fuel basket structure to assist in control of reactivity
- Administrative controls requiring minimum concentrations of soluble boron in the MPC water during fuel loading and unloading, depending upon MPC model and fuel enrichment

The criticality analysis performed for the HI-STORM 100 System assumes only fresh fuel with no credit for burnup as a conservative bounding condition. In addition, no credit is taken for fuel-related burnable neutron absorbers, and it is assumed that the Boron-10 content in the Boral is only 75 percent of the manufacturer's minimum specified content. Other assumptions made to ensure the results of the analysis are conservative are identified in Section 6.1 of the HI-STORM 100 System FSAR. In its storage configuration, the HI-STORM 100 System is dry (no moderator), and the reactivity is very low (k_{eff} less than 0.515). At the Diablo Canyon ISFSI, the fuel will always be in a dry, inert-gas environment. It is sealed within a welded MPC, and no credible accident will result in water entering the MPC.

The limiting reactivity condition occurs in the SFP during fuel loading, where assemblies are loaded into the MPC in close proximity to each other, with moderator between assemblies. All fuel loaded into the MPC-32, regardless of enrichment, requires a certain amount of soluble boron in the MPC during loading to preserve the assumptions of the criticality analyses. Higher enriched fuels loaded into the MPC-32, MPC-24, MPC-24E, or MPC-24EF also require soluble boron in the MPC during loading operations. The Diablo Canyon ISFSI TS ensure that soluble boron is appropriately maintained during fuel loading operations.

The results of the criticality analyses of different fuel types are shown in Chapter 6 of the HI-STORM 100 System FSAR, as amended by LAR 1014-1, for the MPC-24, MPC-24E, MPC-24EF, and MPC-32. The results confirm that the maximum reactivities of the MPCs are below the design criteria (k_{eff} less than 0.95) for fuels with specified maximum allowable enrichments, considering calculational uncertainties. The PWR fuel types for which these analyses were performed are shown in Table 2.1.3 of the HI-STORM 100 System FSAR. With the exception of DCPP fuel assemblies with annular fuel pellets and Zirlo clad fuel with burnup > 45,000 MWD/MTU, all DCPP fuel is bounded by array/classes 17x17A and 17x17B. No credit is taken for neutron poison in the form of gadolinium in the fuel pellets or in the IFBA rods, therefore, fuel assemblies containing these poisons are acceptable for loading.

Accident conditions have also been considered, and no credible accidents have been identified that would result in exceeding the regulatory limit on reactivity. In Section 6.1 of the HI-STORM 100 System FSAR, as amended by LAR 1014-1, Holtec determined that the physical separation between overpacks due to the large diameter and cask pitch, and the concrete and steel radiation shields, are each adequate to preclude any significant neutronic coupling between HI-STORM 100 Systems.

Section 6.4.4 of the HI-STORM 100 System FSAR, as amended by Holtec LAR 1014-1, discusses the results of criticality analyses on MPCs storing damaged fuel in a Holtec damaged fuel container. Analyses were performed for three possible scenarios. The scenarios are:

- Lost or missing fuel rods, calculated for various numbers of missing rods in order to determine the maximum reactivity.
- Fuel assembly broken with the upper segments falling into the lower segment creating a close-packed array. For conservatism, the array was assumed to retain the same length as the original fuel assemblies.
- Fuel pellets lost from the assembly and forming powdered fuel dispersed through a volume equivalent to the height of the original fuel, with the flow channel and cladding material assumed to disappear.

Results of these analyses confirm that, in all cases, the maximum reactivity of the HI-STORM 100 System with design-basis failed fuel in the most adverse post-accident condition will remain well below the regulatory limit within the enrichment range analyzed.

The HI-STORM 100 System is designed such that the fixed neutron absorber (Boral) will remain effective for a storage period greater than 20 years, and there are no credible means to lose the Boral effectiveness. As discussed in Section 6.3.2 of the HI-STORM 100 System FSAR, the reduction in Boron-10 concentration due to neutron absorption from storage of design-basis fuel in a HI-STORM 100SA overpack over a 50-year period is expected to be negligible. Further, the analysis in Appendix 3.M.1 of the HI-STORM 100 System FSAR demonstrates that the sheathing, which affixes the Boral panel, remains in place during all credible accident conditions, and thus the Boral panel remains fixed for the life of the Diablo Canyon ISFSI. Therefore, verification of continued efficacy of the Boral neutron absorber is not required. This is consistent with the requirements of 10 CFR 72.124(b).

For MPCs filled with pure water, the reactivity of any PWR assembly with nonfuel hardware inserted into the guide tubes is bounded by (that is, lower than) the reactivity of the same assembly without the inserts. This is because the inserts reduce the amount of moderator, while the amount of fissile material remains unchanged. In the presence of soluble boron in the water, especially for higher-required soluble boron concentrations, it is possible that the nonfuel hardware in the PWR assembly results in an increase of reactivity. This is because the insert not only replaces water, but also replaces the neutron absorber in the water with a nonpoison material. To account for this effect, analyses with and without nonfuel hardware in the assemblies were performed for higher soluble boron concentrations in support of Holtec LAR 1014-1. The highest reactivities for either case are used as the basis of the criticality evaluation. Section 6.4.8 of the HI-STORM 100 System FSAR, as amended by LAR 1014-1, provides additional discussion of the criticality effect of nonfuel hardware stored with PWR spent fuel assemblies.

During cask loading and unloading activities in the FHB/AB, criticality monitoring requirements of 10 CFR 72.124(c) will be met using a combination of installed and portable monitoring radiation monitoring instrumentation, in accordance with GDC-63 (to detect conditions that may result in excessive radiation levels and to initiate appropriate safety actions). As discussed in PG&E letter DCL-97-058, dated April 3, 1997, the radiation monitoring instrumentation generally conforms to the guidance of Regulatory Guide 8.12, "Criticality Accident Alarm Systems," and ANSI/ANS 8.3-1979, "Criticality Accident Alarm System." As discussed in DCPP FSAR Update Section 9.1.2.2, spent fuel pool radiation monitors RM-58 and RM-59 provide personnel protection and general surveillance of the spent fuel pool area. As discussed in DCL-97-058, portable radiation monitors will be placed in the cask washdown area to provide personnel protection and general surveillance of this area. On November 12, 1997, the NRC granted PG&E an exemption from the requirements of 10 CFR 70.24 concerning criticality monitors. In DCL-02-044 dated April 15, 2002, which submitted License Amendment Request 02-03, Spend Fuel Cask Handling, PG&E requested an exemption from the 10 CFR 72. 124(c) criticality monitoring requirement by requesting an extension of the NRC's

November 12, 1997, exemption for the FHB/AB to envelop the activities associated with the Diablo Canyon ISFSI SAR.

In PG&E letter DCL-02-117, "Change in Licensing Basis Compliance from 10 CFR 70.24 to 10 CFR 50.68(b)," dated October 2, 2002, "PG&E informed the NRC that PG&E will revise the DCPP licensing basis to reflect compliance with 10 CFR 50.68(b) in lieu of 10 CFR 70.24 and that the exemption request in DCL-02-044 will be revised to request a similar exemption from 10 CFR 50.68(b) in lieu of 10 CFR 70.24.

The Holtec design, associated procedural controls, the proposed Diablo Canyon ISFSI Technical Specifications, and SAR Section 10.2 preclude accidental criticality when the spent fuel has been properly placed in the storage cask confinement system and the confinement system has been adequately drained, dried, inerted, and sealed.

The analysis of a fuel assembly drop onto the racks, and the drop of a fuel cask in the SFP, will show criticality is prevented and is also addressed in the 10 CFR 50 LAR in support of ISFSI licensing.

The above discussion demonstrates that the HI-STORM 100 System as deployed at the Diablo Canyon ISFSI meets the requirements of 10 CFR 72.124 and 72.236(c) for criticality design.

4.2.3.3.6 Confinement Design

Confinement design for the HI-STORM 100 System is addressed in Chapter 7 of the HI-STORM 100 System FSAR, as amended by LAR 1014-1. The confinement vessel of the HI-STORM 100 System is the MPC, which provides confinement of all radionuclides under normal, off-normal, and accident conditions in accordance with 10 CFR 72.122(h). The MPC consists of the MPC shell, bottom base plate, MPC lid, vent and drain port cover plates, and the MPC closure ring, which form a totally welded vessel for the storage of spent fuel assemblies. The MPC requires no valves, gaskets, or mechanical seals for confinement. All components of the confinement system are classified as important to safety.

The MPC is a totally welded pressure vessel designed to meet the stress criteria of ASME Section III, Subsection NB. No bolts or fasteners are used for closure. All closure welds are examined using the liquid-penetrant method and helium leak tested to ensure their integrity. Two penetrations are provided in the MPC lid for draining, drying, and backfilling during loading operations. Following loading operations, vent and drain port cover plates are welded to the MPC lid. A closure ring, which covers the penetration cover plates and welds, is welded to the MPC lid to provide redundant closure of the MPC vessel. The loading and welding operations are performed inside the DCPP FHB/AB. There are no confinement boundary penetrations required for MPC monitoring or maintenance during storage.

The confinement features of the HI-STORM 100 System meet the requirements of 10 CFR 72.122(h).

4.2.4 INSTRUMENTATION SYSTEM DESCRIPTION

Monitoring of the loaded casks on the storage pad is necessary to ensure that the passive, air- cooled, convective heat transfer system for the MPC and overpack remains operable. Rather than install an active temperature monitoring system, PG&E has chosen to visually monitor overpack inlet and outlet air duct screens, as required by the Diablo Canyon ISFSI Technical Specifications, to verify the screens are free of blockage and intact.

4.2.5 COMPLIANCE WITH GENERAL DESIGN CRITERIA

Table 4.2-5 provides a tabular presentation of the locations in this SAR and/or the HI-STORM 100 System FSAR where compliance with the General Design Criteria of 10 CFR 72, Subpart F, is shown to be met.

4.2.6 REFERENCES

1. Final Safety Analysis Report for the HI-STORM 100 System, Holtec International Report No. HI-2002444, Revision 0, July 2000.

2. License Amendment Request 1014-1, Holtec International, Revision 2, July 2001 including Supplements 1 through 4 dated August 17, 2001; October 5, 2001; October 12, 2001; and October 19, 2001; respectively.

3. ANSYS Finite Element Modeling, ANSYS Inc., Southpointe 275 Technology Drive; Canonsburg, PA.

4. ACI-349-97, Code Requirements for Nuclear Safety Related Concrete Structures, American Concrete Institute (with 10/01/00 Draft Appendix B).

5. 10 CFR 72, Licensing Requirements for the Independent Storage of Spent Nuclear Fuel and High-Level Radioactive Waste.

6. ANSI N14.6, Special Lifting Devices for Shipping Containers Weighing 10,000 Pounds (4,500 kg) or More, American National Standards Institute, 1993 Edition.

7. Control of Heavy Loads at Nuclear Power Plants, USNRC, NUREG- 0612, July 1980.

8. Boiler and Pressure Vessel Code, Section III, Division I, American Society of Mechanical Engineers, 1995 Edition including 1996 and 1997 addenda.

9. Submittal of Holtec Proprietary and Non-Proprietary Drawing Packages, PG&E Letter to the NRC, DIL-01-008, dated December 21, 2001.

10. ACI 349-85, Code Requirements for Nuclear Safety Related Concrete Structures, American Concrete Institute.

11. Classification of Transportation Packaging and Dry Spent Fuel Storage System Components According to Importance to Safety, USNRC, NUREG/CR-6407, February 1996.

12. Diablo Canyon Power Plant Units 1 & 2 Final Safety Analysis Report Update, Revision 14, November 2001.

13. 10 CFR 72 Certificate of Compliance No. 1014 for the HI-STORM 100 System, Holtec International, Revision 0, May 2000.

14. FLUENT Computational Fluid Dynamics Software, Fluent, Inc., Centerra Resource Park, 10 Cavendish Court, Lebanon, NH 03766.

15. PG&E Calculation No, 52.27.100.705 (PGE-009-CALC-001), "Embedment Support Structure."

16. Calculation PGE-009-CALC-006, "ISFSI Cask Storage Pad Concrete Shrinkage and Thermal Stresses."

17. Calculation PGE-009-CALC-007, ISFSI Cask Storage Pad Steel Reinforcement."

18. PG&E Calculation 52.27.100.718 (GEO.DCPP.01.08), "Determination of Rock Anchor Design Parameters for DCPP ISFSI Cutslope."

19. Holtec International Report No. HI-2002474, "Analysis of the Loaded HI-STORM 100 System Under Drop and Tipover Scenarios," Revision 2.

20. Holtec International Report No. HI-992252, "Topical Report on the HI-STAR/HI-STORM Thermal Model and its Benchmarking with Full-Size Cask Test Data," Revision 1.

21. PG&E Calculation M-1058, "Cask Transfer Facility Seismic Restraint Configuration."

22. ACI 349-01, Code Requirements for Nuclear Safety Related Concrete Structures, American Concrete Institute.

23. Holtec International Report No. HI-2002570, "Design Criteria Document for the Diablo Canyon Cask Transfer Facility."

24. PG&E Calculation 52.27.100.708 (PGE-009-CALC-002), "Cask Transfer Facility (Reinforced Concrete)."

25. PG&E Calculation OQE-10 (HI-2012626), "Structural Evaluation of Diablo Canyon Cask Transfer Facility."

26. PG&E Letter DIL-03-003 to the NRC, Revised Response to NRC Request for Additional Information 5-1 for the Diablo Canyon ISFSI Application, March 27, 2003.

27. PG&E Letter DIL-03-004 to the NRC, Supplemental Slope Stability Response to Additional NRC Questions for the Diablo Canyon ISFSI Application, March 27, 2003.

28. PG&E Letter DIL-03-007 to the NRC, Supplemental Slope Stability Design Mitigation Features Information to Additional NRC Questions for the Diablo Canyon ISFSI Application, May 6, 2003.

4.3 TRANSPORT SYSTEM

The cask transporter is designed and used to safely lift, handle, and transport a HI-TRAC transfer cask or a HI-STORM 100SA overpack, loaded with spent fuel and associated nonfuel hardware, between the DCPP FHB/AB, the CTF, and the Diablo Canyon ISFSI storage pad site as described below. The movement is conducted exclusively on the DCPP site as shown in Figure 2.1-2. Due to its important-to-safety classification, the transporter is licensed under 10 CFR 72 (Reference 1). The cask transporter is designed to withstand all design-basis, natural-phenomena events while lifting, handling, and moving the loaded transfer cask or overpack without impairing its ability to safely hold the load.

4.3.1 FUNCTION

The functions of the cask transporter considered important to safety are:

- Transporting the loaded transfer cask, in the horizontal orientation, between the FHB/AB and the CTF.
- Upending and downending the loaded transfer cask between the horizontal and vertical orientations at the CTF.
- Lifting the loaded transfer cask and placing it atop the overpack at the CTF.
- Facilitating the transfer of the loaded MPC between the transfer cask and the overpack.
- Lifting the loaded overpack at the CTF.
- Transporting the loaded overpack between the CTF and its storage location on the Diablo Canyon ISFSI storage pad.

The cask transporter is capable of traveling over all of the road surfaces on the transport route. The road surfaces and underground facilities (see Section 4.3.3) will be evaluated to ensure the capability to support the weight of a cask transporter plus a loaded transfer cask or overpack.

4.3.2 COMPONENTS

This section describes the components used to lift, handle, and transport the loaded transfer cask and overpack to the CTF and Diablo Canyon ISFSI storage pad. Sections 3.3.3 and 3.4 provide discussion of the design criteria for the cask transportation system. Section 8.2.1 summarizes the results of the stress analyses under seismic loading, which bound the normal operation loads. Table 4.3-1 summarizes the functions of, and applicable design codes for, the transport system components that are considered important to safety and covered by an approved 10 CFR 72 quality assurance program.

4.3.2.1 Cask Transporter

4.3.2.1.1 Description

The cask transporter, shown in Figures 4.3-1 through 4.3-3, is a self-propelled, open-front, tracked vehicle used for handling and onsite transport of overpacks and the transfer cask with an MPC contained therein. It is nominally 25 ft long, 19 ft wide, and weighs approximately 85 tons, unloaded. It is designed with two steel tracks to spread out the load on the transport route surface as a distributed pressure load. These tracks provide the means to maneuver the cask transporter around the site. On top of the main structure is a lifting beam supported by two lifting towers that use hydraulic cylinders to provide the lifting force. The industrial-grade hydraulic cylinders are made of carbon steel to ensure high strength and ductility for all service conditions. The cask transporter is diesel-powered and is limited to a fuel volume of 50 gallons to comply with the Diablo Canyon ISFSI TS. The functional specification for the transporter is provided in Reference 6.

4.3.2.1.2 Design

The cask transporter is custom-designed for conditions at the Diablo Canyon ISFSI site, including the transport route with its maximum grade of approximately 8.5 percent. It will remain stable and will not overturn, experience structural failure, or leave the transport route should a design-basis seismic event occur while the loaded transfer cask is being moved to the CTF; while transferring an MPC at the CTF; or while moving a loaded overpack from the CTF to the storage pad. In addition, the cask transporter is designed to withstand DCPP design-basis tornado winds and tornado-generated missiles without overturning, dropping the load, or leaving the transport route. Other natural phenomena, such as lightning strikes, floods and fires have been evaluated and accounted for in the cask transporter design. All design criteria for natural phenomena used to design the cask transporter are specific to the Diablo Canyon ISFSI site (see Sections 3.2 and 3.4 for detailed information).

A lightning strike on the cask transporter would not structurally affect the transporter's ability to hold the load. Due to the massive amount of steel in the structure, the current would be transmitted to the ground without significantly damaging the transporter. However, the driver may be affected by a lightning strike. Therefore, the transporter design includes fail-safe features to automatically shutdown the vehicle if the operator is injured or incapacitated for any reason.

Flooding is not a concern on the transport route for reasons discussed in Section 3.2.2. Sources of fires and explosions have been identified in Sections 2.2 and 3.3.1.6 and in Table 3.4-1, and have been evaluated with respect to cask integrity in Sections 8.2.5 and 8.2.6. Fixed sources of fire and explosion are sufficiently far from the transport route to be of no concern. Mobile sources of fire and explosion, such as fuel tanker trucks, will be kept at a safe distance away from the transporter during loaded cask movement through the use of administrative controls.

The cask transporter is capable of forward and reverse movement as well as turning and stopping. It includes an on-board engine that is capable of supplying enough power to perform its design functions. The cask transporter includes fail-safe service brakes (that is, setting brakes that automatically engage in any loss of power) and an independent parking brake. The brake system is capable of stopping and holding a fully loaded cask transporter on the maximum design grade. The cask transporter is also equipped with an automatic drive brake system that applies the brakes if there is a loss of hydraulic pressure or the drive controls are released. Additionally, the fully loaded cask transporter is not capable of coasting on a 10 percent downward grade with the brakes disengaged, due to the resistance in the drive system.

The cask transporter is equipped with a control panel that is suitably positioned on the transporter frame to allow the operator easy access to the controls located on the control panel and, at the same time, allow an unobstructed view of the cask handling operations. The control panel provides for all-weather operation or will be enclosed in the cab. The control panel includes controls for all cask transporter operations including speed control, steering, braking, load raising and lowering, cask restraining, engine control and "dead-man" and emergency stop switches. Additional emergency stop switches are located at ground level both in the front and rear of the transporter.

Figures 4.3-1 through 4.3-3 show the cask transporter (and associated components) performing its required functions. The cask transporter works with certain other ancillary components to facilitate the lifting and movement of the transfer cask and the overpack. Each ancillary component is described in Sections 4.3.2.2 through 4.3.2.8. Lifting of the loaded transfer cask and cask transport frame is accomplished using the transfer cask horizontal lift rig and the transfer cask lift slings. Transfer cask vertical handling, using the cask transporter, is performed using the transfer cask lift links. Likewise, overpack handling is performed only with the overpack in the vertical orientation using the HI-STORM lifting brackets.

The cask transporter and associated lifting components are classified important to safety, purchased commercial grade, and qualified for MPC and overpack transfer operations at the CTF by testing prior to service. These lifting components are defined as those components in the load path of the supported load. Special lifting devices, defined as any suspended load-bearing component below the integral load links, are designed in accordance with ANSI N14.6 (Reference 2) per the applicable guidance of NUREG-0612 (Reference 3). Table 4.3-1 provides a summary of the design code(s) applicable to each of the lifting and handling components.

On top of the main structure of the transporter is a lifting beam supported by two lifting towers that use hydraulic cylinders to provide the lifting force. Mechanical design features and administrative controls provide a defense-in-depth approach to preventing load drops during lifting and handling. The primary load-retaining devices of the cask transporter are the hydraulic cylinders. In combination, the hydraulic system is designed to carry twice the rated load, including a 15 percent hoist load factor, or 2.3 times the rated load (828,000 lb).

Once the cask is raised to its travel height by the cylinders, a redundant load support system is used. This may take the form of either locking pins and/or wedge brakes. Wedge brakes, by their shape, limit tower movement to the lift (up) direction only. Any failure of the lifting hydraulics will not result in an uncontrolled lowering of the load. Locking pins are inserted into each gantry leg to independently support the load when no vertical movement is needed. The wedge brakes are operable at all times when a load is being lifted or lowered. To remove the pins or wedge locks, the cylinder must first be extended slightly to take the load off the pin or wedge. The load may then be lowered using the lifting cylinders. Requiring the cylinders to take the load ensures that they are operational before lowering the load. Any failure of the hydraulic system at this time will be mitigated by the cylinder safety systems as described below.

The cask transporter hydraulic system wedge brake design prevents uncontrolled lowering of the load upon a loss of hydraulic fluid. A minimum amount of hydraulic fluid system pressure is required to disengage the wedge brakes to allow movement of the load. A loss of hydraulic fluid would drop the pressure in the system and engage the wedge brakes, preventing further movement of the load until corrective actions can be implemented.

The cask transporter is used to lift and place the loaded transfer cask atop the overpack for MPC transfer. During the MPC transfer process, the transfer cask trunnion connections to the cask transporter (that is, lift links) must be disconnected to provide access for the MPC downloader. Prior to disconnecting the lift links, the transporter is restrained. The restraint limits movement of the cask transporter during the time the cask transporter is disengaged from the transfer cask trunnions. Section 5.1 of this SAR provides additional detail on storage system operations.

The design of the cask transporter includes a lateral cask restraining system to secure the load during transport operations. The restraint system is designed to prevent lateral and transverse swinging of the load.

4.3.2.1.3 Radiation Protection

The driver of the cask transporter is the only person in proximity to the transfer cask during onsite transfer operations who requires specific radiation protection consideration. Dose rate and accumulated dose estimates for the driver during cask transport operations are included in Section 7.4 using DCPP design-basis spent fuel source terms. All necessary radiation protection measures will be determined by DCPP radiation protection personnel at the time of fuel loading based on the actual dose rates in the immediate vicinity of the loaded transfer cask.

4.3.2.1.4 Functional Testing and Inspection

As part of normal storage system operations, the cask transporter is inspected for operating conditions prior to each ISFSI loading campaign typically consisting of several casks. During the operational testing of this equipment, procedures are followed that will affirm the correct performance of the cask transporter features that provide for safe fuel-handling operations.

4.3.2.2 Transfer Cask Horizontal Lift Rig

The transfer cask horizontal lift rig transmits the load of the lifted transfer cask from the transfer cask lift slings to the cask transporter lift points (Figure 4.3-1). The horizontal lift rig is a rectangular, structural-steel component that includes two attachment points at the top that connect to the cask transporter lift links and four attachment points at the bottom for the transfer cask lift slings. Because the transfer cask horizontal lift rig is designated as a special lifting device in the load path of the transfer cask during lifting and movement between the FHB/AB and the CTF, it is classified important to safety, and is designed in accordance with ANSI N14.6 per the guidance of NUREG-0612, Section 5.1.6.

4.3.2.3 Transfer Cask Lift Slings

The transfer cask lift slings are used to support the weight of the loaded transfer cask and cask transport frame during horizontal lifting by the cask transporter (Figure 4.3-1). Two lift slings are used to support the transfer cask near the top and bottom of the cask. The two ends of each sling are attached to the transfer cask horizontal lift rig. The lifting slings are made from high-strength synthetic material suitable for the load and service conditions. The lifting slings are important to safety and are designed in accordance with ASME B30.9 (Reference 4) per the guidance of NUREG-0612, Section 5.1.6.

4.3.2.4 Cask Transport Frame

The cask transport frame is an L-shaped steel cradle (Figure 4.2-12) used for rotating the transfer cask between the horizontal and vertical orientations (that is, upending and downending) in the receiving/shipping area of the FHB/AB and on the approach pad at the CTF (Figures 4.3-4 through 4.3-6). It is also attached to, but does not support, the transfer cask while the transfer cask is suspended from the transporter in the transfer cask horizontal lift rig during transport between the FHB/AB and the CTF (Figure 4.3-1). The use of the cask transport frame during cask transport operations is described in detail in Section 5.1.

Movement of the loaded transfer cask through the FHB/AB door is performed with the transfer cask and cask transport frame in the horizontal orientation using Hilman-type heavy-load rollers attached to the long side of the cask transport frame. The transfer cask and cask transport frame are rotated down directly onto a temporary length of track that runs from inside the FHB/AB to the access road located outside the FHB/AB roll-up door. The loaded cask transport frame exits the FHB/AB to the east and travels approximately 60 ft to the cask transporter. The route is level and straight. The roller device travels on a temporary rail system that distributes the load to selected areas of the roadway. The rollers are industrial-grade items that are designed appropriately to support the cask load. Because the cask transport frame is never in the load path for the lifted load, it is classified as not important to safety and is designed in accordance with the AISC Manual of Steel Construction (Reference 5).

4.3.2.5 HI-TRAC Lift Links

The HI-TRAC lift links are load-bearing, structural steel components used to connect the cask transporter lift points to the lifting trunnions on the transfer cask. The HI-TRAC lift links transfer the force of the loaded HI-TRAC transfer cask from the lifting trunnions to the cask transporter lifting points through connector pins. The lift links are important to safety, and are designed in accordance with ANSI N14.6 per the guidance of NUREG-0612, Section 5.1.6.

4.3.2.6 MPC Downloader Slings

The MPC downloader slings are used to lower (or raise) the loaded MPC during MPC transfer operations between the transfer cask and the overpack. The MPC downloader slings transmit the force of the loaded MPC from the MPC lift cleats to the MPC downloader. The MPC downloader slings are important to safety, and are designed in accordance with ASME B30.9 per the guidance of NUREG-0612, Section 5.1.6.

4.3.2.7 MPC Lift Cleats

The MPC lift cleats are ancillary devices temporarily attached to the MPC lid and used during transfer of the loaded MPC between the transfer cask and the overpack. The MPC lift cleats transmit the weight of the loaded MPC to the MPC downloader slings. The MPC lift cleats are classified as important to safety. The MPC lift cleats are special lifting devices that are designed in accordance with ANSI N14.6 per the guidance of NUREG-0612, Section 5.1.6.

4.3.2.8 HI-STORM Lifting Brackets

The HI-STORM lifting brackets (Figure 4.3-3) are load-bearing, structural steel components used to connect the cask transporter lifting points to the lid studs on the overpack. The HI-STORM lifting brackets transfer the weight of the loaded overpack from the lid studs to the cask transporter lift points through connector pins. The HI-STORM lifting brackets are special lifting devices that classified as important to safety, and are designed in accordance with ANSI N14.6 per the guidance of NUREG-0612, Section 5.1.6.

4.3.2.9 HI-STORM Lift Links

The HI-STORM lift links are load-bearing structural steel components used to connect the cask transporter lift points to the HI-STORM lifting brackets. The HI-STORM lift links are used to retrieve a loaded overpack from the CTF upon loss of the CTF lift system. The lift links are important to safety and are designed in accordance with ANSI N14.6 per the guidance of NUREG-0612, Section 5.1.6.

4.3.3 CASK TRANSPORT ROUTE

The cask transport route between the FHB/AB and the CTF and the Diablo Canyon ISFSI storage pads is shown in Figure 2.1-2. The route begins in the radiological control area (RCA) behind the FHB/AB, extends through the protected area past the Unit 2 cold machine shop (U2 CMS), along Plant View Road near Parking Lot 6, Shore Cliff Road (the main access road), and Patton Cove Bypass (Sections 2.6.1.2, 2.6.1.3.3, and 2.6.1.6.1) and then up along Reservoir Road. The route descends a maximum 8.5 percent grade (for approximately 200 ft) from the RCA to the U-2 CMS and then along Plant View Road, which is essentially flat. From the intersection of Plant View Road and Shore Cliff Road, there begins an approximate 6 percent uphill grade (for approximately 3,600 ft) that continues along Reservoir Road. The route ends with a right-hand turn to the CTF and ISFSI storage pad areas. This route consists of an asphalt roadway. The transport route has a 2 percent transverse slope into the hill from the southeast entry outside the plant protected area and south along Plant View Road up to where the road joins the main plant access road. The main plant road has a 2 percent crown for about 50 to 100 ft until the Patton Cove Bypass Road. The Patton Cove Bypass Road will have a 2 percent transverse slope towards its radius until it joins Reservoir Road at which the transverse slope is 2 percent into the uphill side of the road. The transport route is built to AASHTO H-20 and HS-20 pressure ratings, except for the turntables as discussed below. The roadway capacity to withstand the transporter weight has been verified. The underground utilities and structures will be evaluated and temporarily reinforced with steel plates, cribbing, and/or shoring as necessary to withstand the load from the loaded cask transporter. The transporter position on the road will be controlled to ensure an adequate standoff distance is maintained from potential hazards. The following is a discussion of underground utilities along the transport route.

Underground utilities and related valve boxes, pull boxes, catch basins, concrete pipeways, and the retaining wall east of the DCPP Unit 2 CMS are rated for H-20 traffic loads. Administrative controls will be established to preclude the transporter traversing the turntables that are located on the 115-ft Elevation. The turntables, used in the transfer of resin containers from the AB to the radwaste storage building, are only rated for 30 tons. Most pipes and conduits are buried 3 ft deep, except for utilities installed during the plant construction period and ground grid which are shallower, generally 1.5-ft deep. Pipes and conduits are generally nonmetallic, for example, asbestos-cement or polyvinyl chloride (PVC). Firewater line fittings are of ductile or cast iron. Valves are most commonly metallic.

None of the water lines or drains to be crossed are safety related for the 10 CFR 50 power plant. Firewater lines are 10 CFR 50 nonsafety-related, but they are subject to prescribed quality assurance requirements. Radwaste and makeup water lines in the RCA are encased in concrete. 10 CFR 50 safety-related, or nonsafety-related, circuitry passing beneath the route are contained in plastic conduits and are protected by a concrete cap or encasement.

Inside the RCA, the cask transporter will cross: makeup water; radwaste drainage; firewater; storm drains and pipeway drains; hydrogen and nitrogen gas lines in pipeways; electrical, lighting, and security system conduits and grounding; related concrete pipeways, valve boxes and pullboxes; and embedded rails.

From the Elevation 115-ft bench to the protected area (PA) gate near the Unit 2 CMS, utilities that cross the path include: 12-kV conduits near the road to the main warehouse; a drainage pipeway near the access road to the warehouse; domestic water and sanitary sewer lines near the CMS; and electrical and security conduits near the PA fence.

Along Plant View Road, from the PA to Area 10, and along Shore Cliff Road to Warehouse B, utilities include: PVC domestic water lines and asbestos cement pipe (ACP) raw water lines that run along the edge of the road; shallow steel water lines that cross the road near the south end of Building 201; electrical and telephone lines that run along the other lane; culverts; firewater lines, electrical and telecommunications conduits run from the Area 10 intersection near Warehouse B.

Utilities on Reservoir Road include: an ACP raw water pipeline, a fiberglass seawater reverse osmosis permeate pipeline with combination air valves, and electrical and telecommunications conduits. Abandoned sanitary sewer lines cross the road near the leach field. Culverts cross the road at various locations.

As the transporter ascends the hill along Reservoir Road, it passes beneath the Unit 2 500-kV transmission lines, which are approximately 55 ft above the road surface. To ensure there remains an electrically safe working distance between the transporter and the transmission lines, the maximum height of the lifting beam on the transporter will be administratively controlled in accordance with plant procedures.

4.3.4 DESIGN BASES AND SAFETY ASSURANCE

The design criteria and associated design bases for the transporter are presented in Section 3.3.3. The components of the transportation system in the direct load support path while the load is suspended (lifting points) are considered important to safety. The design and construction of important-to-safety items are conducted under an approved 10 CFR 72 quality assurance program. The design approach to classify certain load path members as important to safety with enhanced safety factors is taken to render all hypothetical transfer cask and overpack drop events outside the FHB/AB not credible. Section 8.2.4 describes this approach in more detail. As a defense-in-depth measure, however, the transportation system design and administrative controls are such that the transfer cask and overpack will be lifted only to those heights necessary for cask handling operations. These transporter design bases and administrative controls are in compliance with 10 CFR 72.128 (a) with regard to ensuring adequate safety under normal and accident conditions.

4.3.5 REFERENCES

1. 10 CFR 72, Licensing Requirements for the Independent Storage of Spent Nuclear Fuel and High-Level Radioactive Waste.

2. ANSI N14.6, Special Lifting Devices for Shipping Containers Weighing 10,000 Pounds (4,500 kg) or More, American National Standards Institute, 1993 Edition.

3. Control of Heavy Loads at Nuclear Power Plants, USNRC NUREG-0612, July 1980.

4. ASME B30.9-1996 through B30.9C-2000 Addenda, Slings, American Society of Mechanical Engineers.

5. Manual of Steel Construction, American Institute of Steel Construction, 9th Edition.

6. Holtec International Report No. HI-2002501, "Functional Specification for the Diablo Canyon Cask Transporter."

4.4 OPERATING SYSTEMS

4.4.1 LOADING AND UNLOADING SYSTEM

The dry storage cask handling systems are provided to lift, move, handle, and otherwise prepare an MPC loaded with DCPP spent fuel for storage at the Diablo Canyon ISFSI. Equipment is also available to unload an MPC in the unlikely event this becomes necessary. This section provides an overview of the functions and design of the equipment used to deploy the HI-STORM 100 System at the Diablo Canyon ISFSI for normal, off-normal, and accident conditions. Regulatory Guide 3.62 uses the term "emergency conditions." This SAR uses the term "accident conditions" for consistency with more recent regulatory guidance (that is, NUREG-1567). Movement of spent fuel assemblies between the spent fuel racks and the MPC is conducted in accordance with existing plant equipment and procedures, which will be modified, as necessary, to meet handling requirements and commitments as described in the DCPP 10 CFR 50 LAR, and is not specifically addressed here. Chapter 5 provides a detailed operating guidance regarding use of the structures, systems, and components to perform the various cask-handling activities.

Personnel radiation exposures occurring as a result of dry storage operations will be planned and monitored in accordance with the DCPP radiation protection program (Section 7.1).

4.4.1.1 Function

The function of the loading system is to safely accomplish the following major objectives while maintaining occupational doses ALARA:

- Place the empty MPC and HI-TRAC transfer cask into the DCPP SFP using the FHB/AB crane.
- Load the MPC using 10 CFR 50 fuel handling equipment.
- After fuel loading, place the MPC lid and lid retention device on the MPC.
- Remove the loaded MPC and transfer cask from the SFP and place the assemblage down in the cask washdown area in the FHB/AB.
- Remove MPC lid retention device.
- Weld the MPC lid to the MPC shell.
- Helium leak test the MPC.
- Drain, dry, and backfill the MPC with helium.

- Weld the vent and drain port cover plates and closure ring to the MPC lid and shell.
- Install the transfer cask top lid.
- Lift and place the loaded transfer cask onto the cask transport frame.
- Downend the cask transport frame and loaded transfer cask from the vertical to the horizontal position.
- Move the loaded transfer cask out of the FHB/AB horizontally.
- Move the loaded transfer cask from just outside the FHB/AB to the CTF using the cask transporter.
- Pre-stage an empty HI-STORM 100SA overpack for MPC transfer at the CTF.
- Upend the loaded transfer cask to the vertical position and place it atop the empty overpack at the CTF using the cask transporter.
- Transfer the loaded MPC from the transfer cask to the overpack.
- Remove the empty transfer cask and place it in its designated storage area.
- Install the overpack lid.
- Move the loaded overpack to a storage pad using the cask transporter and place it in its designated position.

The same lifting and handling equipment is used in reverse order to return the loaded MPC to the cask washdown area in the FHB/AB in the unlikely event that an MPC needs to be unloaded. Loading and unloading operations are summarized below, including descriptions of the equipment used in performing these operations.

4.4.1.2 Major Components and Operating Characteristics

Detailed operational guidance is provided in Section 5.1. The following discussion provides an overview of the cask loading and unloading operations, including normal, off-normal, and accident conditions.

4.4.1.2.1 Component Arrival and Movement to the Preparation Area

The MPC is a cylindrical, stainless steel pressure vessel containing an internal honeycomb fuel basket that is designed to house the spent fuel assemblies chosen for storage at the Diablo Canyon ISFSI. The nominal thicknesses of the MPC shell, lid, and baseplate are 1/2 inch, 9-1/2 inches, and 2-1/2 inches, respectively. See Section 4.2.3.2.1 for detailed description of the MPC.

The MPC is shipped to the DCPP site with the fuel basket having been installed at the fabrication facility. Upon arrival at the site, the MPC is removed from the delivery vehicle, receipt inspected, and cleaned, as necessary, prior to being declared ready for installation into the transfer cask. The MPC is upended and removed from its transport frame.

The transfer cask is used to lift and move the MPC located inside it. It is used both before and after the MPC has been loaded with spent fuel assemblies. The transfer cask is designed to provide radiation shielding while maintaining the total weight of the loaded MPC and transfer cask within the load rating of the FHB crane (125 tons). The 125-ton transfer cask design includes a nominal 3/4-inch thick inner shell and a 1-inch thick outer shell, both made of carbon steel. The approximately 4-1/2 inch wide annulus between the inner and outer shells is filled with lead for gamma shielding. A water jacket attached to the outer shell provides a radial dimension of approximately 5.4 inches of water for neutron shielding. The top lid is composed of 2 carbon steel plates with a combined thickness of approximately 1-1/2 inches. Between the plates are 3-1/4 inches of Holtite neutron shielding material. The bottom lid is composed of two carbon steel plates with a combined thickness of approximately 3 inches. Between these plates are 2-1/2 inches of lead. The bottom lid also includes a drain to remove water during preparation activities. The top lid is bolted to allow reuse and has a nominal 27-inch diameter hole in the center. This hole and the bolted connection of the bottom lid allow raising and lowering of the loaded MPC during transfer operations between the overpack and the transfer cask, as described below. The transfer cask is designed for repetitive, transient use to facilitate the movement of the MPC between the overpack and the SFP. All surfaces exposed to the SFP water are coated with coatings compatible with the SFP water chemistry and any uncoated items are compatible with the SFP water chemistry. The Holtec proprietary drawings for the HI-TRAC 125D transfer cask design to be used at the Diablo Canyon ISFSI have been provided to the NRC (Reference 1) and non-proprietary drawings will be included in Section 1.5 of Revision 1 to the HI-STORM 100 System FSAR (Reference 2). Section 4.2.3.4 describes the modified version of the HI-TRAC 125 transfer cask to be used for Diablo Canyon ISFSI operations.

Like the MPC, upon arrival onsite, the transfer cask is removed from the delivery vehicle, inspected, cleaned as necessary, and upended to the vertical position with a lifting device such as a mobile crane. The pool lid is bolted to the bottom flange and the transfer cask is declared ready for use. The transfer cask lid is removed and the empty MPC is lifted and placed inside the transfer cask using the four lift lugs welded to the inside of the shell. The combined empty MPC and transfer cask assemblage is then attached to the cask transport frame, downended to the horizontal orientation and moved into the FHB/AB through the roll-up door on the east side of the building. All of the outdoor lifts of nonfuel bearing components are performed with suitably designed, commercial-grade lifting and rigging equipment or the transporter.

As discussed in the 10 CFR 50 LAR, an auxiliary lift component, custom designed for compatibility with both the DCPP FHB/AB cranes, provide an attachment point for one end of the redundant tension links used during horizontal load movements. A lift yoke, custom designed for compatibility with both the DCPP FHB/AB crane, the transfer-cask lifting trunnions, the redundant tensions links and SFP water chemistry, is used to upright the transfer cask and MPC while in the cask transport frame.

4.4.1.2.2 Cask Preparation and Fuel Loading

Once in the FHB/AB, the transfer cask, with the empty MPC inside, is detached from the cask transport frame, and the transfer cask and MPC are moved to the cask washdown area. While in the FHB/AB, the transfer cask and cask transport frame are restrained to preclude an unanalyzed tip-over. While in the cask washdown area, an impact limiter is attached to the transfer cask using the bolt holes in the outermost bottom flange that were used to attach the bottom of the transfer cask to the cask transport frame (see Figure 4.4-1). The impact limiter is designed to limit cask deceleration to within the design-basis limit of 45 g under a postulated drop event. The cask is then placed on the floor, the lift yoke is disconnected, and the cask is prepared for movement to the SFP.

The annulus between the transfer cask and the MPC is filled with uncontaminated water (borated as necessary to match or exceed the MPC water concentration as described below) and an inflatable annulus seal is installed to prevent contamination of the outer MPC shell while it is submerged in the SFP. The MPC is then filled with water of the proper boron concentration, as required by the Diablo Canyon ISFSI TS. The lift yoke is reconnected and the transfer cask is lifted above the SFP wall, redundant tension links are installed between the crane auxiliary lift component and the yoke, and the lift component is raised slightly until the cask is suspended fully by the links. The cask is then traversed over the SFP wall into position over the cask recess area of the SFP and lowered using the lift component until the lower set of guides on the cask are engaged in corresponding guide channels of the permanent, in-pool, SFP frame structure. The SFP frame provides lateral support to the cask during its vertical load movement in the cask recess area of the spent fuel pool. The frame is a 10 CFR 50 structure described in the further detail in the DCPP 10 CFR 50 LAR supporting dry cask storage. The transfer cask water jacket remains empty to minimize the lifted weight of the cask.

The annulus overpressure system is attached; the cask is raised to remove the tension links and then lowered until resting on the bottom of the cask recess area of the SFP. The annulus overpressure system is a defense-in-depth measure to ensure that any breach of the annulus seal or bottom lid seal will force leakage of clean borated water into the SFP, and not contaminated SFP water into the annulus. The lift yoke is disconnected and the selected fuel assemblies are loaded into the MPC in accordance with plant procedures.

The drain line is attached to the MPC lid and, after fuel loading is complete, the MPC lid and lid restraint system are lowered into position on top of the MPC lift lugs. The lift yoke is attached to the transfer cask, the cask is lifted out of the SFP, and the annulus overpressure system is disconnected. Before moving laterally beyond the edge of the SFP wall, tension links are reinstalled on the FHB/AB crane from the auxiliary lift component to the yoke, which prevent downward vertical movement of the load. The tension links provide redundant drop protection during lateral crane movement, precluding the need to postulate a drop event between the SFP and the cask washdown area. After arriving above the cask washdown area, the tension links are removed to allow downward vertical load movement.

4.4.1.2.3 MPC and HI-TRAC Preparation for Storage

The loaded transfer cask and MPC are lowered to the cask washdown area inside a seismic restraint structure and the cask is decontaminated. Water is added to the water jacket (this water may be unborated since it is contained within a separate pressure boundary and there is no potential for it to mix with the water in the MPC). The water jacket provides neutron shielding and replaces the shielding lost when the water in the MPC is drained.

The water level in the MPC is lowered slightly, and the MPC lid is welded to the MPC shell using the automated welding system (AWS) augmented by manual welding as necessary. Liquid penetrant (PT) examinations will be performed on the root and final weld layers, and each approximately 3/8-inch of weld depth. For the MPC-24, -24E, and –32, which have a 3/4-inch deep MPC lid-to-shell weld, this will require one or two intermediate PT examinations. For the MPC-24EF, which has a 1-1/4 inch deep lid-to-shell weld, four intermediate PTs will be required. The examinations are performed in accordance with the commitments in the HI-STORM 100 System FSAR.

After MPC-lid welding, the water in the MPC is raised again and a hydrostatic test is performed. Upon successful hydrostatic test completion, the MPC is drained of a small amount of water and a helium blanket is applied between the top of the water and the MPC lid. Helium leak testing is performed in accordance with ANSI N14.5-97 (Reference 3) to meet the acceptance criterion defined in SAR Section 10.2 and controlled in the Diablo Canyon ISFSI TS programs. Performance of the helium leak testing at this time allows detection of any leakage through the lid-to-shell weld before the MPC is drained of water. This sequence of activities allows the neutron shielding provided by the water in the MPC to be retained as long as possible in the loading process.

After successful helium leakage testing, the MPC is completely drained of water using the MPC blowdown system. The last of the water is removed via evaporation through the use of a vacuum drying system (as the pressure in the MPC is reduced, the saturation temperature for the water is reduced, causing evaporation of residual water) or through the use of a forced helium dehydration (FHD) system (required for high burnup fuel). The design criteria for the FHD system are provided in Section 10.2. The Diablo Canyon ISFSI TS program controls and SAR Section 10.2 specify the dryness acceptance criteria for both methods of drying. After meeting the drying acceptance criteria, the MPC is backfilled with 99.995 percent pure helium to within a pressure range defined by SAR Section 10.2.

When the MPC has been satisfactorily drained, dried, backfilled with helium, and the lid-to-shell weld has been leak tested, the MPC vent and drain port cover plates are welded on, inspected, and leak tested in accordance with the commitments in the HI-STORM 100 System FSAR, including ANSI N14.5-97. Then, the MPC closure ring is welded in place and inspected in accordance with the commitments in the HI-STORM 100 System FSAR. The inner diameter of the closure ring is welded to the MPC lid and the outer diameter is welded to the top of the MPC shell. The MPC-to-transfer cask annulus may be drained at any time after the MPC has been successfully backfilled with helium.

The MPC lift cleats are attached to the MPC lid, and the MPC is now ready for transfer to storage. The transfer cask top lid is installed. The impact limiter is unbolted from the bottom of the transfer cask and the lift yoke is re-engaged with the transfer-cask-lifting trunnions. The bolts attaching the impact limiter are removed. The FHB crane is used to lift the loaded transfer cask to a height sufficient to detach the impact limiter from the transfer cask, and the crane tension links are installed (the transfer cask remains directly above the impact limiter until the tension links are operable). The seismic restraint system in the cask washdown area is then opened. The height to which the transfer cask is lifted is carefully controlled to be equal to the thickness of the cask transport frame plus a minimal clearance needed to move the cask onto the cask transport frame.

The transfer cask is then moved laterally to the cask transport frame, staged nearby in the upright position. The transfer cask is attached to the cask transport frame and the cask transport frame stabilizer is removed. After the crane tension links are removed, an impact limiter is positioned to protect the loaded transfer cask, and to protect the FHB/AB in case of a crane load-handling equipment failure (see Figure 4.4-2). As the loaded transfer cask and cask transport frame are lowered to just above the impact limiter, the impact limiter is removed from the downending path to allow completion of the downending operation onto the rail dolly for movement outside the FHB/AB. The cask transport frame is moved out of the FHB/AB on rails to a position just outside the FHB/AB door.

4.4.1.2.4 MPC Transfer and Overpack Storage at the ISFSI

Outside the FHB/AB, the loaded transfer cask and cask transport frame are rigged to the cask transporter and moved to the CTF in the horizontal position. These evolutions and the cask transport system design, including associated lifting components, are described in more detail in Sections 4.3 and 5.1. The design of the CTF is discussed in Section 4.4.5.

At the CTF, the empty overpack is prestaged in the subterranean vault with approximately the top 3 ft of the overpack extending above grade level. At this stage of the loading process, the platform is in its full-down position, supported by the CTF base pad supports and fitted with a cask-mating device. When the cask transporter arrives at the CTF, the loaded transfer cask and transport frame are placed on the ground horizontally. The horizontal lift rig is removed and the HI-TRAC lift links are installed on the transporter. The lift links are compatible with the HI-TRAC lifting trunnions and are used to upend the loaded transfer cask out of the transport frame to the vertical position. Once in the vertical position, the transfer cask is removed from the cask transport frame and the cask transporter moves the transfer cask over to the overpack and places it atop the cask mating device on the overpack.

After the transfer cask is placed atop the overpack, the MPC downloader and MPC lift slings are used to lift the MPC by the lift cleats just enough to take the weight of the MPC off the transfer cask bottom lid. The MPC downloader system is integral to the cask transporter and is located on the bottom flange of the horizontal lift beam of the cask transporter. Once the weight of the loaded MPC is taken off the bottom lid, the bottom lid is unbolted and the cask-mating device is used to remove the lid, creating a clear path between the transfer cask and the overpack. The MPC is then lowered into the overpack using the MPC downloader slings and the slings are lowered onto the top of the MPC. The transfer cask is removed from the top of the overpack and placed out of the way, allowing the downloader slings and MPC lift cleats to be removed. The overpack lid is installed and the overpack is transported to the storage pad using the cask transporter.

4.4.1.2.5 Off-Normal and Accident Conditions

For off-normal and accident conditions, the necessary response is a function of the nature of the event. Chapter 8 of this SAR describes the off-normal and accident events for which the cask system is designed and provides suggested corrective actions. The HI-STORM 100 System is designed to maintain confinement integrity under all design-basis, off-normal, and accident conditions, including natural phenomena and drop events. For Diablo Canyon, the only credible drops are limited to the FHB/AB as described in Sections 4.4.1.3.1 and 4.4.1.3.2. Based on the circumstances of an actual event, plant personnel will take appropriate action ranging from inspections of the affected cask components to movement of the cask back into the SFP and unloading of the spent fuel assemblies.

4.4.1.2.6 Unloading Operations

To unload a HI-STORM 100 System, the loading operations are essentially performed in reverse order, using the same lifting and handling equipment. Once the transfer cask is returned to the cask washdown area in the FHB/AB, the MPC closure ring and vent and drain port cover plates are removed by cutting their attachment welds. Fuel cooldown is performed, if necessary, using the vent and drain and the helium cooldown system until the helium temperature is reduced to the maximum temperature specified in SAR Section 10.2. Helium cooldown is required prior to reflooding the MPC with water (borated as necessary) to prevent flashing of the water and the associated pressure excursions. Once the fuel is sufficiently cool, the MPC is flooded with borated water and the lid weld is removed using the weld removal system. Then, the lid retention system is installed, and the transfer cask and MPC are lowered into the SFP using the lift yoke and FHB crane. Finally, the lid retention system and MPC lid are removed, and the fuel assemblies are transferred from the MPC to the spent fuel racks.

4.4.1.3 Safety Considerations and Controls

The MPC shell is designed in accordance with ASME Section III (Reference 4), Subsection NB. The MPC fuel basket is designed in accordance with ASME Section III, Subsection NG. As discussed in Reference 4, the MPC is designed to retain its confinement boundary integrity under all normal, off-normal, and accident conditions. The MPC is a fully welded vessel that does not require the use of mechanical seals or leakage monitoring systems. The cask system is completely passive by design and does not require the operability of any supporting systems to safely store the spent nuclear fuel at the ISFSI storage pads. The design features that ensure safe handling of the fuel are described in Section 4.4.1.2 and the ISFSI operations are provided in Section 5.1.

The transfer cask and overpack steel structures are designed in accordance with ASME Section III, Subsection NF with some of the NRC-approved Code exceptions applicable to DCPP (Table 3.4-6). Both the transfer cask and the overpack are designed to withstand the design-basis normal, off-normal, and accident loadings (including natural phenomena) for the Diablo Canyon ISFSI site. The transfer cask design includes shielding design features that keep dose rates ALARA during fuel loading operation and transport of the loaded cask to the storage pads.

The transfer cask shielding is optimized to provide the maximum practicable protection from radiation while staying within the size and weight limits necessary for compatibility with the DCPP facility and the capacity of the FHB/AB crane. Additionally, the design of the transfer cask includes as few pockets and crevices as practicable in the design to minimize the amount of radioactive crud that could be retained in these areas. The paint on the transfer cask is suitable for ready decontamination and removal of loose particles through the use of a standard decontamination practices. The overpack provides the maximum shielding possible while keeping the cask at a reasonable size and weight, compatible with commercially available crawler vehicles. Details of the transfer cask and overpack shielding design features are provided in Chapter 5 of the HI-STORM 100 System FSAR and Section 7.3.1 of this SAR.

4.4.1.3.1 Considerations Inside the 10 CFR 50 Facility

NUREG-0612 provides guidelines to licensees to ensure the safe handling of heavy loads. The guidelines define acceptable alternatives for heavy load movements, which include using a single failure proof handling system or analyzing the effects of a load drop.

Inside the FHB/AB, the cask and any ancillary components are lifted, handled, and moved in accordance with DCPP procedures and the DCPP Control of Heavy Loads Program for lifting heavy loads, as applicable. The FHB/AB crane hoist and auxiliary lift component, as applicable, will be used with a lift yoke to perform all lifts of the cask inside the FHB/AB. The transfer-cask-lifting trunnions and the lift yoke are designed, fabricated, inspected, maintained, and tested in accordance with NUREG-0612 to ensure that structural failures of these items are not credible. PG&E's Control of Heavy Loads Program controls the design of special lifting devices in accordance with ANSI N14.6 (Reference 5). This program is fully described in DCPP FSAR Update, Section 9.1.4.3.5. The existing FHB/AB crane was not designed and purchased as single-failure proof, as defined in NUREG-0612, Section 5.1.2 (Reference 6). The FHB/AB crane auxiliary lift component is a modification to the crane to provide a single failure proof lift capable of limited vertical travel to facilitate the transition of load support between the crane hoist and the auxiliary lift component. The FHB/AB crane auxiliary lift component is a 10 CFR 50 modification described in further detail in the DCPP 10 CFR 50 LAR to support dry cask storage.

Certain load drops during vertical crane movements have been postulated in the FHB/AB as required by NUREG-0612, Section 5.1.2. Two vertical drops have been analyzed to ensure the consequences of such drops are acceptable and do not cause forces on the cask in excess of its design basis of 45 g under 10 CFR 72. The generic design of the transfer cask has been modified to accommodate a removable (or temporary) impact limiter (see Figure 4.4-1) to meet this acceptance criterion. A temporary impact limiter (see Figure 4.4-2) is also used for the tipover event in the cask washdown area with the cask in the cask transport frame to ensure the consequences of the tipover are acceptable and do not cause deceleration values on the fuel in excess of its design-basis limit. These load drop and tipover analyses are summarized in the DCPP 10 CFR 50 LAR supporting the Diablo Canyon ISFSI project.

Loaded cask drops during the loading operation where only horizontal movement of the lifted load is required are precluded by the use of tension links on the FHB/AB crane auxiliary lift component. Tension links are required for certain horizontal movements to preclude any postulated drop that would cause deceleration forces on the loaded cask in excess of its design basis of 45 g under 10 CFR 72 or apply loads to the 10 CFR 50 structure in excess of their capacity. The tension links are engineered to provide redundant support for the case when large vertical movement of the load is not required. This redundancy provides the requisite temporary, single-failure proof protection during these operations.

4.4.1.3.2 Considerations Outside the 10 CFR 50 Facility

Cask drop events are precluded during transport of the loaded cask from the FHB/AB to the CTF, and from the CTF to the storage pad, through the design of the cask transport system, including the cask transporter (Section 4.3). Drop events are precluded by lift devices designed, fabricated, operated, inspected, maintained, and tested in accordance with NUREG-0612. The cask transport system is designed in accordance with these requirements and appropriate design codes and standards to preclude drop events on the transport route. The cask transporter is also designed to withstand applicable, site-design-basis natural phenomena, such as seismic events and tornadoes, without dropping the load or leaving the transport route. The load-path parts of the cask transporter are designed as specified in Section 4.3.2.1. The cask transporter is procured commercial grade and is qualified by functional testing prior to service for MPC and overpack transfer operations at the CTF. Uncontrolled movement of the cask transporter is prevented by setting the brakes, an emergency stop switch, and a dead-man switch, as discussed in Section 4.3.2.1.2; these components also are procured commercial grade and are qualified by functional testing prior to service.

Similarly, the CTF is designed, fabricated, inspected, maintained, and tested in accordance with NUREG-0612 to make drop events non-credible.

4.4.2 DECONTAMINATION SYSTEM

Standard decontamination methods will be used to remove surface contamination, to the extent practicable, from the transfer cask and accessible portions of the MPC (that is, the lid) resulting from their submersion in the SFP. The cask and MPC lid will be rinsed with clean borated water while over the SFP. Final decontamination of the transfer cask and MPC lid will be performed in the cask washdown area in the FHB/AB. Decontamination will typically be performed manually. While the entire MPC is submerged in the SFP during fuel loading, the annulus seal and annulus overpressure system prevent contaminated water from coming in contact with the sides of the MPC, leaving the MPC lid as the only exterior surface of the HI-STORM 100 System at the ISFSI storage pad that has been exposed to SFP water.

4.4.3 STORAGE CASK REPAIR AND MAINTENANCE

Chapter 9 of the HI-STORM 100 System FSAR describes the required maintenance for the storage cask system. The HI-STORM 100 System is totally passive by design. There are no active components or monitoring systems required to ensure the performance of its safety functions in the final storage configuration. As a result, only minimal maintenance is required over its lifetime, and this maintenance primarily results from cask handling and weathering effects in storage. Typical of such maintenance is the reapplication of corrosion inhibiting materials on accessible external surfaces. Visual inspection of the overpack inlet and outlet air duct screens is required by the Diablo Canyon ISFSI TS to ensure that they are free from obstruction, including clearing of debris, if necessary.

Repairs and maintenance will be performed by maintenance personnel either in-situ or in another appropriate location, based on the nature of the work to be performed. Radiation protection personnel will provide input to and monitor as necessary these maintenance work activities through the work control process.

4.4.3.1 Structural and Pressure Parts

PG&E anticipates that it will use a cask loading campaign where multiple storage casks are loaded in an essentially continuous work effort. Prior to each transfer cask fuel loading, a visual examination is performed on the transfer-cask-lifting trunnions. The examination consists of inspections for indications of overstress such as cracking, deformation, or wear marks. Repair or replacement is required if unacceptable conditions are identified. The transfer-cask trunnions are maintained and inspected in accordance with ANSI 14.6.

As described in the HI-STORM 100 System FSAR, Chapters 7 and 11, there are no credible normal, off-normal, or accident events that can cause the structural failure of the MPC. Therefore, periodic structural or pressure tests on the MPCs, following the initial acceptance tests, are not required as part of the storage maintenance program.

4.4.3.2 Leakage Tests

There are no seals or gaskets used on the fully welded MPC confinement system. Therefore, confinement boundary leakage testing is not required as part of the storage system maintenance program.

4.4.3.3 Subsystem Maintenance

The HI-STORM 100 System does not include any subsystems that provide auxiliary cooling during loading operations or in its final storage configuration. Normal maintenance and calibration testing is required on the vacuum drying, helium backfill, recirculation and cooldown, and leakage testing systems. Rigging, remote welders, cranes, and lifting beams are inspected prior to each loading campaign to ensure this equipment is ready for service.

4.4.3.4 Pressure Relief Valves

The pressure relief valves used on the water jacket for the transfer cask require calibration on an annual basis (or prior to the next transfer cask use if the period the transfer cask is out of use exceeds 1 year) to ensure the pressure relief setting is within tolerance as controlled by PG&E's DCPP Maintenance Program.

4.4.3.5 Shielding

The gamma and neutron shielding materials in the overpack, transfer cask, and MPC degrade negligibly over time or as a result of usage. Radiation monitoring of the ISFSI provides ongoing evidence and confirmation of shielding integrity and performance. If the monitoring program indicates increased radiation doses, additional surveys of the overpacks will be performed to determine the cause of the increased dose rates.

The Boral panels installed in the MPC baskets are not expected to degrade. The use of Boral as the fixed neutron absorber is discussed in Section 4.2.3.3.5. Therefore, no periodic verification testing of neutron poison material is required on the HI-STORM 100 System.

4.4.3.6 Thermal Performance

In order to ensure that the HI-STORM 100 System continues to provide effective thermal performance during storage operations, surveillance of the passive heat removal system is performed in accordance with the Diablo Canyon ISFSI TS. This involves a periodic inspection to verify that the air duct screens are not blocked.

4.4.4 UTILITY SUPPLIES AND SYSTEMS

Electric power is provided for the CTF lifting platform, CTF and storage-pad-area lighting, and the storage-pad-area security system. As the HI-STORM 100 System is a passive system, no other utilities are required for ISFSI operation.

4.4.4.1 Electrical Systems

Electric power is not required to support functions of the Diablo Canyon ISFSI important-to-safety SSCs. Normal power is supplied from the nonsafety-related 12-kV distribution system for the CTF lifting platform, the CTF, and the storage-pad-area normal lighting. Power for the storage-pad-area security equipment is provided by the DCPP security power system. There are no motorized fans, dampers, louvers, valves, pumps, electronic monitoring systems, and no electrically operated cranes. In the event of a DCPP loss of offsite power, power will not be supplied to the ISFSI components, except for the security loads. A discussion of the normal and emergency power for security equipment is provided in the Physical Security Plan (Section 9.6). Section 8.1.6 describes recovery actions to mitigate this event.

4.4.4.1.1 Normal Power Supplies

The existing DCPP 12-kV distribution system is connected to the DCPP power distribution system in the existing DCPP 12-kV startup buses. Either DCPP Unit 1 or Unit 2 can supply the 12-kV system. The 12-kV underground distribution system is connected to the 12-kV startup bus by existing 3-way switches. The existing 12-kV underground distribution system is routed throughout the DCPP site, including near the location of the CTF and ISFSI storage pad area. A combination of new and existing switches and 12-kV/480-V transformers are used to connect the CTF and ISFSI storage-pad-area loads.

4.4.4.1.2 Grounding

The ISFSI storage pad area, perimeter fencing, lighting and poles, and security equipment will be located below the DCPP Unit 1 500-kV transmission lines. The existing DCPP station-to-switchyard ground grid below the ISFSI location will be maintained. The ISFSI area will be provided with a ground grid, and it will be connected to the station-to-switchyard ground grid. Each storage cask will be grounded to the ISFSI-area ground grid.

4.4.5 CASK TRANSFER FACILITY

The design criteria for the CTF are provided in Section 3.3.4. Holtec CTF drawing 3770 is provided in Figure 4.4-3. The site-specific structural details of the CTF design and analysis for the Diablo Canyon ISFSI are provided in Section 4.2.1.2. The mechanical design aspects are discussed below.

4.4.5.1 CTF Function

The function of the CTF is to facilitate transfer of a loaded MPC between the transfer cask and the overpack. These operations are discussed in Sections 4.4.1.2.4 and 5.1.1.3.

4.4.5.2 CTF Design

Design criteria for the CTF are provided in Section 3.3.4 of this SAR Section 2.3.3.1 of the HI-STORM 100 System FSAR, and in Reference 7. The CTF is used in conjunction with the Diablo Canyon cask transporter to permit MPC transfers between the transfer cask and the overpack. The CTF is designed to position an overpack sufficiently below grade where the transfer cask can be mated to the overpack using a cask transporter and a suitably designed mating device. The CTF lifting platform acts as an elevator to raise and lower an overpack. In the full-up position, the overpack base is approximately 40 inches below grade. At the full-down position, the overpack top surface is approximately 30 inches above grade.

The main components of the CTF include the main shell, lifting jacks, drive and control system, and lift platform (Figure 4.4-3). A description of each of these components and the related design criteria are given in Section 3.3.4.

The analysis of the concrete structure housing the cask transfer facility (CTF) utilized the static and dynamic rock properties provided in References 8 and 9. Reference 8 provides the ultimate and design allowable values for lateral resistance of the rock while Reference 9 provides the ultimate and design allowable values for bearing on the rock at the bottom of the CTF.

4.4.5.2.1 Lifting Jacks

The jacks are designed to safely raise and lower a fully loaded overpack (180 tons). The load-bearing structural steel members are designed and fabricated in accordance with Reference 4.

4.4.5.2.2 Mechanical Design Criteria

The design for the cask-lifting platform is based on a dead load of 180 tons.

4.4.5.2.3 Functional/Technical Requirements

The CTF and its components are designed to operate in conjunction with the cask transporter. Together, the cask transporter and the CTF design ensures that there will be no uncontrolled lowering of the lifted load under all design-basis conditions of service, including environmental phenomena.

4.4.5.2.3.1 Main Shell

The CTF main shell supports the jack screws. The cask-lifting platform is raised inside the CTF main shell. As discussed in Sections 4.2.1.2 and 4.4.5.2.3.6, the main shell is equipped with a sump to collect water from the CTF cylinder.

4.4.5.2.3.2 Lifting Platform

The cask-lifting platform is a horizontal, steel-beam structure. Radial stability of the lifting platform is provided by the main shell. Vertical guides or runners are provided to prevent damage of the main shell or lifting platform at the interface locations. These are either wheeled or low friction pads. The guides (or runners) are capable of restraining the lifting platform when applied with the maximum horizontal load from the earthquake applied in two simultaneous orthogonal directions.

The lifting platform is lifted by three, ACME, thread-traveling, nut-type, inverted screw jacks located on the outside edge of the main shell. Raising and lowering of the lifting platform is performed by the simultaneous rotation of the lifting jackscrews. The platform is parked in the up position, with the jackscrews protected from corrosion and dirt by protective boots. The platform bottoms out at the full-down position against the base pad supports to prevent loading of the jacks with the combined weight of the loaded transfer cask and the overpack.

Provisions are provided for personnel access to inspect, maintain, and repair CTF components. Access to the underside of the platform may be via ladder through removable access ports. Access is not allowed if the platform is loaded.

4.4.5.2.3.3 Lifting Jacks

Even loading of the platform is ensured by the simultaneous operation of the lifting jacks. The range of travel of the lifting platform is a minimum of 160 inches. The upper range of travel positions the overpack with its baseplate approximately 30-40 inches below grade. Lift speed is between 6 and 12 inches/minute. The jacks are capable of performing the lift in one continuous motion. The jacks do not require an interim cooling period during the lift. The jacks are designed to preclude unwinding during a loss-of-power event.

The CTF screw jacks are commercially designed equipment, typically used to raise large, heavy objects, such as train cars, to facilitate maintenance. The CTF screw jacks are Important-to-Safety, Category B, because they support the loaded overpack as it is raised to the full-up position in preparation for transport to the ISFSI pad. Combined, the screw jacks are designed to support 450 tons, which is two and one-half times the weight of a bounding loaded overpack and essentially eliminates the potential for jack structural failure due to overload. The screw jacks do not support the stacked casks during MPC transfer because the lift platform is resting on a support pedestal that transmits the load directly into the concrete and rock foundation below with no load applied to the jacks. With the lift platform in the full down position, the top of the overpack remains above grade, so the overpack cannot become wedged in the CTF

4.4.5.2.3.4 Drive and Control System

The cask-lifting platform is operated from a fixed position control station or a pendant. The control station may be located above or below grade as long as reasonable access is provided. The cask-lifting platform drive system ensures coordination of the lifting jacks.

The CTF drive and control systems are commercial components that are not unique to nuclear facilities. The drive and control systems are not important to safety because their failure modes do not result in an uncontrolled lowering of the load or the inability to retrieve the cask. As stated in SAR Section 3.3.4.2.3, the drive and control systems will be designed in accordance with NUREG-0612, Section 5.1.6(2), which refers to NUREG-0554, "Single Failure Proof Cranes for Nuclear Power Plants." Because the CTF is not a crane, the guidelines of NUREG-0554 will be implemented to the extent practical. The CTF load handling equipment drive and control systems will be functionally checked.

4.4.5.2.3.5 Facility Power

Power for the facility is electric. Power lines are sufficiently protected from interaction with the cask transporter and other operations. Section 8.1.6 describes recovery actions for loss of power to the CTF during operations.

4.4.5.2.3.6 Sump

During periods of nonusage, the CTF will have a cover installed to prevent water entry. To collect any accumulated water, the CTF is equipped with a sump. Any sump water will be collected, sampled for radioactivity, and processed in accordance with applicable administrative procedures.

4.4.5.3 CTF Analysis

The load path parts of the CTF are conservatively designed in accordance with the ASME Code, Section III, Subsection NF. NUREG-0612 was reviewed and the intent of applicable guidance was applied in the design criteria for the load path parts of the CTF. The CTF is purchased commercial grade and is qualified for MPC and overpack transfer operations by functional testing prior to service.

The failure modes of the power supply and the drive and control systems are discussed below:

Loss of Electrical Power Supply

The three screw jacks lift the lifting platform via the rotation of the long threaded screw through a traveling nut. The traveling nuts are attached to the lifting platform and the platform runs up and down the screws as the screws rotate through the nuts. The threaded connection is an ACME-type thread, which is designed not to "unwind" under any condition, such as a loss of power, as described in SAR Section 8.1.6.3.2. The three screw jacks stop simultaneously on a loss of all power to the system. The system will shut down on an out-of-level condition if one or two of the screw jack motors fail and the remaining motor(s) do not. Therefore, a loss of electrical power will not cause an uncontrolled lowering of the load or the inability to retrieve the cask.

Loss of Level Control

The three CTF screw jacks are electronically coupled with position feedback to ensure that the platform remains level at all times during travel. In addition to the primary electronic level control and feedback system, the lifting platform is equipped with independent level monitors which trip the drive system if an out-of-level condition is detected. Therefore, a loss of level control will not cause an uncontrolled lowering of the load or the inability to retrieve the cask.

Loss of Travel Control

The CTF lift platform travel on the screw jacks is controlled by redundant limit switches that trip the drive system in the event that the primary, pre-programmed position feedback circuits fail. These serve to provide redundant assurance that the CTF does not create a situation where it is jacking against a hard point. Failure of both redundant travel limit control systems would result in an eventual trip of the drive motors due to over-torque or over-current when the lift platform reaches a physical hard stop at the top or bottom of the CTF. Therefore, a loss of travel control will not cause an uncontrolled lowering of the load or the inability to retrieve the cask.

Operator Action

The design features of these control systems will be backed up by operator action, if necessary. The CTF operator will be able to tell by observation if the cask is significantly out-of-level or moving past established travel limits because the lifting/lowering speed is on the order of inches per minute. Upon detection of a malfunctioning automatic control feature, the operator can take appropriate action to shut down the system.

Analyses have been performed to verify that, during MPC transfer from the HI-TRAC to the HI-STORM overpack, the main shell of the CTF and its surrounding foundation are sufficient to maintain the overpack in the vertical position.

All load-bearing components have been evaluated to ensure that they have been sized in compliance with the intent of the applicable sections of ANSI 14.6, NUREG-0612, and ASME Subsection NF.

There are no impact factors considered in the CTF analysis. After the empty overpack is positioned in the CTF, any radial gaps between the CTF shell and the body of the overpack just below the top of the CTF are closed to the extent practical by adding metallic shim material at the top of the CTF shell. The overpack base is restrained from sliding, relative to the platform, by vent plates welded to the platform top plate. The lifting platform is restrained against lateral movement by compression bars that ride up and down with the platform as the traveling nut moves along the jack screw. Assumption 3.5 in Section 3 of Holtec Calculation HI-2012626 (Reference 10) recognizes that small gaps may still remain even after the addition of shims to close the gap. These very small gaps (compared to the scale of the structure) may give rise to high frequency impact forces upon contact. However, since the structural analysis for Code qualification focuses on the response to low frequency loads from a seismic loading, any high frequency impact loads arising from the existence of any remaining very small gaps after shimming have been omitted.

After MPC transfer, the HI-TRAC transfer cask and mating device are removed, the lid is installed on the loaded overpack, the shims are removed, and the CTF lift platform raises the overpack to the full up position. The time the loaded overpack may be in the CTF is limited to 22 hours by proposed Diablo Canyon ISFSI Technical Specification Limiting Condition for Operation (LCO) 3.1.2. The actual time between MPC transfer into the overpack and raising the overpack out of the CTF is expected to be less than an operating shift, or 8 hours. The thermal implications of installing these shims are bounded by the 22-hour time limit of this LCO. In the "Applicable Safety Analysis" section of the bases for LCO 3.1.2, it is reported that if the loaded MPC is in the transfer cask and the transfer cask is located in a cask pit, the fuel cladding temperatures remain below the short term limit for up to 22 hours. This 22-hour limit is computed assuming only 10 percent of normal heat transfer capability while the MPC is in the transfer cask. This accident event is discussed in more detail in HI-STORM FSAR Section 4.5.2.1. With the seismic restraint shims in place between the loaded overpack and the CTF walls, there will still be some convective heat transfer through the overpack, albeit not at a rate commensurate with the conditions on the ISFSI pad. However, the analysis supporting the 22-hour time limit in the CTF provides a bounding case to ensure fuel cladding temperature limits are not exceeded.

The analyses performed in Holtec Calculation HI-2012626 (Reference 10) considered the lifting/lowering operation to be a normal condition subject to dead and wind loading. Loadings involving seismic events were considered only for the longer duration scenario when the loaded stack was supported by the base of the CTF. In this configuration, the lowest frequencies are associated with lateral bending of the stacked configuration as a beam-like structure. These lateral frequencies are computed in Attachment E of HI-2012626 and are use to establish load amplifiers for lateral loads imposed by the stacked casks due to seismic effects. The vertical frequency of the stacked casks is in the rigid range, so no amplifier is used for vertical loads when the system is resting on the base of the CTF.

The screw jacks are only loaded in the short duration when the HI-STORM is being raised or lowered. When the HI-STORM is in the full-up position, the screw jacks have a minimal free length and the vertical natural frequency of the screw jack/loaded cask plus platform system is in the rigid range. The screw jacks are hung from the top; the lower screw jack support is to provide lateral support to the long screw. When loaded, the screw jack tensile load is always reacted at the top of the screw jack by the screw jack support structure. There is no mechanism by which large compression can be applied to the screw jack supports. Therefore, screw jack stability under compressive loading is not considered, nor is it a concern. Nevertheless, a straightforward calculation of the classical Euler buckling load of one screw jack, based on considering the maximum travel length of the platform as the unsupported length of the screw jack, gives the classical buckling load as greater than 1.5 million lb. This classical buckling load is over five times the rated capacity of the screw jack in tension.

4.4.5.4 Functional Testing and Inspection

As part of normal storage system operations, the CTF is inspected for operating conditions prior to each ISFSI loading campaign typically consisting of several casks. During the operational testing of this equipment, procedures are followed that will affirm the correct performance of the CTF features that provide for safe fuel-handling operations.

4.4.6 REFERENCES

1. Submittal of Holtec Proprietary Design Drawing Packages, PG&E Letter to the NRC, DIL-01-008, December 21, 2001.

2. Final Safety Analysis Report for the HI-STORM 100 System, Holtec International Report No. HI-2002444, Revision 0, July 2000.

3. ANSI N14.5, Leakage Tests on Packages for Shipment, American National Standards Institute, 1997 Edition.

4. Boiler and Pressure Vessel Code, Section III, Division 1, Subsection NF, American Society of Mechanical Engineers, 1995 Edition including 1996 and 1997 addenda.

5. ANSI N14.6, Special Lifting Devices for Shipping Containers Weighing 10,000 Pounds (4,500 kg) or More, American National Standards Institute, 1993 Edition.

6. Control of Heavy Loads at Nuclear Power Plants, NUREG-0612, USNRC, July 1980.

7. Holtec International Report No. HI-2002570, "Design Criteria Document for the Diablo Canyon Cask Transfer Facility."

8. PG&E Calculation No. 52.27.100.716 (GEO.DCPP.01.06), "Development of Lateral Bearing Capacity for DPCP CTF Stability Analysis."

9. PG&E Calculation No. 52.27.100.513 (GEO.DCPP.01.03), "Development of Allowable Bearing Capacity for DCPP ISFSI Pad and CTF Stability Analysis."

10. PG&E Calculation No. OQE-10 (HI-2012026), "Structural Evaluation of Diablo Canyon Cask Transfer Facility."

4.7 OPERATING ENVIRONMENT EVALUATION

In accordance with NRC Bulletin 96-04 and consistent with Interim Staff Guidance (ISG) 15 (References 1 and 2), a review of the potential for chemical, galvanic, or other reactions among the materials of the HI-STORM 100 dry storage system, its contents, and the operating environments, which may produce adverse reactions, has been performed.

4.7.1 MULTI-PURPOSE CANISTERS

The passive, non-cyclic nature of dry storage conditions does not subject the MPC to conditions that might lead to structural fatigue failure. Ambient temperature and insolation cycling during normal dry storage conditions and the resulting fluctuations in MPC thermal gradients and internal pressure is the only mechanism for fatigue. These low-stress, high-cycle conditions cannot lead to a fatigue failure of the MPC enclosure vessel or fuel basket structural materials, that are made from austenitic stainless steel, known as "Alloy X." "Alloy X" is a fictitious stainless steel used in the design basis analyses of the MPC to ensure any of the permitted austenitic stainless steels used in MPC fabrication will be bounded by the analyses. (See HI-STORM FSAR Section 1.2.1.1 for a detailed discussion of Alloy X.) A typical MPC construction material specification, ASME SA240-304 stainless steel, has a fatigue endurance limit well in excess of 20,000 psi. All other off-normal or postulated accident conditions are infrequent or one-time occurrences, which cannot produce fatigue failures. The MPC also uses materials that are not susceptible to brittle fracture.

The MPC enclosure vessel and fuel basket will be in contact with air, helium, and spent fuel pool (SFP) water during it various stages of use. The MPC enclosure vessel and fuel basket, with the exception of the Boral neutron absorber panels, and aluminum seal washers used in the vent and drain port caps, is fabricated entirely of austenitic stainless steel. Aluminum heat conduction elements, offered as optional equipment in the HI-STORM 100 System generic MPC design (Section 1.2.1.1 of the HI-STORM FSAR, as modified by LAR 1014-1), will not be used in any of the MPCs deployed at the Diablo Canyon ISFSI. There is no significant chemical or galvanic reaction of stainless steel with air or helium. The aluminum seal washers used with the vent and drain port caps never are in contact with water, so combustible gas generation is not a concern. There are no coatings of any kind used in or on the MPC. The control of combustible gases generated by the interaction of the Boral neutron absorber with the SFP water is discussed in Section 4.7.1.1.

The moisture in the MPC is removed during loading operations to a point where oxidizing liquids and gases are at insignificant levels. The MPC cavity is then backfilled with dry inert helium at the time of closure to maintain an atmosphere in the MPC that provides corrosion protection for the SNF cladding and MPC materials throughout the dry storage period. The specific limits on MPC moisture removal and helium backfilling are included in the technical specifications. Insofar as corrosion is a long-term time-dependent phenomenon, the inert gas environment in the MPC minimizes the incidence of corrosion during storage on the ISFSI to an insignificant amount.

4.7.1.1 Boral Neutron Absorber

The Boral neutron absorber panels consist of a boron carbide powder-aluminum powder mixture sandwiched between two solid aluminum surfaces. The corrosion-resistant characteristics of such materials for dry SNF storage canister applications, as well as the protection offered by these materials against other material degradation effects, are well established in the nuclear industry in both wet and dry spent fuel storage applications. The preservation of this non-corrosive atmosphere is assured by the inherent seal-worthiness of the MPC confinement boundary integrity (there are no gasket joints in the MPC).

The Boral neutron absorber panels will be submerged in borated water during fuel loading operations in the SFP, and during MPC lid welding and potential MPC lid cutting in the unlikely event the MPC needs to be unloaded. The aluminum in the as-manufactured Boral panels reacts with water, producing hydrogen gas. Therefore, all Boral surfaces are pre-passivated or anodized before installation in the MPC to minimize the rate of hydrogen production and ensure a combustible concentration of hydrogen does not accumulate under the MPC lid prior to, or during MPC lid welding or cutting operations.

Because the Boral water reaction cannot be completely eliminated by pre-passivation and the Boral material in the MPC will be under varying hydrostatic pressure levels (up to approximately 40 ft of water pressure during fuel loading or unloading in the SFP, and up to approximately 15 ft during lid welding or cutting), continued generation of limited quantities of hydrogen is possible. Pre-passivation has been shown by analysis to preclude the accumulation of combustible quantities of gas under the MPC lid during the welding or cutting operations for over 24 days (Reference 3). The operating procedures for the Diablo Canyon ISFSI will include provisions to address combustible gas control in the MPC lid area, consistent with the controls discussed in Sections 8.1.5 and 8.3.3 of the HI-STORM 100 System FSAR, Revision 1, for loading and unloading operations, respectively.

4.7.2 HI-TRAC TRANSFER CASK

The HI-TRAC transfer cask will be used in an air and borated water environment during the various stages of loading and unloading operations. The use of appropriate coatings and the controlled environment in which the transfer cask is used minimize damage due to direct exposure to corrosive chemicals that may be present during loading and unloading operations. The transfer cask is designed for repeated normal condition handling operations with high factors of safety, particularly for the lifting trunnions, to assure structural integrity. The resulting cyclic loading produces stresses that are well below the endurance limit of the trunnion material, and therefore, will not lead to a fatigue failure in the transfer cask. All other off-normal or postulated accident conditions are infrequent or one-time occurrences that do not contribute significantly to fatigue. In addition, the transfer cask utilizes materials that are not susceptible to brittle fracture during the lowest temperature permitted for loading.

The transient use and relatively low neutron fluence to which the transfer cask materials are subjected do not result in radiation embrittlement or degradation of the transfer cask's shielding materials that could impair its ability to perform its intended safety function. The transfer cask materials are selected for durability and wear resistance for their deployment.

The load-bearing portions of the transfer cask structure are fabricated from carbon steel. Other materials included in the transfer cask design are Holtite-A (in the top lid for neutron shielding); elemental lead (in the body and bottom lid for gamma shielding) and brass, bronze or stainless steel appurtenances (pressure relief valves, drain tube, etc.). A complete description of materials is provided on the transfer cask drawing in Chapter 1 of the HI-STORM 100 System FSAR, Revision 1. The Holtite and lead shielding materials are completely enclosed by the welded steel construction of the transfer cask. Therefore, there will be no significant galvanic or chemical reactions between these shielding materials and the air or borated water. A detailed description of Holtite-A may be found in Section 1.2.1.3.2 of the HI-STORM 100 System FSAR.

The internal and external steel surfaces of the transfer cask, (except threaded plugs and holes, seal areas and trunnions) are sandblasted and coated with an epoxy-based coating system, qualified for borated water use, to preclude surface oxidation. Lid bolts are plated and the threaded holes in the top flange are plugged or sealed during water immersion to prevent borated water intrusion. The transfer cask coating system was chosen based on manufacturer's literature that confirms that the coatings are designed for use in the conditions that the transfer cask will experience. Table 4.7-1 provides the specific coatings to be used on the transfer cask. With the coating system in place, there is no significant galvanic or chemical interaction between the air or SFP water and the steel materials. Minor nicks and dings that may expose the underlying carbon steel will be repaired by maintenance coating between uses of the transfer cask. The small size of any carbon steel exposed by the nicks and dings, the temporary nature of transfer cask use, the relatively short duration of exposure to borated water, and the coating repair maintenance program, combined, eliminate significant corrosion of the carbon steel as a concern.

In summary, significant chemical or galvanic reactions involving the transfer cask and the SFP water are not expected.

4.7.3 HI-STORM OVERPACK

The HI-STORM overpack will be used only in an air environment during the various stages of loading and unloading operations. The overpack is never immersed in the SFP or any other source of water. It will be subjected to the environment at the ISFSI, which includes saline water vapor and rain. The overpack consists of two concentric carbon steel cylinders separated by radial plates, with a carbon steel base plate and lid. The drawing in Section 1.5 of the HI-STORM FSAR, Revision 1 provides details on materials used in the overpack. The annulus between the two cylinders is filled with concrete. All exposed carbon steel surfaces of the overpack, including the anchor studs and nuts, are coated with an epoxy-based coating to prevent corrosion due to salinity or other airborne contaminants at the ISFSI. Table 4.7-1 provides the specific coatings to be used on the overpack. Concrete in the overpack body, lid, and pedestal is non-reinforced and completely encased in steel. Therefore, the potential of environmental-induced degradation in an oceanside environment such as the Diablo Canyon ISFSI, including spalling of concrete, are not possible for the overpack.

Under normal storage conditions, the bulk temperature of the overpack will, because of its large thermal inertia, change very gradually with time. Therefore, material degradation from rapid thermal ramping conditions is not credible for the overpack. As discussed in Appendix 1.D of the HI-STORM 100 System FSAR, the aggregates, cement and water used in the storage cask concrete are carefully controlled to provide high durability and resistance to temperature effects. The configuration of the storage overpack assures resistance to freeze-thaw degradation even though this degradation force is expected to be minimal at the site. All other off-normal or postulated accident conditions are infrequent or one-time occurrences that do not contribute significantly to fatigue. In addition, the overpack utilizes materials that are not susceptible to brittle fracture during the lowest temperature permitted for loading.

A maintenance program for coatings on accessible areas of the overpack ensures that nicks or dings that expose the carbon steel components underneath will be repaired before any significant corrosion can occur.

The relatively low neutron flux to which the storage overpack is subjected cannot produce measurable degradation of the cask's material properties and impair its intended safety function.

In summary, the materials of construction of the overpack design are compatible with the environment in which the overpack will operate. These design features and the coating maintenance program ensure that the overpack can perform its design functions for the life of the ISFSI.

4.7.4 NEUTRON ABSORBER

The effectiveness of the fixed borated neutron absorbing material used in the MPC fuel basket design requires that sufficient concentrations of boron be present to assure criticality safety during worst case design basis conditions over the 40-year design life of the MPC. Information on the characteristics of the Boral neutron absorbing material used in the MPC fuel basket is provided in Subsection 1.2.1.3.1 of the HI-STORM 100 System FSAR. The relatively low neutron flux, which will continue to decay over time, to which this borated material is subjected, does not result in significant depletion of the material's available boron to perform its intended safety function. In addition, the boron content of the material used in the criticality safety analysis is conservatively based on the minimum specified boron areal density (rather than the nominal), which is further reduced by 25 percent for analysis purposes, as described in Section 4.2.3.3.5 of the Diablo Canyon ISFSI SAR. An evaluation discussed in Section 6.3.2 of the HI-STORM 100 System FSAR demonstrates that the boron depletion in the Boral is negligible over a 50-year duration. Thus, sufficient levels of boron are present in the fuel basket neutron absorbing material to maintain criticality safety functions over the 40-year design life of the MPC.

4.7.5 EMBEDDED CASK ANCHORAGE SYSTEM AND PAD

The embedded cask anchorage system (i.e., embedment ring, coupling, rods and embedded plates and jam nuts) is constructed of carbon steel material. Refer to SAR Figure 4.2-6 (Holtec Drawing 3769, item 4) for the cask anchor stud and drawing number PGE-009-SK-301 and –302 for the embedded anchorage in the concrete pad (See Appendix "DOC 1" to Reference 4).

The steel components exposed to the environment (such as the top exposed surface of the embedment ring), will be properly coated per DCPP coating specifications, similar to the components in the power plant also located in the outdoor environment. The ISFSI reinforced concrete pad is located approximately 1/4 mile from the coastline at approximately 300 ft elevation and is not subjected to the harsh saltwater atmosphere that exists at other marine structures (such as the intake structure) located at DCPP. Existing DCPP structures with similar construction (i.e., uncoated reinforcement with minimum concrete cover per ACI Code) and environmental exposure conditions, as proposed for the ISFSI pad (e.g., the containment structure, auxiliary building), have been in service for over 20 years at DCPP and have shown no evidence of adverse degradation due to embedded steel corrosion. In order to provide necessary corrosion protection for the given environmental exposure, construction requirements specified in ACI 349 (Reference 5, Part 3, Chapters 4 and 5), will be followed. These requirements include meeting the concrete durability requirement for the maximum water to cement ratio and a minimum compressive strength and providing the minimum concrete cover for the reinforcing steel based on placement. To provide added protection from the potential of reinforcing steel corrosion, the concrete pad surface will be maintained with a penetrating, breathable, water-repellent sealer to protect the concrete surfaces exposed to weather and marine air.

No corrosion allowance was applied to the embedded anchorage as necessary measures are taken to minimize / prevent the possibility of water intrusion into the pad. The pad will also be periodically and visually inspected as part of the 10 CFR 50 DCPP Maintenance Rule Program to monitor the materiel condition of the facility and its components.

4.7.6 MATERIALS SUMMARY

Table 4.7-1 provides a listing of the materials of fabrication for the HI-STORM 100 dry storage system and summarizes the performance of the material in the expected operating environments during short-term loading/unloading operations and long-term storage operations. As a result of this review, no operations were identified that could produce adverse reactions beyond those conditions already generically evaluated and approved in the licensing of the HI-STORM 100 System.

4.7.7 REFERENCES

1. USNRC Bulletin 96-04, Chemical, Galvanic, or Other Reactions in Spent Fuel Storage and Transportation Casks.

2. USNRC Interim Staff Guidance Document 15, Materials Evaluation.

3. Holtec International Dry Storage Position Paper DS-248, Revision 2, Chemical Stability of the Holtec MPC Internals During Fuel Loading and Dry Storage.

4. ACI 349-01, Code Requirements for Nuclear Safety Related Concrete Structures, American Concrete Institute.

5. ACI 349-97, Code Requirements for Nuclear Safety Related Concrete Structures, American Concrete Institute (with 10/10/00 Draft Appendix B).

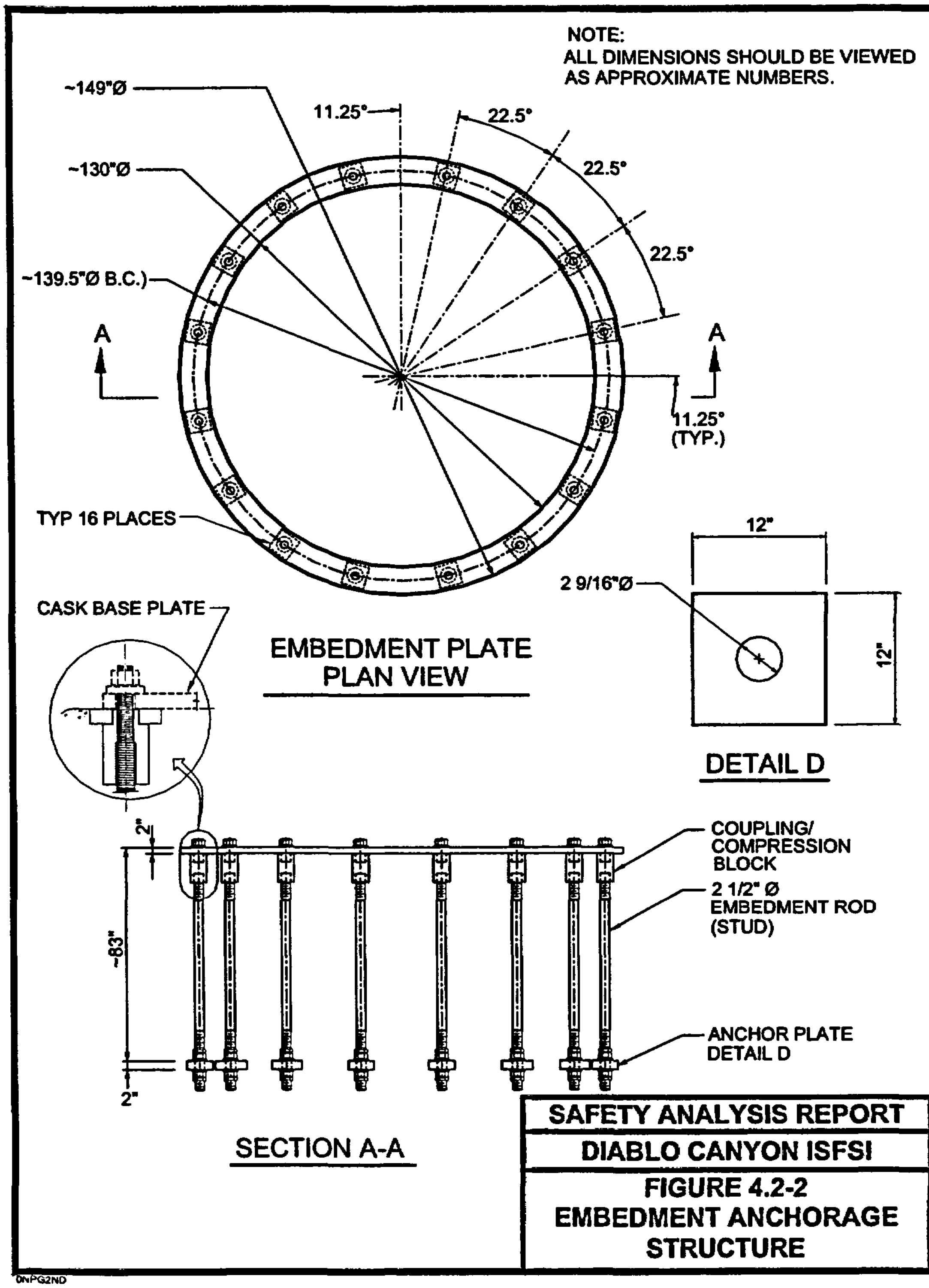

SAFETY ANALYSIS REPORT

DIABLO CANYON ISFSI

FIGURE 4.2-2
EMBEDMENT ANCHORAGE STRUCTURE

DIABLO CANYON ISFSI
SAFETY ANALYSIS REPORT

CHAPTER 5

ISFSI OPERATIONS

CONTENTS

DIABLO CANYON ISFSI
SAFETY ANALYSIS REPORT

CHAPTER 5

ISFSI OPERATIONS

TABLES

CHAPTER 5

ISFSI OPERATIONS

FIGURES

CHAPTER 5

ISFSI OPERATIONS

This chapter describes the operations associated with the Diablo Canyon ISFSI. Fuel handling and cask loading operations in the DCPP fuel handling building/auxiliary building (FHB/AB) will be performed in accordance with the DCPP 10 CFR 50 license. Transfer and storage activities associated with the ISFSI will be performed in accordance with the 10 CFR 72 Diablo Canyon ISFSI license. As indicated in previous chapters, the Diablo Canyon ISFSI, in its final storage configuration, is a totally passive installation. Periodic surveillance is required, by the Diablo Canyon ISFSI Technical Specifications (TS), to ensure the passive air-cooling system is properly operating. Maintenance is limited to minor, touch-up painting of the HI-STORM 100SA overpack and anchorage hardware. The operations described in this chapter relate to the loading and preparation of the multi-purpose canisters (MPCs), transport to the cask transfer facility (CTF) in the HI-TRAC transfer cask, transfer of the MPC from the transfer cask to the overpack at the CTF, and transport of the loaded overpack from the CTF to the ISFSI storage site. Also described is the process for off-normal event recovery, including unloading of fuel from a loaded overpack. An overview of activities occurring in the DCPP FHB/AB is provided. A detailed discussion of these activities is provided in the 10 CFR 50 license amendment request.

5.1 OPERATION DESCRIPTION

The methods and sequences described below provide an overview of the operational controls that the personnel performing spent fuel loading, cask transfer, and storage activities will implement to ensure safe, reliable, long-term spent fuel storage at the ISFSI storage site. Site-specific procedures will be used to implement these activities, including the use of existing procedures, revision of existing procedures, or the creation of new procedures. The specific number, wording, and sequence of site procedural steps may vary from the guidance provided here as long as the steps comply with assumptions and inputs in the governing, design-basis analyses.

Operations to load and place the HI-STORM 100 System at the storage location on the ISFSI pad will be performed both inside and outside the DCPP FHB/AB. MPC fuel loading and handling operations will be performed inside the FHB/AB using existing DCPP systems and equipment for heavy lifts, radiation monitoring, decontamination, and auxiliary support, augmented as necessary by ancillary equipment specifically designed for these functions. The implementing procedures will incorporate applicable 10 CFR 50 license conditions and commitments, such as those governing heavy loads. MPC transfer into the overpack at the CTF and movement of the loaded overpack to the storage location will be performed using procedures developed specifically for these operations.

5.1.1 NARRATIVE DESCRIPTION

The following discussion describes the specifics of the integrated operation, including fuel loading, MPC closure operations, transfer cask handling, overpack handling, and ISFSI pad placement. As described in the HI-STORM 100 System FSAR (Reference 1), as amended by Holtec License Amendment Request (LAR) 1014-1 (Reference 2), the MPC is loaded in a reusable HI-TRAC transfer cask in the spent fuel pool (SFP). The MPC is welded and prepared for storage while in the FHB/AB. The MPC and transfer cask are then transported to the CTF, located adjacent to the ISFSI storage site, where the MPC is transferred into an overpack for storage on the ISFSI pads. Section 5.1.1.1 describes loading operations for damaged fuel and fuel debris. Section 5.1.1.2 describes MPC loading and sealing operations. Section 5.1.1.3 describes the operations for transferring the loaded MPC to the ISFSI storage site and into the overpack for storage. Section 5.1.1.4 describes off-normal event recovery operations.

Specific procedures will identify and control the selection of fuel assemblies, and nonfuel hardware for loading into the HI-STORM 100 System. Candidate fuel assemblies will be selected based on their physical characteristics (for example, dimensions, enrichment, and uranium mass) to ensure they meet the requirements of the Diablo Canyon ISFSI TS and SAR Section 10.2. The selected fuel assemblies then will be classified as intact fuel, damaged fuel, or fuel debris, in accordance with the definitions in SAR Section 10.2. Once an assembly is found to be physically within the limits of the SAR Section 10.2 and correctly classified, the burnup, cooling time, and decay heat of the assemblies will be confirmed to be within SAR Section 10.2 limits using existing records. If any selected assemblies include nonfuel hardware, the particular type of nonfuel hardware also will be confirmed to meet SAR Section 10.2.

Fuel assemblies chosen for loading will be assigned a specific storage location in the MPC in accordance with the Diablo Canyon ISFSI TS and SAR Section 10.2. Criteria such as the classification of the assembly (that is, intact, damaged, or debris), the presence of nonfuel hardware in the assembly, and the use of a uniform or regionalized storage strategy (burnup, cooling time, decay heat) as defined in SAR Section 10.2 are used to determine the acceptable fuel storage locations for each assembly. Records will be kept that track the fuel assembly, and nonfuel hardware and its assigned MPC and specific fuel storage location. Videotape (or other visual record) will be used during fuel loading operations in the SFP to record fuel assembly and associated nonfuel hardware serial numbers and to provide an independent record of the MPC inventory.

Once the fuel inventory for an MPC is identified, the "time-to-boil" for that MPC is calculated based on the total decay heat rate of the fuel and the temperature of the SFP at the time of loading. This calculation establishes the time duration within which MPC sealing operations must reach the point where draining of the water in the MPC is complete and boiling of the water in the MPC is avoided. The commencement for time-to-boil starts when the MPC lid is installed in the SFP, effectively segregating the fuel in the MPC from the cooling provided by the SFP cooling system. The time-to-boil may be determined on an MPC-specific basis or a bounding time may be determined for a group of MPCs to be loaded, using a worst-case fuel decay heat value and initial water temperature. The methodology described in Section 4.5.1.1.5 of the HI-STORM 100 System FSAR shall be used to determine the time-to-boil.

Additional administrative controls will be used, as necessary, to govern the placement and use of impact limiters, special load-handling devices, allowable travel paths, and lift heights, both inside and outside of the FHB/AB, to ensure compliance with the DCPP and Diablo Canyon ISFSI licensing and design bases, as applicable.

The loading, unloading, and handling operations described in this section have been developed based on the Holtec International field experience in loading HI-STAR 100 dry cask storage systems at other ISFSIs. The equipment and operations used at these sites have been evaluated and modified, as necessary, based on this experience to reduce occupational exposures and further minimize the likelihood of human error in performing the activities needed to successfully deploy the HI-STORM 100 System at the Diablo Canyon ISFSI.

5.1.1.1 Damaged Fuel and Fuel Debris Loading

Damaged fuel containers (DFCs) are used to house damaged fuel assemblies and fuel debris in the MPC in accordance with the requirements of the Diablo Canyon ISFSI TS and SAR Section 10.2. Any qualified fuel assembly that is classified as damaged fuel may be loaded into an MPC-24E. Up to a total of four DFCs containing damaged fuel may be stored in an MPC-24E, with the balance being intact fuel assemblies. Fuel classified as fuel debris must be stored in a DFC and must be loaded into an MPC-24EF. The MPC-24EF may also be used to store damaged fuel. Up to a total of four DFCs containing either damaged fuel or fuel debris may be stored in the MPC-24EF, with the balance being intact fuel assemblies. The fuel assembly is placed in the DFC either before or after the DFC is placed into the MPC. Storage of damaged fuel and fuel debris in the HI-STORM 100 System is discussed, and the containers analyzed, in Section 2.1.3 and Appendix 3.AS, respectively, of the HI-STORM 100 System FSAR, as amended by LAR 1014-1. Figure 2.1.2B in the HI-STORM 100 System FSAR, as amended by LAR 1014-1, shows the Holtec pressurized water reactor (PWR) DFC.

5.1.1.2 MPC Loading and Sealing Operations

This section describes the general sequence of operations to load and seal the MPC, including the movement of the transfer cask within the FHB/AB. Site-specific procedures will control the performance of the operations, including inspection and testing. At a minimum, these procedures will control the performance of activities and alert operators to changes in radiological conditions around the cask. As described in this section, several operational sequences have important time limitations including time-to-boil following MPC lid attachment, and evacuation and helium backfill time. These sequences are controlled by Diablo Canyon ISFSI TS and SAR Section 10.2. Several components (that is, impact limiters, crane links, auxiliary lift component, and SFP frame) are used during the cask loading process. A discussion of these items is provided for the sole purpose of describing the loading process. These items, along with their design and use, are controlled under the DCPP Control of Heavy Loads Program.

A removable work platform is positioned in the cask washdown area to assist in transfer cask and MPC preparation and closure operations. The work platform also serves as a transfer cask seismic restraint.

For movements between the SFP and the cask washdown area, a removable impact limiter will be temporarily affixed to the base of the transfer cask. The impact limiter serves to limit loads on the cask system and loads imparted to the FHB/AB in the unlikely event of a vertical cask drop event.

During horizontal cask movements (that is, cask movements between the SFP and over the cask washdown area and movements between the cask washdown area and the cask transport frame), the crane is configured with a set of fixed length redundant load links (tension links). The tension links provide a redundant load path between the lift yoke and the crane eliminating the potential for cask drops as credible events during these cask handling evolutions.

Placement of loaded overpacks at the ISFSI is a cyclical process involving the movement of a loaded overpack to the ISFSI and returning with an empty transfer cask for the next loading process. The operations described herein start at the time the empty MPC is loaded into the transfer cask and is ready for movement into the FHB/AB.

Prior to bringing the transfer cask into the FHB/AB, the transfer cask is visually verified to have the pool lid bolted to the cask, and an empty MPC has been cleaned, inspected, raised, and inserted into the transfer cask. Alignment marks are checked to ensure correct rotational alignment between the MPC and the transfer cask.

The transfer cask containing an empty MPC is brought into the FHB/AB through the roll-up door in the horizontal orientation on a cask transport frame. Affixed to the bottom end of the transfer cask is a temporary shield. The transfer cask bottom shield is used during loaded transport operations to provide supplemental shielding to the operators. During transport of the empty transfer cask back to the FHB/AB, the bottom shield is used only as a spacer to ensure proper fit of the transfer cask in the cask transport frame. The cask transport frame is an L-shaped structure with front and rear saddles to support the transfer cask. The cask transport frame is used for horizontal transport of the transfer cask between the FHB/AB and the CTF and for cask upending and downending operations. (Upending is the process of rotating the cask from the horizontal to the vertical orientation. Downending is the process of rotating the transfer cask from the vertical to the horizontal orientation.) The cask transport frame is equipped with heavy-duty rollers that engage with a temporary track that runs from inside the FHB/AB to the access road located outside the FHB/AB roll-up door. The track and rollers are used because dimensional limitations of the FHB/AB roll-up door prevent access of the cask transporter inside the FHB/AB. The short side of the cask transport frame is designed to ensure that the transfer cask and cask transport frame rotate smoothly to the vertical orientation (without sudden load shifts normally experienced when a load's center of gravity traverses its corner). Heavy-duty rollers are affixed to the cask transport frame so the load will automatically position itself as it is lifted. The rollers also serve to strategically control the impact location should a hypothetical crane failure occur during cask upending or downending. An impact limiter is placed over the identified impact location (selected to be over a load-bearing wall). In the event of a crane failure, the transfer cask weight is directed through the upper saddle into the impact limiter and, in turn, into the strategic location on the floor.

After bringing the transfer cask into the FHB/AB, the transfer cask is positioned under the overhead crane, that is configured with the lift yoke. The lift yoke engages the transfer cask lifting trunnions, and the transfer cask and cask transport frame are tilted up slightly. A cask transport frame impact limiter is placed on the floor below the upper saddle portion of the cask transport frame. The transfer cask and cask transport frame are rotated integrally to the vertical position. The cask transport frame stabilizer is attached to secure the cask transport frame in the vertical orientation. Tension links are attached between the lift yoke and the auxiliary lift component to prevent a load drop during transfer cask horizontal movement. Bolts securing the transfer cask bottom shield to the transfer cask are removed and the straps securing the transfer cask to the cask transport frame are released. The transfer cask is moved horizontally from the frame. Specially designed bumpers are attached to the transfer cask prior to moving the transfer cask to the SFP. These bumpers are attached in eight locations (four at the top and four at the bottom) on the transfer cask using attachment holes fabricated on the transfer cask at 90-degree intervals around the cask body. Figures 4.2-9 and 4.2-10 show the bumper attachment configuration. The bumpers are employed to minimize swing-induced impacts of the transfer cask with the SFP seismic restraint structure.

The cask work platform main gate is opened to receive the transfer cask. A transfer cask impact limiter is positioned on the floor in the cask washdown area. The transfer cask then is positioned over the impact limiter. The main gate is closed and the cask work platform seismic restraints are closed. The tension links are disconnected and the transfer cask is lowered onto the transfer cask impact limiter (see Figure 4.4-1). Attachment bolts connect the transfer cask to the transfer cask impact limiter.

The annulus between the transfer cask and the MPC is filled with borated water, in accordance with the Diablo Canyon ISFSI TS and SAR Section 10.2, and a seal is installed in the top part of the annulus to minimize the risk of contaminating the external shell of the MPC. The MPC cavity is filled with water and borated in accordance with the Diablo Canyon ISFSI TS. MPC and annulus filling may occur in the cask washdown area, over the SFP, or any other intermediate location.

The seismic restraints are opened and the transfer cask, along with its attached impact limiter and empty MPC, are raised approximately 12 inches above the floor of the FHB/AB (140 ft elevation). A second set of crane tension links are attached to provide the redundant load drop protection during horizontal movement over the SFP wall. The transfer cask is positioned adjacent to the SFP.

An annulus purge line is connected to the annulus drain port. The transfer cask is positioned over the cask recess area of the SFP and lowered using the FHB/AB crane auxiliary lift until the lower set of guides on the cask are engaged in corresponding guide channels of the SFP frame structure. The SFP frame provides lateral support of the cask during its vertical load movement in the cask recess area of the spent fuel pool frame structure. The transfer cask is lowered into the SFP, and an annulus purge of water is performed on the annulus through the annulus purge line. The annulus purge applies a slight overpressure to the annulus to protect the MPC external shell from contamination from the SFP water in the event there is a leak in the annulus seal. When the cask is fully lowered to the bottom of the cask recess area in the SFP, the lift yoke is remotely disconnected and removed from the SFP.

Fuel-loading and post-loading verification of fuel assembly identification is conducted in accordance with approved fuel-handling procedures. For damaged fuel assemblies and fuel debris, the assembly is loaded into the DFC, and the DFC is loaded into the MPC. Optionally, an empty DFC may be first loaded into the appropriate fuel storage location in the MPC and then the damaged fuel assembly or fuel debris loaded into the DFC.

The MPC lid, with the drain line and the lid restraint attached, are placed in position in the MPC after the completion of fuel loading, while the transfer cask is in the SFP. The MPC lid restraint is bolted on while the MPC is in the pool. The transfer cask and lift yoke are raised until the top of the MPC breaks the water surface. Rinsing of exterior surfaces is performed as the transfer cask emerges from the SFP. The transfer cask is raised completely out of the SFP to clear the SFP wall and the redundant crane tension links are attached. The annulus purge line is disconnected, the bumpers are removed, and the transfer cask is moved laterally (the crane tension links prohibit vertical movement and provide the necessary redundancy to make a drop event noncredible when installed) and positioned over the cask washdown area. The cask seismic restraints in the cask washdown area are positioned to prevent tipover if the cask should be dropped. The crane tension links are disconnected and the transfer cask is lowered into the cask washdown area. The eight guides are removed from the upper and lower gussets of the transfer cask. The cask seismic restraints are positioned for cask stability during a seismic event, the MPC lid retention device is removed, and the lift yoke is disconnected and removed from the area. Activities involving decontamination, water jacket filling, disconnection of cask rigging, and placement of auxiliary equipment may occur in parallel or in a different sequence based on cask-loading experience at DCPP.

The transfer cask water jacket is filled with water. A temporary shield ring may be installed in the area of the lifting trunnions to provide supplemental personnel shielding. Preparation for MPC sealing operations may now proceed. This may include the erection of scaffolding, staging of auxiliary equipment, additional cask decontamination, dose-rate surveys, and installation of temporary shielding.

As described above, fuel-assembly decay heat could eventually cause boiling of the water in the MPC after it is removed from the SFP. Therefore, MPC draining must be completed within the time-to-boil limit previously determined, which is measured beginning at the time the MPC lid is installed in the SFP and terminating at the completion of MPC draining. Should it become evident that the time-to-boil limit may be exceeded, a recirculation of the MPC water (borated as necessary in accordance with the Diablo Canyon ISFSI TS) will be performed to reduce the temperature of the water and allow a new time-to-boil value to be determined, if necessary. When the MPC water recirculation is complete, the time-to-boil clock is reset. This process may be repeated as necessary.

During welding operations, the MPC water volume is reduced to provide enough space between the water surface and the lid to avoid a water-weld interaction. Oxidation of Boral panels and aluminum components contained in the MPC may create hydrogen gas while the MPC is filled with water. Appropriate monitoring for combustible gas concentrations shall be performed prior to, and during, MPC lid welding operations. In addition, the space below the MPC lid shall be exhausted or purged with inert gas prior to, and during, MPC lid welding operations to provide additional assurance that explosive gas mixtures will not develop in this space. The automated welding system is installed. The MPC-lid welding, including nondestructive examinations, is completed.

Once the MPC-lid welding is complete, the MPC is filled with borated water, vented, and hydrostatically tested. After an acceptable hydrostatic test has been completed, a small amount of water is displaced with helium gas for leakage testing of the MPC lid-to-shell weld. MPC leakage testing is performed in accordance with ANSI N14.5 (Reference 4).

Following successful completion of the leakage testing, the remaining MPC water is displaced from the MPC by blowing pressurized helium gas into the vent port of the MPC, thus displacing the water through the drain line. The moisture removal system is connected to the MPC and is used to remove the remaining liquid water from the MPC and to reduce the moisture content of the MPC cavity to an acceptable level. This can be accomplished using a vacuum drying process (moderate burnup [that is, < 45,000 MWD/MTU] fuel only) or the forced helium dehydration (FHD) system (moderate or high burnup fuel). During the drying process, the annular gap between the MPC and the HI-TRAC will be continuously flushed with water.

Following the successful completion of moisture removal from the MPC, the MPC is backfilled with helium. If the vacuum drying process was used for moisture removal, no additional preparation of the MPC cavity is necessary prior to helium backfill operations. If the FHD system was used, the bulk residual gas must be evacuated from the MPC cavity to ensure the amount of helium being introduced into the MPC can be correctly determined. This evacuation (to 10 torr or less, where 760 torr equal 1 atmosphere) should be completed expeditiously to minimize fuel heatup, once completed, backfilling with helium must be initiated within 2 hours. If the 2-hour guideline is exceeded, the MPC should be refilled with helium and the pressure reduction process started again. Then, the helium backfill system (HBS) is attached, and the MPC is backfilled with helium to within the required pressure range in accordance with the Diablo Canyon ISFSI TS. Helium backfill to the required pressure and purity level ensures that the conditions for heat transfer inside the MPC are consistent with the thermal analyses and provides an inert atmosphere to ensure long-term fuel integrity.

After successful helium backfill operations, the MPC vent and drain port cover plates are installed, welded, inspected, examined, and leak tested. The MPC closure ring is then installed, welded, and examined. The MPC closure ring provides a second welded boundary, in addition to the confinement boundary, and is described further in Section 3.3.1.1.1 with references to the design drawings in the HI-STORM 100 System FSAR for additional details.

The transfer cask water recirculation equipment is detached and remaining water in the transfer cask annulus is drained. The temporary shield ring is removed. The transfer cask and accessible portions of the MPC are checked to ensure any removable contamination is within applicable limits. Additional decontamination and surveys may be performed throughout the loading process. The MPC lift cleats are installed. The transfer cask top lid is installed and the fasteners are torqued.

The lift yoke is re-attached to the transfer cask, and the fasteners securing the impact limiter to the transfer cask bottom are disconnected. The transfer cask is raised and, while the transfer cask is maintained directly above the detached impact limiter, the crane tension links are attached. With the crane tension links attached and the cask suspended from the lift yoke, the bottom surface of the transfer cask is decontaminated using long-handled tools or other remotely-operated devices which do not require personnel to directly access the bottom of the transfer cask.

The seismic restraint is opened and the transfer cask is moved laterally away from the cask washdown area. The transfer cask is positioned in the bottom shield located in the transport frame (Figure 4.2-12). The transfer cask is fastened to the bottom shield and secured to the cask transport frame with straps. The cask transport frame impact limiter (Figure 4.4-2) is positioned on the floor in the same manner as described earlier to mitigate the effects on the transfer cask and building structure of an unrestrained tipover of the cask transport frame and cask. The cask and cask transport frame are supported by the crane, cask transport frame stabilizers, and the tension links. The tension links are disconnected and the cask transport frame stabilizers are removed. The crane hook is slowly lowered, causing the transfer cask and cask transport frame to gently roll, in its tracks, to the horizontal orientation. When the cask is about to contact the cask transport frame impact limiter, the impact limiter is removed and the cask transport frame is lowered to the full horizontal position. The loaded transfer cask is now positioned horizontally in the cask transport frame on the roller tracks.

If not performed earlier, the transfer cask and cask transport frame are surveyed to ensure that any fixed contamination is within acceptable limits. The loaded transfer cask and cask transport frame are then rolled out of the FHB/AB to the cask transporter.

5.1.1.3 Transfer to the ISFSI Storage Site

The cask transporter and associated ancillaries, described in Section 4.3, are positioned outside the FHB/AB doors to receive the horizontal transfer cask and cask transport frame. The transporter will undergo preoperational testing and maintenance and will be operated in accordance with the Cask Transportation Evaluation Program in the Diablo Canyon ISFSI TS, which evaluates and controls the transportation of loaded MPCs between the DCPP FHB/AB to the CTF and ISFSI. The transfer cask is positioned under the lift beam of the cask transporter and the transfer cask lift slings are rigged around the cask. The horizontal lift rig is attached to the slings and the transporter lift beam as described in Section 4.3. The horizontal lift rig supports the transfer cask directly and does not rely on the cask transport frame to support the cask. The transfer cask and cask transport frame are raised and secured within the transporter for the trip to the CTF. The transfer cask is transported to the CTF along the approved transportation route as described in Section 4.3.3 and shown in Figure 2.1-2.

In preparation for receiving the MPC, the overpack is positioned in the CTF and lowered to the full down position. The overpack lid is removed (if previously installed). The mating device (Figure 4.2-11) is secured to the overpack.

To restrain the cask against seismically-induced impact loads on the main shell of the CTF, shimmed seismic restraints will be installed to transmit the load from the overpack to the CTF shell (SAR Section 3.3.4.2.6). The cask transporter tie downs are described in SAR Section 4.2.1.2 and depicted in plan view in Figure 4.2-4. The tie downs function to prevent the transporter from seismically interacting with the storage cask while in the CTF during MPC transfer operations. During the transporter lifting of the HI-STORM, the probability of an earthquake occurring is so small as to make this event non-credible.

The cask transport frame is set down in the upending area near the CTF. The horizontal lift rig is disconnected, and the HI-TRAC lift links are attached. The HI-TRAC lift links are attached to the transfer cask lifting trunnions and the transfer cask is upended to the vertical orientation. Once vertical, the base of the cask transport frame is supported for stability. The cask transport frame straps are disconnected. A mobile crane attaches to the long leg of the cask transport frame. Fasteners connecting the long leg of the cask transport frame to its base are removed and the mobile crane removes the long leg of the frame. This step is performed to enable the transfer cask to be removed from the cask transport frame. The transfer cask bolts securing the transfer cask to the bottom shield are removed. The transfer cask is removed from the cask transport frame, and the transfer cask is aligned over the mating device and secured. Restraints connect the cask transporter to the CTF pad. The transfer cask lift links are then disconnected. The MPC downloader slings are attached between the cask transporter towers and the MPC lift cleats, and the MPC is raised slightly to remove the weight of the MPC from the pool lid. The pool lid is supported by the mating device while the pool lid bolts are removed. The pool lid is removed from under the transfer cask.

The cask transporter towers are used to lower the MPC into the overpack. The MPC downloader slings are disconnected from the cask transporter and lowered onto the MPC lid. The pool lid is reinstalled. The HI-TRAC lift links are reconnected to the cask transporter and the cask transporter restraints are disconnected.

The transfer cask is unfastened and lifted from the mating device and raised from the top of the overpack and placed back on the cask transport frame base and bolted to the bottom shield. The long leg of the frame is reattached. The cask transport frame straps are reinstalled. The cask and frame are lifted and the parabolic shapes are reinstalled. The cask is downended and placed beside the CTF. The lift cleats and MPC downloader slings are removed, and threaded inserts are installed in the MPC lid lift holes where the lift cleats were attached. The mating device containing the transfer cask pool lid is removed from the overpack and placed in a nearby location.

The overpack lid is installed. The overpack lifting brackets are attached. The cask transporter is positioned with its lift beam above the overpack. The overpack is raised to the up position in the CTF and the overpack lifting brackets are attached to the overpack. The top shell seismic restraints are removed. The overpack is lifted out of the CTF and moved to the ISFSI pad, where it is placed in its designated storage location.

Prior to the loaded overpack arriving at the ISFSI pad, the designated storage location will have been prepared for the cask to be placed on the pad. Specifically, a small number of alignment pins will have been installed in the anchor stud locations. These alignment pins ensure that the cask is properly located and the holes in the cask bottom flange match with the holes in the ISFSI pad embedment plate. When the cask is properly located and seated, the alignment pins are removed and the 16 anchor studs are threaded into the top of the embedded coupling (see SAR Figure 4.2-2). The studs will be pre-tensioned using a stud tensioner and the nuts tightened in a cross-pattern, roughly 180 degrees apart, to avoid uneven loads on the baseplate.

The preload on the cask anchor studs is applied without employing a torque wrench. Therefore, no torque is induced on the embedded anchor rods or compression couplings during the preload operation. A stud tensioner is used to apply preload on the anchor studs using hydraulic pressure to elastically "stretch" the bolt. The nuts are then tightened on the "stretched" stud to maintain the pre-load. This tension is transferred to the cask base/embedment plate interface as a compressive force via the stud nut and compression coupling. There is no significant torque applied on the nuts during tightening (i.e., hand-tightening is adequate).

Once the overpack is in position, the remaining overpack lid studs and nuts are installed. The cask transporter is disconnected from the overpack and driven away from the ISFSI pad. The grounding cables are attached to the overpack. The overpack duct photon attenuators (also known as gamma shield cross plates) are installed in the upper and lower air ducts and screens are secured.

5.1.1.4 Off-Normal Event Recovery Operations

The analysis of off-normal and accident events, as defined in ANSI/ANS-57.9 (Reference 5) and as applicable to the Diablo Canyon ISFSI, is presented in Chapter 8. Each postulated off-normal and accident event analyzed and discussed in Chapter 8 addresses the event cause, analysis, and consequences. Suggested corrective actions are also provided for off-normal events. The actual cause, consequences, corrective actions, and actions to prevent recurrence (if required) will be determined through the DCPP corrective action program on a case-specific basis. All corrective actions will be taken in a timely manner, commensurate with the safety significance of the event. Of primary importance in the early response to any event will be the verification of continued criticality prevention, the protection of fuel cladding integrity (that is, heat removal), and the adequacy of radiation shielding while longer-term corrective actions are developed. This may also involve the need for temporary shielding or cask cooling in accordance with the recommendations of PG&E technical staff personnel, based on the event conditions.

Should the need arise, the MPC can be returned to the SFP for unloading. To unload an overpack or transfer cask, the operations described above are effectively executed in reverse order from the point in the operation at which the event occurred. Once the transfer cask is back in the FHB/AB, the transfer cask top lid is removed, and preparations are made to reopen the MPC in the SFP. This involves first grinding out the welds and removing the MPC closure ring and vent and drain port cover plates. A sample of the gas inside the MPC may be drawn to determine the extent of fuel cladding failure, if any. Then, the helium cooldown system is connected and used to recirculate the helium in the MPC to cool it to a temperature at or below the maximum-allowed temperature for reflooding in accordance with the Diablo Canyon ISFSI TS and SAR Section 10.2. Cooling the helium allows the MPC to be reflooded with water (borated as necessary) with a minimal amount of flashing and the associated undesirable pressure spikes in the MPC cavity. Based on the time the cask has been in storage, a new time-to-boil may be determined using a lower decay heat value than was used when the cask was loaded. When the MPC has been reflooded, the time-to-boil clock is started. The weld removal system is used to cut the MPC lid weld, freeing the lid for subsequent removal.

Oxidation of Boral panels and aluminum components contained in the MPC may create hydrogen gas while the MPC is filled with water. Appropriate monitoring for combustible gas concentrations shall be performed prior to, and during, MPC lid cutting operations. In addition, the space below the MPC lid shall be exhausted prior to, and during, MPC lid welding operations to provide additional assurance that explosive gas mixtures will not develop in this space. When the lid weld has been successfully cut, the lid retention device and lift yoke are installed, and the transfer cask is returned to the SFP using the same procedures and equipment as used to remove the transfer cask from the SFP after fuel loading.

Once in the SFP, the MPC lid is removed, and the spent fuel assemblies are removed from the MPC and placed back into the wet storage racks. The time-to-boil consideration is stopped once the MPC lid is removed.

5.1.2 FLOWSHEETS

Figure 5.1-1 shows the operation sequence flowchart for cask system loading, sealing, testing, onsite transport, MPC transfer, and storage operations.

Figure 5.1-2 shows the operation sequence flowchart for overpack off-normal event recovery operations.

A detailed description of the operations is provided in Section 5.1.1. Radiation source terms are discussed in Chapter 5 of the HI-STORM 100 System FSAR for the generic cask analyses and in Section 7.2 of this SAR for site-specific dose analyses. Equipment descriptions, with dimensions, design and operating characteristics, materials of construction, special design features, and operating characteristics are provided in Sections 3.3, 4.2, 4.3, and 4.4. Generic cask component design drawings are found in Section 1.5 of the HI-STORM 100 System FSAR.

5.1.3 IDENTIFICATION OF SUBJECTS FOR SAFETY AND RELIABILITY ANALYSIS

5.1.3.1 Criticality Prevention

A summary description of the principal design features, procedures, and special techniques used to preclude criticality in the design and operation of the HI-STORM 100 System is provided in Section 3.3.1.4. Additional detail on the criticality design of the storage cask is provided in Section 4.2.3.3.5.

5.1.3.2 Instrumentation

No instrumentation is required to detect off-normal operations of the HI-STORM 100 System while in its final storage configuration at the ISFSI storage site. The cask system is designed to maintain confinement integrity under all design-basis normal, off-normal, and accident conditions. Detection of degradation in the HI-STORM 100 heat removal system is accomplished by a Diablo Canyon ISFSI TS that requires periodic visual surveillance of the overpack inlet and outlet air ducts to ensure they remain free of blockage. If blockage is detected, action can be taken to remove the source of the blockage in a short time period, typically within one operating shift.

Examples of measuring and test equipment (M&TE) used during the preparation of the cask for storage operations are listed in Table 5.1-1. Additional, or different M&TE, may be used as determined through the development of site-specific operating procedures, including the revision of those procedures as experience in cask loading operations is gained and the state of the art evolves.

5.1.3.3 Maintenance Techniques

The HI-STORM 100 System is designed to safely store spent nuclear fuel with no regularly required maintenance. The only expected maintenance is to apply touch-up repair coatings to the overpack and/or the anchorage hardware due to exposure to the elements and normal wear and tear.

5.1.4 REFERENCES

1. Final Safety Analysis Report for the HI-STORM 100 System, Holtec International Report No. HI-2002444, Revision 0, July 2000.

2. License Amendment Request 1014-1, Holtec International, Revision 2, July 2001, including Supplements 1 through 4 dated August 17, 2001; October 5, 2001; October 12, 2001; and October 19, 2001; respectively.

3. 10 CFR 72 Certificate of Compliance No. 1014 for the HI-STORM 100 Dry Cask Storage System, Holtec International, Revision 0, May 2000.

4. ANSI N14.5-1997, Leakage Tests on Packages for Shipment, American National Standards Institute.

5. ANSI/ANS-57.9-1992, Design Criteria for an Independent Spent Fuel Storage Installation (dry type), American National Standards Institute.

6. PG&E Calculation M-1058, "Cask Transfer Facility Seismic Restraint Configuration."

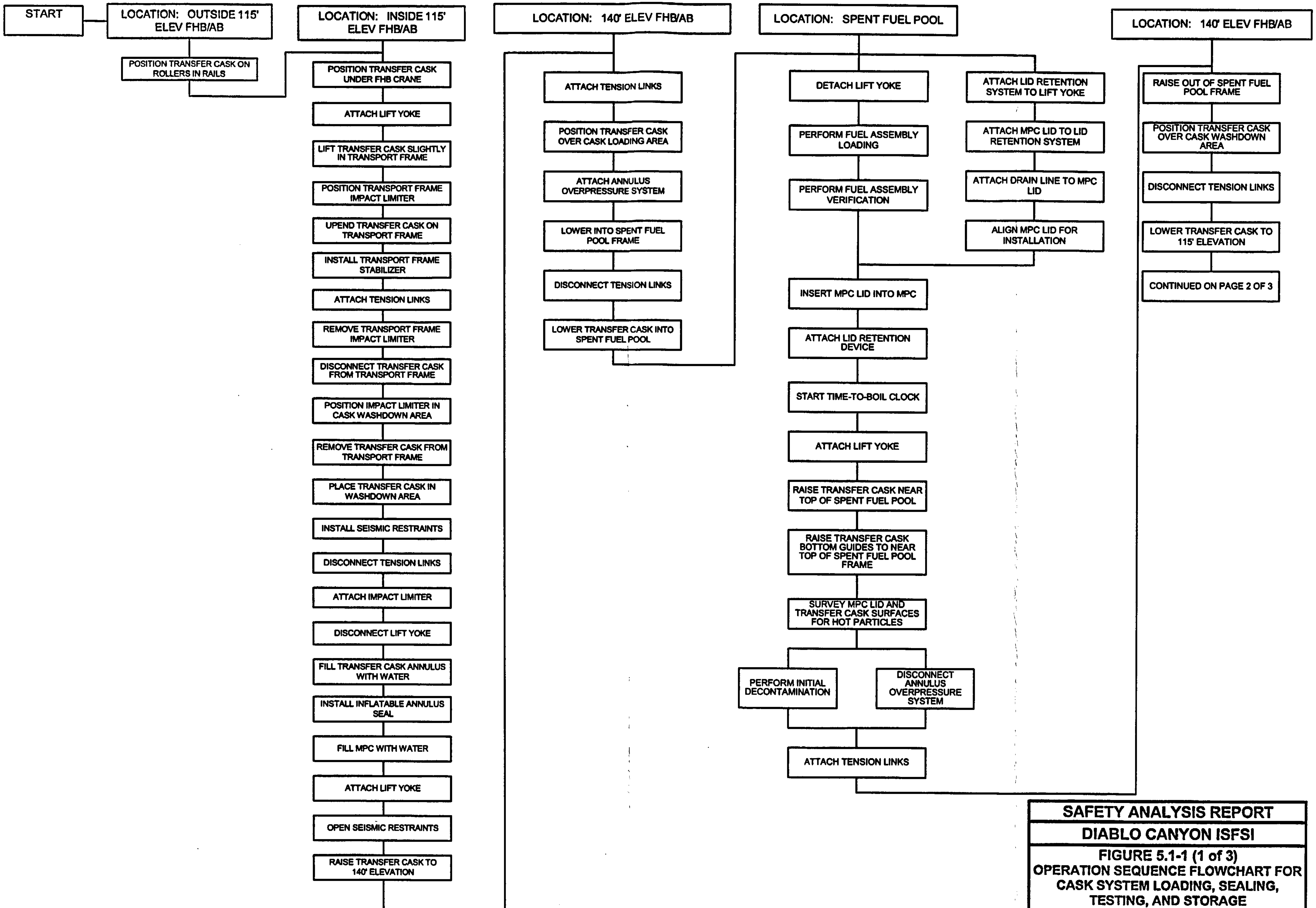

SAFETY ANALYSIS REPORT

DIABLO CANYON ISFSI

FIGURE 5.1-1 (1 of 3)
OPERATION SEQUENCE FLOWCHART FOR CASK SYSTEM LOADING, SEALING, TESTING, AND STORAGE

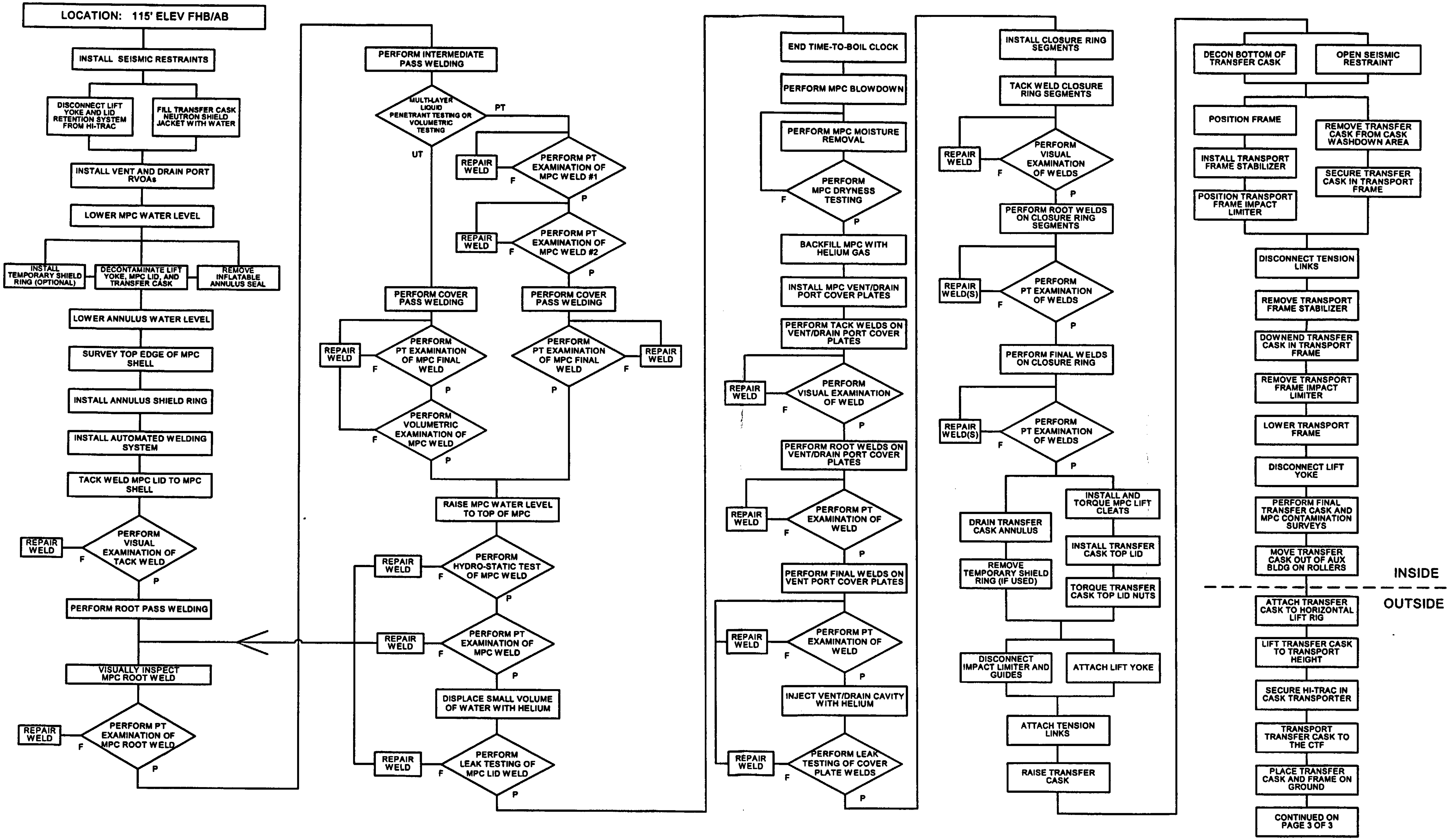

Note: F = Fail
P = Pass

SAFETY ANALYSIS REPORT

DIABLO CANYON ISFSI

FIGURE 5.1-1 (2 of 3)
OPERATION SEQUENCE FLOWCHART FOR CASK SYSTEM LOADING, SEALING, TESTING, AND STORAGE

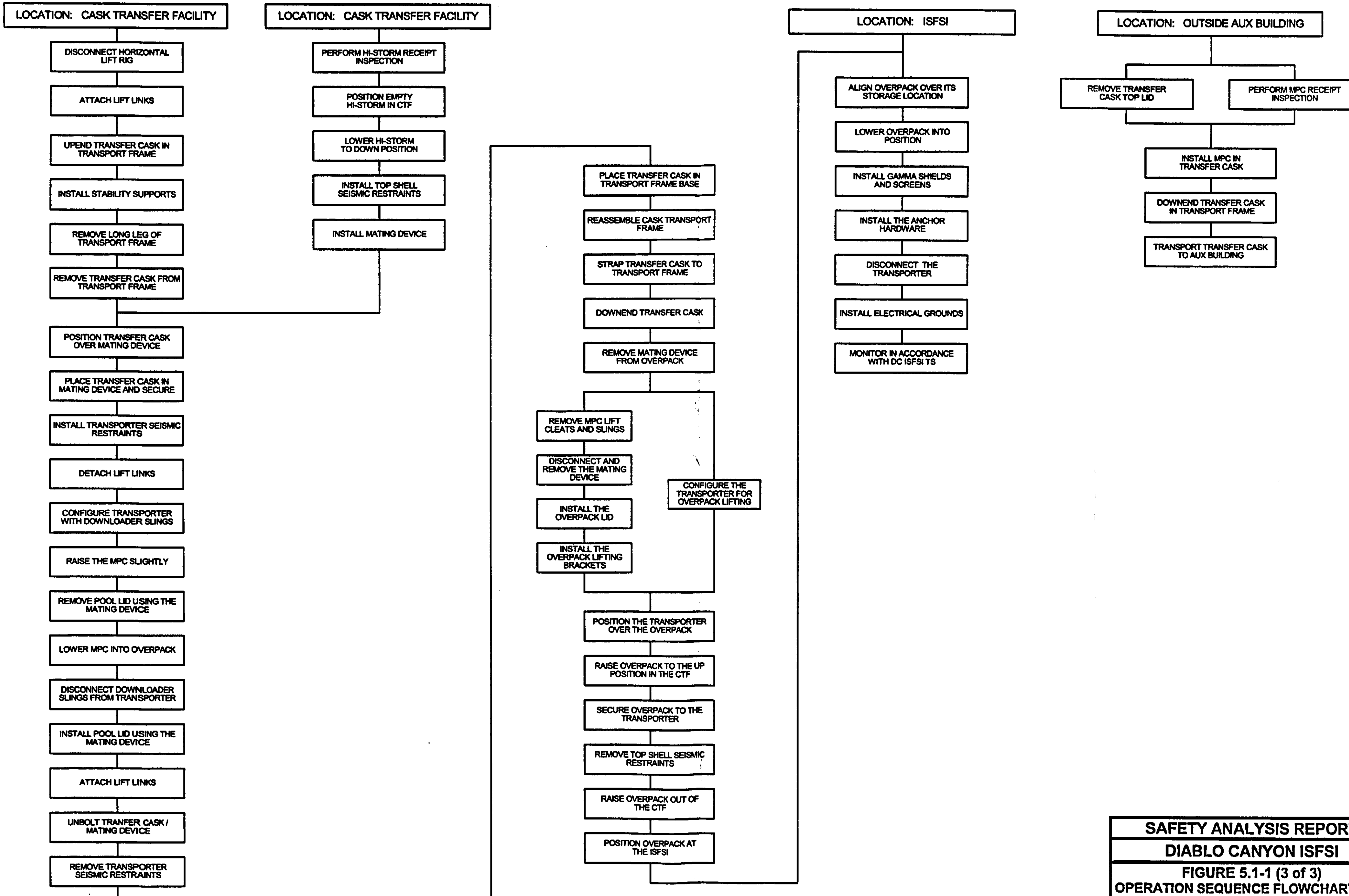

SAFETY ANALYSIS REPORT

DIABLO CANYON ISFSI

FIGURE 5.1-1 (3 of 3)
OPERATION SEQUENCE FLOWCHART FOR CASK SYSTEM LOADING, SEALING, TESTING, AND STORAGE

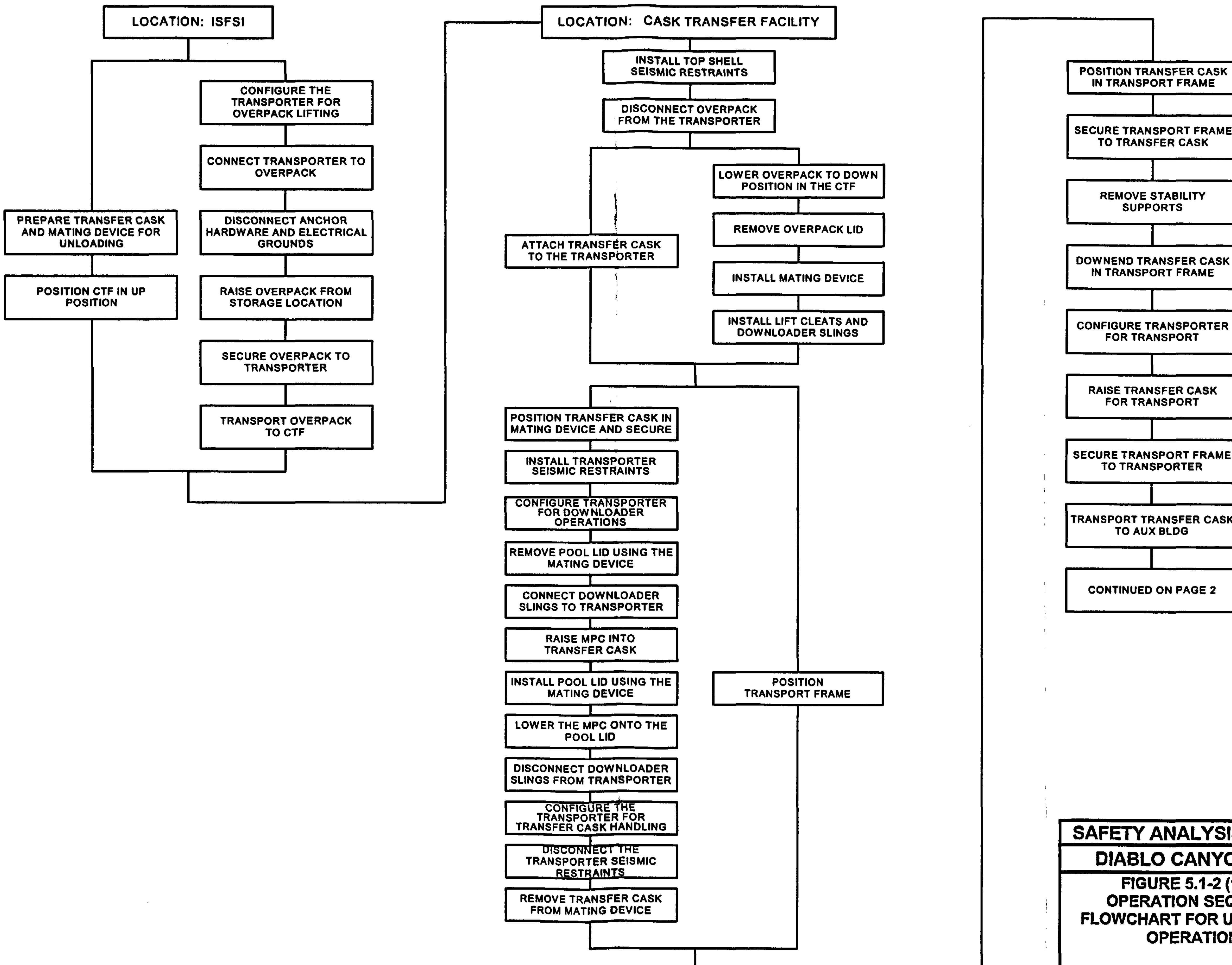

SAFETY ANALYSIS REPORT

DIABLO CANYON ISFSI

**FIGURE 5.1-2 (1 of 2)
OPERATION SEQUENCE FLOWCHART FOR UNLOADING OPERATIONS**

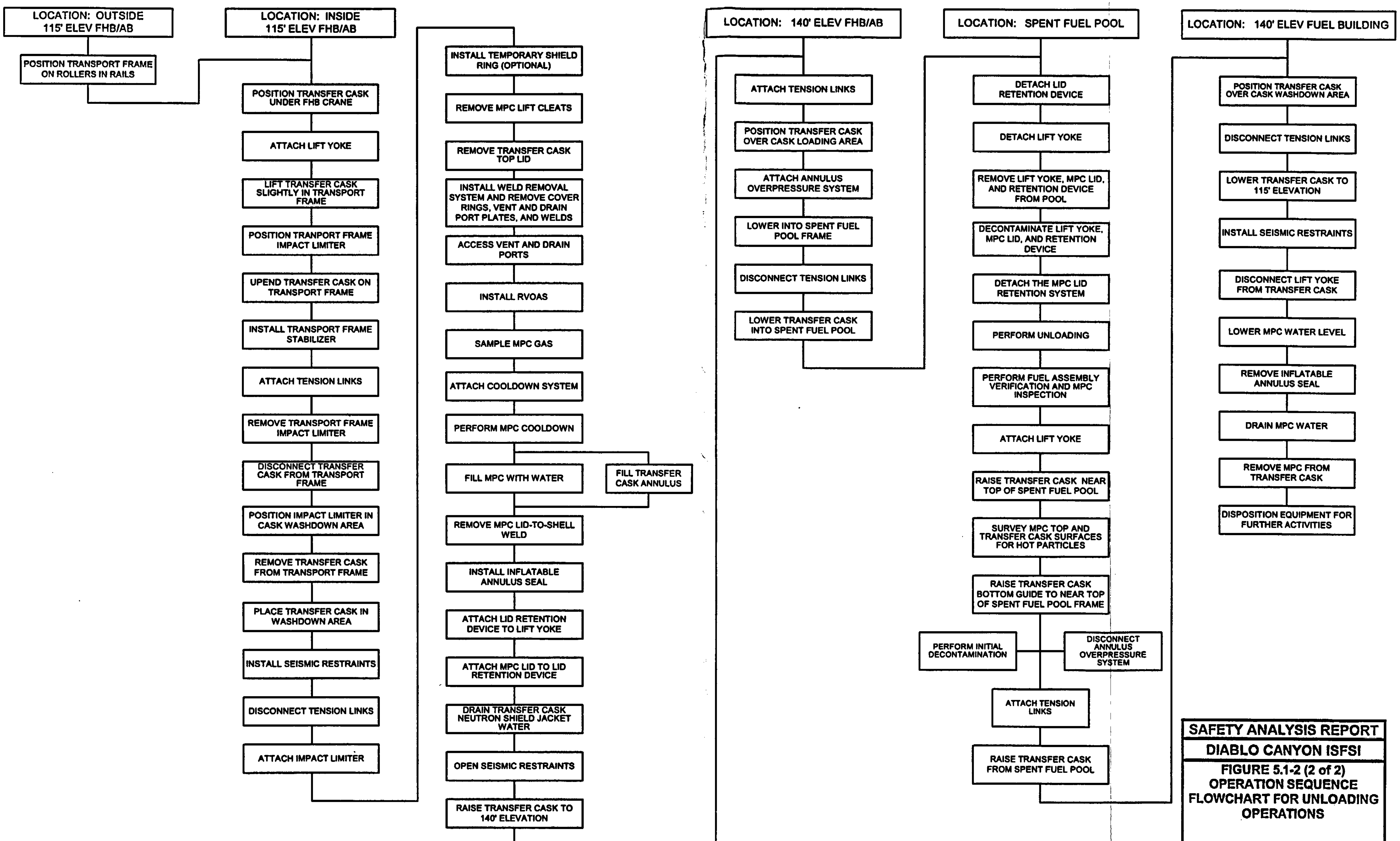

SAFETY ANALYSIS REPORT

DIABLO CANYON ISFSI

FIGURE 5.1-2 (2 of 2)
OPERATION SEQUENCE FLOWCHART FOR UNLOADING OPERATIONS

DIABLO CANYON ISFSI
SAFETY ANALYSIS REPORT

CHAPTER 7

RADIATION PROTECTION

CONTENTS

DIABLO CANYON ISFSI
SAFETY ANALYSIS REPORT

CHAPTER 7

RADIATION PROTECTION

CONTENTS (Continued)

DIABLO CANYON ISFSI
SAFETY ANALYSIS REPORT

CHAPTER 7

RADIATION PROTECTION

TABLES

CHAPTER 7

RADIATION PROTECTION

TABLES (Continued)

CHAPTER 7

RADIATION PROTECTION

FIGURES

7.4 ESTIMATED ONSITE COLLECTIVE DOSE ASSESSMENTS

The results presented in this section are based on the analysis of the overpack and the transfer cask using design basis fuel, including BPRAs (bounding nonfuel hardware). The discussion in Section 7.2 states that the transfer cask was analyzed with the MPC-24 and the overpack was analyzed with the MPC-32 because these were the bounding MPCs for those overpacks. Consistent with that approach, the analysis presented in this section assumed the transfer cask was loaded with an MPC-24 with a design basis burnup and cooling time of 55,000 MWD/MTU and 12 years, respectively. This analysis also conservatively assumed that the overpack was loaded with an MPC-32 with a design basis burnup and cooling time of 32,500 MWD/MTU and 5 years, respectively (Reference 1).

Table 7.4-1 provides the estimated occupational exposures to DCPP personnel during the following phases of ISFSI operation:

(1) Loading of fuel into the MPC in the transfer cask.

(2) Decontamination of the transfer cask and MPC preparation for storage.

(3) Transport of the transfer cask from the FHB/AB to the CTF adjacent to the ISFSI storage area.

(4) Transfer of the MPC from the transfer cask to the overpack at the CTF.

(5) Closing of the overpack and emplacement on the ISFSI pad.

Table 7.4-2 provides the estimated occupational exposures during the unloading of an overpack (the reversal of the steps listed above). In Tables 7.4-1 and 7.4-2, the total duration of the operation is shown, as well as the time the personnel will be located in the higher dose rate areas. Therefore, total dose for each operation is a product of the number of personnel, dose at location, and time in dose field.

The list of operation steps is provided in Tables 7.4-1 and 7.4-2. Numerous operations have been lumped together for ease of presentation. The duration of the operation and the time the personnel will be located in the higher dose rate areas are based on industry experience with the Holtec HI-STAR and HI-STORM casks and casks from other vendors. The dose rates used for this analysis are conservatively estimated using design-basis fuel. Diablo Canyon radiation protection personnel will assure that the appropriate radiation monitoring is performed and that all operations are performed in a manner consistent with ALARA.

The results presented in Tables 7.4-1 and 7.4-2 are conservatively estimated. By the time the Diablo Canyon ISFSI begins operation, other utilities will have loaded numerous overpacks using the transfer cask and a CTF. Based on the experience to be gained and the lessons to be learned, it is expected that the dose rates from loading an overpack will be somewhat less than those listed here (that is, fewer activities and shorter durations).

Table 7.4-3 provides the estimated annual occupational exposure as a result of daily ISFSI walkdowns, occasional maintenance repairs, and construction of additional ISFSI pads. The dose associated with the clearing of debris from a blocked ventilation duct is presented in Sections 8.1.4 and 8.2.15.

The daily walkdown of the ISFSI requires a person to walk the full length of the ISFSI outside each pad of casks and between each row of casks. This walkdown is to look for obstructions that may be blocking the air vents of the overpack. It was assumed, based on a walking speed of 2 miles/hour, that it would take a person 20 minutes to perform the walk-down at the completion of the ISFSI when all pads are filled with overpacks. This results in a total occupancy time of 122 hours per year. The dose rates shown in Table 7.4-3 for the walk-downs are conservatively based on the 1-meter dose rates, times 4 casks.

The doses for the repair operations assume 1 repair operation per month of 1-hour duration with 2 people performing the operation. The dose rates were conservatively calculated inside an infinite array of casks.

The dose during construction of additional storage pads was calculated for the construction of Pad 7. It was assumed that the previous six pads were completely filled. Doses estimated for the construction of Pad 7 bound the construction of any other pad. The dose rate was conservatively estimated at the center of Pad 7 with no credit for temporary shielding. It was assumed that construction would take 3 months at 40 hours per week in the dose field. The number of personnel was assumed to be 15.

Table 7.4-4 presents the dose rate at the assumed location for the restricted area fence, the makeup water facility (the nearest normally occupied location), and the power plant. The occupancy time was assumed to be 2,080 hours, which is the equivalent of a 40-hour workweek for 52 weeks per year. Also, the dose rates at these locations were conservatively calculated perpendicular to the long side of the storage array. This table demonstrates that the dose rate at the restricted area fence for the assumed location will be below 2 mrem/hr. This table also demonstrates that the dose rates in the normally-occupied locations, due to the ISFSI, are well below the 10 CFR 20 limits for monitored radiation workers. Table 7.4-4 indicates that workers at the makeup water facility may have to become monitored workers as the storage pad approaches the full capacity. Compliance with 10 CFR 20 for these and other workers will be assured via personnel dose monitoring in accordance with the DCPP Radiation Protection Program.

The dose rates presented in Tables 7.4-3 and 7.4-4 demonstrate that the estimated occupational exposures from the Diablo Canyon ISFSI meet the regulatory requirements of 10 CFR 20. The actual doses from the ISFSI are expected to be considerably less than the conservatively estimated values in Tables 7.4-3 and 7.4-4.

7.4.1 REFERENCES

1. Holtec Report No. HI-2002563, "Dose Evaluation for the ISFSI at Diablo Canyon Power Plant."

7.5 OFFSITE COLLECTIVE DOSE

The annual offsite dose is calculated for both direct radiation (neutrons and gammas) and from radionuclide releases from the MPC (Reference 8). Since the MPC is welded and designed to maintain confinement integrity under all normal, off-normal, and accident conditions of storage, there will not be any release of radionuclides during normal operation. Nonetheless, an analysis of the offsite dose consequences from a nonmechanistic confinement boundary leak from the ISFSI was calculated for normal, off-normal, and accident conditions. This section addresses doses for normal conditions. Off-normal and accident analyses are provided in Sections 8.1.3 and 8.2.7, respectively. The direct radiation dose from the ISFSI is the same for normal and off-normal conditions.

Since the loading of the MPC into the overpack occurs outside the FHB/AB at the CTF, the offsite dose due to loading operations was also calculated and included in the total annual dose estimate.

The controlled area boundary is located 1,400 ft (427 m) from the ISFSI. However, the nearest resident is located 1.5 mi (7,920 ft or 2,414 m) from the ISFSI. Therefore, consistent with ISG-13 (Reference 1), the occupancy time at the controlled area boundary for the dose calculation was assumed to be 2,080 hr based on a 40-hr work week and 52 weeks per yr while the occupancy time at the nearest resident location was assumed to be 8,760 hr (24 hr per day 365 days per yr).

7.5.1 DIRECT RADIATION DOSE RATES

Table 7.5-1 presents the dose rate and annual doses at the site boundary and the nearest residence from direct radiation from the Diablo Canyon ISFSI after it is completely filled with 140 overpacks loaded with the MPC-32 at design-basis burnup and cooling times. As described in Section 7.3.2.3, these dose rates and doses were calculated at distances that were perpendicular to the long side of the ISFSI and it was assumed that eight overpacks were loaded per year.

7.5.2 DOSE RATES FROM NORMAL OPERATION EFFLUENT RELEASES

The source term used for the offsite dose assessment from the effluent release from the MPC is discussed in Section 7.2.2. The dose assessment from effluent release was calculated for normal conditions. Effluent doses for off-normal operations are discussed in Section 8.1.3 of this SAR. Effluent doses for an accident condition are discussed in Section 8.2.7.

7.5.2.1 Release of MPC Contents Under Normal Occurrences

The MPC is designed to maintain confinement boundary integrity under all normal, off-normal, and accident conditions of storage. Nevertheless, a hypothetical, non-mechanistic confinement boundary leak was evaluated in the effluent dose analysis.

For normal conditions, it was assumed that 2.5 percent of the total source term of each assembly is available for release to the MPC cavity. This was based on the assumption, from ISG-5 (Reference 2), that 1 percent of the fuel rods have ruptured. In addition to the 1 percent, it was assumed, consistent with ISG-11 (Reference 3), that an additional 3 percent of fuel rods had cladding oxide thicknesses greater than 70 micrometers and therefore had 50 percent of the source term in these rods available for release. The spent fuel is stored in a manner such that the spent fuel cladding is protected during storage against degradation that could lead to fuel cladding ruptures. The MPC cavity is filled with the inert gas helium after the MPC has been evacuated of air and moisture that might produce long-term degradation of the spent fuel cladding. The HI-STORM 100 System is additionally designed to provide for long-term heat removal to ensure that the fuel is maintained at temperatures below those at which cladding degradation occurs. It is therefore highly unlikely that a spent fuel assembly with intact fuel cladding will undergo cladding failure during storage, and the assumption that 2.5 percent of the source term is available for release is conservative.

The assumption that 10 percent of the fuel rods have ruptured was incorporated into the postulated pressure increase within the MPC cavity to determine a bounding pressure of the MPC cavity for effluent release calculations for the normal and off-normal cases. This pressure, combined with the maximum MPC cavity temperature was used to determine a postulated leakage rate. This leakage rate was based on an assumed leakage of 5.0×10^{-6} atm-cm^3/sec during the helium leak rate test and was adjusted for the higher temperature and pressure during the off-normal condition to result in a calculated leak rate of 7.37×10^{-6} atm-cm^3/sec.

The radionuclide release fractions, which account for the radionuclides trapped in the fuel matrix and radionuclides that exist in a chemical or physical form that is not releasable to the environment, were based on ISG-5 and are presented in Table 7.2-8. Additionally, only 10 percent of the fines released to the MPC cavity were assumed to remain airborne long enough to be available for release from the cask MPC (Reference 4). It was conservatively assumed that 100 percent of the volatiles, crud, and gases remain airborne and available for release. The release rate for each radionuclide was calculated by multiplying the quantity of radionuclides available for release in the MPC cavity by the leakage rate calculated above, divided by the MPC cavity volume.

7.5.2.2 Effluent Dose Calculations for Normal Conditions

The nearest distance from the ISFSI to the DCPP site boundary is 1,400 ft. A χ/Q value of 3.44×10^{-6} sec/m^3 (Reference 5) at the site boundary was used for this analysis. This χ/Q value is the highest χ/Q in any direction and is based on duration of an entire year. The dose conversion factors for internal doses due to inhalation and submersion in a radioactive plume were obtained from the EPA Federal Guidance Report No. 11 (Reference 6) and EPA Federal Guidance Report No. 12 (Reference 7), respectively. An adult breathing rate of 3.3×10^{-4} m^3/sec was assumed (Reference 2). For site boundary dose, an annual occupancy of 2,080 hr was assumed. For the nearest resident, full-time occupancy was assumed (8,760 hr).

The annual dose equivalent for the whole body, thyroid, and other critical organs to an individual at the DCPP site boundary as a result of a non-mechanistic normal effluent release were calculated for an ISFSI containing 140 overpacks, each loaded with an MPC-32. Table 7.5-2 summarizes the dose results for normal conditions. As can be concluded from Table 7.5-2, the estimated doses are a fraction of the limits specified in 10 CFR 72.104(a) for normal operations.

7.5.3 OFFSITE DOSE FROM OVERPACK LOADING OPERATIONS

The transfer of the MPC from the transfer cask to the overpack will occur outside the FHB/AB at the CTF. As a result, the impact of this operation on the offsite dose was considered. There are only two conditions that need to be considered in this analysis. The first is the condition of the MPC inside the transfer cask. The second condition is the MPC inside the overpack with the transfer cask no longer positioned above the overpack and the lid on the overpack not installed. Table 7.5-3 presents the results of these analyses.

7.5.4 TOTAL OFFSITE COLLECTIVE DOSE

Table 7.5-4 presents the annual dose at the site boundary and for the nearest resident from the combined dose rates from direct radiation and non-mechanistic effluent release for normal ISFSI operations and off-normal operations. The dose rates from other uranium fuel cycle operations (that is, DCPP) are also shown in this table to demonstrate compliance with 10 CFR 72.104. Table 7.5-4 demonstrates that the Diablo Canyon ISFSI will meet the 10 CFR 72.104 regulatory requirements. However, ultimate compliance with the regulations will be demonstrated through the DCPP environmental monitoring program.

The actual dose from the ISFSI will be considerably less than the conservatively estimated values in Table 7.5-4. The following are some of the conservative assumptions used in the calculating the dose rates presented.

- The design basis assembly and design basis burnup and cooling time were conservatively chosen.

- All fuel assemblies in the MPC are assumed to be identical with the design basis burnup and cooling time.

- BPRAs are assumed to be present in all fuel assemblies in all casks.

- The assumed ISFSI loading plan was conservatively chosen to result in the highest offsite dose rate.

- The dose rate was calculated at the most conservative location around the ISFSI.

7.5.5 REFERENCES

1. Real Individual, USNRC, Interim Staff Guidance Document-13, Revision 0, June 2000.

2. Normal, Off-Normal and Hypothetical Dose Estimate Calculations, USNRC, Interim Staff Guidance Document-5, Revision 1, June 1999.

3. Transportation and Storage of Spent Fuel Having Burnups in Excess of 45 GWD/MTU, USNRC, Interim Staff Guidance Document-11, Revision 1, May 2000.

4. Y.R. Rashid, et al, An Estimate of the Contribution of Spent Fuel Products to the Releasable source Term in Spent Fuel Transport Casks, SAND88-2778C, Sandia National Laboratories, 1988.

5. 1999 Annual Radioactive Effluent Release Report, PG&E Letter DCL-00-061, April 28, 2000.

6. Limiting Values of Radionuclide Intake and Air Concentration and Dose Conversion Factors for Inhalation, Submersion, and Ingestion, US EPA, Federal Guidance Report No. 11, DE89-011065, 1988.

7. External Exposure to Radionuclides in Air, Water, and Soil, US EPA, Federal Guidance Report No. 12, EPA 402-R-93-081, 1993.

8. Holtec Report No. HI-2002563, "Dose Evaluation for the ISFSI at Diablo Canyon Power Plant."

TABLE 7.4-1 Sheet 1 of 3

OCCUPATIONAL EXPOSURE DURING OVERPACK LOADING OPERATIONS

	Operation	Duration of Operation (hours)	Time in Dose Field (minutes)	Dose Rate at Location (mrem/hr)	Number of Personnel	Total Dose (mrem)
1	Insert MPC into transfer cask	2	120	0	3	0
2	Place transfer cask in cask washdown area	2	120	0	4	0
3	Attach impact limiter	0.5	10	0	2	0
4	Fill annulus	1	60	0	2	0
5	Fill MPC with water	2	20	0	2	0
6	Move transfer cask over the spent fuel pool	2	60	2	3	6
7	Place transfer cask in the spent fuel pool	1.5	60	2	3	6
8	Load fuel assemblies into MPC	8	480	2	2	32
9	Perform fuel assembly identification check	2	60	2	2	4
10	Install MPC lid and lid retention system	2	120	2	2	8
11	Remove transfer cask from spent fuel pool and washdown external portion	1.5	45	23	2	34.5
12	Place transfer cask in the cask washdown area	1	5	46	2	7.7
13	Install the seismic restraints	0.5	30	46	2	46
14	Disconnect lid retention system and lift yoke	1	60	24	2	48
15	Fill water jacket with water	1	5	38	2	6.3
16	Perform initial decontamination	2	120	23	3	138
17	Install temporary shield ring	0.5	15	39	2	19.5
18	Lower MPC water level	0.5	15	29	2	14.5
19	Install automated welding system	1.5	30	29	2	29
20	Perform MPC lid welding and NDE	12	210	29	1	101.5
21	Hydro test MPC	1	30	29	2	29
22	Perform leakage testing	1	30	29	1	14.5
23	Blowdown MPC	3	15	29	2	14.5
24	Perform MPC moisture removal	20	60	29	2	58
25	Perform helium backfill	3	30	29	2	29
26	Install/weld vent and drain cover plates	2	120	29	2	116

TABLE 7.4-1 Sheet 2 of 3

	Operation	Duration of Operation (hours)	Time in Dose Field (minutes)	Dose Rate at Location (mrem/hr)	Number of Personnel	Total Dose (mrem)
27	NDE vent and drain cover plate welds	0.5	30	29	1	14.5
28	Leak test cover plates	0.5	30	29	1	14.5
29	Install/weld closure ring	2	60	29	2	58
30	NDE closure ring welds	1	60	29	2	58
31	Remove automated welding system	1	15	29	2	14.5
32	Drain annulus	1	5	36	1	3
33	Remove temporary shield ring	0.5	15	39	2	19.5
34	Decontaminate MPC lid and transfer cask	2	120	23	3	138
35	Install transfer cask top lid	0.5	30	33	2	33
36	Install lift cleats	0.5	30	45	2	45
37	Remove impact limiter	0.5	5	49	2	8.2
38	Raise transfer cask and decontaminate bottom	2	90	36	2	108
39	Remove seismic restraints	0.5	30	46	2	46
40	Remove transfer cask from cask washdown area	1	60	18	2	36
41	Install bottom shield	1	60	49	2	98
42	Place transfer cask in transport frame	1	45	23	2	34.5
43	Downend transfer cask in transport frame	1	10	23	2	7.7
44	Perform transfer cask surveys	1	30	61	2	61
45	Transport transfer cask to cask transporter	1	60	23	2	46
46	Attach transfer cask to the cask transporter	0.5	30	23	2	23
47	Transport transfer cask to the cask transfer facility	3	180	12	2	72
48	Prep overpack for receiving MPC	3	180	0	3	0
49	Upend transfer cask in the transport frame	1.5	30	23	2	23
50	Remove transfer cask from the transport frame	0.5	30	23	2	23
51	Remove bottom shield	0.5	30	49	2	49
52	Mate transfer cask with overpack	0.5	30	36	2	36
53	Secure transfer cask to cask transporter	1	60	23	2	46
54	Attach MPC downloader	0.5	15	45	2	22.5
55	Remove transfer cask pool lid	0.5	30	49	2	49

Table 7.4-1 Sheet 3 of 3

	Operation	Duration of Operation (hours)	Time in Dose Field (minutes)	Dose Rate at Location (mrem/hr)	Number of Personnel	Total Dose (mrem)
56	Transfer MPC into overpack	1	60	23	2	46
57	Disconnect MPC downloader slings	0.5	30	2	2	2
58	Remove transfer cask from mating device	0.5	30	2	2	2
59	Remove MPC downloader slings/cleats	0.5	15	45	2	22.5
60	Remove mating device	0.5	30	6	2	6
61	Install overpack lid	1	15	6	2	3.0
62	Raise overpack to full up position	0.5	30	18	2	18
63	Attach overpack lift bracket	0.5	30	5	2	5
64	Transport overpack to ISFSI	1	60	18	2	36
65	Attach overpack to ISFSI pad	1	60	16	2	32
66	Perform post loading testing	3	30	18	2	18
Total dose during loading operations						2.1 rem

TABLE 7.4-2

OCCUPATIONAL EXPOSURE DURING OVERPACK UNLOADING OPERATIONS

	Operation	Duration of Operation (hours)	Time in Dose Field (minutes)	Dose Rate at Location (mrem/hr)	Number of Personnel	Total Dose (mrem)
1	Recover overpack from ISFSI pad	6	360	16	2	192
2	Attach overpack lift bracket	0.5	30	5	2	5
3	Transport overpack to CTF	1	60	18	2	36
4	Lower overpack to full down position	0.5	30	18	2	18
5	Remove overpack lid	1	15	6	2	3
6	Attach mating device	0.5	30	6	2	6
7	Install MPC downloader slings/cleats	0.5	30	45	2	45
8	Install transfer cask into mating device	0.5	30	2	2	2
9	Attach MPC downloader	0.5	30	2	2	2
10	Secure transfer cask to cask transporter	1	60	2	2	4
11	Transfer MPC into transfer cask	1	60	23	2	46
12	Install transfer cask pool lid	0.5	30	49	2	49
13	Disconnect MPC downloader	0.5	15	45	2	22.5
14	Disconnect transfer cask from overpack	0.5	30	36	2	36
15	Install bottom shield	1	60	49	2	98
16	Place transfer cask in the transport frame	1	45	23	2	34.5
17	Downend transfer cask in the transport frame	1	10	23	2	7.7
18	Attach transfer cask to the cask transporter	0.5	30	23	2	23
19	Transport transfer cask to the fuel building	3	180	12	2	72
20	Transport transfer cask into the fuel building	1	60	23	2	46
21	Upend transfer cask in transport frame	1.5	30	23	2	23
22	Remove transfer cask from transport frame	1	60	23	2	46
23	Remove bottom shield	0.5	30	49	2	49
24	Place transfer cask in cask washdown area	0.5	5	46	2	7.7
25	Install the seismic restraints	0.5	30	46	2	46
26	Remove lift cleats	0.5	30	45	2	45

TABLE 7.4-2 Sheet 2 of 2

	Operation	Duration of Operation (hours)	Time in Dose Field (minutes)	Dose Rate at Location (mrem/hr)	Number of Personnel	Total Dose (mrem)
27	Remove transfer cask top lid	0.5	30	37	2	37
28	Attach impact limiter	0.5	10	49	2	16.3
29	Install temporary shield ring	0.5	15	39	2	19.5
30	Fill annulus	1	6	53	2	10.6
31	Install weld removal system	1.5	30	29	2	29
32	Core drill vent and drain cover plates	1	60	29	2	58
33	Perform MPC gas sampling	2	10	29	2	9.7
34	Perform MPC helium cooldown	20	60	29	2	58
35	Flood MPC	3	15	29	2	14.5
36	Remove MPC lid weld	12	210	29	1	101.5
37	Remove weld removal system	1	15	29	2	14.5
38	Remove temporary shield ring	0.5	15	39	2	19.5
39	Drain water jacket	1	5	49	2	8.2
40	Install lid retention system and lift yoke	0.5	20	65	2	43.3
41	Remove the seismic restraints	0.5	30	65	2	65
42	Raise transfer cask to spent fuel pool level	1	5	61	2	10.2
43	Place transfer cask over spent fuel pool	1.5	60	2	2	4
44	Place transfer cask in spent fuel pool	1.5	45	2	2	3
45	Remove lid retention system bolts	2	120	2	2	8
46	Remove MPC lid	0.5	30	2	2	2
47	Unload fuel assemblies from transfer cask	8	480	2	2	32
48	Remove transfer cask from spent fuel pool	1.5	45	2	3	4.5
49	Place transfer cask in cask washdown area	1	6	2	2	0.4
50	Drain MPC and transfer cask annulus	6	30	2	2	2
51	Remove MPC from transfer cask	2	20	2	2	1.3
52	Decontaminate MPC and transfer cask	8	240	2	2	16
Total dose during unloading operations						1.5 rem

TABLE 7.5-3

DOSE RATES AT THE SITE BOUNDARY
FROM OVERPACK LOADING OPERATIONS

Condition	Dose Rate (mrem/hr)	Event Duration (hours)	Loadings per year	Annual Dose (mrem)
MPC in transfer cask	2.0E-03[a]	9	8	1.44E-01
MPC in overpack without a lid	9.0E-04	1.5	8	1.1E-02
Total				15.5E-02

[a] The dose rate for the transfer cask was calculated by scaling the highest dose rate on the surface of the transfer cask (not including the pool lid) by the ratio of the highest contact dose rate to distance dose rate calculated for the overpack. Specifically, 389.3 mrem/hr (Table 7.3-2) was multiplied by 1.8E-04 (Table 7.3-4 (400 m))/34.8 (Table 7.3-1).

TABLE 7.5-4

TOTAL ANNUAL OFFSITE COLLECTIVE DOSE (MREM) AT THE SITE BOUNDARY AND NEAREST RESIDENT FROM THE DIABLO CANYON ISFSI

	Normal Operations				Off-Normal Operations		
Organ	Effluent Release[c]	Direct Radiation[c]	Overpack Loading Operations[d]	Other Uranium Fuel Cycle Operations[a]	Effluent Release[d]	Total (normal + off-normal)	10 CFR 72.104 Regulatory Limit
Site Boundary (1,400 ft / 427 m)							
Whole body ADE[b]	0.064	5.6	15.5E-02	4.357E-02	1.27E-03	5.86	25
Thyroid ADE	0.010	5.6	15.5E-02	1.260E-01	1.02E-04	5.89	75
Critical organ ADE (Max)	0.35	5.6	15.5E-02	5.590E-02	9.31E-03	6.17	25
Nearest Resident (1.5 miles / 7,920 ft / 2414 m)							
Whole body ADE	0.27	3.5E-04	15.5E-02	4.357E-02	5.33E-03	0.47	25
Thyroid ADE	0.043	3.5E-04	15.5E-02	1.260E-01	4.31E-04	0.32	75
Critical organ ADE (Max)	1.46	3.5E-04	15.5E-02	5.590E-02	3.92E-02	1.71	25

(a) Data for uranium fuel cycle operations were obtained from the DCPP FSAR Update, Rev. 11, Table 11.3-32. Table 11.3-32 was selected based on the highest dose values in the sectors at the site boundary (0.5 miles). These dose values for the site boundary were conservatively applied to the nearest resident. The critical organ dose listed was based on the total liver dose in Table 11.3-32. The values listed in Table 11.3-32 should bound the results calculated from effective dose equivalent methodology.
(b) ADE is annual dose equivalent.
(c) 140 casks
(d) Single cask

DIABLO CANYON ISFSI
SAFETY ANALYSIS REPORT

CHAPTER 8

ACCIDENT ANALYSES

CONTENTS

CHAPTER 8

ACCIDENT ANALYSES

TABLES

CHAPTER 8

ACCIDENT ANALYSES

FIGURES

CHAPTER 8

ACCIDENT ANALYSES

This chapter describes the accident analyses for the Diablo Canyon ISFSI. Sections 8.1 and 8.2 evaluate the safety of the ISFSI under off-normal operations and accident conditions, respectively. For each event, the postulated cause of the event, detection of the event, and evaluation of the event effects and consequences, corrective actions, and radiological impact are presented. Unless otherwise identified in Chapter 8 or other SAR sections, the MPC 32 was evaluated as a bounding condition. The results of the evaluations performed herein demonstrate that the HI-STORM 100 System can withstand the effects of off-normal events and accidents without affecting function and are in compliance with the applicable acceptance criteria. Section 8.3 summarizes site characteristics that affect the safety analysis.

8.1 OFF-NORMAL OPERATIONS

This section addresses events designated as Design Event II, as defined by ANSI/ANS-57.9 (Reference 1). The following are considered off-normal events for the Diablo Canyon ISFSI:

- Off-normal pressures
- Off-normal environmental temperatures
- Confinement boundary leakage
- Partial blockage of air inlets
- Cask drop less than allowable height
- Loss of electric power
- Cask transporter off-normal operation

For each event, the postulated cause of the event, detection of the event, an evaluation of the event effects and consequences, corrective actions, and radiological impact are presented. The results of the evaluations performed herein demonstrate that the HI-STORM 100 System can withstand the effects of off-normal events without affecting function and are in compliance with the applicable acceptance criteria. The following sections present the evaluation of the HI-STORM 100 System for the design-basis, off-normal conditions that demonstrate that the requirements of 10 CFR 72.122 are satisfied and that the corresponding radiation doses satisfy the requirements of 10 CFR 72.104(a).

8.1.1 OFF-NORMAL PRESSURES

The HI-STORM 100SA overpack is a ventilated cask design. The sole pressure boundary of the storage system is the multi-purpose canister (MPC). The off-normal pressure for the MPC internal cavity is a function of the initial helium fill pressure, variations in the helium temperature, and leakage of any gases contained within the fuel rods. The analyzed off-normal environmental temperature is 100°F and peak solar insolation is assumed. This bounds the Diablo Canyon ISFSI maximum off-normal site ambient temperature and solar insolation values. The MPC off-normal pressure evaluation includes the conservative assumption that 10 percent of the fuel rods rupture, allowing 100 percent of the fill gas and 30-percent of the fission gases from these fuel rods to be released to the MPC cavity. This assumption is consistent with the guidance in NUREG-1536 for the review of dry storage cask designs (Reference 2).

8.1.1.1 Postulated Cause of Off-Normal Pressure

After fuel assembly loading, the MPC is drained, dried, and backfilled with an inert gas (helium) to ensure long-term fuel cladding integrity during dry storage. The pressure of the gas in the MPC cavity is affected by the initial fill pressure, the MPC cavity volume, the decay heat emitted by the stored fuel, the presence of nonfuel hardware, fuel-rod gas leakage, ambient temperature, and solar insolation. Of these, the initial fill pressure, presence of non-fuel hardware, and MPC cavity volume do not vary with time in storage and can be ignored as a cause of off-normal pressure. The decay heat emitted by the stored fuel decreases with time and is conservatively accounted for in the analysis by using the highest rate of decay heat for a given fuel cooling time. Off-normal pressure is conservatively evaluated considering a concurrent non-mechanistic rupture of 10 percent of the stored fuel rods during a time of maximum off-normal ambient temperature (100°F) and full solar insolation.

8.1.1.2 Detection of Off-Normal Pressure

The HI-STORM 100 System is designed to withstand the MPC off-normal internal pressure without any effects on its ability to perform its design safety functions. No personal actions or equipment are required to respond to an off-normal pressure event. Therefore, no detection instrumentation is required.

8.1.1.3 Analysis of Effects and Consequences of Off-Normal Pressure

The evaluation of MPC pressure for this off-normal event was initially performed assuming normal ambient temperature (80°F), 10 percent of the fuel rods ruptured, peak insolation, maximum decay heat, and the effect of nonfuel hardware. The MPC-32 was used as the bounding MPC in this analysis because it provides the maximum internal pressure for all MPCs to be used at the Diablo Canyon ISFSI (see Section 4.2.3.3.2.2 for justification). The resulting pressure for MPC-32 with 80°F ambient temperature is 76.0 and 87.90 psig for the storage and transport conditions respectively. Using this initial pressure, the added effect of increasing the ambient temperature from

80°F to the maximum off-normal temperature of 100°F was conservatively evaluated using the Ideal Gas Law. Assuming the MPC cavity gas temperature increased by the full 20°F, the resulting absolute pressure $P_2$for the storage condition is computed as follows:

$$P_2 = P_1 \times [(T_1 + \Delta T)/T_1]$$

Where,

P_1 = Absolute pressure at T_1 = 76.0 psig (90.7 psia)

T_1 = Absolute bulk temperature of the MPC cavity gas with design basis fuel decay heat = 513.6°K (Reference 4, Section 11.1.1.3)

ΔT = Absolute bulk MPC cavity gas temperature increase = 20°F, or 11.1°K

The resulting absolute pressure (P_2) was computed to be 92.7 psia, or 78.0 psig. Applying the same formula, the transport condition temperature can be calculated to be 89.84 psig. Both are below the normal/off-normal MPC internal design pressure of 100 psig.

8.1.1.4 Corrective Action for Off-Normal Pressure

The HI-STORM 100 System is designed to withstand the off-normal pressure without any effects on its ability to maintain safe storage conditions. There are no corrective actions associated with off-normal pressure.

8.1.1.5 Radiological Impact from Off-Normal Pressure

The off-normal pressure event has no radiological impact because the confinement barrier and shielding integrity are not affected.

8.1.2 OFF-NORMAL ENVIRONMENTAL TEMPERATURES

The off-normal temperature ranges for which the HI-STORM 100 System is designed are summarized in the HI-STORM 100 System FSAR (Reference 3) Section 2.2.2. The off-normal temperature evaluation is described in HI-STORM 100 System FSAR Section 11.1.2, as amended by LAR 1014-1 (Reference 4). Off-normal environmental temperature ranges of –40 to 100°F (for the HI-STORM 100SA overpack and ISFSI storage pads) and 0 to 100°F (for the HI-TRAC transfer cask, cask transporter, and cask transfer facility) conservatively bound off-normal temperatures at the Diablo Canyon ISFSI site (24°F to 97°F). The off-normal environmental temperature ranges are used as the design criteria for the concrete storage pad, cask transporter, and CTF. The ranges of off-normal temperatures evaluated bound the historical temperature variations at the Diablo Canyon ISFSI.

This off-normal event is of a short duration. Therefore, the resultant fuel cladding temperatures for the cask evaluations are compared against the accident condition (short-term) temperature limits.

8.1.2.1 Postulated Cause of Off-Normal Environmental Temperatures

The off-normal environmental temperature is postulated as a constant ambient temperature caused by unusual weather conditions. To determine the effects of off-normal temperatures, it is conservatively assumed that these temperatures persist for a sufficient duration to allow the HI-STORM 100 System to achieve thermal equilibrium. Because of the large mass of the HI-STORM 100 System with its corresponding large thermal inertia and the limited duration for the off-normal temperatures, this assumption is conservative.

8.1.2.2 Detection of Off-Normal Environmental Temperatures

The HI-STORM 100 System is designed to withstand off-normal environmental temperatures without any effects on its ability to maintain safe storage conditions. There are no personnel actions or equipment required for mitigation of an off-normal temperature event. Deleterious effects of off-normal temperatures on the cask transporter, CTF, and concrete storage pad are precluded by design. Administrative procedures based on Diablo Canyon ISFSI TS 5.1.3 will prohibit cask handling if temperatures fall outside the off-normal temperature limits. Ambient temperature is available from thermometers used for the DCPP site meteorological measurement program.

8.1.2.3 Analysis of Effects and Consequences of Off-Normal Environmental Temperatures

There are no adverse safety effects resulting from off-normal environmental temperatures on the cask transporter, CTF, or concrete storage pads, since they are designed for these temperature ranges.

The off-normal event, considering a maximum off-normal ambient temperature of 100°F has been evaluated for the HI-STORM 100 System and is described in the HI-STORM 100 System FSAR Section 11.1.2.3, as amended by LAR 1014-1. The evaluation was performed for the loaded transfer cask and the loaded overpack, assuming design-basis fuel with the maximum decay heat and the most restrictive thermal resistance. The 100°F environmental temperature was applied with peak solar insolation.

The HI-STORM 100 System maximum temperatures for components close to the design-basis temperatures are conservatively calculated at an environmental temperature of 80°F as an initial condition for this off-normal event. These temperatures (for MPC-32, MPC-24E, and the overpack) are shown in Tables 4.4.26, 4.4.27, and 4.4.36 of the HI-STORM 100 System FSAR, as amended by LAR 1014-1. The maximum off-normal environmental temperature is 100°F, which is an increase of

20°F over the normal design temperature. The resulting limiting component maximum off-normal temperatures are shown in Table 11.1.1 of the HI-STORM 100 System FSAR, as amended by LAR 1014-1. The temperatures are all below the applicable material short-term temperature limits.

The off-normal event considering a limiting low environmental temperature of -40°F and no insolation for a duration sufficient to reach thermal equilibrium has been evaluated with respect to overpack material brittle fracture at this low temperature. The overpack and MPC are conservatively assumed to reach -40°F throughout the structure. The minimum off-normal environmental temperature specified for the transfer cask is 0°F and the transfer cask is conservatively assumed to reach 0°F throughout the structure. This evaluation is discussed in the HI-STORM 100 System FSAR Section 3.1.2.3 and the results are acceptable. Administrative procedures based on Diablo Canyon ISFSI TS 5.1.3 prohibit cask handling operations at environmental temperatures below 0°F.

8.1.2.4 Corrective Action for Off-Normal Environmental Temperatures

The HI-STORM 100 System is designed to withstand the off-normal environmental temperatures without any effects on its ability to maintain safe storage conditions. The cask transporter, CTF, and ISFSI pad are designed for temperature ranges consistent with the dry storage cask components used at these facilities. Therefore, no corrective actions are required for off-normal environmental temperature conditions.

8.1.2.5 Radiological Impact of Off-Normal Temperatures

Off-normal environmental temperatures have no radiological impact as the integrity of the confinement barrier and shielding are unaffected by off-normal temperatures. The effect of elevated temperatures does not significantly increase the doses associated with the design-basis leak rate from the MPCs and is bounded by the results of the off-normal failure of fuel cladding event assessed in Section 8.1.3.

8.1.3 CONFINEMENT BOUNDARY LEAKAGE

The HI-STORM 100 System MPC has a welded confinement boundary to contain radioactive fission products under all design-basis normal, off-normal, and accident conditions. The radioactivity confinement boundary is defined by the MPC shell, baseplate, MPC lid, and vent and drain port cover plates. A non-mechanistic failure of fuel cladding in conjunction with allowable leakage in the MPC confinement boundary has been evaluated as both an off-normal and an accident condition (Reference 7). The difference between the two evaluations is in the radioactive source term, the bounding temperature and pressure determined in the thermal analysis of the HI-STORM 100 System FSAR, as amended by LAR 1014-1, and the χ/Q value used for each of the two conditions. The analytical technique and assumptions used in both evaluations are consistent with Interim Staff Guidance (ISG) Document 5 (Reference 5). All other inputs to the confinement boundary leak dose analysis are identical for the off-normal and accident analyses. The accident condition is addressed in Section 8.2.7 of this SAR and is not discussed further here.

Since this event is applicable only to the MPC, the evaluation is applicable for all locations (that is, in the cask transporter, at the CTF, or on the ISFSI pad) and is independent of whether the MPC is inside the transfer cask or the overpack. Due to the close proximity of these three locations, the two χ/Q values used for the off-normal and accident condition evaluations are the same for all three postulated release locations.

8.1.3.1 Postulated Cause of Confinement Boundary Leakage

Based on the design of the MPC vessel and the protection provided by the transfer cask and the overpack, a leak in the MPC confinement boundary is not considered credible, so no cause is identified. Also, there is no credible mechanism for inducing the level of fuel failure assumed for this event. This off-normal condition is evaluated as a non-mechanistic event.

8.1.3.2 Detection of Confinement Boundary Leakage

The MPC is a welded cylindrical enclosure. There are no mechanical joints or seals in the confinement boundary. The confinement boundary is designed to maintain its integrity under all design basis normal, off-normal, and accident conditions. Therefore, leakage detection equipment is not required.

8.1.3.3 Analysis of Effects and Consequences of Confinement Boundary Leakage

The MPC confinement boundary is designed to remain intact under all design basis normal, off-normal, and accident conditions. However, as a defense-in-depth measure, the MPC closure ring, which provides a redundant weld for the MPC lid-to-shell weld and the vent and drain port cover plate welds, is designed to withstand full MPC cavity pressure. Therefore, the closure ring would provide the confinement boundary in this event. The dose consequences of a hypothetical, non-mechanistic confinement boundary leak are discussed in Section 8.1.3.5.

8.1.3.4 Corrective Action for Confinement Boundary Leakage

There is no corrective action required for the assumed leakage in the MPC confinement boundary because leakage in excess of allowable is not considered credible. Also, the assumed level of fuel failure is not considered credible.

8.1.3.5 Radiological Impact of Confinement Boundary Leakage

The dose consequences of a non-mechanistic leak in the MPC confinement boundary have been analyzed on a site-specific basis for the Diablo Canyon ISFSI using appropriate source terms, release fraction, leak rate, meteorology, breathing rate, and occupancy times. The analysis of this abnormal event considers the rupture of

10 percent of the stored fuel rods. The evaluation of this event under normal conditions is discussed in Section 7.5.2. The same methodology with the unique off-normal source is used here. Annual doses at the site boundary and nearest resident were calculated. The results are provided in Table 8.1-1 for the analysis of a single HI-STORM cask in the off-normal condition. The calculated doses are less than the regulatory limits in 10 CFR 72.104(a).

8.1.4 PARTIAL BLOCKAGE OF AIR INLETS

The HI-STORM 100 System overpack is designed with inlet and outlet air ducts, four each at the top and bottom of the overpack structure with the lid installed. Each duct opening includes a fine mesh screen across its outer face. These screens ensure the air ducts are protected from the incursion of foreign objects. Each set of four air inlet and outlet air ducts are spaced 90 degrees apart around the circumference of the overpack and it is highly unlikely that blowing debris during normal or off-normal operation could block all of the air inlet ducts. It is conservatively assumed, as an off-normal condition, that two of the four air inlet ducts are blocked. Blockage of the inlet air ducts is assumed to be thermally equivalent to blockage of the outlet air ducts. The evaluation of this off-normal event, as well as the blockage of three inlet ducts, is discussed in Section 11.1.4 of the HI-STORM 100 System FSAR, as amended by LAR 1014-1. The blocked air inlet ducts are assumed in the HI-STORM 100 System FSAR to be completely blocked, with an ambient temperature of 80°F, peak solar insolation, and maximum spent fuel decay heat values. The HI-STORM 100 System FSAR generic assumption of an annual average temperature of 80°F and peak solar insolation value of 800 g-cal/cm^2, respectively, bounds the Diablo Canyon site annual average temperature of 55°F and peak solar insolation value of 766 g-cal/cm^2.

8.1.4.1 Postulated Cause of Partial Blockage of Air Inlets

It is conservatively assumed that the affected air inlet ducts are completely blocked, although the protective screens prevent foreign objects from entering into the ducts. The mesh screens are inspected periodically, as required by the Diablo Canyon ISFSI TS. Any duct blockage would be detected by visual inspection and removed to restore the heat removal system to full operational condition. Depending on the size and number of debris pieces, it is possible that blowing debris may simultaneously block two air inlet ducts of the overpack.

8.1.4.2 Detection of Partial Blockage of Air Inlets

Detection of partial blockage of air inlet ducts would occur during the routine visual surveillance of the storage cask air duct screens required by the Diablo Canyon ISFSI TS. The frequency of inspection is conservatively based on an assumed complete simultaneous blockage of all four air inlet ducts (Diablo Canyon ISFSI TS Bases).

8.1.4.3 Analysis of Effects and Consequences of Partial Blockage of Air Inlets

Blockage of the overpack air inlet ducts can affect the heat removal process of the dry storage system. The magnitude of the effect is dependent upon the rate of decay heat emission from the stored fuel (itself dependent upon the fuel burnup and cooling time) and the ambient air temperature. Bounding evaluations were performed for the blockage of two and three inlet air ducts with the MPC-32 inside the overpack, at its maximum decay heat load at the ambient air temperature of 80°F. As stated above, the HI-STORM 100 System FSAR assumes an annual-average ambient air temperature of 80°F, which bounds the annual-average ambient air temperature for the Diablo Canyon Site of 55°F. The MPC-32 decay heat load bounds the MPC-24, MPC-24E, and MPC-24EF heat loads due to the presence of eight additional fuel assemblies. The largest component temperature rise for two ducts blocked is 25°F. The largest component temperature rise for three ducts blocked is 81°F. (Blocking of four ducts is treated as an accident in Section 8.2.15.) This maximum temperature rise was conservatively added to all cask component temperatures for comparison with the respective component short-term temperature limits. The results are shown in Table 11.1.2 of the HI-STORM 100 System FSAR, as amended by LAR 1014-1. All temperatures are less than the applicable component short-term temperature limits.

The MPC cavity pressure as a result of this limiting component temperature increase was also evaluated. An MPC cavity gas bulk temperature rise of 25°F was evaluated using the Ideal Gas Law method as described in Section 8.1.3 and the resulting MPC internal pressure was computed to be 78.4 psig, which is less than the normal condition MPC design pressure of 100 psig.

8.1.4.4 Corrective Action for Partial Blockage of Air Inlets

The corrective action for the partial blockage of air inlet ducts is the removal of the cause of the blockage, and the cleaning, repair, or replacement, as necessary, of the affected mesh screens. After clearing of the blockage, the cask heat removal system is restored to its design condition, and temperatures will return to the normal range. Partial blockage of air inlet ducts does not affect the ability of the HI-STORM 100 System to safely store spent fuel for the long term.

Inspection of the overpack air duct screens is performed at a 24-hour frequency as required by the Diablo Canyon ISFSI TS. This inspection ensures blockage of air inlet ducts is detected and appropriately corrected.

8.1.4.5 Radiological Impact of Partial Blockage of Air Inlets

For partial blockage of air inlet ducts, it is estimated that the removal, cleaning, and replacement of the affected mesh screens will take two people approximately 1 hour. The dose rate at this location is estimated to be 58 mrem/hr. The total exposure for personnel to perform these corrective actions is 0.116 man-rem.

8.1.5 CASK DROP LESS THAN ALLOWABLE HEIGHT

Cask drops outside the fuel handling building/auxiliary building (FHB/AB) are not credible due to the design of the cask transporter and the CTF, as discussed in Section 8.2.4. The structural load path members of both the CTF and the cask transporter used in Diablo Canyon ISFSI operations are designed, operated, fabricated, tested, inspected, and maintained in accordance with the guidelines of NUREG-0612 (Reference 6). Therefore, a drop of the loaded MPC during inter-cask transfer operations is not a credible event. Although the cask and any ancillary components are lifted, handled, and moved in accordance with DCPP procedures and the DCPP Control of Heavy Loads Program, which provide assurance of safe heavy load handling, drop events inside the FHB/AB are nevertheless postulated and analyzed as described in the 10 CFR 50 license amendment request supporting the Diablo Canyon ISFSI license application, since the FHB/AB crane is not single failure proof.

8.1.6 LOSS OF ELECTRIC POWER

A total loss of external AC electric power is postulated to occur as a result of either a disturbance in the offsite electric supply system or the failure of equipment in the electrical distribution system feeding the ISFSI storage site and the CTF. A loss of electric power does not affect the cask transporter because all active functions of the transporter, such as cask lifting and MPC downloading, are driven from the onboard diesel engine.

8.1.6.1 Postulated Cause of Loss of Electric Power

Loss of the external power supply may occur as the result of natural phenomena, such as lightning strike or high winds, or as a result of undefined factors causing a disturbance in the offsite electrical grid. Loss of electrical power may also result from an electrical system fault or the failure of electrical distribution equipment such as a transformer.

8.1.6.2 Detection of Loss of Electrical Power

Loss of electrical power will be detected by the failure of electric-powered equipment.

8.1.6.3 Analysis of Effects and Consequences of Loss of Electrical Power

8.1.6.3.1 ISFSI Storage Site

There is no effect on the ability of the HI-STORM 100 System to safely continue storing the spent fuel at the ISFSI storage site during a loss of electric power event because the dry storage system is a completely passive design. No electric-powered equipment is used with the storage overpack while it is in its storage configuration on the concrete storage pads.

8.1.6.3.2 Cask Transfer Facility

The lift jacks of the CTF are the only functional component requiring electric power to operate. In a loss of electrical power, all lighting, power to the lift jacks, and any auxiliary power outlets will be unavailable. If the lift jacks are in operation at the time of the event, they will stop in place upon loss of power to preclude an uncontrolled lowering of the load. Upon restoration of power, the lift jacks will remain stopped by design of the electrical circuitry and will require manual action to restart.

8.1.6.4 Corrective Action for Loss of Electric Power

Corrective actions following a loss of electric power may vary widely, depending on the cause of the power loss. Restoration activities are generally straightforward. If electrical power to the CTF is lost with the loaded overpack in the lowered position, the overpack must be raised to grade level within 22 hours to ensure that the short-term, fuel-peak-cladding temperature limit is not exceeded. This is accomplished using the cask transporter and the HI-STORM lift links and lifting brackets.

8.1.6.5 Radiological Impact of Loss of Electric Power

The off-normal event of loss of electric power has no radiological impact because the MPC confinement barrier is not breached and shielding is not affected. The transfer cask is designed to provide adequate shielding and decay heat removal from the canisters. The sides of the transfer cask have both gamma and neutron shields, and the combination of the pool lid and bottom shield are designed to prevent excessive dose rates below the transfer casks. In the event the transfer operation is interrupted due to a loss of external power, operators would take measures as necessary to assure adequate distance and/or additional shielding between themselves and the transfer cask to minimize doses until electrical power is restored and the transfer process can resume.

8.1.7 CASK TRANSPORTER OFF-NORMAL OPERATION

Off-normal operation of the cask transporter includes postulation of the following human performance and active component failures during transport of the loaded transfer cask and the loaded overpack:

- Driver error
- Driver incapacitation
- Transporter engine failure
- Loss of hydraulic fluid

8.1.7.1 Postulated Cause of Cask Transporter Off-Normal Operation

Cask transporter driver error may be caused by driver inattentiveness, poor visibility, incorrect instructions, poor training, or any of several human performance-related causal factors. Driver incapacitation would be most likely caused by a sudden medical emergency. Transporter engine failure may be caused by a variety of mechanical problems typical of combustion engines. A loss of hydraulic fluid may be caused by a leak anywhere in the hydraulic system.

8.1.7.2 Detection of Cask Transporter Off-Normal Operation

Driver error or driver incapacitation would be detected by the support staff walking along with the transporter on the transport route observing the driver in distress or erratic transporter motion. Transporter engine failure would be detected by the halt of any engine-driven activity taking place at the time. A hydraulic fluid leak would be detected by the pressure instrumentation in the hydraulic system and possibly by visual observation of leaking fluid.

8.1.7.3 Analysis of Effects and Consequences of Cask Transporter Off-Normal Operation

In addition to the transporter driver, transport operations will be conducted with a support team consisting of security and other personnel affiliated with the fuel movement walking along with the transporter to ensure a safe and efficient move of the loaded cask from its point of origin to its destination. These personnel will be observing the movement of the transporter to ensure the designated travel path is being followed. Should the transporter start to veer from the travel path, the transporter will be stopped (either by the driver or by a support team member using either of two external stop switches mounted on the outside of the transporter), the cause investigated, and corrective actions taken to get the vehicle back on the correct path.

Incapacitation of the driver will be addressed by the design of an automatic shutoff control where the vehicle will stop whenever the control is released. The same control is used to move the transporter vehicle and operate the cask lifting apparatus integral to the transporter. A selector switch is used to ensure only one function can be performed by the transporter at a time. Also, either of two emergency stop switches, mounted on the outside of the transporter, can be operated to stop the transporter.

A transporter engine failure will result in the vehicle stopping or the hydraulic brakes engaging to stop any lift operations in progress.

A loss of hydraulic fluid will cause a loss of pressure in the hydraulic system that will engage the hydraulic brakes and stop movement of the lifting apparatus.

8.1.7.4 Corrective Action for Cask Transporter Off-Normal Operation

The corrective action for cask transporter off-normal operation will be developed and implemented based on the nature and safety significance of the problem. Corrective actions may include additional training for the driver, replacement of the driver, improved operating procedures, and repair or replacement of failed mechanical parts. The transporter is designed "fail-safe" to preclude uncontrolled lowering of the loaded transfer cask or overpack if a failure of an active component occurs, so no corrective actions related to the cask are necessary. If necessary, cribbing could be used to support the loaded transfer cask or overpack if the transporter needs to be replaced or detached from the load for repairs.

8.1.7.5 Radiological Impact of Cask Transporter Off-Normal Operation

The cask transporter off-normal event has no radiological impact since the confinement barrier is not breached and shielding is not affected.

8.1.8 REFERENCES

1. ANSI/ANS 57.9-1992, Design Criteria for an Independent Spent Fuel Storage Installation (dry type), American National Standards Institute.

2. Standard Review Plan for Dry Cask Storage Systems, USNRC, NUREG-1536, January 1997.

3. Final Safety Analysis Report for the HI-STORM 100 System, Holtec International Report No. HI-2002444, Revision 0, July 2000.

4. License Amendment Request 1014-1, Holtec International, Revision 2, July 2001, including Supplements 1 through 4 dated August 17, 2001; October 5, 2001; October 12, 2001; and October 19, 2001; respectively.

5. Normal, Off-Normal, and Hypothetical Dose Estimate Calculations, USNRC, Interim Staff Guidance Document-5, May 2000.

6. Control of Heavy Loads at Nuclear Power Plants, USNRC, NUREG-0612, July 1980.

7. PG&E Calculation STA-140 (HI-2002513), "Diablo Canyon ISFSI Site Boundary Confinement Analysis."

8.2 ACCIDENTS

8.2.1 EARTHQUAKE

An earthquake is classified as a natural phenomenon Design Event IV as defined in ANSI/ANS-57.9 (Reference 1). The effects of seismic events on cask loading operations inside the fuel handling building/auxiliary building (FHB/AB) are discussed in the 10 CFR 50 License Amendment Request submitted in support of Diablo Canyon ISFSI licensing. This section addresses the effect of a seismic event on the operations related to the Diablo Canyon ISFSI that occur outside the FHB/AB. Cask handling activities outside the FHB/AB were reviewed to identify potential risk significant configurations during a seismic event. The seismic evaluations address the following potentially seismic risk significant configurations (all configurations are analyzed with an MPC loaded with spent fuel):

(1) HI-TRAC transfer cask suspended horizontally from the cask transporter on the transport route between the FHB/AB and the cask transfer facility (CTF).

(2) HI-TRAC transfer cask suspended vertically from the cask transporter at the CTF, prior to being placed atop the HI-STORM 100SA overpack.

(3) HI-TRAC transfer cask mounted atop the HI-STORM 100SA overpack at the CTF and the transporter restrained to the ground. The overpack is in the fully lowered position in the CTF.

(4) HI-STORM 100SA overpack being transported to the ISFSI storage pad, suspended vertically from the cask transporter. In terms of seismic stability, this configuration bounds configuration (2) because the HI-STORM 100SA overpack is heavier than the HI-TRAC transfer cask.

(5) HI-STORM 100SA overpack anchored to the ISFSI storage pad in its long-term storage configuration.

Additionally, the slopes above the ISFSI and transport route were analyzed for stability during a seismic event (see Section 2.6.5).

8.2.1.1 Cause of Accident

Earthquakes are natural phenomena caused by the movement of large geological plates under the earth's surface.

8.2.1.2 Earthquake Accident Analysis

Two methods were used for seismic analysis of SSCs, that is, equivalent static analysis load method and dynamic analysis method. These methods were used as follows:

Equivalent Static Analysis Method

(1) Design of CTF reinforced concrete support structure.

(2) Pad design.

(3) Design of CTF shell structural steel.

Dynamic Analysis Method

(1) Determination of slope stability.

(2) Determination of transporter stability while carrying a transfer cask or loaded overpack.

(3) Determination of ISFSI storage pad sliding.

(4) Design of storage cask anchorage to the pad.

As discussed in SAR Section 2.6.2.2, the design earthquake (DE), double-design earthquake (DDE), Hosgri earthquake (HE) and Long Term Seismic Program (LTSP) earthquakes are the DCPP seismic licensing basis. The DE and DDE spectra are defined for periods up to 1 second. The Hosgri spectra are defined for periods up to 0.8 seconds. The LTSP spectra are defined for periods up to 2 seconds.

The statistically independent free-field DE, HE and LTSP ground acceleration time histories in two horizontal and vertical directions were regenerated and updated based on the free-field response spectra and time histories from strong ground motion recorded at the Lucerne Valley site from the June 28, 1992 Landers magnitude 7.3 earthquake and from a rock site located approximately 8 km fault rupture distance from the September 20, 1999 Chi Chi magnitude 7.6 earthquake. These time histories are referred in this SAR as the DE, DDE, HE and LTSP time histories. The DDE is twice the DE. The regenerated DE, DDE, HE and LTSP free-field time histories meet the NRC Standard Review Plan (SRP) spectral matching criteria, Section 3.7.1 of NUREG-0800, (Reference 2) and the three components of the time-histories for each earthquake were verified to be statistically independent in accordance with ASCE 4-86 (Reference 3). The spectra generated from the time-histories were compared to existing DCPP DE, DDE, HE, and LTSP ground spectra. The regenerated DE, DDE, HE, and LTSP time histories were used in the seismic time history analysis of the cask anchorage; since the storage cask is anchored to the ISFSI storage pad long period energy will have a negligible impact on the analysis results.

As discussed in Section 2.6.2, PG&E developed the ISFSI Long Period (ILP) earthquake spectra to be used for the analyses of transporter stability, slope stability and ISFSI storage pad sliding to provide extra design margin since these analyses' results could be affected by long period energy. The ILP are 84th percentile spectras at damping values of 2 percent, 4 percent, 5 percent and 7 percent for the horizontal and vertical components that extend out to 10 seconds and which include near fault effects of directivity and fling. The ILP spectra envelops the DDE spectra at 2 percent and 5 percent damping, the Hosgri spectra at 4 percent, 5 percent, and 7 percent damping, and the LTSP spectra at 5 percent damping. Five sets of spectrum compatible time histories were generated from recordings of large magnitude earthquakes (M>6.7) recorded at short distances (<15 km from the fault), and they contain a range of characteristics of the near fault effects.

The modal damping ratios expressed as a percentage of critical damping for the seismic analyses are provided in Table 8.2-1. These damping values are from the DCPP FSAR Update (Reference 4). The analysis approach, results, and conclusions for each of the configurations are discussed separately below.

8.2.1.2.1 Seismic Evaluation of Operations Involving the Cask Transporter - Seismic Configurations 1, 2 and 4

This section discusses the seismic stability evaluation of the spent fuel cask transporter used at the Diablo Canyon ISFSI.

The HI-TRAC transfer cask, containing a loaded MPC, exits the FHB/AB on the cask transport frame in a horizontal orientation. The cask transporter lifts the HI-TRAC and the horizontal lift rig and moves along the road approximately 1.2 miles to the ISFSI storage site, in the process traversing an 8.5 percent (nominal) grade decline and climbing a 6 percent (nominal) grade incline. Figure 4.3-1 shows the cask transporter/transfer cask during this operational mode. At the CTF upending site, the transfer cask is rotated by the cask transporter to a vertical orientation and then moved to the CTF. Figure 4.3-2 shows the HI-TRAC transfer cask in the vertical orientation prior to mating to the overpack. After the MPC transfer operation is executed, the cask transporter carries the loaded overpack in a vertical orientation to its final position on the ISFSI storage pad. Figure 4.4-3 shows the loaded HI-STORM 100SA overpack en route to the ISFSI pad.

The transport route is approximately 1.2 miles long, approximately one third on bedrock and the remaining two thirds crossing surficial deposits over bedrock (Section 2.6.2.6). Because the transport route is about the same distance from the Hosgri fault zone as the DCPP and the ISFSI sites, the ILP spectra are appropriate for use along the transport route where the route is constructed on bedrock and where the transport route crosses surficial deposits over bedrock (approximately two-thirds of the route) as described in Reference 50. Seismic stability analyses of the transporter on the road are provided in References 31 and 46. A transporter stability analysis (Reference 31), described below, was performed for ground acceleration associated with the ILP earthquake. The analysis determined that the transporter would not overturn or leave the roadway (Configurations 1, 2, and 4, and a portion of Configuration 1).

PG&E also performed a seismic evaluation of the cask transporter under ground accelerations twice those of the ILP earthquake accelerations to account for any amplification due to surficial deposits over bedrock beneath the road. This evaluation is documented in Reference 46 and demonstrates that even under these hypothetical conditions, the cask transporter would remain stable and would not overturn or leave the roadway.

PG&E evaluated the risk of an earthquake causing ground accelerations twice those of the ILP occurring simultaneously with cask transport activities (12 hours per year) and concluded that the risk is not credible (less than 10^{-7}) as described in Reference 51.

In summary, the transporter will remain stable under seismic conditions while the transporter is traversing the portions of the route over bedrock and the surficial deposits over bedrock. In addition, PG&E analyses for ground accelerations twice those of the ILP demonstrate that the transporter will remain stable and the risk of such a ground acceleration occurring during cask transport is not credible (less than 10^{-7}).

Methodology

The ILP seismic events for the Diablo Canyon ISFSI, described in Section 8.2.1.2, were evaluated and analyzed for the transporter stability analysis. Five sets of ILP time-histories were used to demonstrate transporter stability as it carries a loaded cask on the transport route. As discussed in Section 2.6.2.6, the ILP spectra and associated time histories are appropriate for use along the transport route.

VisualNastran 4-D (VN) (formerly Working Model 4-D) (Reference 5) serves as the simulation engine to obtain the response to the 3-dimensional seismic events. This computer code has previously been used in licensing the HI-STORM 100 System as described in the HI-STORM 100 System FSAR (Reference 6).

The time-domain dynamic simulations model the cask transporter, the HI-STORM 100SA overpack, the HI-TRAC transfer cask, the MPC (including the fuel basket, fuel, and lid), and the cask lids as rigid bodies. The mass of the MPC and the contained spent fuel is lumped in a free-standing rigid cylinder that, during the earthquake, is free to rattle in the cask cavity.

The cask transporter sits on grade that is subjected to a ground acceleration time history appropriate to the free field ILP event. The simulations use the Holtec generic model of the cask transporter with a track width identical to that planned for the Diablo Canyon cask transporter, but with a reduced track length. This ensures that the results from the dynamic simulations will conservatively bound the response of the real system using a transporter with a longer track length along the roadway.

Acceptance Criteria

The cask transporter plus its carried load must remain stable (not overturn) and remain on the travel path under all seismic events applicable to the Diablo Canyon ISFSI site. The minimum roadway width is 26 ft, which sets the allowable transporter lateral sliding distance. The maximum acceptable sliding movement along the roadway is limited to the DCPP cask transporter track length to ensure that the transporter will remain on the roadway after exiting a turn in the roadway.

Assumptions

The following key assumptions were employed to construct the models for the simulations:

(1) The time domain dynamic analyses of the transporter seismic stability simulate the modeled components (cask transporter, transfer cask, overpack and MPC) as rigid bodies with specified geometry and bounding mass. The connections between the cask body and the lids were assumed to be rigid. These are conservative assumptions for the seismic analysis since energy dissipation in the dynamic system is neglected by virtue of the rigid body modeling.

(2) The time domain dynamic simulations model the MPC and the contained fuel by a solid cylinder with total mass that bounds the heaviest PWR MPC-32 (90,000 lb). This is conservative since all energy dissipation due to fuel assembly rattling inside the MPC is neglected and any reduction in amplitude due to chaotic fuel assembly motion over time is ignored.

(3) The analyses in time domain are simplified by assuming the rigid bodies to have uniform mass density when calculating their mass moments of inertia and mass center locations. Any shift in the centroid due to this assumption has a negligible effect on the results of the analysis.

(4) The coefficient of restitution for the internal contact surfaces (MPC/overpack) is set to zero. The coefficient of restitution between the transporter treads and the ground was set to 0.0 - 0.25 (the exact value has no influence on the solution when sliding motions predominate). For the coefficient of friction at the transporter tread/ground interface, an upper bound value of 0.8 was conservatively assumed to emphasize tipping action. A lower bound value for the tread/roadway surface of 0.4 was assumed to determine the sliding behavior of the transporter. The coefficient of friction between the MPC and the HI-TRAC transfer cask cavity side surfaces is set at 0.5. This is realistic because experience indicates a variation from 0.8 down to 0.2 for steel-on-steel depending on the relative velocity between the two surfaces.

(5) The time domain dynamic simulations use a generic model of the cask transporter with a track length that is shorter than the length of the Diablo Canyon cask transporter tracks. The analyses considered the stability of the cask transporter when supported by a horizontal ground surface.

(6) In all stability analyses, the positioning of the cask in the cask transporter is set slightly higher than the anticipated carry height to ensure that overturning moments are conservatively computed at each time point during the dynamic simulations.

(7) All bodies are assumed to be rigid for the global analysis. The cask transporter design specification includes a requirement that the transporter be designed such that its lowest global natural frequency is in the rigid range (>33 Hz).

Key Input Data

The key input data used in the cask transporter seismic analyses are shown in Tables 8.2-2 through 8.2-4. Input time histories used for the dynamic simulations are five sets of ILP design earthquake excitations. These seismic events are identified below with their duration:

Set 1: Lucerne Valley (48 sec)
Set 2a: Yarimca (40 sec)
Set 3: LGPC (22 sec)
Set 5: El Centro (40 sec)
Set 6: Saratoga (40 sec)

Results of Analyses

A series of nonlinear dynamic simulations were performed using the VisualNastran 4-D computer code to assess the seismic stability of the cask transporter during the five ILP earthquakes. Table 8.2-5 lists the simulations performed for the stability evaluation. The combinations of grade, coefficient of friction, and seismic events have been chosen to be bounding for the site-specific conditions.

For each case considered, the loaded transporter was assumed to be on a flat or inclined surface with specified coefficients of friction. The simulations performed under Phase 1 serve to identify potentially bounding events from among the five candidate time histories. The choice of simulations for the remaining phases was based on the results from the simulations in Phase 1. The combination of grade and coefficient of friction were chosen to induce sliding as opposed to tipping.

Table 8.2-6 summarizes the estimates of the maximum transporter horizontal excursions in the transverse and longitudinal direction for each phase of the dynamic simulations performed. The reported maximum excursions are at the top of the transporter relative to the ground.

These results are bounding for all Diablo Canyon cask transporter operational modes and for all ILP earthquakes. The maximum value of 10.7 inches reported for the transverse excursion with a coefficient of friction of 0.4 demonstrates that in the event of seismic excitation, the transporter will not leave the road while moving from the FHB/AB to the Diablo Canyon CTF or while moving from the CTF to the ISFSI. The small relative movements reported for the case with friction coefficient of 0.8 demonstrate that overturning of the loaded cask transporter is not a credible event under the ILP seismic events. For the case where the transporter is on the 8.5 percent grade when the seismic event is postulated to occur, the results demonstrate that, the maximum sliding movement along the axis of the road (30.2 inches) is less than one transporter track length. In addition, the transverse movement of the transporter during a seismic event is small, 10.7 inches, compared to the distance between the edge of the transporter and the edge of the roadway (roadway minimum width is 26 ft and the width of the transporter from outside of track to outside of track is approximately 17.5 ft), provides additional margin of safety.

The time domain dynamic simulations of the cask transporter demonstrate that the cask transporter, carrying either a loaded HI-TRAC transfer cask in the horizontal orientation or a loaded HI-STORM 100SA overpack in the vertical orientation, will not overturn during a seismic event and will not leave the road while moving from the FHB/AB to the CTF or from the CTF to the storage pads. When the transporter is carrying a HI-TRAC horizontally, up or down the 8.5 percent grade, the magnitude of sliding displacement along the axis of the road is less than the length of the transporter track.

Cask drop during transport (seismic)

As discussed in Section 8.2.4, the load path portions of the cask transporter and the lifting devices attached to the cask components will be designed to preclude drop events, either through redundancy or enhanced safety factors. The design will include consideration of seismic loads. Therefore, a seismic event occurring during transport would not result in a cask drop. In addition, Holtec has qualified the HI-TRAC with an MPC for a horizontal cask drop of 42 inches (Section 3.4.9 of Holtec's Hi-STORM 100 System FSAR).

8.2.1.2.2 Seismic Analysis of Cask Transfer Facility Seismic Configuration 3

8.2.1.2.2.1 CTF Steel Structure

The CTF at the Diablo Canyon ISFSI is used in conjunction with the cask transporter to perform MPC transfers between the HI-TRAC transfer cask and the HI-STORM 100SA overpack. Prior to the transfer operation, the empty HI-STORM 100SA overpack is placed in the CTF. The overpack is lowered to the full down position in the CTF and a mating device is installed on the top of the overpack. This mating device serves as a structural connection and an alignment device between the top of the overpack and the bottom of the HI-TRAC transfer cask. The transfer cask is positioned over the overpack by the cask transporter, which remains in position during the transfer operation. Restraints are used to secure the cask transporter to ground during the MPC transfer operation.

The cask transfer facility is shown in Figure 4.4-3 and includes the following main structural components:

Main Shell – A cylindrical shell is positioned into a larger vertical hole in the rock with concrete backfill providing an interface connection with the rock walls of the hole. The bottom of the shell is anchored to a reinforced concrete base. This cylindrical shell serves as the cavity liner into which the overpack is lowered and provides the support for the lifting jacks and a set down location for the lifting platform when the lifting platform is fully lowered. Three vertical stiffening extensions (U-shaped) run the length of the cylinder shell and act as the main structural members that transfer the loads from the lifting jacks to the shell and down to the base. Restraints are installed at the top of the shell, which serve to restrain the cask under lateral loads from seismic events (Reference 47).

Lifting Jacks – Three lifting jacks are used to raise or lower the lifting platform. They are located in the three vertical stiffening extensions on the circumference of the main shell. The lifting jacks are supported at the top end and have traveling nuts that operate in unison to keep the platform level.

Jack Supports – Jack platform plates and gussets are welded to the top of the shell extensions to provide support for the lifting jacks.

Lifting Platform – A lifting platform of built-up plates provides vertical support of the HI-STORM 100SA overpack and transmits the load to the lifting jacks. During the lifting operation, a uniform loading of the lifting platform is afforded by the location and controlled movement of the lifting jacks. Support plates together with the top and bottom platform plates form the lifting platform structural frame. A cover plate covers the lifting platform plate and provides a base on which the overpack rests. The lifting platform has extensions that reach into each main shell stiffening extension to interface with the lifting jacks. Gussets are welded to the platform outer plates to provide a stiff structural member in the vicinity of the lifting jacks.

Reinforced Concrete Support Structure -The CTF steel structure is placed on a steel reinforced concrete foundation slab and surrounded by heavily reinforced concrete up to the surface. The concrete structure will carry all the compressive loadings on the base and the side-walls (cylindrical in shape) to the ground rock. The structure will have an adjoining gravity fed sump for drainage.

This section discusses the seismic structural analyses and evaluations of the CTF at the Diablo Canyon ISFSI. The capacity of the CTF structural components is evaluated including the lifting jacks, the jack supports, the shell extensions, and the lifting platform. The calculations provide the loads on the CTF base, CTF shell, and surrounding concrete under the specified ASME Section III (Reference 7), Subsection NF service (Level A and Level B) load conditions and Appendix F seismic (Level D) load conditions. A description of the analysis of the reinforced concrete support structure is also included.

Methodology- Structural Analysis

The analysis (Reference 32) evaluates the capacity of the CTF structural components under static loads (dead weight and factored dead load) and under static plus seismic and wind loads. Bounding values for the weights of the spent fuel casks and canisters are used to evaluate the dead loads applied on the CTF structure. In accordance with the HI-STORM 100 System FSAR (Reference 6), the dead loads incorporate an inertia amplification of 15 percent during the lifting operation (factored dead load). Quasi-static stability analyses provide the magnitudes of the seismic loads on the CTF steel structure during the governing LTSP earthquake excitation. The natural frequencies of the cask transporter, the HI-TRAC transfer cask, and the HI-STORM 100SA overpack stack was calculated. The actual horizontal spectral acceleration value corresponding to 19.85 Hz was used in the seismic analysis. Under vertical excitation, the ground vertical zero period acceleration value was used in the seismic analysis since the stacked configuration is rigid in the vertical direction. Examination of the response spectra for the four DCPP seismic events (DE, DDE, HE and LTSP) shows that the bounding spectral accelerations for CTF structural design are those from the LTSP spectra.

The analysis considers the most critical combinations of design loads for the loading scenario wherein a loaded HI-TRAC transfer cask is stacked on top of the HI-STORM 100SA overpack in the full down position (Configuration 3) (Figure 4.4-4).

The seismic analysis considers two critical combinations of the specified design earthquake components when the CTF structure is subjected either to upward vertical inertia forces or downward vertical inertia forces. The Newmark 100-40-40 Method is used to combine the three specified directions of the seismic load.

Using the calculated inertia loadings together with known dead loading, strength-of-materials solutions from the theory of elasticity are used to determine the stresses in the CTF structural components and weld connections. The ratio of the allowable stresses to the calculated stresses in the components and welds defines safety factors for service (Level A) and seismic (Level B and Level D) load conditions.

Acceptance Criteria

The stresses in the CTF structural components and welded connections under the service loads must be below the limits prescribed in ASME Section III, Subsection NF (Level A and Level B). The stresses in the CTF structural components and welded connections under the combination of dead plus seismic loads must be below the limits prescribed by ASME Section III, Appendix F (Level D).

The lifting jacks, as the primary load-bearing components, must meet the design criteria of Section 4.2 of ANSI N14.6 (Reference 8) and Section 5.1.6 of NUREG-0612 (Reference 9) applied to the lifted load, including any dynamic effects.

The seismic connectors at the CTF (cask transporter to ground, and between the . transfer cask and the overpack) must have sufficient structural capacity to prevent extensive motions of the transfer cask during MPC transfer operations that could put the contained fuel at risk. The load capacity of all necessary connectors is designed to meet the applicable limits of ASME Section III, Subsection NF and Appendix F.

Assumptions

The following conservative assumptions are employed in the linear elastic structural analyses:

- The stability analysis of the CTF shell extensions conservatively neglects any contributory stiffening from the main shell and ignores the support from the concrete fill between the shell and the rock walls.

- The structural analysis of the lifting platform built-up plate structure is conservatively analyzed as a beam structure, thus neglecting any two-dimensional plate bending that would decrease the computed stress.

Key Input Data

The key input data used in the CTF seismic analyses are shown in Table 8.2-7. The seismic inputs for the analyses are obtained from ground acceleration response spectra for DCPP. The ZPAs for the vertical direction were used because the stacked casks in the CTF are rigid (>33 Hz) in the vertical direction. The spectral accelerations in the horizontal directions corresponding to 19.85 Hz were used. The ZPAs and spectral accelerations used in the analysis are shown in Table 8.2-8. Where load combinations are required for the strength evaluation, the Newmark 100-40-40 Method (for LTSP seismic event) is used to combine the three specific directions of the seismic load.

Results of Analyses

The results from the CTF structural analyses demonstrate that all structural members and welds stresses satisfy the condition that safety factors are greater than 1.0. Safety factors are defined as:

SF= (Allowable stress or load)/(Calculated stress or load).

In addition to the structural analysis of the CTF components, mandated by the appropriate design codes, analyses of the connector restraints (that inhibit relative movements between the cask transporter and ground) and the mating device (between the transfer cask and the overpack) will also be performed to ensure that any relative motion between the transfer cask and the overpack during the cask transfer operation will not compromise the integrity of the MPC. Load/stress limits on these ancillary items meet applicable requirements of Subsection NF and Appendix F. In order to optimize the design of connector restraints and mating device, it may be necessary to restrain the HI-TRAC transfer cask to ground.

8.2.1.2.2.2 CTF Reinforced Concrete Support Structure

Methodology - Structural Design/Analysis

A static analysis (Reference 30) was performed to appropriately size the base slab and the side cylindrical wall to accommodate the applied forces generated by the CTF as discussed in 8.2.1.2.2.1.

Acceptance Criteria

ACI-349 97 (Reference 10), in compliance with NUREG-1536 (Reference 13), concrete stress allowables and DG-1098 (Reference 11), as applicable are used.

Assumptions

None

Key Input Data

The surrounding rock properties and the functional requirements of the CTF steel structure (as described earlier in this section) and the loads developed in the CTF analysis (Section 8.2.1.2.2) are the key input parameters.

Results

The reinforced concrete structure meets the stress requirements of ACI 349-97 and the functional requirements of the facility.

8.2.1.2.3 Seismic Analyses of the HI-STORM 100SA Overpack Anchored to the ISFSI Storage Pad in its Long-Term Storage Configuration Seismic Configuration 5

8.2.1.2.3.1 Cask and Anchorage Seismic Analysis

The HI-STORM 100SA overpack design differs from the HI-STORM 100S only in that it includes an extended bottom flange and gussets that enhance the structural resistance of the flange/shell around the bottom periphery of the overpack (see Figure 4.2-7). This flange includes a bolt circle to permit structural "mating" of the overpack to the ISFSI storage pad steel embedment plate by 16, 2-inch diameter, SA193-B7 preloaded cask anchor studs. The preloaded cask anchor studs are threaded into compression/coupling blocks to ensure a continuous compressive state of stress at the interface between the lower surface of the HI-STORM 100SA overpack and the top surface of the embedment plate. The continued contact ensures development of interface friction forces sufficient to resist lateral movement of the overpack base relative to the embedment plate. It also ensures that the ISFSI storage pad embedment structure provides the resisting moment to stabilize the system under seismic loading. The cask anchor studs are threaded into compression/coupling blocks that bear against the lower surface of the embedment plate from the action of the preload. The embedment plate is held to the concrete by 16 longer embedment anchor rods that are threaded into the same compression/coupling blocks, but are not preloaded. The embedment anchor rods are only loaded, as the seismic event proceeds, to the extent necessary to maintain vertical force and moment equilibrium. Oscillations in the cask anchor stud load are minimized due to the presence of the initial preload. Figure 4.2-2 shows a section depicting the embedment plate, the compression block, the cask anchor studs and the embedment anchor rods. The cask is not shown in this figure.

The cask and anchorage seismic analyses are not sensitive to long period ground motion. Therefore, these analyses (Reference 38) were performed using the four DCPP seismic events (DE, DDE, HE, and LTSP). The DE, DDE, HE, and LTSP are characterized by free-field acceleration time-histories, in each of three orthogonal directions, with durations of 41 seconds for the DE and DDE cases and 48 seconds for the HE and LTSP cases. The HE and LTSP events have the highest, zero-period accelerations, and the largest, free-field excursions. Therefore, the results from these events are bounding and the dynamic simulations to obtain time-history behavior of the system are performed using the VisualNastran (VN) simulation code described previously only for these two events.

<u>Methodology</u>

The dynamic model of the HI-STORM 100SA overpack in VN consists of the following major components:

(1) The HI-STORM 100SA overpack plus the embedment plate is modeled as a six degree-of-freedom (rigid body) component.

(2) The loaded MPC is also modeled as a six degree-of-freedom (rigid body) component that is free to rattle inside the overpack shell. Gaps between the two bodies reflect the nominal dimensions from the design drawings in Reference 12.

(3) The embedment anchor rods provide the vertical connection between the embedment plate and ISFSI slab. The embedment anchor rods are

modeled as individual linear springs connecting the periphery of the extended baseplate to the ISFSI storage pad section. The concrete pad/embedment compression resistance at the interface is simulated with compression-only stiffness elements around the periphery.

(4) For the global dynamic analysis of the anchored cask, the slab section under the cask is assumed rigid and the three components of acceleration and time-history are applied simultaneously at the base of the slab. Since the HE and LTSP events provide the bounding loads to the anchorage, the importance of directional effects on the responses is evaluated for both the HE and LTSP events by repeating the simulations with the only change being the negative of the vertical seismic time history is used in conjunction with the specified horizontal time histories.

(5) The contact between the MPC and the overpack is simulated by a classical impulse-momentum equation. The coefficient of restitution (COR) is set to 0.0 reflecting the large contact areas involved and the coefficient of friction is set to 0.5, which is representative of steel-on-steel. This is a realistic assumption and allows for energy loss during contact between the two, large rigid bodies.

(6) The interface contact between the base of the overpack and the ISFSI storage pad embedment is modeled by discrete linear springs to simulate the embedment anchor rods and by compression-only elements to simulate the balancing force from the embedment. The spring rates are computed using established methodology for embedment anchor components. Damping is consistent with that specified for steel and concrete components in Table 8.2-1. These are realistic assumptions that appropriately model the expected interface behavior.

(7) Bounding (high) weights for the cask components are used for conservative results; inertia properties are computed consistent with these bounding weights.

Each VN dynamic simulation produces time-history results for the tensile loads in each of the 16 embedment anchor rods, as well as time-history results for the total interface compression load between the base of the embedment plate and the ISFSI pad concrete. The results of the VN-time-history analyses are stored in spreadsheet form and a FORTRAN computer code is used to post-process the results to determine vertical-load and overturning-moment time-histories for subsequent structural-integrity evaluation. Figure 8.2-1 shows an expanded model of the components (excluding the 16 anchor rods) that make up the dynamic model.

To ensure the capture of all energy from a seismic event, while at the same time eliminating high frequency components not pertinent to satisfying Code requirements in a structural evaluation, the filtering frequency for processing the "raw" numerical results is set as 40 Hz. The use of filtering of dynamic results in cask structural integrity analysis has been previously licensed for the HI-STORM 100 System as described in the HI-STORM 100 System FSAR.

__Acceptance Criteria:__

The design criteria for the HI-STORM 100 SA overpack are discussed in Chapter 2 of the HI-STORM 100 System FSAR, as amended by Holtec LAR 1014-1 (Reference 12). The anchorage system, being an integral part of the overpack structure, is subject to the same design requirements. The anchorage (cask anchor studs, sector lugs, and adjacent shell structure) is designed to meet the static stress limits of ASME Section III, Subsection NF and Appendix F (Reference 7).

Two conditions for analysis are defined as follows:

(1) Level A (Preload) - The anchor stud preload is established at approximately 157 kips in each stud. Under this load and the corresponding balancing load from the ISFSI storage pad, the sector lug structural components must meet the allowable stress limits for plate and shell structures given in Article NF-3200. The stress limits at 200°F for SA-516, Grade 70 material (used for the sector lugs) listed in Table 3.1.10 of the HI-STORM 100 System FSAR are used in the acceptance evaluation.

(2) Level D (Preload plus Seismic Load) - In accordance with Appendix F of ASME Section III, the tensile stress in the stud, averaged through the cross-section is limited to 70 percent of the ultimate strength of the stud material. The extreme fiber stress in the stud is limited to ultimate strength per F-1335.1. The design criteria and stress intensity limits for the sector lug components are given in Chapter 2 and Table 3.1.12, respectively, of the HI-STORM 100 System FSAR, as amended by LAR 1014-1. The stud alternating stress intensity under the dynamic loading induced by the seismic event must be sufficiently low to ensure a safety factor greater than 1.0 against fatigue failure for the number of stress intensity cycles associated with the seismic event.

In addition to the above anchorage acceptance criteria, it is required to demonstrate that the seismic events do not induce acceleration levels in the body of the cask that exceed the cask design basis (45 g) as defined in the HI-STORM 100 System FSAR (Reference 6).

__Assumptions__

The key assumptions used in the dynamic model are listed and explained within the methodology description given above.

Key Design Inputs

Bounding weights of 270,000 lb for an empty HI-STORM 100SA and 90,000 lb for a loaded MPC are used in the analyses (References 6 and 12, Table 3.2.1). SA193-B7 material is used for the anchor stud material. For the dynamic analyses, anchor stud minimum yield and ultimate strengths of 105 ksi and 125 ksi, respectively, are used. Dimensions for the two cask bodies are taken from Drawing 3187 in Reference 12. Mass moment of inertia properties are determined based on cylindrical body assumptions with the specified mass uniformly distributed.

The spring rate of the embedment anchor rods is equivalent to a 2-inch diameter carbon steel rod, 48 inches long.

Seismic inputs for the dynamic analyses are obtained from acceleration time histories developed from the response spectra for each of the DCPP earthquakes.

Results of Analyses

The results from the series of analyses performed for the anchored cask can be summarized as follows:

(1) The anchored HI-STORM 100SA overpacks do not exceed the generic cask design basis deceleration limit of 45 g under any of the seismic events.

(2) The state of stress in the cask anchor studs and in the overpack bottom flange, gussets, and the shell structure remain below the stress limits of ASME Section III, Subsection NF and Appendix F under all seismic events.

(3) The interface loads on the embedment structure determined for the ISFSI pad structural qualification are summarized in Table 8.2-9. The peak values are obtained from the filtered, time-history results for embedment anchor rod tension and for interface compression from the dynamic simulations.

A finite element analysis of the sector lug was performed using as input the tensile load in the cask anchor stud. Structural integrity evaluations were performed for both Level A (where the preload is balanced by compression between the extended flange and the embedment plate) and for Level D conditions (where local lift-off of the flange is assumed and the stud maximum load capacity is conservatively assumed). The results from the finite element analyses are reported in Table 8.2-10.

The maximum values obtained for the interface loads at the embedment structure are summarized in Table 8.2-9 and form the input for the structural integrity evaluation of the ISFSI pad.

The bounding cask weight is 360 kips. Using the maximum net shear force result from Table 8.2-9 and dividing by the cask weight provides the effective "g" loading on the cask as 1.43 g. This demonstrates that the cask design basis deceleration level (from the HI-STORM 100 System FSAR) of 45 g is not exceeded with a large margin of safety.

The results summarized in Table 8.2-9 provide the information needed to determine the coefficient of friction required at the cask/embedment plate interface to ensure that there is no relative sliding at that location. These results are obtained by dividing the net filtered shear force by the filtered normal force at each instant of time through the simulation. From the simulations performed, the largest required value for the coefficient of friction is 0.18. In accordance with the ASME Code (NF-3324.6, Table 3324.6(a)(4)-1), a minimum coefficient of friction of 0.25 may be assumed to exist at the interface when preload is used. Therefore, the minimum safety factor against sliding of the cask relative to the embedment plate is 1.39 and the desired benefit of the preload is assured.

To evaluate the propensity for a failure by fatigue in the sector lug, the results from the finite element stress analysis of the sector lug under the limiting tensile load was used. Using the recommended methodology for fatigue analysis as outlined in ASME Section III and determining the likely number of stress cycles by using the results from the dynamic analyses, large margins of safety against a fatigue failure during a single seismic event were obtained. Therefore, fatigue failure of the overpack anchorage is not credible at the Diablo Canyon ISFSI.

To ensure continued maintenance of the design bases assumptions for preloading of the anchorage connections, PG&E will develop an inspection program that periodically visually checks a sampling of the exposed portions of the anchor studs, washers, nuts, and storage cask baseplate surrounding the nuts to note any degradation or relaxation of these connections. This program will verify that the studs, washers, and nuts have not turned from their as-left preloaded position, are not loose to the touch, and that visually their mating surfaces remain engaged. This verification will be performed as part of the 10 CFR 50 DCPP Maintenance Rule Program developed for compliance to the maintenance rule and will have similar periodic inspection requirements.

8.2.1.2.3.2 Storage Pad Seismic Analyses

The objective of the seismic analyses of the concrete pad is to ensure that the steel reinforced concrete pads and the anchored casks remain functional during all seismic conditions. A static analysis was performed to determine the storage pad size and thickness required to resist the loads resulting from seismic accelerations (DE, DDE, HE, and LTSP ground zero period acceleration [ZPAs]) applied to the pad, in addition to the resultant loads from the cask dynamic analysis (Section 8.2.1.2.3.1). Also, a nonlinear time history analysis of the cask/pad set-up was performed to determine the extent of sliding that occurs at the pad/rock interface.

Pad Static Analysis

Methodology

The analysis is a nonlinear static finite element analysis (FEA), Using the ANSYS computer code. The storage pad size and thickness analysis is not sensitive to long period ground motion. Therefore, this analysis (Reference 29) was performed using the four DCPP seismic events (DE, DDE, HE and LTSP). The seismic inputs used for this analysis were HE and LTSP ZPAs. The HE and LTSP spectra were used since these spectra produce the largest ZPAs and the cask/pad interfaces are not sensitive to longer period ground motion. The concrete slab was allowed to lift off the rock support if the loads and geometry dictate that liftoff should occur. All material properties are linear. Compression only gap elements are used at the interface between the slab and the rock. This is the only nonlinear modeling feature in the analysis.

The FEA model consists of the pad, portion of the underlying rock, and elements representing the cask on top of the pad. The casks are modeled up to a plane, 118.5 inches above the slab. This is the location of the center of gravity of the casks and is, therefore, where the loads are applied. The pad uplift and concrete stresses are determined by the FEA analysis. The steel embedment/anchorage structure is designed to meet the ductile anchorage provisions of the proposed new draft Appendix "B," dated October 01, 2000, to ACI-349-97. Other provisions of Appendix B are not applicable due to the thickness of the pad and length of the rod. Specifically, design strength capacity of the embedded base plate; concrete bearing and diagonal tension shear capacity computed must be more than the required ductile design strength of the embedded rod/stud. The Newmark 100-40-40 Method is used to combine the three specified directions of the seismic load.

Acceptance Criteria

Concrete and the embedded steel structures, are designed to the requirements of ACI-349-97 and ductility provisions of Draft Appendix "B" dated October 01, 2000, and NUREG-1536 (Reference 13).

Assumptions

Normal engineering assumptions associated with developing FEA models (for example, boundary conditions, modeling techniques). The anchorage evaluation methodology used assumes the loading imposed on the pad embedment structure is similar to an inverted column and as such diagonal shear provisions of the ACI, Section 11.3, were followed.

Key Input Data

Table 8.2-9 shows the resultant cask loading on the pads. The underlying rock material properties have an impact on the analysis. The rock's Young's modulus range of

0.2×10^6 psi to 2.0×10^6 psi were considered in the analysis to account for variability of the rock types.

Rock elastic properties for the analyses were obtained from References 48 and 49. These properties are stress-strain dependent; that is, they are appropriate only for the range of stresses and strains for which they are determined.

A check was made of the calculation results in Reference 29 to verify that stresses and strains calculated in the underlying rock mass were within the range for which use of the rock properties is appropriate. It was determined that the average values of shear and compressive strain calculated within a volume of rock approximately 35 ft deep beneath an ISFSI pad are comparable to the range of strains for which the rock elastic properties were determined. Therefore, the elastic properties are appropriate for use in pad load-displacement analyses.

Results

The maximum pad stresses and the embedded steel ductility requirements meet the ACI 349 code requirements. The yield strength of the embedded studs is greater than 250 percent of the computed demand load on these studs. The maximum potential uplift on an edge of the pad is less than 1/32 inch to 1/8 inch, depending on the variation in the rock properties.

Pad Sliding Dynamic Analysis

Methodology

A nonlinear time history analysis of the cask/pad structure sliding at the rock/pad interface was performed (Reference 28). The methodology for determining sliding resistance along the base of the pads is provided in Reference 39. Analyses were performed with the five sets of ILP time histories. The ILP time histories were used since the pad sliding analysis may be sensitive to long period ground motion and the use of ILP time histories produces bounding results.

A nonlinear stick model is developed for the purposes of these analyses. A lollypop stick model representing the cask behavior represents the set of 20 casks on a pad. The pad is represented by its mass only. The interface between the rock and the pad surface is modeled using SAP2000N's NLLINK element with friction properties. This element is a biaxial friction element that has coupled friction properties for the two shear deformations, post-slip stiffness in the shear directions, gap behavior in the axial direction. The cask superstructure stick is modeled such that it represents the dynamic properties of the anchored cask. [The cask and anchorage seismic analysis described in Section 8.2.1.2.3.1 models the anchored cask (in the absence of sliding of the pad) and perform dynamic analysis to predict the cask/pad interface design shears, moments, tension, and compression forces to be used in the pad design.] The fundamental frequency of the cask superstructure in sliding analyses is based on best estimate of the rocking frequency of the anchored cask. In the absence of local nonlinearities, it is expected that the fixed base model (no pad sliding) of the cask will yield slightly more conservative results than Section 8.2.1.2.3.1 results. The same model when mounted on the friction element is called the sliding model. The relative ratio of peak response between the sliding model and the fixed base model will yield an adjustment factor, which if found to be greater than unity, would have to be applied to the design shears and moments predicted by the analysis described in Section 8.2.1.2.3.1. This approach identifies any potential increases in design responses due to sliding.

For the vertical direction, the tensile component of cask/pad reactions is studied. This component is judged to be an important parameter that controls the normal resisting force at the interface, thus affecting the sliding displacement during a seismic event.

All analyses are performed based on the nonlinear time-history analysis option using Fast Nonlinear Analysis (FNA) approach of SAP2000N computer FEA program.

<u>Acceptance Criteria</u>

The pad must maintain its ability to perform its functional requirements with insignificant impact on the cask design qualifications.

<u>Assumptions</u>

Net Vector sliding is conservatively calculated assuming simultaneous peak X and Y horizontal sliding displacements.

<u>Key Input Data</u>

The analysis was performed assuming two pad-to-rock interface sliding friction coefficients $\mu = 1.19$ corresponding to a friction angle of 50 degrees, and $\mu = 0.73$ corresponding to a friction angle of 36 degrees. This represents the range of the sliding friction coefficient expected at this interface.

Cask Weight:	W = 360 kips
No. of Casks on a pad	20

<u>Results</u>

Based on the results of these analyses, the following is concluded:

(1) The best estimate of maximum pad sliding for a lower bound friction coefficient of 0.73 corresponding to a rock friction angle of 36 degrees is estimated as 1.21 inches.

(2) The best estimate of maximum pad sliding for an upper bound friction coefficient of 1.19 corresponding to a rock friction angle of 50 degrees is estimated as 0.41 inches.

(3) The above pad sliding displacements are considered small and not large enough to cause any damage to the pad or the casks. The acceptance criteria for pad sliding is defined as whether pad sliding results in increased design shears and moments at the cask-to-pad interface, which is discussed further below.

(4) After pad sliding is considered, it is concluded that the cask design shear of 515 kips (load on to the pad) remains valid for design. The best estimate of the adjustment factor to account for the effects of pad sliding is calculated as 0.95 for a friction coefficient of 1.19, and 0.90 for a friction coefficient of 0.73. Both of these ratios are below unity, as such the design shear of 515 kips (and associated moments) remains valid for design.

(5) The best estimate of maximum vertical tensile load after sliding remains unchanged. Thus the design axial bolt tensions of the analysis described in Section 8.2.1.2.3.1 remain valid.

(6) The response spectra comparison plots of the rock versus pad sliding indicate that the responses at the cask-to-pad interface generally do not vary up to about 16 Hz. However, above this frequency some differences in the responses are seen as a result of sliding. An evaluation by the cask supplier determined that there were no components inside the cask are sensitive to changes in input motion in this higher frequency range. The highest peak spectral ordinate associated with change in motion as a result of pad sliding is 4.1 g at approximately 26 Hz and 5 percent critical damping well below the cask qualifications.

(7) Given that the base shear (and therefore base moments) and axial tension do not change as a result of pad sliding, it is concluded that analyses described in Section 8.2.1.2.3.1 remain valid.

8.2.1.3 Earthquake Accident Dose Calculations

The HI-STORM 100SA overpack and the HI-TRAC transfer cask were explicitly analyzed for, and shown to withstand the seismic ground motion during transport to the CTF, during activities conducted at the CTF, during movement from the CTF to the storage pads, and during storage operations, as applicable. The seismic ground motion does not cause stresses above allowable limits in the MPC confinement boundary, the transfer cask, or the storage overpack during canister transport, transfer, or storage operations. The CTF and cask transporter structures are also designed to withstand the

DCPP ground motion. No radioactivity would be released in the event of an earthquake and there would be no resultant dose.

8.2.2 TORNADO

A tornado is classified as a natural phenomenon Design Event IV, as defined in ANSI/ANS-57.9. This event involves the potential effects of tornado-induced wind, differential pressure, and missile impact loads on the ISFSI SSCs that are important to safety. The design basis wind and tornado evaluation is provided in Reference 27.

8.2.2.1 Cause of Accident

The cause of this event is the occurrence, at or near the ISFSI site, of meteorological conditions that are favorable to the generation of a tornado. The design-basis tornado wind speed for the ISFSI is based on a conservative estimate appropriate for DCPP (annual probability of 10^{-7}), which was developed by the NRC (SSER No. 7). The specific topography associated with the plant site indicates that the postulated tornado event is unlikely. However, it has been included in the ISFSI design basis as a potential accident event.

8.2.2.2 Accident Analysis

The accident analysis for tornado effects involves evaluation of the loaded transfer cask during transport to the CTF, MPC transfer activities at the CTF, transport of a loaded HI-STORM 100SA overpack to the ISFSI pad, and long-term storage of the loaded overpack at the ISFSI pad. As discussed in Section 3.2.1 and 4.2.3.3.2.6, tornado-wind and missile design criteria are a combination of Diablo Canyon site-specific winds and missiles and the design-basis missiles described in the HI-STORM 100 System FSAR. In the evaluation of the Diablo Canyon ISFSI for tornado effects, the missiles were categorized as large, intermediate, or small missiles and were compared with those missiles for which the HI-STORM 100 System was generically designed to withstand. The description, mass, and velocity of all missiles considered for evaluation are listed in Table 3.2-2. As noted in Table 3.2-2, some of the additional Diablo Canyon ISFSI missiles were conservatively evaluated for the generic Region II missile velocities described in NUREG-0800, Section 3.5.1.4. The 1800 kg automobile and the 4 kg, 1-inch-diameter steel rod were determined to be the bounding large, and small missiles, respectively. For the intermediate missile category, the 500-kV insulator string was found to be bounding for penetration resistance and the 8-inch-diameter steel rod was determined to be bounding for the global stress evaluation.

The bounding large and intermediate (for penetration only) missiles were chosen by comparison of the kinetic energies of the missiles. The small missile was chosen based on the guidance of NUREG-0800, Section 3.5.1.4, for selecting a missile that can pass through an opening in a protective barrier. For the global stress evaluation of the intermediate category missile, the bounding missile was chosen based on a comparison of safety factors (SF), the missile producing the lower SF being bounding. If the generic analysis described in the HI-STORM 100 System FSAR was bounding, no additional evaluation was performed. If a DCPP site or Diablo Canyon ISFSI-specific missile was bounding, an analysis was performed for the applicable component (that is, the overpack and/or the transfer cask). The following is a summary of the evaluations performed for the four operating ISFSI configurations: transport to the CTF, MPC transfer activities at the CTF, transport to the ISFSI pad, and long-term storage at the ISFSI pad.

The missile impacts are analyzed using formulas from Bechtel Power Corporation Topical Report BC-TOP-9A (Reference 14), ORNL Report TM-1312 (Reference 33), and energy balance methods. In all cases, at all locations away from the impact locations, missile-induced stresses in the transfer cask and overpack are below ASME Level D stress intensity limits.

Another possible consequence of a tornado is to cause the collapse of a nearby 500-kV transmission tower. This event is discussed in Section 8.2.16.

8.2.2.2.1 Transport to the CTF

The transfer cask is transported between the DCPP FHB/AB and the CTF in a horizontal position. Section 3.4.8.2.2 of the HI-STORM 100 System FSAR discusses the side impact from a large missile and concludes loads are below ASME Level D stress intensity limits. The small missile is bounded by the intermediate missile. The evaluations for the side, top, and bottom impact from an intermediate missile (344.7 kg insulator string traveling at 157 mph) are as follows.

- For the side impact, conservatively neglecting the water jacket and the lead shielding, the intermediate missile will penetrate the outer steel shell, but will not penetrate the 3/4-inch inner shell of the transfer cask. Using this conservative model, the minimum inner shell thickness required to withstand the missile impact is 0.266 inch. The design inner shell thickness is 0.75 inch.

- A bottom shield is attached to the transfer cask while suspended horizontally in the cask transporter. On the bottom of the transfer cask, the missile impact occurs on the bottom shield, which covers the pool lid. The HI-STORM 100 System FSAR contains an evaluation for the impact of the intermediate missile on the HI-TRAC transfer lid door. The analysis shows that the intermediate missile would not penetrate the 2-1/4-inch, carbon-steel top plate of the transfer lid door. The minimum required steel thickness to withstand the missile impact is 0.619 inch. This evaluation is conservative for the configuration used at the Diablo Canyon ISFSI, which includes the pool lid (3 inches of steel) and the bottom shield (7-1/4 inches of steel).

- On the top of the transfer cask, the top lid has a hole for rigging, lowering, and raising the MPC during transfer of the canister between the transfer cask and the overpack. While suspended horizontally, this hole is shielded from tornado missiles by the cask transporter body. Conservatively neglecting credit for the missile protection provided by the transporter, an analysis was performed for the 500-kV insulator string intermediate missile entering the transfer cask through the hole in the top lid and impacting the MPC lid. If the insulator string missile directly impacts the MPC, it will not penetrate the 9-1/2-inch-thick, stainless-steel lid. The global stress analysis of the 8-inch steel cylinder missile impacting the MPC lid yielded a safety factor against failure of the peripheral MPC lid-to-shell (LTS) weld of 1.23 versus a safety factor of 7.1 for the insulator string.

8.2.2.2.2 Transfer Operations at the CTF

During MPC transfer operations at the CTF, the transfer cask and the overpack are oriented vertically with the transfer cask stacked on top of the overpack. All but approximately the top 3 ft of the overpack are below grade and not susceptible to tornado missile strikes. The top of the overpack is shielded by the transfer cask until the transfer cask is removed to allow installation of the HI-STORM lid. As discussed in Section 8.2.3.1, cask transport and transfer operations will not be conducted during severe weather. The top of the MPC will only be exposed for a short duration (nominally less than 4 hours). Therefore, in the configuration with the lid removed, a tornado missile impact is not credible. With the top of the MPC exposed during this time, the evaluation of an intermediate missile impact on the MPC lid, described in Section 8.2.2.2.1 ensures the MPC integrity is maintained.

In the vertical orientation, the top of the transfer cask is not subject to direct impacts from these missile strikes and the bottom of the transfer cask is not exposed to tornado-missile strikes. The evaluation of the missile strike on the side of the transfer cask described in Section 8.2.2.2.1 is applicable for this configuration.

8.2.2.2.3 Overpack Transport to the ISFSI Pad

The effect of tornado missiles impacting the transporter while carrying an overpack during transport to the ISFSI pad was evaluated for a horizontal large tornado missile. The transporter with overpack will not turnover from the impact.

Tornado wind effects are enveloped by the HI-STORM 100 System FSAR analysis of a freestanding HI-STORM on a pad. The overpack is lifted only to those heights necessary to travel from the CTF to the ISFSI storage pad. Typically, this is only several inches. This small lift height eliminates tornado missiles striking the bottom of the cask as a credible event.

8.2.2.2.4 Long-Term Storage at the ISFSI Pad

The HI-STORM 100 and 100S free-standing overpack designs have been analyzed for steady state tornado wind loads with a concurrent, large-missile impact, as well as intermediate and small-sized missiles for penetration, as described in Appendices 3.C and 3.G of the HI-STORM 100 System FSAR. The anchored version of the HI-STORM 100S overpack (HI-STORM 100SA) to be deployed at the Diablo Canyon ISFSI is bounded by the free-standing analysis because the anchorage provides additional protection against overturning. The wind loading evaluated in the HI-STORM 100 System FSAR bounds the maximum wind loading at the Diablo Canyon ISFSI site (Table 3.2-1). The loads on the MPC confinement boundary due to the design-basis, 3.0-psi pressure differential are bounded by the 100-psi normal design internal pressure for the MPC described in Section 3.4.4.3.1.2 of the HI-STORM 100 System FSAR, as amended by LAR 1014-1. The HI-STORM 100SA overpack is a ventilated design that includes four air inlet ducts and four air outlet ducts at the bottom and top, respectively. Therefore, no tornado-induced pressure differential analysis was performed for the overpack.

The HI-STORM 100SA overpack is generically designed to withstand three types of tornado missiles in accordance with Section 3.5.1.4 of NUREG-0800.

Sections 3.4.8 and 3.4.8.1, as well as Appendices 3.C and Appendix 3.G of the HI-STORM 100 System FSAR, provide discussions of the generic design criteria and the effects of the large (automobile), intermediate (rigid cylinder) and small (sphere) tornado missiles on the overpack. The Diablo Canyon ISFSI-specific intermediate missile (344.7-kg insulator string) is a more limiting design-basis missile for penetration and was evaluated for penetration after impacting the outer shell and the top lid of the overpack at design-basis velocity. The 8-inch-diameter steel cylinder was evaluated generically for global stresses induced after a strike on the top lid of the overpack. The Diablo Canyon ISFSI-specific small missile (1-inch-diameter steel rod) was evaluated for puncture and whether it will enter the overpack air ducts and impact the MPC at design-basis velocity.

The small missile, while less energetic than the intermediate missile, was analyzed specifically due to its unique ability to travel through one of the overpack air inlet ducts and directly impact the MPC pedestal. The evaluations of the effects of the large, intermediate, and small categories of missiles impacting the overpack are described below.

- The free-standing overpack is capable of withstanding the combination of tornado wind (or instantaneous pressure drop) and a large-missile-load impact with a conservative safety factor against overturning of greater than two. The anchored cask system, which provides additional resistance to overturning, is bounded by the free-standing overpack analysis. Local damage to the cask surface by a large-missile impact is bounded by the small and intermediate category missiles.

- Conservatively neglecting the concrete in the overpack, the 500-kV insulator string intermediate missile will penetrate the outer shell of the overpack, but will not penetrate the 1-1/4-inch inner shell of the overpack or result in loss of MPC retrievability. Using this conservative model, the minimum inner shell thickness required to withstand the missile impact is 0.619 inches.

- The 500-kV insulator string intermediate missile will not penetrate the 2-inch top lid of the overpack. The minimum required thickness to withstand the missile impact is 1.089 inches.

- The 8-inch steel cylinder intermediate missile will not cause an over-stress condition on the overpack lid. The factor of safety is 1.4 for this event. The factor of safety for the 500-kV insulator string for this event is 1.6.

- The 1-inch diameter steel rod (that is, small missile) is postulated to enter an overpack inlet duct and impact the pedestal shell. The analysis shows that the rod will pierce the shell and penetrate the concrete to a depth of 6.179 inches, which is significantly less than the radius of the pedestal shield. The damage to the concrete pedestal shield does not affect the confinement boundary or the ability of the MPC to remain standing on the pedestal, nor does it affect the retrievability of the MPC.

The effects of large and small missiles on the free-standing HI-STORM 100 overpack, which were determined in the generic evaluations, are applicable to and bounding for the anchored HI-STORM 100SA overpack to be deployed at the Diablo Canyon ISFSI. The Diablo Canyon ISFSI-specific intermediate missile has been evaluated for penetration and found to have acceptable consequences. The effect of the intermediate missile impact on the overpack lid has been evaluated and found to have acceptable consequences.

8.2.2.3 Conclusions

The above discussion demonstrates that the HI-STORM 100SA overpack and the HI-TRAC transfer cask provide effective missile barriers for the MPC. No missile strike will cause instability of the overpack, compromise the integrity of the confinement boundary or jeopardize retrievability of the MPC. In addition, global stress intensities arising from the missile strikes satisfy ASME Code Level D limits for an ASME Section III Subsection NF structure. For the case where the transfer cask is being transported to the CTF in the horizontal position, the MPC top lid has been evaluated for an intermediate missile strike. The stress intensities from this missile strike satisfy the ASME Section III Subsection NB Level D limits. Therefore the requirements of 10 CFR 72.122(b) are met with regard to tornadoes.

The cask transporter has redundant drop protection by design (Section 3.3.3). Therefore, a loss of load due to a direct missile strike on the transporter is not credible.

Since the CTF structure at DCPP is underground, it is not exposed to missile impacts (Section 3.3.4).

8.2.2.4 Accident Dose Calculations

Extreme winds in combination with tornado missiles are not capable of overturning a storage cask or of damaging an MPC within a storage cask resulting in a loss of shielding. Therefore, no radioactivity would be released due to tornado effects on the overpack in the event of a tornado. Dose rates at the controlled area boundary and onsite would not be affected by the minor damage to the transfer or storage cask from tornado-driven missile strikes.

8.2.3 FLOOD

A flood is classified as a natural phenomenon Design Event IV in accordance with ANSI/ANS 57.9.

8.2.3.1 Cause of Accident

The probable maximum flood is classified as a severe natural phenomenon. In general, floods are caused by extended periods of rainfall, tsunamis, storm surges, or structural failures, such as a dam break.

The Diablo Canyon ISFSI storage pads are located at an elevation of over 300 ft mean sea level (MSL). The Diablo Canyon ISFSI site surface hydrology is described in Section 2.4. It is concluded in Section 2.4 that there is no potential for flooding in the vicinity of the ISFSI storage pads. Therefore, flooding is not a consideration for ISFSI operations or on the capability of the dry storage cask system to safely store the spent fuel. Likewise, due to the elevation of the ISFSI site, a tsunami (about 35 ft MSL) as discussed in the DCPP FSAR Update (Reference 4), Section 2.4.6, is not a threat to the HI-STORM 100 Systems being stored on the pad. Since the CTF is located adjacent to the ISFSI pads, it is similarly concluded that there is no potential flooding and tsunami impact on the CTF.

Floods are generally predictable events. As such, administrative controls contained in ISFSI operating procedures will be used to preclude transport of the MPC in a transfer cask, CTF MPC handling activities, and transport of a loaded overpack between the CTF and storage pads during severe weather. Therefore, flooding during these configurations is also not considered credible. Also, the minimum elevation of the transport route (about 82 ft MSL) precludes a tsunami flooding the transport route while in use.

The potential for flooding at the CTF is further reduced by the CTF having a removable cover that is installed when the CTF is not in operation. As a further precautionary measure, the CTF is equipped with a sump as described in Section 4.4.5.

8.2.3.2 Accident Analysis

The HI-STORM 100 System is designed to withstand the pressure and water forces associated with a flood. The design criteria for a flood are discussed in Section 2.2.3.6 of the HI-STORM 100 System FSAR. The flood is assumed to submerge the HI-STORM 100 System to a depth of 125 ft with a water velocity of 15 ft/sec (HI-STORM 100 System FSAR, Table 2.2.8).

No additional flooding analyses have been performed for the Diablo Canyon ISFSI because flooding of the ISFSI is not considered credible.

8.2.3.3 Accident Dose Calculations

Flooding is not a credible event for the Diablo Canyon ISFSI because of the elevation of the ISFSI site. There will be no releases of radioactivity and no resultant doses.

8.2.4 DROPS AND TIP-OVER

The hypothetical drop/tip-over of a storage cask is classified as Design Event IV, as defined by ANSI/ANS-57.9. The design for the Diablo Canyon ISFSI, as explained below, eliminates the need to postulate and analyze cask drop and non-mechanistic tip-over events (Reference 40). The load path portions of the cask transporter and the lifting devices attached to the cask components (that is, the HI-TRAC lifting trunnions and the overpack lift bolt anchor blocks) are designed to preclude drop events, either through redundancy or enhanced safety factors. Table 2.2.6 of the HI-STORM 100 System FSAR, as amended by LAR 1014-1, discusses the design codes and standards applicable to the transfer cask and the overpack. Sections 3.3.3, 4.3, and 8.2.1 discuss the design criteria, applicable codes and standards, and design features of the cask transporter that demonstrate that the transporter will not leave the transport route, tip over, or drop the loaded transfer cask or overpack under all design basis conditions, including natural phenomena. Since the CTF lifting devices are designed, fabricated, inspected, maintained, operated, and tested in accordance with applicable guidelines of NUREG-0612, a drop of the transfer cask and MPC will not occur.

Section 8.2.1 describes the analysis of a seismic event, verifying that the CTF and the cask transporter will not drop a loaded transfer cask or overpack, and the cask transporter will remain stable on the transport route for the duration of the earthquake. Therefore, transfer cask and overpack drop events are not analyzed outside the FHB/AB, nor are maximum lift heights established for handling the casks. Administrative controls in operation procedures will ensure the casks are lifted only to those heights necessary to complete the required activities for cask loading and unloading.

The design of the Diablo Canyon ISFSI also includes a requirement to anchor the overpack to the concrete ISFSI pad. This design concept is necessary to accommodate a design-basis seismic event at the site without the cask sliding or tipping over. The anchored overpack concept eliminates the need to postulate a non-mechanistic tip-over of the loaded overpack when anchored to the ISFSI storage pad. Section 8.2.1 describes the analysis that verifies the anchored overpack will not slide or tip over during a seismic event. Section 8.2.2 describes the analysis that demonstrates that the overpack will not tip over as a result of tornado wind concurrent with a large tornado missile impact.

8.2.4.1 Cause of Accident

Cask drop or tip-over is not a credible event outside the DCPP FHB/AB as discussed above. Cask drop events have been postulated as part of the 10 CFR 50 licensing basis inside the FHB/AB due to the nonsingle-failure-proof design of the FHB/AB crane, which will be used to lift and move the unloaded and loaded transfer cask. The description of the drop events, necessary ancillary equipment (that is, impact limiters), and the analyses performed to show the cask and building structure remain within acceptable limits are included in the 10 CFR 50 license amendment request supporting the Diablo Canyon ISFSI license application.

At the Diablo Canyon ISFSI, transfer of the loaded MPC between the transfer cask and the overpack is accomplished at the CTF using the cask transporter to lift the transfer cask to the height necessary to accomplish this objective. The CTF and the cask transporter used in Diablo Canyon ISFSI operations are designed, fabricated, operated, inspected, maintained, operated, and tested in accordance with the applicable guidelines of NUREG-0612. Therefore, a drop of the loaded MPC during inter-cask transfer operations is not a credible event.

8.2.4.2 Accident Analysis

As discussed above, cask drop or tip-over or MPC drop are not credible events outside the FHB/AB.

8.2.4.3 Dose Calculation for MPC Drop Event

Cask drop or tip-over or MPC drop are not credible events. Thus, there is no breach of the MPC confinement boundary and no release of radioactivity.

8.2.5 FIRE

Fires are classified as human-induced or natural phenomena design events in accordance with ANSI/ANS 57.9 Design Events III and IV. To establish a conservative design basis, the following fire events are postulated:

(1) Onsite transporter fuel tank fire

(2) Other onsite vehicle fuel tank fires

(3) Combustion of other local stationary fuel tanks

(4) Combustion of other local combustible materials

(5) Fire in the surrounding vegetation

(6) Fire from mineral oil from the Unit 2 transformers

The potential for fire is addressed for both the overpack and the transfer cask. Locations where the potential for fire is addressed include the ISFSI storage pads, the area immediately surrounding the ISFSI storage pads, including the CTF, and along the transport route between the DCPP FHB/AB and the ISFSI storage pads. The evaluations performed for these postulated fire events (Reference 41) are discussed in the following sections.

8.2.5.1 Cause of Accident

Multiple causes, both human-induced and natural, are assumed for each of the fire events postulated above. For the purposes of this SAR, all conservatively postulated fire events are classified as ANSI/ANS 57.9, Design Event IV, events that are postulated because they establish a conservative design basis for important-to-safety SSCs.

There are several potential mechanisms for the initiation of Events 1, 2, 3, 4, and 6, listed above, including both human-induced (electrical shorts, vehicle accidents, transmission line strikes, etc.) and natural (lightning strikes, tornado missiles, etc.) phenomena. While the probability of occurrence of these mechanisms would be very low, the classification of these fire events as ANSI/ANS 57.9, Design Event IV, requires performing an evaluation.

The postulated fire in the vegetation surrounding the ISFSI storage pad (Event 5) could be caused by the spread of an offsite fire onto the site or as the result of natural phenomena such as a lightning strike or a transmission line strike. Unlike the other fire events, it is reasonable to expect that some type of vegetation fire will occur during the ISFSI license period. While plant personnel would quickly act to suppress or control vegetation fire, it is postulated that no fire suppression activity occurs. Thus, this fire event is conservatively classified as an ANSI/ANS 57.9, Design Event IV.

8.2.5.2 Accident Analysis

For the evaluation of the onsite transporter and other onsite, vehicle-fuel-tank fires (Events 1 and 2), it is postulated that the fuel tank is ruptured, spilling all the contained fuel, and the fuel is ignited. The fuel tank capacity of the onsite transporter is limited by the Diablo Canyon ISFSI TS to a maximum of 50 gallons of fuel. The maximum fuel tank capacity for other onsite vehicles in proximity to the transport route and the ISFSI storage pads is assumed to be 20 gallons. On the storage pad, the fuel is postulated to be burning in a pool surrounding the cask, therefore, the concrete short-term temperature limit will be exceeded and is an expected consequence of the event. Recovery from a fire event on the ISFSI pad will require a technical evaluation of the ability of the ISFSI pad, in the affected area, to perform its design function, and appropriate corrective actions taken as necessary

A potential fire in the CTF due to the release of the 50 gallons of fuel from the cask transporter has been addressed. The cask transporter will be designed with features (e.g., a removable fuel tank) that ensure the fuel, if spilled, will not migrate into the CTF structure. The CTF opening will be located at a higher elevation than the local surrounding area such that any fuel spilled will flow away from the CTF by gravity. This ensures that any fire that may occur is bounded by the fire analysis described in Section 11.2.4 of the HI-STORM System FSAR.

Section 11.2.4 of the HI-STORM 100 System FSAR presents an evaluation of the effects of an engulfing 50-gallon fuel fire for both overpack and transfer cask. Results of these analyses indicate that neither the storage cask nor the transfer cask undergoes any structural degradation and that only a small amount of neutron shielding material (concrete, Holtite-A, and water) is damaged or lost. This analysis bounds any onsite, 20-gallon vehicle-fuel-tank fire (Event 2).

The location of any transient sources of fuel in larger volumes, such as tanker trucks, will be administratively controlled to provide a sufficient distance from the ISFSI storage pads (at all times), the CTF, and the transport route during transport operations to ensure the total energy received is less than the design-basis fire event. In addition, when the tanker truck is moving on the roadway past the ISFSI, the roadbed in all cases is below the level of the ISFSI pad, which ensures that even if there were a tank rupture, the fuel would not run toward the ISFSI. An analysis was performed for a ruptured 2000-gallon gasoline tanker truck, which determined that at a distance of more than 4 meters it does not result in exceeding the design basis of the storage casks (Reference 34).

Administrative controls are imposed to ensure no combustible materials are stored within the protected area fence around the ISFSI storage pads. Prior to any cask transport, a walkdown will be performed to ensure all local combustible materials (Event 4), including transient combustibles, are controlled in accordance with ISFSI fire protection requirements. All stationary fuel tanks (Event 3) are at least 50 ft from the ISFSI storage pad security fence and at least 100 ft from the transport route and the CTF. These existing stationary tanks have been evaluated. Due to their distances to the transport route or the ISFSI pad, the total energy received by the storage cask or the transporter is insignificant compared to the design-basis fire event.

The native vegetation surrounding the ISFSI storage pad is primarily grass, with no significant brush, and no trees. Maintenance programs prevent uncontrolled growth of the surrounding vegetation. As previously stated, no combustible materials will be stored within the ISFSI protected area. A conservative fire model was established for evaluation of grass fires. Analysis has demonstrated that grass fires are bounded by the 50-gallon, transporter-fuel-tank fire evaluated in the HI-STORM 100 System FSAR (Event 5). The wildfire evaluation uses predictive models called FARSITE and FLAMMAP (Reference 36) to determine the potential characteristics of wildfire in the Diablo Canyon. Both models utilize mapped data about the type of vegetation (fuel model), slope, aspect, elevation, wind, and moisture to predict wildfire characteristics such as flame length, rate of spread, heat per unit area, etc. The proposed ISFSI site, located immediately southeast of the power plant's raw water reservoirs, is surrounded on the south, southeast, and north sides by a vegetation type of "annual grassland" (Reference 37) The main access road forms the northwest boundary of the proposed site. The annual grassland vegetation is grazed and has relatively low cover. Consequently, the fire risk of this fuel type is relatively low.

For Event 6, the physical properties of mineral oil limit the threat of a fire. The pertinent material property for this determination, the flash point, is defined as the lowest temperature at which the vapor pressure of a liquid is sufficient to produce a flammable vapor/air mixture at the lower limit of flammability. In other words, a combustible liquid cannot vaporize sufficiently to detonate if the ambient temperature is below the flash point. Such materials could conceivably burn, but would be incapable of detonation.

The flash point of mineral oil is 275°F. To be classified as flammable, the flash point of a liquid must be less than 100°F as discussed in the National Fire Protection Association Handbook (Reference 15). The highest ambient temperature predicted for the Diablo Canyon ISFSI site (5- to 10-year recurrence interval) is 104°F and would normally (99 percent of the time) be no more than 85°F; and the normal operating temperature of the 13,000 gallons of mineral oil in each of the DCPP Unit 2 main bank transformers is approximately 160°F. These temperatures are considerably less than the flash point of mineral oil. Therefore, under ambient or normal operating temperature, these materials do not represent a credible fire hazard. However, if an electrical fault were to occur in a transformer, the increase in heat within that transformer could cause it to rupture and its contents may support a local fire. The resulting fire is considered to be limited and bound by the design basis fire provided in Section 11.2.4 of the HI-STORM 100 System FSAR, and is further supported by an analysis performed for a ruptured 2000-gallon gasoline tanker truck, which determined that at a distance of more than 4 meters does not result in exceeding the design basis of the transfer cask. (Reference 34)

The probability of this event occurring while the transfer cask is in proximity and it affecting the transporter and transfer cask is extremely low. This is based on the properties of mineral oil, the minimum distance from the transformers to the transporter, the limited amount of exposure time, a dedicated transformer fire suppression system, and a significant difference in elevation between the transformers and the transporter route.

The transformers are approximately 240 ft from the transporter at its closest point during transport and the transporter is within a line of sight of the transformers for no more than

10 hours per year. Each of the transformers is surrounded by a dedicated fire suppression system that will act to control and minimize any fire that could potentially occur. There is also a 30-ft difference in elevation between the transporter route and the transformers that will not allow oil from a transformer to approach within approximately 120 ft of the transporter.

In addition, although a fire from a transformer is considered bounded by the design basis of the transfer cask and not an unacceptable hazard, in an effort to further minimize its probability, PG&E is taking prudent actions to minimize the transformer fire hazards during transport as follows:

For potential external hazards, administrative procedures will not allow any vehicle motion in the vicinity of the transformers during transport operations. In addition, administrative procedures will be in place that will not allow transport of fuel when severe weather (which could result in lightning or other hazards) exists or is predicted to occur during the transport time in the vicinity of the DCPP plant site. To address the potential hazard for an internal short, PG&E administrative procedures will consider offsite power conditions prior to transport operations in the vicinity of the Unit 2 transformers.

Based on the above discussion, the potential hazard from a transformer fire is considered credible; however, its potential effects are limited and considered bounded by the design basis fire analysis for the transfer cask.

In summary, the fire evaluations performed generically in the HI-STORM 100 System FSAR, the physical layout of the Diablo Canyon ISFSI, the fire analysis for the surrounding vegetation, and the administrative controls on fuel sources ensure that the general design criteria related to fire protection specified in 10 CFR 72.122(c) are met.

8.2.5.3 Accident Dose Calculations

The effects of an onsite transporter, or other onsite vehicle-fuel-tank fire postulated for the Diablo Canyon ISFSI, are enveloped by the design basis transporter fire evaluated in the HI-STORM System FSAR. Section 11.2.4 of the HI-STORM 100 System FSAR describes how the MPC confinement boundary remains intact after a design basis fire for both the overpack and the transfer cask. Therefore, there is no release of the contained radioactive material from the MPC and no dose consequences in this regard. The shielding implications of a design basis fire for each of these components are discussed below.

8.2.5.3.1 HI-STORM 100 Overpack

Section 11.2.4.2.1 of the HI-STORM 100 System FSAR discusses the fire analysis for the overpack, including radiological implications. The design-basis fire for the HI-STORM 100 overpack causes a small reduction in the shielding provided by the concrete. No portions of the steel structure of the overpack experience temperatures exceeding the short-term temperature limits. While the temperature in the outer 1-inch of concrete is shown to exceed the material short-term temperature limit, there is no significant reduction in the shielding provided by the overpack. All MPC component and fuel assembly temperatures remain within their short-term temperature limits.

8.2.5.3.2 HI-TRAC Transfer Cask

Section 11.2.4.2.2 of the HI-STORM 100 System FSAR discusses the fire analysis for the transfer cask. The elevated local temperatures due to the fire will cause approximately 11 percent of the water in the water jacket to boil off and relieve as steam through the relief valves on the water jacket. However, it is conservatively assumed for the dose calculations that all of the water in the water jacket is boiled off. The fire could also heat the Holtite-A shielding material in the transfer cask top lid and bottom shield above its temperature limit. Therefore, it is conservatively assumed in the dose calculations that all of the Holtite-A in the transfer cask is lost.

The postulated losses of all neutron shielding, due to the loss of water in the water jacket and all Holtite-A in the transfer cask top lid and bottom shield, will not exceed the 10 CFR 72.106 dose limits at an assumed controlled-area boundary located 100 meters from the ISFSI pad for the 30-day duration of the accident, as discussed in Section 5.1.2 of the HI-STORM 100 System FSAR. The nearest controlled area boundary at Diablo Canyon is approximately 1,400 ft from the ISFSI storage pads, which would further decrease the estimated accident dose to well below the 10 CFR 72.106 limit.

Also, as discussed in Section 8.2.11.2, the increase in fuel cladding and component material temperatures due to the loss of water in the water jacket do not cause the short-term fuel cladding or material temperature limits listed in the HI-STORM 100 System FSAR Table 2.2-3 to be exceeded. The internal MPC pressure also remains below the 200-psig accident design limit. Thus, there is no effect on the integrity of the MPC confinement boundary.

The ISFSI system will not be affected by the postulated combustion of local fuel tanks, combustible materials outside the ISFSI storage pad perimeter or along the transport route, or an unsuppressed vegetation fire. Therefore, there are no dose consequences beyond the 10 CFR 72.106 limits for these postulated events.

8.2.6 EXPLOSION

Explosions are classified as human-induced or natural phenomena design events in accordance with ANSI/ANS 57.9 Design Events III and IV. The following explosion event categories have been evaluated (Reference 42) for the Diablo Canyon ISFSI:

(1) Detonation of a transporter or onsite vehicle fuel tank

(2) Detonation of propane bottles transported past the ISFSI storage pad

(3) Detonation of a compressed gas bottles transported past the ISFSI storage pad

(4) Detonation of large stationary fuel tanks in the vicinity of the transport route

(5) Explosive decompression of a compressed gas cylinder

(6) Detonation of the bulk hydrogen storage facility

(7) Detonation of acetylene bottles stored on the east side of the cold machine shop

Events 1, 2, 3, and 5 are assumed to occur in the vicinity of the ISFSI storage pads, CTF, or transport route; and potentially affect both the overpack and the transfer cask. Events 4 through 7 occur in the vicinity of the transport route and affect only the transfer cask.

As a result of its physical properties, diesel fuel does not pose any real explosion hazard. The pertinent material property for this determination, the flash point, is defined as the lowest temperature at which the vapor pressure of a liquid is sufficient to produce a flammable vapor/air mixture at the lower limit of flammability. In other words, a combustible liquid cannot vaporize sufficiently to detonate if the ambient temperature is below the flash point. Such materials could conceivably burn, but would be incapable of detonation.

The flash point of diesel fuel is 125°F. To be classified as flammable, the flash point of a liquid must be less than 100°F as discussed in the National Fire Protection Association Handbook (Reference 15). The highest ambient temperature predicted for the Diablo Canyon ISFSI site (5- to 10-year recurrence interval) is 104°F and would normally (99 percent of the time) be no more than 85°F. These temperatures are considerably less than the flash point of diesel fuel. Therefore, under ambient or normal operating temperature, diesel fuel oil does not represent a credible explosive hazard. Therefore, Event 1 for vehicles containing diesel fuel oil is excluded from further consideration.

Since the cask transporter is powered by diesel fuel, which cannot detonate as discussed above, explosion Event 1 is reduced to the explosion of onsite, gasoline-powered vehicles. The fuel tank capacity of these vehicles is an average of 20 gallons. Administrative controls will be used to keep onsite, gasoline-powered vehicles and tanker trucks carrying flammable liquids either: (a) at sufficient distance from the ISFSI storage pad (at all times), the CTF (while transferring an MPC), and the transport route during cask transport to ensure the total explosion overpressure is less than 1 psi, (b) a risk assessment will be performed using Regulatory Guide 1.91 risk acceptance criteria, or (c) diesel-powered vehicles will be used. The administrative controls will include, but are not limited to, speed limits, single vehicle zones, no entry zones, no stopping zones, designated parking for various types of vehicles, and limitations on the size and contents of vehicles passing the ISFSI facility or the CTF during transport operations. In addition, vehicle movement will be controlled in the vicinity of the transporter when it is transporting fuel. These administrative controls are further defined in the various referenced calculations provided in support of these sections.

To meet the Regulatory Guide 1.91 overpressure criterion, for a vehicle with a maximum of a 20-gallon fuel capacity, the separation distance to the ISFSI pads has been calculated as no less than 175 ft. As a result, there is the possibility that these vehicles may pass within that separation distance momentarily on their way past the ISFSI facility. No gasoline- powered vehicles will be allowed to park or stop within 175 ft of the ISFSI. A probabilistic risk assessment (Reference 35) was performed and it was determined that, based on use of administrative controls and the restrictions for movement and stopping within the separation distance, the risk of exceeding the Regulatory Guide 1.91 overpressure criterion from vehicles driving past the ISFSI is insignificant.

In addition, although not considered credible, the potential explosion of a parked vehicle along the transport route was evaluated in a probabilistic risk assessment using Regulatory Guide 1.91 criteria (Reference 35). In that evaluation, it was determined that the risk was insignificant and not a credible source. This was based on the limited time the transporter is exposed (less than 10 hours per year), the lack of any ignition source in a parked car, the lack of a single vehicle explosion in the 35-year history of the Diablo Canyon project, and the administrative controls restricting vehicle movement during transport (no vehicle movement within 175 ft of the transporter).

A 2,000-gallon gasoline tanker truck passes using the transport route near the ISFSI pad. The truck will only be in this area momentarily while passing by the ISFSI facility and will be under administrative controls for its speed and continued movement through the area on its way to and from the vehicle maintenance shop that is located approximately 2,000 ft northeast of the ISFSI pad. A probabilistic risk assessment was performed (Reference 35) and it was determined, based on the use of administrative controls and the restrictions for movement and stopping within the 812 ft separation distance calculated based on the 1 psi Regulatory Guide 1.91 criterion, the risk is insignificant.

For Explosion Events 2 and 3, a probabilistic risk assessment was performed (Reference 35). The transport of gas bottles past the ISFSI pads is controlled by administrative controls and will maintain the same separation distance as the 2,000-gallon fuel truck requirements. Under these controls and proper restraint of the bottles in transport, the risk of exceeding the Regulatory Guide 1.91 overpressure criteria was determined to be insignificant.

The large fuel tanks referred to in Event 4 are located along the main plant access road from the Avila Gate, approximately 1,200 ft from the onsite transport road at the closest point. The tanks include a 250-gallon propane tank, a 2,000-gallon diesel fuel tank, and a 3,000-gallon gasoline tank. The diesel fuel cannot detonate, so Event 4 is limited to the detonation of the 250-gallon propane and 3,000-gallon gasoline tanks. As shown in Section 8.2.6.2.1, Event 4 does not exceed the Regulatory Guide 1.91 1 psi criterion. These tanks will be periodically filled by standard tanker trucks with a capacity of three to four thousand gallons. The location of any tank truck will be administratively controlled to ensure the total energy potentially received by the ISFSI is less than the design basis event. In addition, during transport operations all filling will be suspended and all of the gasoline tanker trucks, which fill these tanks, will not be allowed within the owner-controlled area. This will be administratively controlled in accordance with the Diablo Canyon ISFSI Technical Specification Cask Transportation Evaluation Program.

Although the risk of a gas bottle explosion was found to be insignificant as discussed above, an Event 5 explosive decompression event for a compressed-gas cylinder was evaluated. The cylinder is evaluated as a projectile, similar to a tornado-generated missile and is discussed in Section 8.2.6.2.2.

Event 6 includes a potential source of detonation and is discussed in Section 8.2.6.2.3.

For Event 7, the probability of an explosion that would exceed the Regulatory Guide 1.91 criteria of 1 psi for the transporter is not considered credible and the hazard is bounded by the analysis of the hydrogen facility discussed in Section 8.2.6.2.3. This is documented in a probabilistic risk assessment (Reference 35) that determined that the risk from this hazard is not credible. This is based on the seismic procedural requirements for chaining the bottles in the upright position in the facility, the lack of any ignition sources in the area, the administrative controls eliminating vehicle movement when transporter is in the area, and the limited exposure time of the transporter, which conservatively would be less than 10 hours per year.

8.2.6.1 Cause of Accident

There are several potential mechanisms for the initiation of the postulated explosion events listed above, including both human-induced (electrical shorts, vehicle accidents, transmission line strikes, etc.) and natural (lightning strikes, tornado missiles, etc.) phenomena. While the probability of occurrence of these mechanisms is expected to be very low, the credible explosion events are classified as ANSI/ANS 57.9, Design Event IV, and are evaluated.

8.2.6.2 Accident Analysis

8.2.6.2.1 Explosive Overpressure Due to Detonation Events

During a detonation event, the overpack and/or transfer cask would be subjected to an external overpressure. Regulatory Guide 1.91 states: "...for explosions of the magnitude considered in this guide and the structures, systems, and components that must be protected, overpressure effects are controlling." The magnitude of the overpressure would be a function of the calorific energy released and the distance between the overpack/transfer cask and the explosion source. Due to the extremely short duration of explosion events, any heat input to the casks would be negligible (fires are evaluated in Section 8.2.5).

Events 1 through 4 are evaluated under the following assumptions:

(1) The fuel tanks are ruptured, releasing all contained flammable material, and all spilled flammable liquids are completely vaporized.

(2) The flammable gas or vapor is mixed with air at the lower flammability limit of the material.

(3) The flammable fuel/air mixture is detonated, releasing a portion of the total heating value as a hemispherical overpressure wave front. The fraction of the available energy that contributes to the overpressure, called the explosive yield, is between 3 percent and 6 percent for hydrocarbon/air mixtures, as discussed in the Handbook of Chemical Hazards Analysis (Reference 17).

To determine the magnitude of the explosive overpressure incident on the overpack and transfer cask, the energy released during detonation is converted to an equivalent weight of trinitrotoluene (TNT). This is accomplished by dividing the explosion energy by the detonation energy of TNT, which is 4.5 megajoules per kilogram as discussed in Perry's Chemical Engineers' Handbook (Reference 18).

Once the equivalent weight of TNT is known, the explosive overpressure can be determined as a function of the separation distance between the explosion and the cask systems using a methodology developed by the U.S. Army (Reference 19) and endorsed by the NRC through Regulatory Guide 1.91. This methodology requires the calculation of a scaled ground distance, Z_G, which is the ratio of the physical separation distance divided by the cube root of the equivalent weight of TNT and has units of ft/lb$^{1/3}$. The incident overpressure at a given scaled ground distance is then obtained directly from Figure 2-15 of Reference 19.

For Event 4, the minimum physical separation distance to the transport route or the ISFSI is 1,200 ft. based on the maximum quantities of flammable material having an equivalent weight of TNT of 12,100 lb, the resultant setback distance to ensure that the 1 psi maximum overpressure acceptance criteria is met per Regulatory Guide 1.91, is 1,033 ft. Therefore, further evaluation, is unnecessary.

The site-specific explosive overpressures caused by detonation events are bounded by the 1 psi Regulatory Guide 1.91 criterion or are determined not to be risk significant in accordance with Regulatory Guide 1.91. Therefore, 10 CFR 72.122(c) is met.

8.2.6.2.2 Missiles Due to Explosive Decompression of a Compressed Gas Cylinder

Although not considered a credible event, as discussed above, the missile created by the explosive decompression of a gas cylinder (Event 6) is evaluated assuming that a compressed gas cylinder under high-pressure is damaged such that the valve assembly located at the top of the cylinder breaks off. Expansion of the high-pressure compressed gas out of the hole in the cylinder accelerates the cylinder or valve assembly toward the cask systems, resulting in an eventual impact. Cylinders filled with acetylene, air, argon, helium, nitrogen, oxygen, and propane are evaluated.

The acceleration of the cylinder is dependent on the thrust force generated by the escaping high-pressure gas, which reduces over time as the cylinder internal pressure decreases. The thrust force as a function of time is determined from principles of compressible flow, which state that the thrust force is the product of the mass flow and velocity of the gas escaping through the hole in the cylinder wall. While the internal pressure of the cylinder is sufficiently high (that is, greater than the critical pressure), the velocity of the gas is limited to the speed of sound (that is, sonic or choked flow). As the pressure falls below the critical pressure, the velocity becomes subsonic, and eventually reaches zero when the cylinder internal pressure is equal to the atmospheric pressure.

Conservatively neglecting aerodynamic drag (which would decrease the maximum velocity of the cylinder by opposing the thrust force), and assuming bounding discharge coefficients, the cylinder is determined to accelerate from rest to a maximum of approximately 109 mph as the internal pressure drops toward ambient pressure (propane gas). The detached valve assembly is determined to accelerate to a maximum of approximately 342 mph (all gases equal).

Section 8.2.2 of this SAR presents evaluations of the impact of tornado missiles on both the loaded overpack and the transfer cask. Using the same energy method employed in Section 8.2.2, the effects of the impact of cylindrical missiles are evaluated. The maximum penetration into a steel target for the cylinder and valve assembly missiles is less than 1/4 inch. These penetrations are insufficient to completely penetrate either a storage overpack or a transfer cask, thereby precluding damage to the MPC confinement boundary. These missile evaluations conclude that neither the loaded overpack nor the transfer cask undergoes any significant reduction of structural integrity and no shielding material (concrete and water) is damaged or lost, such that the licensing basis acceptance criteria for the casks is met.

8.2.6.2.3 Potential Explosion Event at the Bulk Hydrogen Facility

As shown in SAR Figure 2.2-1, a bulk hydrogen facility is located east of the FHB/AB and approximately 0.14 miles from the ISFSI pad with its elevation several hundred ft below the ISFSI facility. Therefore the hydrogen facility can only potentially affect the transport of fuel and not the ISFSI facility. This facility contains 6 tanks for a total of about 300 cubic ft and is near the transport route (approximately 15 ft) from where the transfer cask enters and leaves the Unit 1 FHB/AB. These tanks are refilled approximately twice a month. They are held in a seismic-qualified rack, which is enclosed, in a seismic-qualified vault. The vault is only open on the side toward the FHB/AB and is provided with a 12-inch-diameter top vent to ensure no possible buildup of gas from leakage. This facility is designed to protect against over pressurization, excessive flow, and vehicle (delivery truck) damage during filling. The transporter will only be in this area for a very short period of time, and during this time, all filling of tanks will be suspended and all vehicle movement will be administratively controlled in accordance with the cask transportation evaluation program. A probabilistic risk assessment (Reference 35) was performed in accordance with the Regulatory Guide 1.91 methodology. Due to the noncredible nature of an explosion and the limited exposure to the transporter, the event is not risk significant using the Regulatory Guide 1.91 acceptance criteria and is considered acceptable.

8.2.6.3 Accident Dose Calculations

As discussed above, the effects of the Diablo Canyon site explosion events involving detonation (Events 1, 2, 3, 4, and 8) are enveloped by the design-basis accident conditions (explosion and transfer cask side drop) in the HI-STORM 100 System FSAR or are not considered risk significant in accordance with Regulatory Guide 1.91. The missile evaluation for Event 6 concludes that only a small amount of the shielding materials may be damaged or lost. The structural evaluations in Chapter 3 of the HI-STORM 100 System FSAR confirm that the MPC confinement boundary remains intact and the shielding effectiveness of the HI-STORM 100 System is not significantly affected by these explosion and missile events. The radiological evaluations presented in Chapter 11 of that document also conclude that the loaded overpack and transfer cask continue to meet the accident dose limits of 10 CFR 72.106 at the controlled area boundary after these events.

8.2.7 LEAKAGE THROUGH CONFINEMENT BOUNDARY

The hypothetical leakage of a single, loaded MPC-32 under accident conditions, where the cladding of 100 percent of the fuel rods is postulated to have ruptured, is described in this section.

8.2.7.1 Cause of Accident

The analyses presented in Chapters 3 and 11 of the HI-STORM 100 System FSAR, as amended by LAR 1014-1, demonstrate that the MPC confinement boundary remains intact during all hypothetical accident conditions, including the associated increased internal temperature and pressure due to the decay heat generated by the stored fuel.

This section evaluates the consequences of a non-mechanistic, 100 percent, fuel-rod rupture and confinement boundary leak (Reference 43). The breach could result in the release of gaseous fission products, fines, volatiles, and airborne crud particulates to the MPC cavity. Doses resulting from the canister leakage under hypothetical accident conditions were calculated in accordance with Interim Staff Guidance (ISG) Document 5 (Reference 20), ISG 11 (Reference 21) and NUREG/CR-6487 (Reference 22).

8.2.7.2 Accident Analysis

8.2.7.2.1 Confinement Vessel Releasable Source Term

The MPC-32, which holds 32 PWR fuel assemblies, is used in the confinement analysis because it bounds the other, lower-capacity Holtec PWR MPCs for the total quantity of radionuclides available for release from a single cask. The methodology for calculating the spent fuel isotopic inventory for an MPC-32 is detailed in Section 7.2.2. A summary of the isotopes available for release is provided in Table 7.2-8.

8.2.7.2.2 Release of Contents under Accident Conditions of Storage

In this hypothetical accident analysis, it is assumed that 100 percent of the fuel rods have developed cladding breaches, even though, as described below, the spent fuel is stored in a manner such that the spent fuel cladding is protected against degradation that could lead to fuel rod cladding ruptures. The MPC cavity is filled with helium after the MPC has been evacuated of air and moisture that might produce long-term degradation of the spent fuel cladding. Additionally, the HI-STORM 100 System is designed to provide for long-term heat removal capabilities to ensure that the fuel is maintained at a temperature below those at which cladding degradation occurs. It is, therefore, highly unlikely that a spent fuel assembly with intact fuel rod cladding will undergo cladding failure during storage, and the assumption that 100 percent of the fuel rods have ruptured is extremely conservative.

The assumption that 100 percent of the fuel rods have ruptured is incorporated into the postulated pressure increase within the MPC cavity to determine the maximum possible pressure of the MPC cavity. This pressure, combined with the maximum MPC cavity temperature under accident conditions, is used to determine a postulated leakage rate during an accident. This leakage rate is based on the SAR Section 10.2 leakage rate limit of 5.0×10^{-6} atm-cm^3/sec for the helium-leak-rate test, and is adjusted for the higher temperature and pressure during the accident to result in a hypothetical accident leak rate of 1.28×10^{-5} cm^3/sec.

The radionuclide release fractions, which account for the radionuclides trapped in the fuel matrix and radionuclides that exist in a chemical or physical form that is not releasable to the MPC cavity from the fuel cladding, are based on ISG-5. Additionally, only 10 percent of the fines released to the MPC cavity are assumed to remain airborne long enough to be available for release through the confinement boundary based on SAND88-2778C (Reference 23). It is conservatively assumed that 100 percent of the volatiles, crud, and gases remain airborne and available for release. The release rate for each radionuclide was calculated by multiplying the quantity of radionuclides available for release in the MPC cavity by the leakage rate calculated above, divided by the MPC cavity volume. No credit is taken for any confinement function of the fuel cladding or the ventilated overpack.

8.2.7.3 Dose Calculations for Hypothetical Accident Conditions

Doses at the Diablo Canyon ISFSI site boundary resulting from a postulated leaking MPC-32 were calculated using an inhalation and submersion pathway. An ingestion pathway is not included because of the lack of broadleaf vegetation within 4 miles of the site boundary; the lack of fresh surface water; the lack of milk animals or a credible meat pathway within 800 meters of the ISFSI site; and the very low population within a 6-mile radius of the site. The nearest distance from the ISFSI to the DCPP is 1,400 ft. A χ/Q value of 4.50×10^{-4} s/m^3 was assumed. This χ/Q value is conservative because it is based on a 1-hour release period, whereas the hypothetical accident duration is 30 days per ISG-5. The dose conversion factors for internal doses due to inhalation and submersion in a radioactive plume were taken from EPA Federal Guidance Report No. 11 (Reference 24) and EPA Federal Guidance Report No. 12 (Reference 25), respectively. An adult breathing rate of 3.3×10^{-4} m^3/s was assumed.

Doses to an individual present continuously for 30 days were calculated assuming a release from a single cask with the wind blowing constantly in the same direction for the entire duration. The following 30-day doses were determined:

- The committed dose equivalent from inhalation and the deep dose equivalent from submersion for critical organs and tissues (gonad, breast, lung, red marrow, bone surface, thyroid)
- The committed effective dose equivalent from inhalation and the deep dose equivalent from submersion for the whole body
- The lens dose equivalent for the lens of the eye
- The shallow dose equivalent from submersion for the skin
- The resulting total effective dose equivalent and total organ dose equivalent.

The doses were calculated, as appropriate, for both inhalation and submersion in the radioactive plume. Doses due to exposure to soil with ground surface contamination and contamination to a depth of 15 cm have been evaluated generically for the HI-STORM 100 System. The dose due to ground contamination was found to be negligible compared to those resulting from submersion in the plume and are not reported here (HI-STORM 100 System FSAR, Section 7.2.8).

Table 8.2-12 summarizes the accident doses for a hypothetical confinement boundary leak. The estimated doses are a fraction of the limits specified in 10 CFR 72.106(b).

8.2.8 ELECTRICAL ACCIDENT

Electrical accidents considered include a lightning strike and a 500-kV transmission line drop. Both events are postulated to apply high voltage electrical current through the overpack or the transfer cask, the effects of which are evaluated in Reference 44. These events are classified as natural phenomena, Design Event IV, in accordance with ANSI/ANS 57.9.

8.2.8.1 Cause of Electrical Accident

Lightning strikes are natural phenomena caused by meterological conditions conducive to the discharge of large amounts of static electricity to ground. The 500-kV transmission line drop is postulated as a result of a transmission tower collapse or transmission line hardware failure near the ISFSI storage site and the CTF. The worst-case fault condition for a cask is that which places a cask in the conduction path for the largest current. This condition is the line drop of a single conductor of one phase with resulting single, line-to-ground fault current and voltage-induced arc at the point of contact.

A number of transmission line failure modes were postulated. These included the break or drop of: a single conductor of one phase, both conductors of a single phase, and all three phases. The failure modes considered are:

(1) Three-phase drop onto cask structures - The fault would be balanced, most current would return through the phase conductors and only a small amount would pass through the casks and into the earth.

(2) Both conductors of one phase fall onto one cask - The single line-to-ground fault would split evenly between the two conductors (spaced at 18 inches) and effectively reduce the energy at the point of contact by a factor of two. Therefore, it would create two points of contact, each dissipating half the energy.

(3) One conductor of one phase breaks into two and each end falls onto separate casks or onto different points of the same cask - The single, line-to-ground fault would split between the two points of contact reducing the energy at each point of contact.

(4) One conductor falling while remaining intact - The single, line-to-ground fault would be forced into one point of contact, through the cask, and into the earth/ground grid. All energy would be forced to dissipate at this one point. This would be the worst-case for the cask systems.

Protective relaying is assumed to actuate on arc initiation. The time duration from relay actuation to breaker opening is assumed to be 0.1 sec (6 cycles).

8.2.8.2 Electrical Accident Analysis

The overpack and the CTF are sited beneath a 500-kV transmission line. The transmission line connects the Unit 1 main generator to the 500-kV switchyard. The transmission line is protected from direct lightning strikes by two shield wires installed above the line. Similarly, the transmission conductors provide lightning protection for the overpack and the CTF. The transmission lines themselves act as shield wires for metal objects located below them and within their effective shield angle. Inside this effective shield angle, the distance from the lightning arc to the line will be less than from the lightning arc to the top of the cask, and all lightning within this zone will hit the transmission line instead of the cask. Outside of this effective shield angle, the lightning will be so close to the ground that it will directly hit the ground before it strikes any metal object. Thus, the overhead transmission line prevents a direct lightning strike on any overpack or the CTF. Even so, the effects of a lightning strike are evaluated.

The cask transporter provides protection for the transfer cask from direct lightning strikes and transmission line drops. The gantry and rigging metal is sufficiently above the cask material that any line drop would be effectively deflected by this metal before it is able to contact the cask surface.

For the evaluation of the lightning strike, direct atmospheric lightning strikes on the overpack and the transfer cask are postulated. The lightning strike, defined by a current versus time profile, is defined by standard industry practice as a peak current of 250 kiloamps for 260 microseconds followed by a continuing current of 2 kiloamps for 2 additional seconds.

For the evaluation of the 500-kV transmission line drops for both the overpack and the transfer cask, it is postulated that while both DCPP units are operating at full power a single overhead transmission conductor falls onto a cask. The 500-kV system is operated at a nominal voltage of 525-kV phase to phase. The line-to-ground voltage is 303-kV. The transmission line drop sequence of events is defined in three distinct time periods as follows:

- Period 1 free air arc (wire falling but not yet touching cask) - voltage drops from 303 kV to 1 kV and current rises from 0 kiloamps to 18.6 kiloamps over a 0.05 second arc duration.

- Period 2 prior to breaker trip (wire in solid contact with the cask but breaker not yet fully open) - voltage and current are constant at 1 kV and 18.6 kiloamps, respectively, over a 0.05 second breaker trip duration.

- Period 3 during generator coast-down (all breakers open, faulted generator still contributing fault current) - voltage and current are constant at 0.2 kV and 5.08 kiloamps, respectively, over a generator, coast-down duration of 3.9 seconds.

Both electrical events result in an electrical discharge that travels along the least resistive path through the cask to the ground. Both the lightning strike and the transmission line drop originate external to the casks, so the least resistive path for both the overpack and the transfer cask will be through the outermost shell (that is, overpack outer shell and transfer cask enclosure shell). The MPC contained within an overpack or transfer cask will, therefore, be protected from any electrically-induced damage.

For the postulated lightning strike, the electrical discharge deposited into the cask and conducted to ground must overcome the inherent electrical resistance of the conducting material. This resistance to current flow generates heat, called resistance or Joulean heating, and is governed by the following formula:

$$E = I^2 \times t \times R$$

where E is the resistance heat energy, I is the current, t is the current duration and R is the material resistivity. The electrical resistivity value for iron (10 $\mu\Omega$-cm) was obtained from the CRC Handbook of Chemistry and Physics and conservatively increased by 20 percent to obtain an estimated value of 12 $\mu\Omega$-cm for steel, which was used in the lightning strike analysis. Even if the resistivity were doubled from this value (to 24 $\mu\Omega$-cm), the temperature rise from the lightning event would still be less than 1°F.

The heat generated by resistance heating must be absorbed by sensible heating of the affected cask component, governed by the following equation:

$$E = m \times c_p \times \Delta T$$

where m is the mass of the cask component, c_p is the material heat capacity and ΔT is the component temperature rise. These two equations can be used to determine the cask component temperature rise for each cask, the results of which are contained in Table 8.2-13.

All of the computed, electrically-induced, temperature-rise values are less than 1°F. The HI-STORM 100 System FSAR contains evaluations of both the overpack and the transfer cask under normal temperature conditions. The increase in outer shell temperature for both structures is well below the normal temperature condition limits. Accident condition temperature limits for the outer shells of both casks are significantly higher than the normal condition limits. It is therefore concluded that the postulated lightning strike will not cause the affected cask components to exceed either normal or accident condition temperature limits and do not adversely affect the performance of either system.

For the postulated transmission line break, because of the significant influence of the time-varying voltage and the longer time periods involved, a slightly different method of calculating the energy input is used. The electrical energy is governed by the following formula:

$$E = \int_t V(t) \times I(t) dt$$

where V(t) is the time-varying voltage function, I(t) is the time-varying current function and t is the independent time variable. The electrical energy is calculated separately for each time period of the postulated electrical profile.

As the transmission line drops onto a cask, the predominant portion of arc energy is dissipated to the atmosphere, with the remaining portions heating the cask and vaporizing a portion of the steel outer shell. During the arc phase (Period 1) of the postulated accident, it is conservatively assumed that 10 percent of the total energy is dissipated in sublimating (vaporizing) steel at the point of arc, 40 percent of the total energy is dissipated in resistance heating of the affected cask component, and the balance of the arc energy is dissipated to the environment. During the breaker trip and generator coast-down periods (Periods 2 and 3) of the postulated accident, it is conservatively assumed that all energy is dissipated in resistance heating of the affected cask component. The results of these evaluations are contained in Table 8.2-14.

With respect to the computed, electrically-induced, temperature rise values, the HI-STORM 100 System FSAR contains evaluations of both the overpack and the transfer cask under normal temperature conditions. Again, the increase in the outer shell temperature of both structures is well below the normal condition temperature limits. Accident condition temperature limits for these components for both casks are significantly higher than the normal condition limits.

The sublimated hole diameters are calculated assuming that a cylindrical plug of material, with a length equal to the thickness of the component material, is vaporized. Even if a hole is sublimated in the overpack outer shell, there are no negative thermal consequences. Behind the steel outer shell is a thick concrete layer that is unlikely to be significantly affected given the rapidity of the event and the low thermal diffusivity of concrete. Experience with high-fault currents has shown that spalling and crystallization of the concrete surface would be expected at the point of contact of the fault. The maximum depth of the concrete plug affected would be less than the diameter of the surface hole. It should also be noted that the existence of a hole in the overpack outer shell was postulated and evaluated in Section 8.2.2. The cause of the hole in that section was due to a hypothesized tornado missile. Should a hole be formed in the transfer cask, the water jacket used to provide shielding and to help maintain cool conditions inside the MPC could be drained. This condition has an insignificant thermal impact, and the shielding impact is already addressed in Section 8.2.11 and was found to be acceptable. Section 8.2.11 considers a loss of water jacket without considering any specific cause.

These results are considered bounding for the design life of the ISFSI. Even if the fault current increases over the life of the facility, the results remain valid because the resulting damage increase would not be significant. The line-to-ground voltage is the predominant factor in arc ignition. An increase in fault current would have minimal consequences. A larger hole size does not change the radiological dose consequences because there is minimal damage to the concrete shielding in the overpack, no damage to the lead shielding in the transfer cask, and no damage to the inner steel liners in both the overpack and the transfer cask.

It is concluded that the postulated transmission line break will not cause the affected cask components to exceed either normal or accident condition temperature limits and that localized material damage at the point of arc is bounded by accident conditions discussed in Sections 8.2.2 and 8.2.11. As a result of these considerations, it is concluded that the postulated transmission line drop does not adversely affect the thermal performance of either system.

8.2.8.3 Electrical Accident Dose Calculations

The postulated electrical events are shown to result in a negligible increase in the temperatures of the affected components and damage to a small amount of material in the localized area of arc. The resulting temperatures would remain bounded by both the normal and accident condition temperature limits.

The small loss of material is negligible compared to the total mass of shielding materials, so there would be no significant increase in overall cask dose rates. As noted above, the concrete behind the overpack outer shell would not likely be affected. Thus, the change in shielding would be negligible. In any event, a more limiting condition is evaluated in Section 8.2.2.

In the case of the transfer cask, there would be an increase in radiation doses adjacent to the cask should the shielding water in the water jacket be lost. The loss of neutron shielding is evaluated in Section 8.2.11. The addition of a hole in the transfer cask outer shell would have a negligible impact on dose. The impact on personnel exposures is considered to be negligible.

The MPC is protected from electrical damage by the overpack. Thus, there is no release of the contained radioactive material from the MPC. Doses to persons located offsite are not affected by these events.

8.2.8.4 Conclusions

The postulated electrical events may possibly result in a small hole in either the overpack or the transfer cask. Both conditions are conservatively bounded by previously analyzed events in Sections 8.2.2 and 8.2.11.

8.2.9 LOADING OF AN UNAUTHORIZED FUEL ASSEMBLY

The Diablo Canyon ISFSI TS and SAR Section 10.2 specify limiting values for the initial enrichment, burnup, decay heat, and cooling time after reactor discharge for the fuel assemblies to be placed into the MPCs. The possibility of storing a fuel assembly that does not meet the Diablo Canyon ISFSI TS and SAR Section 10.2 has been considered.

8.2.9.1 Cause of Loading an Unauthorized Fuel Assembly

Procedures will be used to administratively control and document the planning and loading of all DCPP fuel assemblies to be stored in each overpack. The cause of this event is postulated to be an error during spent fuel planning or loading operations (for example, a planning error occurs in selecting the fuel assembly to be stored or the wrong fuel assembly is loaded into an MPC).

8.2.9.2 Analysis of the Loading of an Unauthorized Fuel Assembly

The chance of loading of an unauthorized fuel assembly is greatly minimized because of the multiple administrative controls imposed via procedures to ensure a fuel planning or loading error does not remain undetected. These procedures prescribe how the planning is performed and verified to ensure the characteristics of selected fuel assemblies are within the applicable Diablo Canyon ISFSI TS and SAR Section 10.2 limits. Likewise, the spent fuel loading procedures require that a final verification of the identity and location of fuel assemblies be performed prior to placing the lid on the MPC. These procedures are part of the ISFSI operational procedures described in Section 9.4.1.1.4.

The loading of an unauthorized fuel assembly has no consequence while the transfer cask/MPC assembly remains in the spent fuel pool (SFP) as explained below. The borated water in the SFP provides adequate protection against a criticality event, and also provides shielding and heat removal. Loading of an unirradiated fuel assembly will not cause a criticality event because the MPC design precludes criticality assuming all loaded fuel assemblies are unirradiated (that is, no burnup credit taken). Loading of a fuel assembly with gross cladding defects will not cause further damage to the cladding or result in the release of radioactive material. Loading of a fuel assembly with structural defects will likely be detected during placement into the MPC. These events will not go undetected because fuel condition will be verified as part of the loading process.

8.2.9.3 Conclusion

As discussed above, the use of procedures, which prescribe and verify the rigorous planning and loading activities, provides reasonable assurance that only fuel assemblies meeting Diablo Canyon ISFSI TS and SAR Section 10.2 requirements will be loaded for storage.

8.2.10 EXTREME ENVIRONMENTAL TEMPERATURE

Extreme environmental temperature is classified as a natural phenomenon Design Event IV as defined in ANSI/ANS-57.9. The extreme environmental temperature accident involves the postulation of an unusually high ambient temperature at the Diablo Canyon ISFSI site. Unlike the off-normal high temperature evaluated in Section 8.1.2, the postulated, extreme-high temperature is beyond what can be reasonably expected to occur over the life of the ISFSI and represents a bounding, worst-case scenario.

8.2.10.1 Cause of Extreme Environmental Temperature

The extreme environmental temperature event for the HI-STORM 100 System is analyzed at an environmental temperature of 125°F in the HI-STORM 100 System FSAR, as amended by LAR 1014-1, Section 11.2.15, and -40°F in LAR 1014-1, Section 4.4.3. To determine the effects of the extreme temperature, it is conservatively assumed that the temperature persists for a sufficient duration to allow the HI-STORM 100 System to achieve thermal equilibrium. Because of the large mass of the HI-STORM 100 System, with its corresponding large thermal inertia and the limited duration for the extreme temperature, this assumption is conservative.

8.2.10.2 Extreme Environmental Temperature Analysis

8.2.10.2.1 Upper Temperature Limit

The accident condition considered in the HI-STORM 100 System FSAR, as amended by LAR 1014-1, assumes an extreme environmental temperature of 125°F for a duration sufficient to reach thermal equilibrium. This bounds the extreme-maximum-site ambient temperature for the Diablo Canyon ISFSI site of 104°F (Section 3.4.). This condition is evaluated with respect to accident condition component design temperatures listed in Table 2.2.3 of the HI-STORM 100 System FSAR. The evaluation was performed with the HI-STORM 100 System FSAR design-basis fuel with the maximum decay heat and the most restrictive thermal resistance. The HI-STORM 100 generic evaluation of a 125°F environmental temperature is applied with the peak solar insolation as described in the HI-STORM 100 System FSAR. The solar insolation assumed in the generic analysis bounds that for the Diablo Canyon ISFSI site.

The HI-STORM 100 System maximum temperatures for components close to the design-basis temperatures are discussed in the HI-STORM 100 System FSAR, Section 4.4. These temperatures are calculated at a normal environmental temperature of 80°F. The extreme environmental temperature is 125°F, which is an increase of 45°F. This event is simplistically evaluated by adding the 45°F difference to each of the limiting normal component temperatures. This yields conservatively bounding temperatures for all of the HI-STORM 100 System components because the thermal inertia of the HI-STORM 100 System is not credited. The resulting component temperatures under extreme environmental temperature condition are reported in the HI-STORM 100 System FSAR, Table 11.2.7, as amended by LAR 1014-1. As illustrated by the table, all the temperatures are well below the accident-condition, design-basis component temperatures. Since the extreme environmental temperature is of a short duration (several consecutive days would be highly unlikely), the resultant temperatures are evaluated against short-term accident condition temperature limits.

Therefore, the HI-STORM 100 System component temperatures meet design requirements under the extreme environmental temperature condition.

Additionally, the effect of extreme environmental temperature on MPC internal pressure was evaluated. The resultant pressure was bounded by the pressure calculated for complete blockage of the inlet duct. In the case of complete duct blockage, the calculated temperatures are much higher than the temperatures that result from the extreme environmental temperature. The accident condition pressure for the bounding MPC (MPC-32) was determined for concurrent 100 percent fuel rod rupture and was found to be below the accident design pressure of 200 psig.

8.2.10.2.2 Lower Temperature Limit

The HI-STORM 100 System was also evaluated for a -40°F extreme low ambient temperature condition, as discussed in Section 4.4.3 of the HI-STORM 100 System FSAR. Zero decay heat generation from spent fuel and no solar insolation were conservatively assumed. All materials of construction for the MPC and overpack will perform their design function under this extreme cold condition. Since the minimum temperature at the Diablo Canyon ISFSI is greater than or equal to 24°F (Table 3.4-1), the extreme low ambient temperature evaluation in the HI-STORM 100 System FSAR bounds the conditions at the Diablo Canyon ISFSI.

8.2.10.3 Extreme Environmental Temperature Dose Calculations

The extreme environmental temperature range at the Diablo Canyon ISFSI will not cause the overpack concrete to exceed its normal design temperature. Therefore, there will be no degradation of the concrete shielding effectiveness. The extreme temperature range will not cause a breach of the confinement system and the short-term fuel cladding temperature limit is not exceeded. Therefore, there is no radiological impact on the HI-STORM 100 System for the extreme environmental temperature range, and the dose rates under this accident condition are equivalent to the normal condition dose rates.

8.2.10.4 Extreme Environmental Temperature Corrective Action

There are no consequences of this accident that require corrective action.

8.2.11 HI-TRAC TRANSFER CASK LOSS-OF-NEUTRON SHIELDING

This accident event postulates the loss-of-neutron shielding provided by the transfer cask water jacket and the Holtite-A solid neutron shielding in the transfer cask top lid and bottom shield. A loss-of-neutron shielding is classified as a Design Event IV, as defined in ANSI/ANS-57.9.

8.2.11.1 Cause of Loss-of-Neutron Shielding

Throughout all design-basis-accident conditions, the axial location of the fuel will remain fixed within the MPC because of the upper and lower fuel spacers. Chapter 3 of the HI-STORM 100 System FSAR, as amended by LAR 1014-1, shows that the fuel spacers, transfer cask inner shell, lead, and outer shell remain intact throughout all design-basis normal, off-normal, and accident loading conditions. (The 10 CFR 50 LAR in support of the Diablo Canyon ISFSI addresses the effect of lead slump on the transfer cask shielding after a vertical drop inside the FHB/AB.) Localized damage of the transfer cask outer shell could be experienced, but no loss of shielding results.

Two potential causes for the loss of neutron shielding provided by the transfer cask are:

(1) Elevated temperatures as a result of a fire accident could result in the temperature of the Holtite-A exceeding the design-accident temperature. The pressure of the water jacket could also increase due to a fire, to the point where the overpressure relief valve on the water jacket would vent steam and water to the atmosphere. This would result in the loss of some amount of the water used for neutron shielding.

(2) Puncture of the transfer cask outer neutron shield jacket by a small object traveling at high speed, such as a tornado-borne missile, would cause the shield water to drain out at the point of puncture.

Other shielding credited in the shielding analyses includes the steel transfer cask and overpack structures, concrete, and lead. There are no credible events that could cause a significant degradation or loss of these solid forms of shielding.

8.2.11.2 Loss-of-Neutron Shielding Analysis

In the transfer cask, which uses Holtite-A in the top lid and bottom shield for neutron shielding, a fire could cause the Holtite-A to exceed its design-accident-temperature limit. For the dose analysis, it is conservatively assumed that all of the Holtite-A in the transfer cask top lid and bottom shield is lost. The potential reduction in shielding effectiveness of the Holtite-A in the transfer cask top lid results in a dose rate that is bounded by the normal dose rates in the area of the access hole in the transfer cask top lid. Therefore, no additional evaluation of this scenario is required. The accident condition dose rate through the transfer cask bottom shield with no Holtite-A is bounded by the accident dose rate at the side of the transfer cask with an assumed loss of all water in the water jacket, as discussed below. This is based on the accident dose rate adjacent to the empty water jacket being greater than the normal condition dose rate adjacent to the transfer cask pool lid without the bottom shield installed as discussed in the HI-STORM 100 System FSAR, as amended by the LAR 1014-1, Tables 5.1.8 and 5.1.10.

The bounding consequence that affects the shielding materials of the transfer cask is the potential for damage to the water jacket shell and the loss of all of the neutron shield (water). In the accident consequence analysis, it is conservatively assumed that the neutron shield (water) is completely lost and replaced by a void. The assumed loss of all water in the water jacket results in an increase in the radiation dose rates at locations adjacent to the water jacket. The shielding analysis results presented in Section 5.1.2 of the HI-STORM 100 System FSAR, as amended by LAR 1014-1, demonstrate that the dose limits of 10 CFR 72.106 are not exceeded if all of the water in the water jacket is lost. It is shown in Section 11.2.4 of the HI-STORM 100 System FSAR, as amended by LAR 1014-1, that the increase in fuel cladding and component material temperatures due to the loss of water in the water jacket do not cause the short-term fuel cladding or material temperature limits listed in the HI-STORM 100 System FSAR Table 2.2.3 to be exceeded. The internal MPC pressure also remains below the 200-psig-accident design limit. Therefore, there is no affect on the integrity of the MPC confinement boundary.

8.2.11.3 Loss-of-Neutron Shield Dose Calculations

The complete loss of the transfer cask neutron shield along with the water-jacket shell is assumed in the shielding analysis for the post-accident analysis of the loaded transfer cask in Section 5.1.2 of the HI-STORM 100 System FSAR, as amended by LAR 1014-1. As shown therein, the complete loss of the transfer cask neutron shield significantly affects the dose rate at mid-height of the transfer cask, and the accident dose rate (calculated using the burnups and cooling times that produce the highest dose rates) is 1.47 mrem/hr at an assumed distance of 100 meters from the ISFSI storage pad. For the 30-day duration of the event, the total dose at this location is 1.058 rem, which is less than the accident dose limit in 10 CFR 72.106. The minimum distance to the controlled-area boundary at the Diablo Canyon ISFSI is approximately 1,400 ft (430 m). Therefore, the generically-calculated doses for this accident from the HI-STORM 100 System FSAR bound those for the Diablo Canyon ISFSI site.

Doses to onsite personnel will be monitored after a loss-of-neutron shielding event and temporary shielding may be employed at the discretion of the DCPP radiation protection organization.

8.2.12 ADIABATIC HEAT-UP

This noncredible accident event postulates that the loaded overpack is unable to reject heat to the environment through conduction, convection, or radiation. This is classified as a Design Event IV, as defined by ANSI/ANS 57.9.

8.2.12.1 Cause of Accident

There is no credible accident that could completely stop heat transfer from the overpack to the environment. Even if the overpack were to be completely buried, with the inlet and outlet vent ducts blocked, some heat transfer would occur via conduction through the overpack structure and the material covering the overpack, and through convection at the surface of the outer material. The Diablo Canyon ISFSI site is located where a portion of the hill has been excavated (Figure 2.1-2). The slope protection of the hill adjacent to the storage pads (Section 4.2.1.1.9) precludes a landslide that completely covers one or more casks on the ISFSI pads. Should a slide occur, minor amounts of material could be removed before excessive heat up would occur. Also, there are no sources of volcanic activity or large amounts of debris located above, and sufficiently close to, the ISFSI site that could cause a complete covering of one or more casks on the ISFSI pads. This is a non-mechanistic accident and is evaluated to yield the most conservative response of the HI-STORM 100 System.

8.2.12.2 Accident Analysis

Section 11.2.14 of the HI-STORM 100 System FSAR, as amended by LAR 1014-1, discusses the "Burial-Under-Debris" accident, which is modeled as an adiabatic heat-up event. The analysis of this event is summarized below.

Burial of the loaded overpack does not impose a condition that would have more severe consequences for criticality, confinement, shielding, and structural analyses than that performed for the other accidents analyzed. The debris would provide additional shielding to reduce radiation doses. The accident external pressure encountered during the flooding accident (Section 8.2.3) bounds any credible pressure loading caused by the burial under debris.

Burial under debris can affect thermal performance because the debris acts as an insulator and heat sink. The insulating effect will cause the HI-STORM 100 System and fuel cladding temperatures to increase. A thermal analysis has been performed to determine the time for the fuel cladding temperatures to reach the short-term, accident-condition temperature limit during a burial under debris accident.

To demonstrate the inherent safety of the HI-STORM 100 System, a bounding analysis that considers the debris to act as a perfect insulator is considered. Under this scenario, the contents of the HI-STORM 100 System will undergo a transient heat up under adiabatic conditions. The minimum time required for the fuel cladding to reach the short-term, design, fuel-cladding-temperature limit depends on the amount of thermal inertia of the cask, the cask initial conditions, and the spent fuel decay heat generation.

Figure 11.2.6 of the HI-STORM 100 System FSAR, as amended by LAR 1014-1, shows that the time to reach the short-term, fuel-cladding-temperature limit varies from approximately 45 hours at a total cask heat load of 30 kW (higher than the maximum authorized cask heat load) to more than 130 hours at a cask heat load of 10 kW.

8.2.12.3 Accident Dose Calculations

Since there is no degradation in shielding or confinement capabilities as discussed above, there is no effect on occupational or public exposures as a result of this event.

As discussed in burial-under-debris analysis, the shielding is enhanced while the HI-STORM 100 System is covered. The elevated temperatures will not cause the breach of the confinement system and the short-term, fuel-cladding-temperature limit is not exceeded. Therefore, there is no radiological impact.

8.2.13 PARTIAL BLOCKAGE OF MPC VENT HOLES

Each MPC basket fuel cell wall has elongated vent holes at the bottom and top. These holes facilitate the natural circulation of helium inside the MPC for convection heat transfer. The partial blockage of the MPC basket vent holes accident has been evaluated to determine the effects on the HI-STORM 100 System due to the reduction in the size of the vent openings. This accident condition is discussed in Section 11.2.5 of the HI-STORM 100 System FSAR, as amended by LAR 1014-1.

8.2.13.1 Cause of Partial Blockage of MPC Vent Holes

After the MPC is loaded with spent nuclear fuel, the MPC cavity is drained, dried, and backfilled with helium. There are three possible sources of material that could block the MPC basket vent holes. These are the fuel cladding, fuel pellets, and crud. Gross fuel cladding rupture is precluded by design in accordance with 10 CFR 72.122(h)(1). Due to the maintenance of relatively low cladding temperatures during storage, it is not credible that the fuel cladding would rupture and that fuel cladding and fuel pellets would fall to block the basket vent holes. Damaged fuel and fuel debris are stored in damaged fuel containers, which have screens to minimize the dispersal of gross particulates. However, it is conceivable that a percentage of the loose crud deposited on the external surfaces of the fuel rods may fall away and deposit at the bottom of the MPC.

Helium in the MPC cavity provides an inert atmosphere for storage of the fuel. During normal storage operations, the design of the HI-STORM 100 System maintains the peak fuel rod cladding temperature below the required long-term storage limits. There are no credible, design-basis accidents that cause the fuel assembly to experience a deceleration loading greater than the limits established in the HI-STORM 100 System FSAR, Section 3.5. (As discussed in Section 8.2.4, the load portions of the transporter and the lifting devices attached to the transfer cask and overpacks are designed to preclude drop events.)

Crud can be made up of two types of layers, namely, loosely-adherent and tightly-adherent. The fuel assembly movement from the fuel racks to the MPC, and subsequent movement of the MPC during cask loading, transfer, and transport operations, may cause a portion of the loosely-adherent crud to fall away. The tightly-adherent crud remains in place during ordinary fuel handling operations.

8.2.13.2 Analysis of Partial Blockage of MPC Vent Holes

The MPC vent holes that act as the bottom plenum for the MPC internal helium circulation are of an elongated, semi-circular design to ensure that the flow passages will remain open under a hypothetical shedding of the crud on the fuel rods. For conservatism, only the minimum semi-circular hole area is credited in the thermal models (that is, the elongated portion of the hole is completely neglected).

The amount of crud on fuel assemblies varies greatly from plant to plant. The maximum crud depths calculated for each of the MPCs is listed in Table 2.2.8 of the HI-STORM 100 System FSAR. The maximum amount of crud was assumed to be present on all fuel rods within the MPC. Both the tightly- and loosely-adherent crud was conservatively assumed to fall off of the fuel rods. The assumed crud depth does not totally block any of the MPC basket vent holes as the crud accumulation depth is less than the elongation of the vent holes. Therefore, the remaining cross-sectional flow area through the vent holes area is greater than that used in the thermal models.

The partial blockage of the MPC basket vent holes has no effect on the structural, confinement, and thermal analysis of the MPC. There is no significant effect on the shielding analysis because the source term from the crud is enveloped by the source term from the fuel and the activated nonfuel hardware of the fuel assemblies. As the MPC basket vent holes are not completely blocked, preferential flooding of the MPC fuel basket is not possible during draining operations and, therefore, the criticality analyses are not affected.

8.2.13.3 Dose Calculations for Partial Blockage of MPC Vent Holes

Partial blockage of basket vent holes will not result in a compromise of the confinement boundary because the thermal model accounts for the partial blockage. Fuel decay heat, burnup, and cooling time limits in SAR Section 10.2 are determined accordingly to ensure that the cask heat transfer remains within the limits of the licensing analysis. Therefore, there will be no loss of confinement or radioactive material release.

Any increase in dose rate through the bottom of the cask due to crud accumulation is inconsequential for several reasons. The total amount of source in the cask is not increased; it is simply relocated by the distance between where the crud particle was located on the fuel assembly and the bottom of the MPC. Any minimal dose increase at the bottom of the cask is inconsequential while the cask is on an ISFSI pad because the bottom of the cask (being flush against the pad surface) is not a source of exposure during storage operations. During vertical handling operations, the overpack and transfer cask are lifted only to those heights necessary to facilitate required cask movements. These heights are typically low enough to physically prevent personnel access. Administrative controls related to prudent, heavy-load movement will preclude personnel from access underneath the lifted cask inside the FHB/AB. During horizontal transportation of the transfer cask between the FHB/AB and the CTF, the additional dose is negligible due to the shielding provided by the bottom of the MPC, the pool lid, and the supplemental transfer-cask bottom shield.

8.2.14 100 PERCENT FUEL ROD RUPTURE

This accident event postulates that all of the fuel rods in a sealed MPC rupture and that fission-product gases and fill gas are released from the fuel rods into the MPC cavity.

8.2.14.1 Cause of Accident

Through all credible accident conditions, the HI-STORM 100 System maintains the spent nuclear fuel in an inert environment while maintaining the peak fuel-cladding temperature below the short-term temperature limits, thereby ensuring fuel-cladding integrity. Although rupture of all the fuel rods is assumed, there is no credible cause for 100 percent fuel rod rupture. This accident is postulated to evaluate the MPC confinement boundary for the maximum possible internal pressure based on the non-mechanistic failure of 100 percent of the fuel rods.

8.2.14.2 Accident Analysis

The 100 percent fuel-rod-rupture accident has no thermal, criticality, or shielding consequences. The event does not change the reactivity of the stored fuel, the magnitude of the radiation source, which is being shielded, the shielding capacity, or the criticality control features of the HI-STORM 100 System. It only has the potential for affecting the internal pressure of the MPC and the leakage from the MPC. The determination of the maximum accident pressure due to a hypothetical 100 percent fuel rod rupture accident was evaluated for the MPC-32 as a bounding case for all MPCs that are licensed for use at the Diablo Canyon ISFSI.

The MPC-32 internal cavity pressure was calculated for the 100 percent rod rupture accident using the methodology from the HI-STORM 100 System generic analysis documented in Section 4.4.4 of the HI-STORM 100 System FSAR. Limiting input values were assumed for initial fuel rod fill pressure (715 psia), fuel burnup (70,000 MWD/MTU), decay heat load (28.74 kW) and minimum MPC cavity volume. The presence of nonfuel hardware and the release of fission gases from the BPRAs was also accounted for. These assumptions bound the characteristics for fuel to be loaded in any MPC to be deployed at the Diablo Canyon ISFSI. The computed MPC internal pressure from the 100 percent rod rupture accident is 185.5 psia (170.8 psig), which is less than the MPC accident design pressure of 200 psig (Reference 12, Table 2.0.2).

8.2.14.3 Accident Dose Calculations

There is no effect on the shielding performance or criticality control features of the system as a result of this event. There is no effect on the confinement function of the MPC as a result of this event. All stresses remain within allowable values, ensuring confinement boundary integrity. Since there is no degradation in shielding or confinement capabilities as discussed above, there is no effect on occupational or public exposures as a result of this event.

The MPC confinement boundary maintains its integrity for this postulated event. There is no effect on the shielding effectiveness, and the magnitude of the radiation source is unchanged. However, the radiation source could redistribute within the sealed MPC cavity causing a slight change in the radiation dose rates at certain locations. In that case though, the radiation dose at the ISFSI site boundary would not be affected. There is no release of radioactive material or significant increase in radiation dose rates.

8.2.15 100 PERCENT BLOCKAGE OF AIR INLET DUCTS

This accident postulates the complete blockage of all four inlet air ducts of the overpack. Blockage of the inlet air ducts is equivalent to the condition where all four outlet air ducts are blocked because either scenario stops air flow through the overpack. While a small amount of warmed air may exit the outlet air ducts and be replaced with cooler ambient air, this mechanism is of second order compared with the heat redistribution effect of the buoyancy-driven, natural-convection circulation that is established in the annular space between the MPC and overpack. As the dominant natural convection circulation is identical for either the inlet or outlet air ducts blockage, the following evaluation is applicable to both conditions. The loss of the small, second-order, air-exchange effect should the top ducts be blocked would be a lesser magnitude than the inherent conservatisms in the analysis resulting from the assumptions of complete blockage, maximum decay heat load, high ambient temperature, conservative conductivity modeling, and conservative solar heat. The complete blockage of air inlet ducts is classified as Design Event IV as defined by ANSI/ANS-57.9.

8.2.15.1 Cause of 100 Percent Blockage of Air Inlet Ducts

In Section 11.2.13 of the HI-STORM 100 System FSAR, as amended by LAR 1014-1, the 100 percent blockage of all overpack air inlet ducts is postulated to occur due to an environmental event such as flooding, snowfall, tornado debris, or volcanic activity. Of these, only blockage by tornado debris is credible at the Diablo Canyon ISFSI (Chapter 2). The slope protection of the hill adjacent to the storage pads (Section 4.2.1.1.9) precludes a landslide that completely covers all air inlet ducts. Should a slide occur, minor amounts of material could be removed before excessive heatup would occur. There is no credible, design-basis event at the Diablo Canyon ISFSI that could completely block all four air inlet ducts for an extended period of time where corrective action could not be taken in a timely manner to remove the blockage.

8.2.15.2 Analysis of 100 Percent Blockage of Air Inlet Ducts

The immediate consequence of a complete blockage of the air inlet ducts is that the normal circulation of air for cooling the MPC is stopped. An amount of heat will continue to be removed by localized air circulation patterns in the overpack annulus and outlet ducts, and the MPC will continue to radiate heat to the relatively cooler storage overpack. As the temperatures of the MPC and its contents rise, the rate of heat rejection will increase correspondingly. Under this condition, the temperatures of the overpack, the MPC, and the stored fuel assemblies will rise as a function of time.

As a result of the large mass, and correspondingly large thermal capacity, of the storage overpack (in excess of 170,000 lb), it is expected that a significant temperature rise is only possible if the completely blocked condition is allowed to persist for a number of days. This accident condition is, however, a short-duration event that will be identified and corrected through the performance of daily surveillance inspections required by the Diablo Canyon ISFSI TS.

There is a large thermal margin between the maximum-calculated, fuel-cladding temperature with design-basis fuel decay heat (HI-STORM 100 System FSAR Tables 4.4.9, 4.4.26, and 4.4.27) and the short-term, fuel-cladding-temperature limit (1,058°F), to accommodate this transient, short-term, fuel-cladding temperature excursion. The fuel stored in a HI-STORM 100 System can heat up by over 300°F before the short-term temperature limit is reached. The concrete in the overpack has a smaller, but nevertheless significant, margin between its calculated, maximum, long-term-temperature and its short-term-temperature limit, with which to withstand the temperature rise caused by this accident.

A detailed discussion of the analysis of this accident is provided in Section 11.2.13.2 of the HI-STORM 100 System FSAR, as amended by LAR 1014-1. This accident has been generically analyzed both with and without considering the effect of the thermosiphon convection heat transfer phenomenon inside the MPC. Since the limiting decay heats, burnups, and cooling times for the DCPP spent fuel authorized for loading into the HI-STORM 100 System are based on credit for thermosiphon convection in the MPC; the convection-based analysis is applicable to the Diablo Canyon ISFSI.

The results of the analysis without thermosiphon bound the Diablo Canyon ISFSI design-basis analysis with thermosiphon and show that the concrete section average (that is, through-thickness) temperature remains below its short-term-temperature limit for the 72-hour duration of the accident. Both the fuel-cladding and the MPC-confinement boundary temperatures remain below their respective short-term-temperature limits at 72 hours, the fuel cladding by over 150°F, and the confinement boundary by almost 175°F. Table 11.2.9 of the HI-STORM 100 System FSAR, as amended by LAR 1014-1, summarizes the temperatures at several points in the HI-STORM 100 System at 33 hours and 72 hours after complete, inlet-air-duct blockage.

The thermosiphon effect is credited in the determination of the maximum allowable fuel heat emission rates (via maximum burnup, maximum decay heat, minimum cooling time limits) in SAR Section 10.2. Incorporation of the MPC thermosiphon internal convection phenomenon, as described in Chapter 4 of the HI-STORM 100 System FSAR, as amended by LAR 1014-1, enables the maximum, design-basis, PWR-decay-heat load to rise to about 29 kW. The thermosiphon effect also shifts the highest temperatures in the MPC enclosure vessel toward the top of the MPC. The peak, MPC-lid, outer-surface temperature, for example, is computed to be about 450°F in the thermosiphon-enabled solution compared with about 210°F in the thermosiphon-suppressed solution, with both solutions computing approximately the same peak cladding temperature. In the 100 percent, inlet-duct-blockage condition, the heated MPC lid and MPC shell become effective heat dissipaters because of their proximity to the overpack outlet ducts and because the thermal radiation heat transfer rises at the fourth power of absolute temperature. As a result of this increased heat rejection from the upper region of the MPC, the time limits for reaching the short-term peak fuel-cladding temperature limits calculated without thermosiphon (72 hours) remains bounding.

Under the complete, air-inlet-duct-blockage condition, it must also be demonstrated that the MPC internal pressure does not exceed its design-basis accident limit. The bounding MPC internal pressure calculated at an ambient temperature of 80°F, 100 percent fuel rods ruptured, design-basis insolation, and maximum decay heat is 185.5 psia, as discussed in Section 8.2.14.2. This calculated pressure is for an MPC cavity bulk gas temperature of 513.6°K. Using this initial pressure, a bounding increase in the MPC cavity temperature of 184°F (102.2°K, maximum of MPC shell or fuel cladding temperature rise 33 hours after blockage of all four ducts; see HI-STORM 100 System FSAR Table 11.2.9), the reduction in the bulk average gas temperature due to increased MPC heat dissipation at higher pressure of 62.1°F (34.5°), and the Ideal Gas Law, the resultant MPC internal pressure is calculated to be 209.9 psia (195.2 psig), which is less than the accident design pressure of 200 psig (HI-STORM 100 System FSAR Table 2.2.1). The HI-STORM 100 System FSAR generic assumption of an annual average temperature of 80°F bounds the Diablo Canyon site annual-average temperature of 55°F. The HI-STORM 100 System FSAR uses 800 g-cal/cm^2 per day for the full insolation level as recommended in 10 CFR 71 (averaged over a 24-hour period as allowed in NUREG-1567). The maximum insolation values for the ISFSI site are estimated to be 766 g-cal/cm^2 per day for a 24-hour period and are therefore bounded by the analysis in the HI-STORM 100 System FSAR, as amended by LAR 1014-1.

8.2.15.3 Dose Calculations for 100 Percent Blockage of Air Inlet Ducts

As shown in the analysis of the 100 percent blockage of air inlets accident in the HI-STORM 100 System FSAR, the shielding capabilities of the HI-STORM 100 System are unchanged because the section average concrete temperature does not exceed its short-term-condition design temperature limit for the duration of the accident. The Diablo Canyon ISFSI TS require the blockage to be cleared within 8 hours of declaring the heat removal system inoperable. Assuming the blockage occurs just after the last 24-hour surveillance is performed, the 8-hour completion time provides a total of 32 hours in this condition, which is less than the 72-hour analyzed duration of the event. The concrete, fuel cladding and MPC shell do not reach their short-term-temperature limits over the entire analyzed 72-hour duration of the event. In addition, the emergency procedures will require an inspection of the ISFSI following a tornado, which will shorten the time to complete clearing the blockage. The elevated temperatures will not cause a breach of the confinement system and the short-term, fuel-cladding-temperature limit is not exceeded. Therefore, there are no direct or airborne radiation consequences of this accident.

For complete blockage of air inlet ducts it is estimated that the removal, cleaning, and replacement of the affected mesh screens will take two people approximately 2 hours. The radiation doses to workers who remove debris blocking the inlet ducts are estimated to be double those conservatively estimated for the analysis of the partial inlet blockage in Section 8.1.4. The dose rate at this location is estimated to be 58 mrem/hour. The total exposure for two people taking 2 hours to perform these corrective actions is 0.232 man-rem.

8.2.16 TRANSMISSION TOWER COLLAPSE

Two 500-kV transmission towers are located in the vicinity of the ISFSI storage pads and CTF. This section addresses the impact of a fallen transmission tower on a loaded overpack. During transportation to the CTF and all handling and lifting activities at the CTF, a loaded transfer cask is protected from the impact of a falling transmission tower at all times by the structure of the cask transporter. Therefore, an analysis of the transfer cask for tower collapse impact loads is not required and has not been performed. A postulated transmission tower collapse at both the ISFSI storage site and CTF was analyzed (Reference 45) to demonstrate that there is no loss of confinement from damage to an MPC during both transfer operations or while stored at the ISFSI pad in an overpack. The collapse of a transmission tower is classified as Design Event IV, as defined by ANSI/ANS-57.9.

8.2.16.1 Cause of Transmission Tower Collapse

The transmission tower collapse is postulated as a consequence of extreme wind speeds (above 84 mph) creating greater than design loads on the tower structure.

8.2.16.2 Analysis of the Transmission Tower Collapse

The location of the transmission towers with respect to the CTF and ISFSI storage pads is shown in Figure 2.1-2. A transmission tower is postulated to collapse by hinging of the legs and failure of braces without incident of leg or pile foundation pullout or lateral failure due to wind- or tornado-wind-generated loads. The transmission tower is a four-legged structure with a "T" shape at the top. Based on the location of the transmission corridor with respect to the CTF and the ISFSI storage pad and the conduct of loading operations, in the unlikely event of a collapse, a tower could impact the loaded overpack in different orientations at the CTF and the storage pad. At the CTF, the tower collapse is modeled with the pointed section of the "T" cross-bar impacting the MPC lid directly because the overpack may not have its top lid installed at the time of the event. At the ISFSI, the flat side of the "T" cross-bar impacts the overpack top lid.

A commercial computer code developed by the Livermore Software Technology Corporation and QA validated by Holtec International, LS-DYNA (Reference 26), was used to numerically model the problem and develop the impact forces of the tower structure on the target. LS-DYNA is a general purpose, explicit finite element program used to analyze the nonlinear dynamic response of two- and three-dimensional inelastic structures.

There are two towers that are close enough in proximity to the CTF and ISFSI storage site to impact a cask if a tower collapse were to occur. The applicable physical characteristics for the two transmission towers are:

(1) One tower has a height of approximately 125 ft, measured from the ground to the highest point. It is located, at its nearest foundation, approximately 100 ft west of the ISFSI pads and 60 ft south of the CTF. It has a total structural weight of approximately 25 kips.

(2) The other tower has a height of approximately 135 ft, measured from the ground to the highest point. It is located, at its nearest foundation, approximately 60 ft east of the ISFSI pads. It has a total structural weight of approximately 31 kips.

The analysis evaluates the impact forces generated by collapse of the second tower as the governing case since it is a taller and heavier tower.

8.2.16.2.1 Tower Collapse at the CTF

The LS-DYNA computer simulation of the tower collapse at the CTF models the pointed portion of the "T" bar impacting the MPC lid. The force of the tower impact on the MPC lid is 427 kips. This force is much smaller than the allowable impact force for the weld (2,789 kips) determined in the tornado-missile analysis, and thus will not cause a breach of the MPC confinement boundary. The maximum local stress of the MPC lid due to the impact is 14.6 ksi, which is smaller than the yield stress of the lid material (18.8 ksi). The potential for MPC-lid puncture due to this event is bounded by the intermediate-missile evaluation described in Section 8.2.2. The design-basis intermediate missile (a 760-lb insulator string traveling at 157 mph) is shown not to penetrate the 9-1/2-inch-thick MPC lid.

8.2.16.2.2 Tower Collapse at the ISFSI Storage Pad

The LS-DYNA computer simulation of the tower collapse at the ISFSI storage pad models the flat side of the "T" bar impacting the overpack top lid. The unfiltered impact force was computed to be 534 kips. To convert this to an equivalent g-load on the overpack, the 534 kips is divided by the weight of the loaded overpack:

$$534 / 360 = 1.48 \text{ g}$$

The overpack structure is designed to withstand a 45-g deceleration. Therefore, the impact of the force due to the transmission tower collapse is bounded with margin. The horizontal component of the impact force is less than 93 kips, which is bounded by the large tornado missile load of 122 kips described in Section 8.2.2. The overturning moments are also bounded for the effects on the anchorage to the ISFSI pad. MPC confinement boundary integrity related to tower impact discussed in Section 8.2.16.2.1 is applicable at the pad.

8.2.16.3 Dose Calculation for Transmission Tower Collapse

There are no offsite dose consequences as a result of this accident because the MPC confinement boundary remains intact. Potential damage to the overpack structure as a result of this event will vary based on the actual location and severity of the impact on the overpack. Based on the loads described above, no significant damage to the shielding effectiveness of the overpack is expected. If necessary, corrective actions will be implemented based on the nature of the damage in a time frame commensurate with safety significance.

8.2.17 NONSTRUCTURAL FAILURE OF A CTF LIFT JACK

This section addresses the nonstructural failure of one CTF lift jack on a loaded overpack requiring convective cooling. Three lift jacks are used simultaneously to raise and lower the CTF lifting platform on which the overpack rests. A postulated failure of one lift jack at the CTF was evaluated as a hypothetical accident. The nonstructural failure of a lift jack at the CTF is classified as Design Event IV, as defined by ANSI/ANS-57.9.

The lift jacks and platform are designed using the applicable guidelines of NUREG-0612 and seismically analyzed to ensure that structural failure is not a credible event. The CTF design criteria, facility description, and operations and maintenance activities are presented in Sections 3.3.4, 4.4.5, and 5.1, respectively.

8.2.17.1 Cause of Nonstructural Failure of a CTF Lift Jack

The nonstructural failure of a lift jack is postulated as a consequence of an electrical or mechanical malfunction of a lift jack component causing all lift jacks to stop.

8.2.17.2 Analysis of the Nonstructural Failure of a CTF Lift Jack

The CTF is designed to position an overpack sufficiently below grade where the transfer cask can be mated to the overpack using the cask transporter. In this position, the top approximately 3 ft of the overpack remains above grade while the base of the overpack is in a confined air space. The CTF lift platform, suspended by each jack screw, raises and lowers the overpack. Three lift jacks provide the lifting force for the lifting platform. The jacks are located on the circumference of the main shell in the extensions, 120 degrees apart. The jacks are supported at the top end and use a traveling-nut design. The captured nut travels along the rotating threaded jack screw shaft to provide the lifting and lowering motion for the lifting platform. All jacks operate in unison to keep the platform level through the entire travel range (approximately 150 inches).

The CTF lifting platform provides the support of the overpack and transmits the lifting jack force to the overpack. The platform provides a level base on which the overpack rests. To interface with the lifting jacks, the platform has extensions that enter into each main shell extension. The location and controlled movement of the jacks afford uniform loading of the lifting platform. The main shell provides radial guidance of the lifting platform.

It is postulated that if one lift jack fails, the platform and potentially a loaded overpack requiring convective cooling would be unable to be raised out of the confined air space for an extended period of time while corrective actions are performed. The design of the jack control system incorporates protective features whereby all jacks are stopped when a mismatch in the performance between operating jacks is detected. Thus, there is no mechanical damage to the overpack, and the only concern in this event is keeping the MPC and overpack sufficiently cooled and removing the overpack from the CTF.

By conservative analysis, the overpack can withstand a loss of normal ventilation cooling for up to 22 hours before the short-term temperature limit of the fuel cladding is reached. The conservative limit of 22 hours is based on the observation that the HI-STORM 100 System FSAR Section 4.5.2 case of a transfer cask in an underground silo envelopes the overpack in the CTF vault due to the overpack's larger thermal mass, greater opportunity for convective cooling, and lower initial temperature. If it is determined that the 22 hours may be exceeded during an actual event, the overpack is capable of being removed using the cask transporter with the HI-STORM lift links and lifting brackets.

The baseplate and outer shell temperatures for the all-inlet-ducts-blocked condition are 182°F and 185°F, respectively. They provide a reasonably bounding set of temperatures for the normal and accident CTF conditions where the steel shims are installed as seismic restraints in the annulus between the overpack and the top circumference of the CTF and natural convective cooling will be reduced below normal values. This is because, although natural convection cooling will be reduced while the overpack is in the CTF, there will be some cooling flow through the inlet and outlet air ducts and up to the environment through the openings between the shims. CTF concrete temperatures will actually be lower than these values as heat is transferred from the outer surfaces of the overpack, through the intervening steel CTF structural components, and air to the surrounding concrete. Therefore, the CTF concrete temperatures during normal conditions will be lower than the 200°F normal and off-normal temperature limit specified in NUREG-1567, Section 6.5.2.3 and the 350°F accident temperature limit specified in Section A.4.2 of Appendix A to ACI-349-97.

It is concluded that the postulated nonstructural failure of a lift jack accident will not result in the breach of MPC confinement, fuel cladding damage, or prevent MPC retrievability.

8.2.17.3 Dose Calculation for Nonstructural Failure of a CTF Lift Jack

Because the confinement boundary is not breached, there are no releases and no corresponding offsite dose consequences as a result of this accident.

The dose consequences to personnel implementing corrective actions for this accident are estimated using the dose rate for the removal of blockage from the air inlet ducts (Section 8.1.4). Using the blockage removal dose rate of 58 mrem/hour for these corrective actions is conservative because it includes contribution from the affected cask, as well as adjacent casks on the ISFSI storage pad. This accident involves only one cask at the CTF. Assuming it takes a crew of 5 a total of one, 8-hour shift spent in close proximity to the cask, the total accumulated dose to mitigate this event would be:

58 mrem/hr x 8 hr x 5 people = 2.32 man-rem

8.2.18 REFERENCES

1. ANSI N57.9-1992, Design Criteria for an Independent Spent Fuel Storage Installation (dry type), American National Standards Institute.

2. Standard Review Plan for the Review of Safety Analysis Reports for Nuclear Power Plants, USNRC, NUREG-0800, July 1981.

3. ASCE 4-86, Seismic Analysis of Safety-Related Nuclear Structures and Commentary on Standard for Seismic Analysis of Safety-Related Nuclear Structures, American Society of Civil Engineers, September 1986.

4. Diablo Canyon Power Plant Units 1 & 2 Final Safety Analysis Report Update, Revision 14, November 2001.

5. Visual Nastran Desktop Code, Version 2001, MSC Software Corp., 2001.

6. Final Safety Analysis Report for the HI-STORM 100 System, Holtec International Report No. HI-2002444, Revision 0, July 2000.

7. Boiler and Pressure Vessel Code, Section III, Division I, American Society of Mechanical Engineers, 1995 Edition including 1996 and 1997 addenda.

8. ANSI N14.6-1993, American National Standard for Radioactive Materials - Special Lifting Devices for Shipping Containers Weighing 10,000 Pounds (4500 kg) or More, Institute for Nuclear Materials Management.

9. Control of Heavy Loads at Nuclear Power Plants, USNRC, NUREG-0612, July 1980.

10. ACI-349-97, Code Requirements for Nuclear Safety Related Concrete Structures, American Concrete Institute (with 10/01/00 Draft Appendix B).

11. Draft Regulatory Guide DG-1098, Safety Related Concrete Structures for Nuclear Power Plants (Other than Reactor Vessel and Containment), USNRC, August 2000.

12. License Amendment Request 1014-1, Holtec International, Revision 2, July 2001, including Supplements 1 through 4 dated August 17,2001; October 5,2001; October 12, 2001; and October 19, 2001; respectively.

13. Standard Review Plan for Dry Cask Storage Systems, USNRC, NUREG-1536, January 1997.

14. Design of Structures for Missile Impact, BC-TOP-9A, Bechtel Power Corporation Topical Report, Revision 2, September, 1974.

15. National Fire Protection Association Fire Protection Handbook, Sixteenth Edition, 1986.

16. Evaluations of Explosions Postulated to Occur on Transportation Routes Near Nuclear Power Plants, USNRC, Regulatory Guide 1.91, Revision 1, February 1978.

17. Handbook of Chemical Hazards Analysis, Federal Emergency Management Agency (FEMA), 1989.

18. Perry and Green, Perry's Chemical Engineers' Handbook, Seventh Edition, 1997.

19. Structures to Resist the Effects of Accidental Explosions, Department of the Army Technical Manual TM 5-1300, November 1990.

20. Normal, Off-Normal and Hypothetical Dose Estimate Calculations, USNRC, Interim Staff Guidance Document-5, Revision 1, June 1999.

21. Transportation and Storage of Spent Fuel Having Burnups in Excess of 45 GWD/MTU, USNRC, Interim Staff Guidance Document-11, Revision 1, May 2000.

22. B. L. Anderson, et al, Containment Analysis for Type B Packages Used to Transport Various Contents, NUREG/CR-6487, Lawrence Livermore National Laboratory, November 1996.

23. Y. R. Rashid, et al, An Estimate of the Contribution of Spent Fuel Products to the Releasable Source Term in Spent Fuel Transport Casks, SAND88-2778C, Sandia National Laboratories, 1988.

24. Limiting Values of Radionuclide Intake and Air Concentration and Dose Conversion Factors for Inhalation, Submersion, and Ingestion, U.S. EPA, Federal Guidance Report No. 11, DE89-011065, 1988.

25. External Exposure to Radionuclides in Air, Water, and Soil, U.S. EPA, Federal Guidance Report No. 12, EPA 402-R-93-081, 1993.

26. LS-DYNA, Version 950, Livermore Software Technology Corporation, 1999.

27. PG&E Calculation No. 52.27.100.703 (HI-2002497), "Design Basis Wind and Tornado Evaluation for DCPP."

28. PG&E Calculation No. 52.27.100.704, "Non-Linear Seismic Sliding Analysis of the ISFSI Pad."

29. PG&E Calculation No. 52.27.100.707 (PGE-009-CALC-003), "ISFSI Cask Storage Pad Seismic Analysis."

30. PG&E Calculation No. 52.27.100.708 (PGE-009-CALC-002), "Cask Transfer Facility (Reinforced Concrete).'

31. PG&E Calculation No. OQE-9 (HI-2012768), "Transporter Stability on Diablo Canyon Dry Storage Travel Paths."

32. PG&E Calculation No. OQE-10 (HI-201626), "Structural Evaluation of Diablo Canyon Cask Transfer Facility."

33. H. A. Nelms, Structural Analysis of Shipping Casks, Effect of Jacket Physical Properties and Curvature on Puncture Resistance, Vol. 3 ORNL TM-1312, Oak Ridge National Laboratories, June 1968.

34. PG&E Calculation No. M-1052, "Determine the Heat Gain of the HI-TRAC Casks Due to a 2000 Gallon Gasoline Fire."

35. Probabilistic Risk Assessment, Calculation File No. PRA01-01, Revision 3, "Risk Assessment of Dry Cask/Spent Fuel Transportation within the DCPP Owner Controlled Area."

36. M. A. Finney, and P. L. Andrews, The FARSITE Fire Area Simulator: Fire Management Applications and Lessons of Summer 1994, In: Fire Management Under Fire (adapting to change): Proceedings, 1994 Interior West Fire Council meeting and program, 1994, Fairfield, CA: Interior West Fire Council, 1998.

37. Michael Fry, Wildlands Fuel Management Program; Annual Report. Diablo Canyon Land Stewardship Program, PG&E, 1999.

38. PG&E Calculation OQE-8 (HI-201618), "Analysis of Anchored HI-STORM Casks at the Diablo Canyon ISFSI."

39. PG&E Calculation 52.27.100.714 (GEO.DCPP.01.04), "Methodology for Determining Sliding Resistance Along Base of DCPP ISFSI Pads."

40. Holtec International Report No. HI-2002474, "Analysis of the Loaded HI-STORM 100 System Under Drop and Tipover Scenarios."

41. PG&E Calculation M-1048 (HI-2012615), "Evaluation of Site-Specific Wild Fires for the Diablo Canyon ISFSI."

42. PG&E Calculation M-1050 (HI-2002512), "Evaluation of Site-Specific Blasts and Explosions for the Diablo Canyon ISFSI."

43. PG&E Calculation STA-140 (HI-2002513), "Diablo Canyon ISFSI Site Boundary Confinement Analysis."

44. PG&E Calculation 378-DC (HI-2002559), "Evaluation of the Effects of Lightning and a 500-kV Line Break on Holtec Casks."

45. PG&E Calculation EQP-828.4 (HI-2012634), "Analysis of Transmission Tower Collapse Accidents at the Diablo Canyon ISFSI Pad and CTF."

46. PG&E Calculation OQE-14, "Seismic Stability Analysis of Transporter on Soil."

47. PG&E Calculation M-1058, "Cask Transfer Facility Seismic Restraint Configuration."

48. PG&E Calculation 52.27.100.711 (GEO.DCPP.01.01), "Development of Young's Modulus and Poisson's Ratios for DCPP ISFSI Based on Field Data."

49. PG&E Calculation 52.27.100.725 (GEO.DCPP.01.15), "Development of Young's Modulus and Poisson's Ratio Values for DCPP ISFSI Based on Laboratory Data."

50. Letter from N. Abrahamson, PG&E, to R. Klimczak, PG&E, "Ground Motion Along the Proposed Transport Route," September 13, 2002.

51. Probabilistic Risk Assessment, Calculation File No. PRA02-10, "Probabilistic Evaluation of Seismically Induced Cask Drop, Overturn of the Transporter, or Sliding of the Transporter Off the Transport Route."

TABLE 8.2-11

Deleted in Amendment 2

DIABLO CANYON ISFSI
SAFETY ANALYSIS REPORT

CHAPTER 10

OPERATING CONTROLS AND LIMITS

CONTENTS

DIABLO CANYON ISFSI
SAFETY ANALYSIS REPORT

CHAPTER 10

OPERATING CONTROLS AND LIMITS

TABLES

CHAPTER 10

OPERATING CONTROLS AND LIMITS

FIGURES

10.2 DEVELOPMENT OF OPERATING CONTROLS AND LIMITS

This section provides an overview of, and the general bases for, operating controls and limits specified for the Diablo Canyon ISFSI.

10.2.1 FUNCTIONAL AND OPERATING LIMITS, MONITORING INSTRUMENTS, AND LIMITING CONTROL SETTINGS

This section provides requirements for the controls or limits that apply to operating variables classified as important to safety and are observable and measurable. The operating variables required for the safe operation of the Diablo Canyon ISFSI are:

- Spent fuel characteristics
- Spent fuel storage cask (SFSC) heat removal capability
- Multi-purpose canister (MPC) dissolved boron concentration level
- Annulus gap water requirement during moisture removal for loading and reflooding for unloading
- Water temperature of a flooded MPC
- MPC vacuum pressures
- MPC recirculation gas exit temperature
- Helium purity
- MPC helium backfill pressures
- Gas exit temperature of a MPC prior to reflooding
- SFSC time limitation while seated in the cask transfer facility (CTF)
- Fuel cladding oxide thickness

Each of the specifications for these characteristics is provided below with the exception of the MPC dissolved boron concentration, SFSC time limitation in the CTF, and heat removal parameters, which are provided in the Diablo Canyon ISFSI Technical Specifications (TS) and their bases. Although provided in the SAR sections below, the TS and bases also provide Limiting Conditions for Operation and bases for maintaining the integrity of the MPC during loading and unloading. These include vacuum pressure, recirculation gas temperature, backfill pressure, and leak rate during loading, and exit gas temperature during unloading.

10.2.1.1 Fuel Characteristics

The Diablo Canyon ISFSI is designed to provide interim storage for up to 4,400 fuel assemblies, which accommodates the number of assemblies predicted to be used during the licensed operating life of the plant. The Diablo Canyon ISFSI storage system will use four MPC types for the storage of fuel assemblies, fuel debris and associated nonfuel hardware. The DCPP fuel will normally be stored as nonconsolidated fuel assemblies both with and without control components. The intact fuel assemblies will be stored in either the MPC-24, MPC-24E, MPC-24EF, or MPC-32 canisters. The damaged fuel assemblies can only be stored in MPC-24E or MPC-24EF canisters, and the fuel debris can only be stored in MPC-24EF canisters. Damaged fuel or fuel debris will be placed in a damaged fuel container before loading into an MPC. The fuel debris can be consolidated, however, the amount of debris is limited to the equivalent of a single intact fuel assembly.

Fuel qualification is based on the requirements for criticality safety, decay heat removal, radiological protection, and structural integrity. The analysis presented in Chapters 4, 7 and 8 of this SAR documents the qualification of DCPP inventory of spent fuel assemblies and associated nonfuel hardware for storage in the Diablo Canyon ISFSI storage system design.

During the operation of DCPP, fuel integrity has been, and continues to be, monitored. Through the detection of radiochemistry changes in the reactor coolant system, most fuel damage is assessed. When damaged rods are suspected, assemblies are inspected as they are removed from the core. All assemblies with positive indication of damage are again inspected in the spent fuel pool (SFP) to determine numbers and location of rods in the assembly that have failed cladding. If the fuel assembly is to be placed back in the reactor core, any failed rods are removed and replaced with nonfuel rods of equivalent dimensional properties. If the suspected damaged fuel assemblies are at the end of their cycle, the assemblies may be stored in the SFP without repair. During this process, all known rod failures are noted and their assemblies are tracked. If the failure is visible from the exterior of the assembly, the damage may be video taped. For assemblies that are removed from the reactor core and were not inspected at that time, similar inspections will be performed prior to loading these assemblies into an MPC for storage. This will ensure that there are no undetected failed rods in any assembly that is placed in an MPC.

Under this failure detection process, inspections to date have found limited failures. Where single failed rods have been identified and removed, they are being stored in the SFP and will ultimately be stored in an MPC that can contain fuel debris. This detection process, along with the past history of plant operations and SFP fuel storage, provide a high level of confidence that the current spent fuel and associated nonfuel hardware will meet the criteria for storage in the appropriate MPC. In addition, based on the condition of the current spent fuel, the continued maintenance of the reactor coolant and SFP water chemistry requirements, and proper handling of the fuel, there is a high level of confidence that future spent fuel assemblies will meet the criteria for storage in the appropriate MPC.

DCPP will develop a cask-loading plan to ensure that no damaged fuel assemblies are loaded into an MPC-24 or MPC-32 canister. Damaged fuel will only be allowed to be stored in either an MPC-24E or MPC-24EF canister. Fuel debris will only be allowed to be stored in an MPC-24EF canister. If the structural integrity criterion is met, then approval for dry storage for a given assembly is made. This qualification will be documented and subsequently referenced in Diablo Canyon ISFSI operating procedures prior to loading spent fuel assemblies into the MPC.

The cask-loading plan will provide a loading sequence based on the various characteristics of the fuel assemblies being loaded. There are two main fuel-loading strategies that are used: uniform fuel loading and regionalized fuel loading. In addition, there is a fuel loading sub-strategy called preferential fuel loading. All of these loading strategies are designed to ensure that the design bases of the fuel, MPCs, and overpacks are maintained.

Uniform fuel loading is used when the fuel assemblies being loaded are all of similar burnup rates, decay heat levels, and post-irradiation cooling times. In this case the actual location of each assembly is less critical and assemblies can be placed at any location in the MPC. However, if the post-irradiation cooling times for any of the assemblies are different by ≥ 1-year, preferential fuel loading is required to be considered.

Preferential fuel loading requires that the fuel assemblies with the longest post-irradiation cooling times be located at the periphery of the MPC basket. Fuel assemblies with shorter post-irradiation cooling times are placed toward the center of the basket. Preferential fuel loading is a requirement in addition to other MPC loading restrictions such as those for nonfuel hardware and damaged fuel containers.

Regionalized fuel loading is used when high heat emitting fuel assemblies are to be stored in an MPC. This loading strategy allows these specific assemblies to be stored in locations in the center of the MPC basket provided lower heat emitting fuel assemblies are stored in the peripheral storage locations. Use of regionalized fuel loading must consider other restrictions on loading such as those for nonfuel hardware and damaged fuel containers. Regionalized fuel loading meets the intent of preferential fuel loading.

The following controls will ensure that each fuel assembly is loaded into a known cell location within a qualified MPC:

- A cask-loading plan will be independently verified and approved.

- A fuel movement sequence will be based upon the written loading plan. All fuel movements from any rack location will be performed under controls that will ensure strict, verbatim compliance with the fuel movement sequence.

- Prior to placement of the MPC lid, all fuel assemblies and associated nonfuel hardware, if included, will be either video taped or visually documented by other means, and independently verified, by ID number, to match the fuel movement sequence.

A cognizant engineer is responsible for performing a third independent verification to ensure that the fuel in the MPCs is placed in accordance with the original cask-loading plan.

Based on the qualification process of the spent fuel and the administrative controls used to ensure that each fuel assembly is loaded into the correct location within an MPC, incorrect loading of an MPC is not considered to be a credible event.

10.2.1.2 Fuel Characteristics (Allowable Content)

The characteristics of the fuel that are allowable for storage in the MPCs are as follows:

- Intact fuel assemblies, damaged fuel assemblies, fuel debris, and nonfuel hardware meeting the limits specified in Tables 10.2-1, 10.2-2, 10.2-3, and 10.2-4 and other referenced tables may be stored in the SFSC system. These SAR tables and specifications are duplicated in Tables 2.2-1 through 2.2-10 of the Diablo Canyon ISFSI TS.

- For MPCs partially loaded with damaged fuel assemblies or fuel debris, all remaining intact fuel assemblies in the MPC shall meet the decay heat generation limits for the damaged fuel assemblies. This requirement applies only to uniform fuel loading.

Fuel proposed for storage at the Diablo Canyon ISFSI is bounded by the thermal analyses described in Chapter 4 of the HI-STORM 100 FSAR, Revision 1. The thermal design is also summarized in Section 4.2.3.3.3 of the Diablo Canyon ISFSI SAR. Off-normal and accident conditions are addressed in HI-STORM FSAR, Revision 1, Sections 11.1 and 11.2, respectively.

10.2.1.3 Uniform and Preferential Fuel Loading

Fuel assemblies used in uniform or preferential fuel loading shall meet all applicable limits specified in Tables 10.2-1, 10.2-2, 10.2-3, 10.2-4, and 10.2-5. Fuel assembly burnup, decay heat, and cooling time limits for uniform loading are specified in Tables 10.2-6 and 10.2-7. Preferential fuel loading shall be used during uniform loading (that is, any authorized fuel assembly in any fuel storage location) whenever fuel assemblies with significantly different post-irradiation cooling times (≥ 1 year) are to be loaded in the same MPC. Fuel assemblies with the longest post-irradiation cooling times shall be loaded into fuel storage locations at the periphery of the basket. Fuel assemblies with shorter post-irradiation cooling times shall be placed toward the center of the basket. Regionalized fuel loading as described in 10.2.1.4 below meets the intent of preferential fuel loading.

10.2.1.4 Regionalized Fuel Loading

Fuel may be stored using regionalized loading in lieu of uniform loading to allow higher heat emitting fuel assemblies to be stored than would otherwise be able to be stored using uniform loading. Figures 10.2-1 through 10.2-3 (these figures are duplicated in the Diablo Canyon ISFSI TS as Figures 2.1-1 through 2.1-3), define the regions for the MPC-24; MPC-24E/MPC-24EF; and MPC-32 models, respectively. Fuel assembly burnup, decay heat, and cooling time limits for regionalized loading are specified in Tables 10.2-8 and 10.2-9. In addition, fuel assemblies used in regionalized loading shall meet all other applicable limits specified in Tables 10.2-1, 10.2-2, 10.2-3, 10.2-4, and 10.2-5. Limitations on nonfuel hardware to be stored with their associated fuel assemblies are provided in Table 10.2-10.

10.2.1.5 For Allowable Content - Functional and Operating Limits Violations

If any fuel specifications or loading conditions above are violated, the following Diablo Canyon ISFSI TS actions shall be completed:

- The affected fuel assemblies shall be placed in a safe condition.
- Within 24 hours, notify the NRC Operations Center.
- Within 30 days, submit a special report that describes the cause of the violation, and actions taken to restore compliance and prevent recurrence.

10.2.2 MPC LOADING CHARACTERISTICS

The confinement of radioactivity during the storage of spent fuel and associated nonfuel hardware in the MPC is ensured by the structural integrity of the strength-welded MPC. However, long-term integrity of the fuel and cladding depends on storage in an inert heat removal environment inside the MPC. This environment is established by removing water from the MPC and backfilling the cavity with an inert gas.

The loading process of an MPC involves placing a transfer cask with an empty MPC in the SFP and loading it with fuel assemblies (intact or damaged that meet the specifications for allowable content discussed above), fuel debris, and/or nonfuel hardware allowed per the type of MPC. Once this is complete a lid is then placed on the MPC. An MPC lid retention device is placed over the MPC lid and attached to the transfer cask. The transfer cask and MPC are raised to the SFP surface. The transfer cask and MPC are then moved into the cask washdown area where dose rates are measured and the MPC lid is welded to the MPC shell and the welds are inspected and tested. The water is drained from the MPC cavity and moisture removal is performed. The MPC cavity is backfilled with helium. Additional dose rates are measured and the MPC vent and drain cover plates and closure ring are installed and welded. Nondestructive examination (NDE) inspections are performed on the welds.

As a part of the loading process there are several characteristics that must be maintained to ensure that the allowable contents placed in any MPC remains stable and intact. These characteristics involve maintaining the MPC cavity temperature. During the loading process there are times when the loaded MPC is water filled and times when it is empty of water. As a result, there are characteristics that must address each of these two conditions. One of these characteristics is MPC water temperature and the other is maintaining the borated water level and recirculation in the annular gap between the transfer cask and the MPC.

Also during the loading process there are several characteristics vital to ensuring that the resulting MPC internal environment is conducive to long-term heat removal and maintaining the integrity of the fuel cladding. These characteristics are; limiting the moisture in the MPC; backfilling the MPC with high quality inert gas; and limiting the leakage of this inert environment over time. The dry, inert and sealed MPC atmosphere is required to be in place during loading, transport and storage operations after an acceptable final NDE on the first weld of the MPC lid to its outer shell.

10.2.2.1 Annulus Gap Water Requirement

During the loading and unloading processes there are time periods when there is no water in the MPC, or it is being removed, or the inert environment in the MPC cavity has not been completely established or maintained at levels that will continue to provide adequate cooling and maintain fuel cladding integrity. During these time periods maintaining the water level in the annular gap and continuous recirculation for high heat fuel (> 22 kw) between the loaded MPC and the transfer cask ensures that the cooling capability is adequate to maintain the fuel cladding integrity. As long as the annular gap water level is maintained with borated water and the temperature of the water in the gap is maintained below boiling through recirculation, there is no time limitation for refilling the MPC with borated water or establishing an acceptable inert environment in the MPC for moderate burnup fuel (≤ 45,000 MWD/MTU). However, without recirculation there is a limit of 2 hours to establish this process or establish an inert environment. For higher burnup fuel (>45,000 MWD/MTU), which requires the use of a forced helium dehydration (FHD) system for drying, once the drying process is completed and if residual helium is not removed from the MPC, there is a limit of 2 hours to re-establish an inert environment in the MPC. This is discussed further in Section 10.2.2.3.

During the loading process, prior to start of the removal of water from the MPC through the drying process, the annular gap shall be filled and maintained full throughout the drying and backfill process. This water level shall be maintained until the MPC inert environment is established at an acceptable level to support long-term storage or the MPC is refilled with water. In addition, during an unloading process the annular gap shall be filled with water prior to removal of the inert environment in the MPC cavity.

10.2.2.2 MPC Water Temperature

During the loading and unloading processes, maintaining the integrity of the fuel in the MPC is the critical activity. As a result of decay heat produced by the spent fuel assemblies, providing a coolant source is imperative to maintaining control of cladding temperature and the fuel integrity. During these processes when there is water in the MPC, the water is considered the coolant source. As long as there is water in the MPC it will continue to perform the coolant function. This water should continue to perform its function as long as it does not reach the boiling temperature. As a result, the parameter that will best indicate the potential reduction of water would be the temperature of the water in the MPC. However, since monitoring the water temperature in the MPC directly may not always be possible, an analysis of the potential for the water to reach the boil-off temperature is performed to ensure that the boil-off temperature cannot be reached. This analysis will be based on the decay heat levels of the contents and the various volumes of water in the MPC as it is loaded. The results of this analysis will provide any time limitation or any requirement for compensatory measures.

While there is water in the MPC, there will be adequate assurance through analysis that the temperature of that water in the MPC will not reach the boil-off level and that the volume of water in the MPC is not allowed to decrease significantly. If the water temperature is shown to potentially reach the boiling level, action will be taken to limit the time of the activity to less than the time to boil off or, as a minimum, continue to replace the volume of water that is boiling off. If no action is possible to correct this condition, then the content loaded in the MPC shall be removed and placed back in the SFP.

10.2.2.3 MPC Drying Characteristics

Dependent on the allowable content of a specific MPC, cavity moisture removal can be performed by using either vacuum drying or a Forced Helium Dehydration (FHD) system after the MPC has been drained of water. See Figure 10.2-4 for a schematic diagram of the FHD system. The Standard Review Plan (SRP) acceptance criterion for dryness is ≤ 1 gram-mole per cask of oxidizing gases. This has been translated by the industry to be 3 torr for vacuum drying. For the recirculation drying process using the FHD system, measuring the temperature of the gas exiting the demoisturizer of the FHD system provides an indication of the amount of water vapor entrained in the helium gas in the MPC. Maintaining a demoisturizer exit temperature of less than or equal to 21°F for 30 minutes or more during the recirculation drying process ensures that the partial pressure of the entrained water vapor in the MPC is less than 3 torr.

If the MPC contains only moderate burnup fuel (≤ 45,000 MWD/MTU) vacuum drying can be used. In this process any water that has not drained from the MPC cavity evaporates from the MPC cavity due to the vacuum. This drying is aided by the temperature increase due to the decay heat of the fuel. To ensure adequate drying the vacuum drying pressure in the MPC must be verified to be at ≤ 3 torr for ≥ 30 minutes. This low vacuum pressure is an indication that the cavity is dry and the moisture level in the MPC is acceptable.

For any MPC that contains fuel assemblies of any authorized burnup, the FHD system can be used to remove the remaining moisture in the MPC cavity after all of the water that can practically be removed through the drain line using a hydraulic pump has been expelled in the water blowdown operation. The FHD system is required to be used for any MPCs containing at least one high burnup fuel assembly (>45,000 MWD/MTU). The recirculation process using the FHD involves introducing dry gas into the MPC cavity that absorbs the residual moisture in the MPC. This humidified gas exits the MPC and the absorbed water is removed through condensation and/or mechanical drying. The dried gas is then forced back through the MPC until the gas exit temperature from the FHD demoisturizer is ≤ 21°F for at least 30 minutes. Meeting these temperature and time criteria ensures that the cavity is dry and the moisture level in the MPC is acceptable. The FHD system shall be designed to ensure that during normal operation (that is, excluding startup and shutdown ramps) the following criteria are met:

(1) The temperature of helium gas in the MPC shall be at least 15°F higher than the saturation temperature at coincident pressure.

(2) The pressure in the MPC cavity space shall be less than or equal to 60.3 psig (75 psia).

(3) The recirculation rate of helium shall be sufficiently high (minimum hourly throughput equal to ten times the nominal helium mass backfilled into the MPC for fuel storage operations) so as to produce a turbulated flow regime in the MPC cavity.

(4) The partial pressure of the water vapor in the MPC cavity will not exceed 3 torr if the helium temperature at the demoisturizer outlet is ≤ 21°F for a period of 30 minutes.

In addition to the above system design criteria, the individual modules shall be designed in accordance with the following criteria:

(1) The condensing module shall be designed to devaporize the recirculating helium gas to a dew point of 120°F or less.

(2) The demoisturizer module shall be configured to be introduced into its helium conditioning function after the condensing module has been operated for the required length of time to ensure that the bulk moisture vaporization in the MPC has been completed.

(3) The helium circulator shall be sized to effect the minimum flow rate of circulation required by the system design criteria described above.

(4) The preheater module shall be engineered to ensure that the temperature of the helium gas in the MPC meets the system design criteria described above.

The design of the FHD system is subject to the confirmatory analyses listed below to ensure that the system will accomplish the performance objectives set forth in this SAR.

(1) System thermal analysis in Phase 1: Characterize the rate of condensation in the condensing module and helium temperature variation under Phase 1 operation (i.e., the scenario where there is some unevaporated water in the MPC) using a classical thermal-hydraulic model wherein the incoming helium is assumed to fully mix with the moist helium inside the MPC.

(2) System thermal analysis in Phase 2: Characterize the thermal performance of the closed loop system in Phase 2 (no unvaporized moisture in the MPC) to predict the rate of condensation and temperature of the helium gas exiting the condensing and the demoisturizer modules. Establish that the system design is capable to ensure that partial pressure of water vapor in the MPC will reach less than or equal to 3 torr if the temperature of the helium gas exiting the demoisturizer is predicted to be at a maximum of 21°F for 30 minutes.

(3) Fuel Cladding Temperature Analysis: A steady-state thermal analysis of the MPC under the forced helium flow scenario shall be performed using the methodology described in HI-STORM 100 FSAR Subsections 4.4.1.1.1 through 4.4.1.1.4 with due recognition of the forced convection process during FHD system operation. This analysis shall demonstrate that the peak temperature of the fuel cladding under the most adverse condition of FHD system operation (design maximum heat load, no moisture, and maximum helium inlet temperature), is below the peak cladding temperature limit for normal conditions of storage for the applicable fuel type (PWR or BWR) and cooling time at the start of dry storage.

If Diablo Canyon is the first user of the FHD system designed and built for the MPC drying function, the system will be subject to confirmatory testing as follows:

(1) A representative quantity of water will be placed in a manufactured MPC (or equivalent mock-up) and the closure lid and RVOAs installed and secured to create a hermetically sealed container.

(2) The MPC cavity drying test will be conducted for the worst case scenario (no heat generation within the MPC available to vaporize water).

(3) The drain and vent line RVOAs on the MPC lid will be connected to the terminals located in the preheater and condensing modules of the FHD system, respectively.

(4) The FHD system will be operated through the moisture vaporization (Phase 1) and subsequent dehydration (Phase 2). The FHD system operation will be stopped after the temperature of helium exiting the demoisturizer module has been at or below 21°F for 30 minutes (nominal). Thereafter, a sample of the helium gas from the MPC will be extracted and tested to determine the partial pressure of the residual water vapor in it. The FHD system will be deemed to have passed the acceptance testing if the partial pressure in the extracted helium sample is less than or equal to 3 torr.

At completion of the drying operation using the FHD system, the partial pressure of the helium/water vapor will be at 3 torr or less, however, the total pressure in the MPC will be approximately 2000 torr or 3 atm. This is the result of the MPC still containing helium and the approved contents continuing to heat that helium. To complete the backfill and loading process when the FHD system is used, the contained helium/water vapor mixture in the MPC must be withdrawn down to an MPC total pressure of 10 torr. This ensures the helium backfill process can be properly completed. Once the residual helium/water vapor mixture is drawn down to 10 torr the cooling capability of the MPC is reduced. As a result, there is a 2-hour limitation during which either the backfill gas must be introduced into the MPC; or as a minimum the MPC must be refilled with helium. Either of these actions will re-establish adequate cooling capability in the MPC and ensure that the fuel cladding short-term temperature limit is not exceeded.

If the cavity moisture removal limits are not met, an engineering evaluation will be necessary to determine the potential quantity of moisture left within the MPC cavity. Once the quantity of moisture potentially left in the MPC cavity is determined, a corrective action plan shall be developed and actions initiated to the extent necessary to return the MPC to an analyzed condition. As the quantity of moisture estimated can range over a broad scale, different recovery strategies may be necessary.

Since moisture remaining in the cavity may represent a potential long-term degradation concern, immediate action is not necessary. The actions to develop and initiate the corrective actions should be undertaken as soon as possible commensurate with the safety significance of the condition. Completion times for the determined corrective actions will be controlled by the DCPP corrective actions program and will be determined and controlled based on the safety significance of the condition.

10.2.2.4 MPC Helium Backfill Characteristics and Purity

Having the proper helium backfill pressure or density ensures adequate heat transfer from the fuel to the fuel basket and surrounding structure of the MPC. During the loading operation, once the dryness limits are met, the MPC cavity is backfilled with helium to provide the inert environment required for long-term storage. To ensure the proper environment is established the helium used in the backfill process shall have a purity of ≥ 99.995 percent. In addition, the helium backfill pressure shall be verified during loading for all MPCs to be ≥ 29.3 psig and ≤ 33.3 psig.

If it has been determined that the helium backfill pressure limit has not been met, an engineering evaluation shall be undertaken to determine the actual helium pressure within the MPC cavity. Since too much or too little helium in the MPC cavity represents a potential overpressure or heat removal degradation concern, the engineering evaluation shall be performed in a timely manner commensurate with the safety significance of the condition (that is, if it is not addressed there is a possibility of a failure to adequately cool the contained fuel resulting in cladding damage).

Once the helium pressure in the MPC cavity is determined, a corrective action plan shall be developed and initiated to the extent necessary to return the MPC to an analyzed condition. Since the helium pressure estimated can range over a broad scale, different recovery strategies may be necessary. Completion times for the determined corrective actions will be controlled by the DCPP corrective actions program and will be determined and controlled based on the safety significance of the condition.

10.2.2.5 MPC Leakage Characteristics

The MPC helium leak rate limit ensures there is adequate helium in the MPC for long-term storage and proper heat removal. The leak rate acceptance limit of ≤ 5.0E-6 atm cc/sec (He) is assumed in the confinement analyses and is bounding for offsite dose. This is a mass-like leakage rate as specified in ANSI N 14.5 (1997). This is defined as the rate of change of the pressure-volume product of the leaking fluid at test conditions. This allows the leakage rate as measured by a mass spectrometer leak detector (MSLD) to be compared directly to the acceptance limit without the need for unit conversion from test conditions to standard, or reference conditions.

During transport operations or storage operations if the helium leak rate limit is determined not to be met, an engineering evaluation shall be performed to determine the impact of increased helium leak rate on heat removal and offsite dose. Since the SFSC is a ventilated system, any leakage from the MPC is transported directly to the environment. An increased helium leak rate represents a potential challenge to MPC heat removal and the offsite doses calculated in the Diablo Canyon ISFSI SAR confinement analyses, reasonably rapid action is warranted.

Once the cause and consequences of the elevated leak rate from the MPC are determined, a corrective action plan shall be developed and initiated to the extent necessary to return the MPC to an analyzed condition. Since the recovery mechanisms can range over a broad scale based on the evaluation performed, different recovery strategies may be necessary. An elevated helium leak rate represents a challenge to heat removal rates and offsite doses, reasonably rapid action and completion of the corrective actions shall be commensurate with the safety significance of the condition. Completion times for the determined corrective actions are controlled by the DCPP corrective actions program and will be determined based on the safety significance of the condition

10.2.2.6 Returning MPC to Safe Condition

If for a loaded MPC the fuel cavity dryness, backfill pressure, or helium leakage rate cannot be successfully met or maintained for any reason, the MPC must be returned to a safe analyzed condition, which may ultimately require the fuel to be placed back in the SFP. The completion time for this effort shall be based on the safety significance of the condition. The completion time shall consider the time required to perform fuel cool-down operations, reflood the MPC, cut the MPC lid welds, move the transfer cask into the SFP, remove the MPC lid, and remove the spent fuel assemblies in an orderly manner and without challenging personnel.

10.2.3 MPC UNLOADING CHARACTERISTICS

In the event that an MPC must be unloaded, the transfer cask with its enclosed MPC is returned to the auxiliary building/fuel handling building to begin the process of fuel unloading. The MPC closure ring, and vent and drain port cover plates are then removed. The MPC gas is sampled to determine the integrity of the spent fuel cladding. The MPC is attached to the cool-down system. The cool-down system is a closed-loop forced ventilation gas cooling system that cools the fuel assemblies by cooling the surrounding helium gas inside the MPC.

During fuel cool-down, the MPC/transfer cask annular gap is reflooded with borated water to ensure adequate cooling capability is maintained. Once the fuel cool-down process is complete the MPC is reflooded with borated water and the MPC lid weld is removed leaving the MPC lid in place. The transfer cask and MPC are placed in the SFP and the MPC lid is removed. The contents are removed from the MPC and the MPC and transfer cask are removed from the SFP and decontaminated.

10.2.3.1 Gas Exit Temperature Of An MPC Prior To Reflooding

The integrity of the MPC depends on maintaining the internal cavity pressures within design limits. During the unloading process, reducing the fuel cladding temperatures significantly reduces the temperature gradients across the cladding, thus minimizing thermally-induced stresses on the cladding during MPC reflooding. In addition, reducing the MPC internal temperatures eliminates the risk of high MPC pressure due to sudden generation of steam during reflooding. This is accomplished by using the cool-down system that reduces the MPC internal temperatures such that there is no sudden formation of steam during MPC reflooding. Monitoring the circulating MPC gas exit temperature from the cool-down system ensures that there will be no large thermal gradient across the fuel assembly cladding during reflooding, which could be potentially harmful to the cladding. The exit gas temperature limit of ≤ 200°F ensures that the MPC gas exit temperature will closely match the desired fuel cladding temperature prior to reflooding the MPC. This temperature was selected to be lower than the boiling temperature of water with additional margin to eliminate the possibility of flashing to steam during reflooding.

During the fuel cool-down process, if the MPC helium gas exit temperature limit is not met, proceeding with reflooding shall be prohibited and actions must be taken to restore the parameters to within the limits before reflooding. In addition, while this parameter is being restored within limits, the proper conditions must be verified to exist for the transfer of heat from the MPC to the surrounding environs to ensure the fuel cladding remains below the short-term temperature limit. Maintaining the annular gap water level between the MPC and the transfer cask will ensure that adequate cooling capability exits.

10.2.4 OTHER OPERATING CONTROLS AND LIMITS

10.2.4.1 Fuel Cladding Oxide Thickness

In determining whether fuel assemblies are considered intact or damaged, several parameters are considered as is discussed in Section 10.2.1. Most of these parameters concern known or suspected cladding failures. However, for high burnup fuel (> 45,000 MWD/MTU), fuel-cladding oxidation is also a concern and shall be evaluated prior to a specific fuel assembly being identified as an intact assembly. A very high oxidation level can mean that a fuel assemble is not structurally sound and may fail in storage causing a change in the conditions inside the affected MPC. The evaluation of fuel cladding oxidation can be performed by actual physical measurement or an appropriate predictive methodology. For a high burnup spent fuel assembly to be classified as an intact fuel assembly, the computed or measured average oxidation layer thickness shall not exceed the applicable maximum allowable average fuel cladding oxidation layer thickness provided in the Diablo Canyon ISFSI Technical Specifications.

For a high burnup fuel assembly, if the fuel cladding oxidation layer thickness that is computed or measured on any fuel rod exceeds the limit, that fuel assembly will be considered a damaged fuel assembly. As such it will require storage in a damaged fuel container and limited to what MPC type it may be stored in.

10.2.5 LIMITING CONDITIONS FOR OPERATION

10.2.5.1 Equipment

All Diablo Canyon ISFSI equipment important to safety is passive in nature, therefore, there are no limiting conditions regarding minimum available equipment or operating characteristics. The MPC, transfer cask, CTF, and overpack have been analyzed for all credible equipment failure modes and extreme environmental conditions. No credible postulated event results in damage to fuel, release of radioactivity above acceptable limits, or danger to the public health and safety. All operational equipment is to be maintained, tested, and operated according to the implementing procedures developed for the ISFSI. The failure or unavailability of any operational equipment can delay the transfer of an MPC to the transfer cask or to the SFSC, but would not result in an unsafe condition.

10.2.5.2 Technical Conditions and Characteristics

The following technical conditions and characteristics are required for the Diablo Canyon ISFSI:

- Spent fuel characteristics
- SFSC heat removal capability
- MPC dissolved boron concentration level
- Annulus gap water requirement during moisture removal for loading and reflooding for unloading
- Water temperature of a flooded MPC
- MPC vacuum pressures
- MPC recirculation gas exit temperature
- Helium purity
- MPC helium backfill pressures
- Gas exit temperature of an MPC prior to reflooding
- SFSC time limitation while seated in the CTF
- Fuel cladding oxide thickness

The spent fuel specifications for allowable content for storage in the ISFSI and their bases are detailed in Section 10.2.1. In addition, the spent fuel specifications are also contained in Diablo Canyon ISFSI TS Section 2.0. A description of bases for selecting the above remaining conditions and characteristics are detailed in Sections 10.2.2 through 10.2.4, with the exception of the heat removal capability, SFSC time limitation in the CTF, and dissolved boron concentration. These are provided in the Diablo Canyon

ISFSI TS bases. Although provided in the above SAR sections, the Diablo Canyon ISFSI TS and TS Bases also provide Limiting Conditions for Operations and bases for maintaining the integrity of the MPC during loading and unloading. These include vacuum pressure, recirculation gas temperature, backfill pressure, and leak rate during loading, and exit gas temperature during unloading.

The technical and operational considerations are to:

- Ensure proper internal MPC atmosphere to promote heat transfer, minimize oxidation, and prevent an uncontrolled release of radioactive material.
- Ensure that dose rates in areas where operators must work are ALARA and that all relevant dose limits are met.
- Ensure that the fuel cladding is maintained at a temperature sufficiently low to preclude cladding degradation during normal storage conditions.

Through the analyses and evaluations provided in Chapters 4, 7, and 8, this SAR demonstrates that the above technical conditions and characteristics are adequate and that no significant public or occupational health and safety hazards exist.

10.2.6 SURVEILLANCE REQUIREMENTS

The analyses provided in this SAR show that the Diablo Canyon ISFSI and the storage system fulfill its safety functions during all accident conditions as described in Chapter 8. Surveillance requirements are provided in the Diablo Canyon ISFSI TS. No continuous surveillance of the MPC is required during long-term storage. Surveillance of the SFSC duct screens is in the Diablo Canyon ISFSI TS and ensures freedom of air movement and adequate heat dissipation during long-term storage.

10.2.7 DESIGN FEATURES

The following storage system design features are important to the safe operation of the Diablo Canyon ISFSI and require design controls and limits:

- Material mechanical properties for structural integrity confinement and shielding
- Material composition and dimensional control for subcriticality
- Decay heat removal

Component dimensions are not specified here since the combination of materials, dose rates, criticality safety, and component fit-up define the operable limits for dimensions (that is, thickness of shielding materials, thickness of concrete, MPC plate thicknesses, etc.) The values for these design parameters are specified in the HI-STORM 100 System FSAR and LAR 1014-1 (References 1 and 2 respectively). Changes to any of these design features will be implemented only after conducting a safety evaluation in accordance with 10 CFR 72.48.

The combination of the above controls and limits and those discussed previously in Section 10.2 define requirements for the Diablo Canyon ISFSI storage system components that provide radiological protection and structural integrity during normal storage and postulated accident conditions.

10.2.8 ADMINISTRATIVE CONTROLS

Use of the existing DCPP organizational and administrative systems and procedures, record keeping, review, audit, and reporting requirements coupled with the requirements of this SAR ensure that the operations involved in the storage of spent fuel at the ISFSI are performed in a safe manner. This includes both the selection of assemblies qualified for ISFSI storage and the verification of assembly identification numbers prior to and after placement into individual MPCs. The spent fuel qualification, identification, and control are discussed in Sections 10.2.1 through 10.2.4 above. Other administrative programs will control revisions to the Diablo Canyon ISFSI TS Bases; radioactive effluents; fuel-cladding-oxide thickness; MPC loading and unloading processes; ISFSI operations, and transportation route conditions. These other programs are defined in the Diablo Canyon ISFSI TS.

10.2.9 OPERATING CONTROL AND LIMIT SPECIFICATIONS

The operating controls and limits applicable to the Diablo Canyon ISFSI, as documented in this SAR, are delineated in the Diablo Canyon ISFSI TS and the TS Bases. These include:

- MPC dryness, backfill pressure and leak rate limitations
- SFSC heat removal capability
- Fuel Cool-Down exit gas temperature limitation
- SFSC time limitation in the CTF
- Dissolved boron concentration

10.2.10 REFERENCES

Detailed information describing the HI-STORM 100 System is provided in the following two references, which must be used together:

1. Final Safety Analysis Report for HI-STORM 100 System, Revision 0, July 2000.

2. License Amendment Request 1014-1, Holtec International, Revision 2, July 2001, including Supplements 1 through 4 dated August 17, 2001; October 5, 2001; October 12, 2001; and October 19, 2001; respectively.

Reference 2 contains information related to MPC-32, MPC-24, MPC-24E, MPC-24EF, and the HI-STORM 100SA. General references to these documents are made in Chapter 10 as needed to supplement SAR information.